

INAF



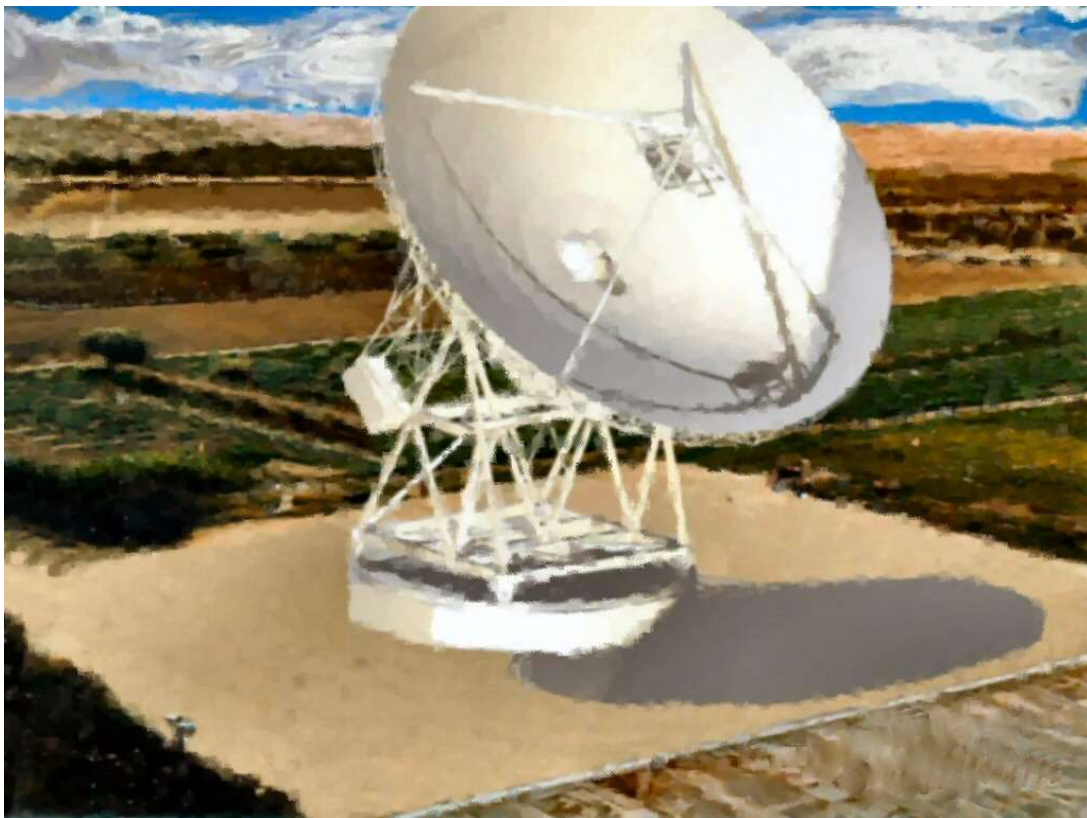
ISTITUTO NAZIONALE DI ASTROFISICA
NATIONAL INSTITUTE FOR ASTROPHYSICS



International VLBI Service for Geodesy & Astrometry

PROCEEDINGS OF THE 17th WORKING MEETING ON EUROPEAN VLBI FOR GEODESY AND ASTROMETRY

Noto - April 22-23, 2005



Edited by Markus Vennebusch and Axel Nothnagel

INAF - Istituto di Radioastronomia - Sezione di NOTO - Italy

Proceedings of the

**17th Working Meeting
on European VLBI for
Geodesy and Astrometry**

April 22-23, 2005

Noto, Italy

Edited by
Markus Vennebusch and Axel Nothnagel

Preface

Geodetic and astrometric VLBI activities have always been linked with each other generating important synergies and major cooperations. It may even be permitted to say that the techniques form a technical symbiosis. In Europe a number of individuals and working groups have contributed considerable resources to successfully carry out observations, to process the recorded bitstreams and to analyse the data. As early as 1980 the first *Working Meeting on European VLBI for Geodesy and Astrometry* has brought together scientists working in the fields of geodetic and astrometric VLBI in order to discuss joint projects, to share experience, and to present results. In a loose sequence these meetings have been repeated almost yearly with the 17th event having taken place at Noto Astronomical Observatory of the Italian *Istituto Nazionale di Astrofisica* (INAF) on April 22 and 23, 2005. We have enjoyed to be the guests of INAF in the pleasant surroundings of the observatory and have appreciated the efficient logistics.

The 17th *Working Meeting on European VLBI for Geodesy and Astrometry* marks a noticeable change in the appearance of these meetings but also in the organisational structure of the geodetic and astrometric VLBI activities in Europe. Prof. Dr. James Campbell who initiated these meetings in the very beginning, and who has been keeping the group together ever since, retired in summer 2004. We have been very glad that he gave us the honour to attend this meeting even though. His departure from the active working life will leave a gap in our ranks since James is the person who made the European geodetic VLBI network to what it stands for today. We hope that he may find the time and interest to attend many more of these meetings to come.

On the organisational side we are proud to announce the formal establishment of the *European VLBI group for Geodesy and Astrometry* (EVGA). In times where funding and idealistic support more than ever depend on widespread visibility, working under an acknowledged umbrella bears many advantages. The EVGA is, thus, planned to serve as an organisational entity to foster geodetic and astrometric VLBI in Europe and to increase its appearance¹. The 17th *Working Meeting on European VLBI for Geodesy and Astrometry* may be considered to be the first scientific meeting of the EVGA. The articles presented during the meeting and published in these proceedings document that the community is very active in addressing interesting topics and scientific challenges.

Axel Nothnagel
Chairman of the EVGA

¹For more details please visit EVGA's charter under <http://www.evga.org>

Table of Contents

Preface	iii
 <i>Franco Mantovani, Monia Negusini, Pierguido Sarti:</i>	
The Italian Infrastructure for Geodetic VLBI	1
 <i>Gino Tuccari, Ying Xiang, Michael Wunderlich, Salvatore Buttaccio, Gaetano Nicotra, Guntars Balodis:</i>	
DBBC Development: Status and First Results	5
 <i>Yasuhiro Koyama, Tetsuro Kondo, Mamoru Sekido, Hiroshi Takeuchi, Moritaka Kimura:</i>	
Developments of the K5 VLBI System	8
 <i>Alan R. Whitney:</i>	
Mark 5 Status Update	13
 <i>Alan R. Whitney:</i>	
e-VLBI Development at Haystack Observatory	20
 <i>Walter Alef, Arno Muskens:</i>	
The Bonn Astro/Geo MKIV Correlator	30
 <i>Thomas Hobiger, Tetsuro Kondo:</i>	
An FX software correlator based on Matlab	34
 <i>Robert M. Campbell:</i>	
Recent Results from the EVN MkIV Data Processor at JIVE	39
 <i>Joerg Wresnik, Rudiger Haas, Johannes Boehm, Harald Schuh:</i>	
Thermal deformation of VLBI antennas	45
 <i>Pierguido Sarti, Monia Negusini, Luca Vittuari, Simonetta Montaguti, Paolo Tomasi:</i>	
GPS - VLBI eccentricity at Noto Observatory: June 2003 survey results	51
 <i>Bitelli, G., Campbell, J., Negusini, M., Sarti, P., Vittuari, L.:</i>	
Determination of vertical motion from levelling data in the wider area of Medicina	56
 <i>Johannes Boehm, Marco Ess, Harald Schuh:</i>	
Asymmetric Mapping Functions for CONT02 from ECMWF	64
 <i>Robert Heinkelmann, Johannes Boehm, Harald Schuh:</i>	
IVS long-term series of Tropospheric Parameters	69

<i>Robert Heinkelmann, Johannes Boehm, Harald Schuh:</i> Homogenization of surface pressure recordings and its impact on long-term series of VLBI tropospheric parameters	74
<i>Robert Heinkelmann, Johannes Boehm, Harald Schuh:</i> Combination of tropospheric parameters within IVS project TROPO	79
<i>Monia Negusini, Paolo Tomasi:</i> Water vapour content and variation estimated at European VLBI sites	84
<i>Rüdiger Haas, Camilla Granström, Jan Johansson:</i> An Investigation of Water Vapor Trends in Europe	90
<i>Jung-ho Cho, Axel Nothnagel, Markus Vennebusch, Dorothee Fischer:</i> Preliminary results of applying WVR calibration to European VLBI data	96
<i>Thomas Hobiger, Tetsuro Kondo, Harald Schuh:</i> Estimation of absolute TEC values by VLBI	102
<i>Markus Vennebusch, Andreas Weinberger:</i> Status of SINEX combination - IVS' Contribution to the IERS Combination Pilot Project	107
<i>Leonid Petrov:</i> Approaches for modeling non-linear site position variations	113
<i>Axel Nothnagel:</i> VTRF2005 - A combined VLBI Terrestrial Reference Frame	118
<i>María Rioja, Richard Dodson, Richard Porcas, Hiroshi Suda, Francisco Colomer:</i> Measurement of core-shifts with astrometric multi-frequency calibration	125
<i>Alexey Melnikov, John Gipson:</i> Running SKED under Linux	131
<i>Patrick Charlot, Alan Fey, Chris Jacobs, Chopo Ma, Ojars Sovers:</i> Densification of the International Celestial Reference Frame: Results of EVN+ Observations	133
<i>Thomas Klügel, Wolfgang Schlueter, Ulrich Schreiber:</i> Ring Laser "G" and Earth Rotation	138
Participants	145
Programme	148

The Italian Infrastructure for Geodetic VLBI

Franco Mantovani, Monia Negusini, Pierguido Sarti

Istituto di Radioastronomia, Bologna

Contact author: Franco Mantovani, e-mail: fmantovani@ira.cnr.it

Abstract

General information on the Italian Infrastructure for Geodetic VLBI are given, together to a short description of the present status of the VLBI observing facilities. The station usage for the last seven years is also provided.

1. General Information

The Italian Infrastructure for Geodetic VLBI is formed by the telescopes of Medicina, Noto and Matera. These telescopes have been actively involved in Geodetic VLBI observations since the late '80 and are now regularly scheduled in agreement with the IVS Observing Program Committee.

The Medicina and Noto Stations are run by the Institute of Radioastronomy (IRA). The Matera dish belongs to the Italian Space Agency (ASI) and it is run under contract by Telespazio.

IRA was one of the many Institutes of the Consiglio Nazionale delle Ricerche (CNR) until December 2004. Since January 1st, 2005, IRA is part of the National Institute of Astrophysics (INAF). ASI, CNR and INAF are under reorganization following a decision taken by the Italian Government a couple of years ago. Such a reorganization is not at present affecting the Geodetic VLBI observing plans at the stations. On the other hand, the reorganization is producing effects on the Italian research groups involved in Geodetic VLBI activities. One of the most critical case is that of the IRA group based at the Centro di Geodesia Spaziale in Matera. The IRA site has been shut down. Consequently part of the staff moved to the IRA Head-quarters in Bologna.

IRA is also managing the construction of an antenna in Sardinia. The project is called Sardinia Radio Telescope (SRT). SRT is a 64 m paraboloidal radio telescope able to work in the frequency range 0.3 – 100 GHz. It is planned that SRT will be dedicated to VLBI observations for 30–40% of its time. The first light of the radio telescope is foreseen for 2007. It is not yet known when a S/X receiver for geodetic VLBI observations will be made available. More information on the SRT project are available at the web-page <http://www.ca.astro.it/srt/index.htm> .

2. Italian VLBI observing facilities

2.1. The Medicina 32-m dish

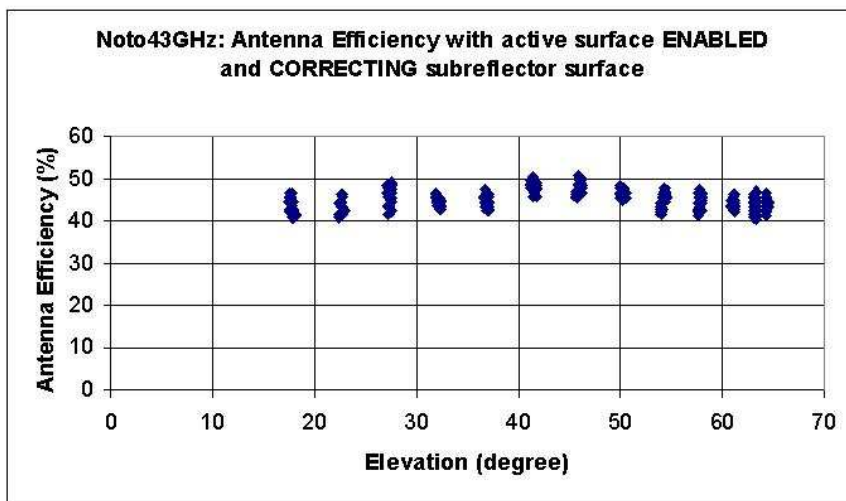
In the recent past the 32-m dish at the Medicina Station gained in reliability upgrading the following parts: a new Vertex room, now able to host seven receivers allowing the telescope to be agile in changing the observing frequency; new Azimuth and Elevation engines; High Accuracy Encoders; new Antenna Control Unit; new Drive Cabinet; new Cabling; a more effective interface between the AZ rail and the telescope foundation.

The Station is equipped with a MKIV terminal and with a MK5A recording system. The upgrading from MK5A to MK5B is planned as soon as the MK5B will be made available.

2.2. The Noto 32-m dish

The major upgrading of the Noto dish is represented by the implementation of the Active Surface for the main mirror of the telescope. The new panels have an accuracy of 0.1 mm rms. The secondary mirror has an accuracy of 0.38 mm rms. The panels are supported by 244 actuators. The set of the actuators is under computer control. The system is refreshed in 7 seconds and the panel positions updated every change in the telescope pointing position by 1 deg in Elevation.

Fig. 1 – The Efficiency of the Noto radio telescope *vs* Elevation at 43 GHz.



The following antenna parts have also been upgraded: High Accuracy Encoders; new Antenna Control Unit; new Drive Cabinet and Cabling.

A cooled multi-feed SXL receiver has been added to the front-end set of receivers . The receiver is now complete and ready to be mounted. It is composed by three sections: one in primary focus,

one in secondary focus, and one in the control room. The sky frequency is transferred from the primary focus to the vertex room using low loss cables. The frequency conversion is performed in the secondary focus room. All the receivers' IFs are routed through the same system to the control room, using fibre optic connections. The implementation of such system will require an antenna stop.

The Station is equipped with both a MKIV and a VLBA formatters and with a MK5A recording system. The MK5A will be upgraded to MK5B as soon as possible.

2.3. The Matera 20-m dish

As previously stated, the Matera 20-m dish is operated by Telespazio under contract with ASI. The antenna is not available for observations since the beginning of 2004 due to severe problems in the AZ rail (see Fig. 2). The repairing plan, hopefully in operation before the end of 2005, requires the replacement of the rail and of the four wheels, a new concrete and high quality grout, a concrete ring added to support the rail upgrade of the rail-concrete interface. This plan is not yet funded. A less 'ambitious' plan, which asks for a minor repairing and less resources, is now in place. It would allow the telescope to temporarily restart the observations in a short period of time.

The Matera Station is equipped with a MKIV Terminal and MK5A recording system.

Fig. 2 – View of the damaged AZ rail of the Matera 20 m dish.



3. Station Usage

The three Italian Stations are involved in different type of observing sessions coordinated by IVS, namely IVS-R1 and IVS-R4 which provide twice weekly EOP results, IVS-T2 which monitor the TRF via monthly sessions, RDV which are astrometric/geodetic experiments that use the full VLBA plus up to 10 geodetic stations, and EUROPE with the aim to determine the station coordinates and their evolution in the European geodetic VLBI network.

The participation of the Italian Stations to the above observing sessions is summarized in Table 1.

Table 1. **Italian Stations Usage**

Station/Year	1999	2000	2001	2002	2003	2004	2005
Matera	25	36	37	72	72	0	0
Medicina	35	10	28	19	9	28	23
Noto	9	7	3	5	9	11	17

4. Activities

In Italy there are 2 IVS Analysis Centres, located at the INAF-Istituto di Radioastronomia (Bologna) and at the Centro di Geodesia Spaziale ASI/Nuova Telespazio (Matera).

Twenty people are IVS affiliated Members. Most of them are staff members of the INAF-Istituto di Radioastronomia and of the Centro di Geodesia Spaziale. They are actively collaborating with several other Italian Groups interested in Geodesy which are affiliated with institutions like the Dept. of Physics of the Bologna University, the Dept. of Engineering of the Bologna University, the Istituto Nazionale di Geofisica e Vulcanologia (INGV), the Milan Polytechnic, the Bari Polytechnic, the Padova and Cagliari University.

DBBC Development: Status and First Results

*Gino Tuccari*¹, *Ying Xiang*², *Michael Wunderlich*³, *Salvatore Buttaccio*¹,
*Gaetano Nicotra*¹, *Guntars Balodis*⁴

¹⁾ *INAF-IRA, National Astrophysical Institute-RadioAstronomy Institute, Italy*

²⁾ *SHAO-CAS, Shanghai Astronomical Observatory, China*

³⁾ *Max Planck Institute fuer Radioastronomie, Germany*

⁴⁾ *Faculty of Electronics and Telecommunications - University of Riga, Latvia*

Contact author: *Gino Tuccari*, e-mail: `g.tuccari@ira.cnr.it`

Abstract

It is reported a description of the DBBC project, having the aim to realize a fully digital backend system to replace the presently used terminals. The need for such replacement is well known and motivated by the necessity to renew an obsolete system and for achieving better performance making use of the more predictable digital techniques. Field Programmable Gate Array (FPGA) components give the opportunity to take advantages within a concept of a fully programmable system, with the possibility to get a variable architecture and to pursuit an upgrading methodology. The DBBC development is in a well advanced stage and a simplified version, named miniDBBC, coming as collaboration between Italy and China, produced the first experimental results in real observations. Indeed two prototypes have been placed in the Noto (Italy) and Seshan (China) VLBI stations, while two complete systems are in construction.

1. Project Overview

The main idea staying behind to this project is to replace the existing terminal with a complete and compact system to be used with any VSI compliant recorder or data transport. Moreover the cost has to be limited making use of commercially available components.

Hardware programmability is a feature in order to optimize the architecture to the needed performance, because different performance involve different number of gates necessary to perform the required functionality. Under this assumptions, maximum input and output data rates are the limitation and they have to be set so to satisfy the present and reasonable future necessities.

The new development needs to be fully compatible with the existing terminals and correlators in order to require a minimum effort to be introduced in the stations and no modification at the correlator side, still maintaining the possibility to be upgraded for wider bands correlators. The upgrades on the other hand have to be mostly software in order to avoid and modify any hardware part, for cost savings and simplification in the operations, so that programmable hardware is planned as main component.

The entire project is based on a flexible architecture, composed by one or more FPGA boards as computation elements, placed in a mixed cascaded/parallel structure, so to guarantee a parallel usage of data input and a shared parallel output data flow. For such a reason the upgrade could also in principle be possible in hardware replacing or adding compatible modules for different or modified performance, even if this is strongly limited by the software programmability.

In the DBBC project a single unit is composed by four IF Input in the ranges 1-512, 512-1024, 1024-1536, 1536-2048 MHz, with each of them feeding a 1.074 GHz clock sampler. Then four

polarizations or bands are available for a single group of output channels selection. In other words, a group of 64 channels is able to handle a shared combination of channels coming from the four bands.

Multiple architecture can be used taking the advantage to adopt fully re-configurable FPGA Core-Modules, where one of such modules is an autonomous board populated with an appropriate number of gates, fed by any of the four IFs, and sharing the output data bus. More narrow or few wide channels per module can be assigned, maintaining the maximum number of gates provided by the CoreModule. Modular realization for possible cascaded processing is provided, that implies the use of one or more Core Modules for achieving more gates number and then more processing capability. The input bus is cascaded, with very low skew, between modules.

An analog monitor, produced by DA conversion, has been added for testing purposes, in order to be able and evaluate with a common spectrum analyzer the different channels content and performance. This has been proved particularly useful in order to adopt standard equipment normally in use in our radio-telescopes.

Field System support is required to configure the different modules and allow standard settings, and still getting total power measurements of the converted channel. Different configurations can be supported for obtain similar, but not identical, functionalities, as SSB down converter, wide band parallel FIR, poly-phase FIR/FFT. The possibility to independently tune different channels, and to have them filtered at different bandwidth, while it is an obvious feature in the analog implementation, it is not the unique so obvious solution in the digital implementation, so that different solutions appear to be more convenient. For this reason the project allows to implement different architectures, and to change them at convenience.

A Core Module can handle a maximum input bandwidth of 8.192 Gbit/s, apart from the IFs cascade (more than 34 Gbit/s), and a maximum output bandwidth of 4.096 Gbit/s. Two high rate buses are present, named HSI and HSO respectively, with the addition of a further Control/Configuration/Monitor bus, named CCM.

2. Digital Down Converter Configuration

Different architectures can be used in the Core Modules, having different performance and behaviors. One possible configuration is the DDC digital down converter in the classical implementation meaning. In such a solution a direct SSB conversion is typically performed between high data rate sampled IF band and lower data rate base band. One or two channels are generated for each converter, as in the analog implementation. Important differences, greatly improving the performance are anyway present: local oscillator is a Numerically Controlled Oscillator (NCO), mixer is complex as Look Up Table multiplier, low-pass band filters are Finite Impulse Response (FIR). Decimation circuitry is adopted because of the high ratio between IF and output data rate and is performed with multirate/multistage FIR. Digital Total Power (DTP) measurement at base band level is adopted, Rescaling/Gain Control (RGC) is adopted for dynamic range control and final data representation. The tuning step is 1 Hz, giving the possibility to finely tune the receiver for spectroscopy or any other precise frequency setting. Moreover a full compatibility with the 10 KHz tuning step of the present backend is assured. Narrow bandwidth typically adopted is defined for this project in the range: 16, 8, 4, 2, 1, 0.5, 0.25 MHz. Output data rate is 32 or 64 MHz at present in order to be able and fit with the standard, now adopted VSI-H data rate.

3. Development Status

Most of the bandwidth configurations have been completed or are under completion. The tuning ranges are now ready as 64 and 128 MHz, while 256 and 512 MHz are ready in simulation and are under implementation.

Preliminary testing has been done in laboratory for the developed configurations. Good performance in conversion and tuning have been measured from 0 up to 2.5 GHz. Today with appropriate Nyquist zone pre-selection, L and S band can be directly down-converted and recorded with modified MK4 formatter.

Testing with real observation started with mDBBC (IRA-SHAO agreement): fringes have been detected in both analog-digital and digital-digital baselines. First digital x analog fringes have been detected on Nov 23, 2004 in the Seshan-Urumuqi baseline, while first digital x digital fringes have been detected on Feb 2, 2005 in the Noto-Seshan baseline.

An upgrade in the critical system components is planned, leaving the structure as it is described in this document, including boards layout. In particular, an experience is going to be acquired before introducing the modification, making use of a different AD chip with 10 bit resolution, LVDS differential output, increased max sampling rate, and a Virtex4 FPGA device. Main improvement are expected due to the increment of the internal system clock from 128 MHz to 256 MHz and to the optimized resources and internal routing performance available with the last generation FPGA Xilinx family. Further element will be to make use of the higher Nyquist sampling zone to directly down-convert from sky frequency with bands where this could be applied.

In conclusion the DBBC system is an high flexible instrument because is able to produce independent tunable channels for a full compatibility with the existing acquisition system and correlators. One CoreModule board is replacing a BBC module. The DBBC system is also able to handle polyphase + FFT architectures for producing contiguous not tunable channels. One CoreModule board is able to produce multiple channels. Both solutions are possible within the same system.

References

- [1] Tuccari, G. Development of a Digital base Band Converter (DBBC): Basic Elements and Preliminary Results. "New Technologies in VLBI", ASP Conference Series, Vol. 306, 2003, ed. Y. C. Minh (San Francisco: ASP), pp. 177-192
- [2] Ferris, D. Digital Filters and Filterbanks for VLBI. Presented at the Symposium of the International VLBI Service for Geodesy and Astrometry "New Technologies in VLBI", held in Gyeong-ju, Korea, 5-8 November 2002
- [3] G. Tuccari, "DBBC-A Wide Band Digital Base Band Converter", IVS Third General Meeting Proceedings, Canada, 2004

Developments of the K5 VLBI System

Yasuhiro Koyama, Tetsuro Kondo, Mamoru Sekido, Hiroshi Takeuchi, Moritaka Kimura

Kashima Space Research Center, National Institute of Information and Communications Technology

Contact author: Yasuhiro Koyama, e-mail: koyama@nict.go.jp

Abstract

At Kashima Space Research Center of National Institute of Information and Communications Technology, developments of the K5 VLBI system have been continuing based on conventional PC systems to realize e-VLBI observations and data processing over the Internet. By using the the K5 system, various geodetic VLBI experiments have already been performed and interoperability with the other VLBI observation systems such as Mark-5 and PC-EVN have been demonstrated.

1. Concept of the K5 System

The K5 VLBI system is designed to perform real-time or near-real-time VLBI observations and correlation processing using Internet Protocol over commonly used shared high speed networks. Various components are being developed to realize the target goal in various sampling modes and speeds. The entire system will cover various combinations of sampling rates, number of channels, and number of sampling bits. All of the conventional geodetic VLBI observation modes will be supported as well as the other applications like single-dish spectroscopic measurements or pulsar timing observations will also be supported. The concept as the family of the K5 system is show in the Figure 1.



Figure 1. Concept of the entire K5 System.

As shown in the Figure 1, if the ADS1000 or ADS2000 sampler units are used, the PC-VSI board is used to interface the VSI (VLBI Standard Interface) compliant signal from the sampler unit and the PCI bus of the PC. Both of the sampler units, ADS1000 and ADS2000, are equipped with two VSI compliant connectors which can support data rates up to 1024Mbps. In addition, ADS2000 unit supports 64MHz clock signalling specified as the option of the VSI specification to support the data rates up to 2048Mbps with a single VSI connector. Whereas the ADS1000 is designed as a single channel high speed sampler unit, the ADS2000 is designed for geodetic VLBI observations by supporting 16 channels at the sampling rates up to 32Mpsps for each channel. When the ADS1000 or ADS2000 sampler unit is used, the PC-VSI board is connected with the sampler unit by using VSI specified data signalling. Although the function is not fully supported at present, the same PC-VSI board will be used to extract data from the K5 system by using VSI.

When relatively low sampling rates are required, PC systems with the IP-VLBI boards are used as shown in the bottom of the Figure 1. The IP-VLBI board is consist of a main board and a daughter board, and it occupies two board slots in the PCI bus of the PC system. Each board is equipped with four BNC connectors from which the base-band signal is supplied and sampled at the Nyquist frequency of the signal. In this configuration, A/D sampling capability is embedded in the board and the PC can be directly connected to the base band converter units. This configuration is called as K5/VSSP and has been used for various geodetic VLBI sessions including IVS routine VLBI sessions and rapid UT1-UTC estimation demonstrations[1].

2. K5/VSSP System

Figure 2 shows the evolution of the VLBI observation and data processing systems developed at the Kashima Space Research Center of the National Institute of Information and Communications Technology (NICT). The K5 system is characterised by the use of conventional PC systems. The data correlation will be performed on the PC systems using software correlator programs. Similarly, the K4 system can be characterised by the use of rotary-head, cassette type magnetic tape recorders, and the K3 system can be characterised by the use of open-reel magnetic tape recorders.

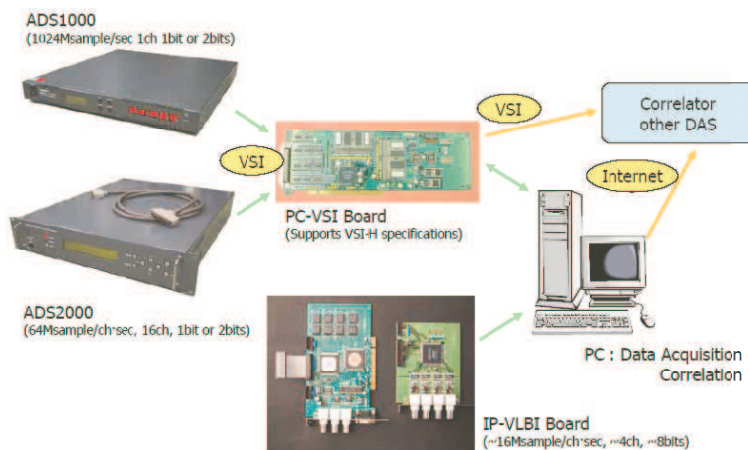


Figure 2. Developments of K3, K4 and K5 VLBI systems.

Figure 3 is one of the combined set of the K5 system and it is specified as the K5/VSSP system. VSSP is an acronym of the Versatile Scientific Sampling Processor. This name is used because the system is designed to be used for general scientific measurements. The system has a capability to sample analog data stream by using the external frequency standard signal and the precise information of the sampled timing. The system is also used to process the sampled data. For geodetic VLBI observations, software correlation program runs on the K5/VSSP system. Therefore, it can be said that the functions of the formatter, the data recorder, and the correlator are combined into the single system. It is consist of four UNIX PC systems. Each UNIX PC system has one IP-VLBI data sampling board on its PCI interfacing bus. Table 1 shows the specifications of the K5/VSSP system. Each board can sample 4 channels of base-band signals at various sampling rates ranging from 40kHz to 16MHz. The timing of the sampling is controlled by the externally provided 10MHz and 1PPS reference signals so that precise timing information can be reproduced from the sampled data. Quantisation bits can be set from 1, 2, 4, and 8. Because the board has these many sampling modes, it has many possibilities to be used not only for VLBI observations but also for various other scientific researches which require precise timing information in the data. Device driver software of the board has been developed on LINUX, FreeBSD, and Windows2000 operating systems, and FreeBSD is used in the K5/VSSP data acquisition terminals. Four PC systems are mounted in the lower part of the 19-inch standard rack. A signal distributor unit for 1-PPS and 10 MHz signals and 16-channel base-band signal variable amplifier unit are mounted in the upper part of the rack. The LCD monitor and the keyboard on the top of the rack are connected to the four PC systems by using a four-way switch. Each PC system is equipped with four removable parallel ATA 3.5 inch hard disk drives. The sampled data can be transferred to the network by using TCP/IP protocol or can be recorded to internal hard disks as ordinary data files. The maximum recording speed is currently restricted by the speed of the CPU and the speed of the PCI internal bus. Currently, the total recording speed of 512 Mbps has been achieved. To process the data sampled with the K5 data acquisition system, software correlation processing program is also under development on conventional PC systems[2]. The correlation processing program receives data from K5 data acquisition systems over the network using TCP/IP protocol and then calculates cross correlation functions without any specially designed hardware. It can also read data files on internal hard disks. These capabilities allow to transfer observed data in real-time if the connecting network is fast enough, or in near real-time if data buffering is required. Since easily re-writable software programs and general PC systems are used, the processing capacity and the function of the correlator can be easily expanded and upgraded. Figure 4 shows the schematic diagram of the data flow of the K5 system.

Table 1. Specifications of the K5/VSSP system.

Reference Signals	10MHz (+10dBm) and 1PPS
Number of Channels	16
A/D bits	1, 2, 4, or 8
Sampling Frequency (for each channel)	40kHz, 100kHz, 200kHz, 500kHz, 1MHz, 2MHz, 4MHz, 8MHz, or 16MHz
Maximum Data Rate	512Mbps



Figure 3. Picture of the K5/VSSP system.

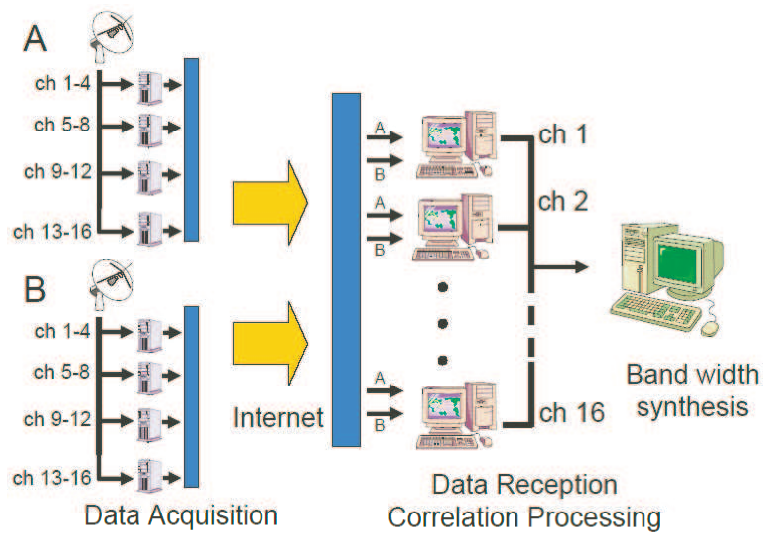


Figure 4. Data flow of the K5/VSSP system in typical geodetic VLBI observations.

3. Concluding Remarks

By using the the K5 system, various geodetic VLBI experiments have already been performed and interoperability with the other VLBI observation systems such as Mark-5 and PC-EVN have been demonstrated. Currently, K5/VSSP system is routinely used as a main observing terminal at five IVS stations, i.e. 34m and 11m station at Kashima, 32m station at Tsukuba, 11m station at

Koganei and 11m station at Syowa. The system is also used at other astronomical VLBI stations in Japan and is currently planned to be used at 32m station in Huancayo, Institute of Geophysics in Peru. On the other hand, the K5 software correlator program is used at Joint Institute for VLBI in Europe, Australia Telescope National Facility and MERLIN in England based on free software license agreements between these institutes and NICT. We are hoping that the K5 VLBI observation system and Software Correlator programs are widely used by as many applications and institutes as possible.

4. Acknowledgements

The authors would like to appreciate many members of the Haystack Observatory and NICT for supporting the e-VLBI developments and observations. Research partners at the NTT Communications Corporation, KDDI R&D Laboratories, NTT Laboratories, JGNII, and Internet2 have made the e-VLBI session possible together. e-VLBI research and developments in Japan have been promoted by a close collaboration of NICT, Geographical Survey Institute, NTT Laboratories, National Astronomical Observatory, Japan Aerospace Exploration Agency, Gifu University and Yamaguchi University.

References

- [1] Koyama, Y., T. Kondo, H. Takeuchi, M. Hirabaru, D. Lapsley, K. Dudevoir, and A. Whitney (2003), Rapid UT1-UTC estimation from Westford-Kashima e-VLBI experiment (2), IVS NICT TDC News, No. 25, pp. 2-6.
- [2] Kondo, T., Y. Koyama, and H. Osaki (2003), Current Status of the K5 Software Correlator for Geodetic VLBI, IVS CRL-TDC News, No. 23, pp. 18-20.

Mark 5 Status Update

Alan R. Whitney

MIT Haystack Observatory

e-mail: `awhitney@haystack.mit.edu`

Abstract

The Mark 5A 1Gbps disk-based VLBI data system has been rapidly adopted with ~ 100 units now deployed around the world, along with ~ 1000 Mark 5 disk modules totaling ~ 1.5 PB of storage capacity. As a result, the majority of VLBI observations are now recorded on disk systems. The Mark 5B system, which will be compatible with the VSI-H specification, is being developed at Haystack Observatory. The Mark 5B includes Station Unit capabilities to allow it to replace the existing Mark 4 Station Units on the Mark 4 VLBI correlator. The Mark 5B system is expected to be available near the end of 2005.

1. Introduction

The Mark 5 VLBI disk-based data system is being developed in two stages:

1. Mark 5A: A 1 Gbps disk-based record/playback system that is a plug-compatible replacement for a Mark 4 or VLBA tape transport
2. Mark 5B: A 1 Gbps disk based record/playback system that supports the VLBI Standard Interface Specification (VSI). Mark 5A and Mark 5B use the same disk modules, but record different data formats onto disk.

The Mark 5A system was placed into operation in 2003; ~ 100 Mark 5A units are now deployed worldwide and have largely displaced the Mark 4 and VLBA tape transports. Mark 5B is expected to be ready for deployment in late 2005. Complete information on the Mark 5 system is available on-line [Ref 1].

2. Mark 5A Data System

The primary characteristics of the Mark 5A data system (Figure 1) are:

- Direct plug-compatible replacement for 64-track Mark4 or VLBA tape drives
- Record/Playback at rates up to 1024 Mbps
- Two independent removable ‘8-pack’ disk modules per system that can be used in ‘ping-pong’ fashion for near-continuous recording
- Can record 8, 16, 32 or 64 tracks from Mark4 formatter (1024 Mbps max) or VLBA formatter (512 Mbps max)
- Parity bits are stripped before recording and re-inserted on playback
- Arbitrary mixing of modes (#tracks, data rate, bits/sample) is allowed, always using 100% of installed disk capacity

The Mark 5A is based on a standard PC platform with two specialized interface cards:

1. A high-speed 'StreamStor' disk interface card from Conduant Corporation which supports recording and playback at 1Gbps to/from a bank of 8 commodity IDE disks
2. A specialized VLBI interface card designed at Haystack Observatory which emulates the data interfaces of a Mark 4 or VLBA tape transport.

The Mark 5A system is now used routinely for both geodesy and astronomy VLBI experiments at data rates up to 1024 Mbps.

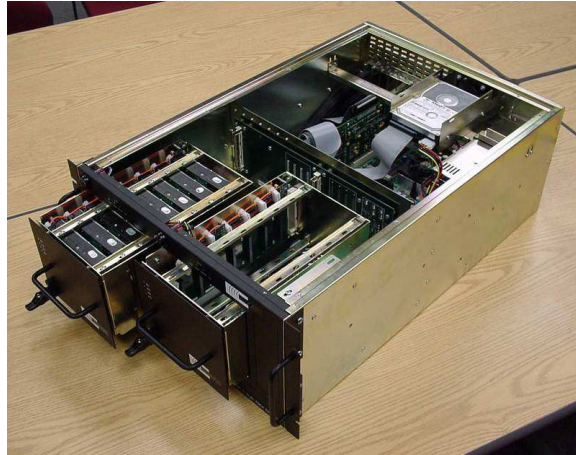


Figure 1. Mark 5A data system

3. Disk-Media Status

The original impetus for the development of the Mark 5 system, starting in 2001, was the rapidly falling price of disk storage and the expectation that disk storage would be less expensive than tape storage within a few years. Now, just four years later, these expectations have already been met and exceeded (see Figure 2):

- Hard disk price vs capacity/performance continues to drop
 - Now approaching $\sim \$0.50/\text{GB}$ and will continue to drop
 - (Mark 4/VLBA tape is $\sim \$2.00/\text{GB}$)
- 250 GB disks are now common
 - 8-disk module of 250GB disks is comparable to ~ 3.5 VLBA/Mark 4 tapes
- 400 GB disks are available
 - 8-disk module of 400GB disks is comparable to ~ 5 VLBA/Mark 4 tapes
- 700 GB disks expected by end 2005
 - 8-disk module of 700GB disks is comparable to ~ 9 VLBA/Mark 4 tapes; 2 modules will support ~ 24 hours @ 1 Gbps unattended!

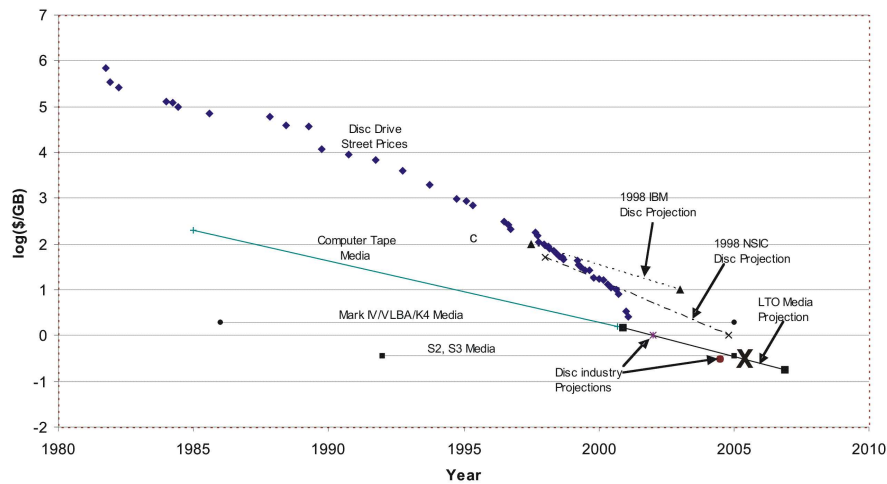


Figure 2. Comparison of disk and tape prices vs. time

Though disks have, by and large, been much more reliable than tape, disks are not completely problem-free:

- Based on statistics collected at Haystack, average disk drive failure rate is $\sim 0.5\%$ /year
- Failure rate of Hitachi 250GB has been higher than expected and Conduant recommends discontinuing their use
- Conduant has qualified drives from Maxtor, WD and Seagate and is shipping the following disks in assembled Mark 5 disk modules:
 - 400GB - Seagate
 - 250GB - Western Digital RAID Edition (high-reliability)
 - 250GB - Maxtor Maxline III (high-reliability)
- Disk reliability at high altitudes is under investigation. Most disks are specified to operate only to $\sim 3000\text{m}$ altitude

4. Mark 5A Software/Firmware Upgrades

The Mark 5A continues to be upgraded for both more capability and reliability. Some of the recent upgrades include:

- Improved capabilities to deal with bad or slow disks on both write and read
- Ability to recover from inadvertent operational errors using ‘recover’ command
 - recover data from interrupted recording
 - recover from accidental use of ‘sstest’ or ‘WRSpeed’ test programs

- recover data from accidentally erased module
- Support of ‘disk-FIFO’ mode up to 512Mbps
- Implementation of ‘disk state mask’ (being used by NRAO)
- Improved data-buffer handling for support of faster network transfers

Considerable effort has been expended to allow the Mark 5A to continue to operate with slow or bad disks. In particular:

- Record: Shift the writing load away from the bad disk(s) and continue writing on the good disks. In most circumstances, this will still allow the full data rate to be captured, but at a reduced disk-module capacity (since the storage of at least one disk is typically lost)
- Playback: Substitute a ‘fill pattern’ for data that is not received in a timely manner from slow or bad disks. This special fill pattern is recognized by the Mark 5A playback electronics and causes wrong parity to be inserted, which in turn invalidates the data to the correlator. Since data from all recorded channels are spread evenly over the disks, the loss on one disk drive typical means the loss of about 12.5% data from each channel, resulting in an SNR loss of $\sim 6\%$, which is usually tolerable.

5. Plans for Serial-ATA (SATA) Disk Support

IDE-interface disk drives (also know as Parallel-ATA or ‘PATA’) are being rapidly replaced in the marketplace by Serial-ATA (‘SATA’) disk drives. Currently, the Mark 5 supports only disk modules with PATA drives, but support for SATA disks is planned:

- PATA and SATA disk modules will be interchangeable in Mark 5 systems
- Biggest challenge was finding module SATA connectors with sufficient durability for many insertion/removal cycles
- Requires upgrade kit for current Mark 5 systems - new chassis backplane with separate connectors for PATA and SATA (same for both Mark 5A and Mark 5B)
- New SATA disk modules have been designed
- SATA disk module should be able to support 2048 Mbps in the future with Mark 5B, next-generation StreamStor board, and next-generation disk drives
- SATA module price will be about same as current module
- Expect SATA modules to be available late 2005; upgrade kit will be available from Conduant

6. Mark 5B Data System

The Mark 5B system is being designed to adhere to the VSI-H specification [Ref 2]. It is particularly attractive for new stations as it directly accepts sampler data without the need for an expensive external formatter. The Mark 5B system is being designed with the following characteristics:

- Full VSI compatibility

- Same chassis as Mark 5A; uses same disk modules; requires Mark 5B I/O card
- 1024 Mbps record/playback
- Plans for expansion to 2048 Mbps with next-generation StreamStor card using 64 MHz data clock
- Full e-VLBI capability
- Eliminates need for external formatters
- With a 14-BBC Mark4 or VLBA4 system, up to 1792 Mbps can be recorded with two parallel Mark 5B systems
- Requires sampler adapter for Mark 4/VLBA DASs to provide VSI-compatible output [but will not be needed when digital BBC's become available in the future]
- Station Unit capabilities for connection to Mark 4 correlators is being designed into Mark 5B
- Built-in phase-cal extraction and state counting
- Front-panel status display - 8 tri-color LEDs
- DIM and DOM capabilities are separate FPGA downloads
- FPGA is in-place programmable via software

7. Mark 5A/Mark 5B Compatibility

The Mark 5A records data in a parity-stripped version of the Mark 4 or VLBA tape format and is thus highly specialized. The Mark 5B, being governed by VSI specifications, is freed from the legacy constraints of magnetic tape and allows the adoption of a more logical data format on disk. Hence, the disk-data format of Mark 5A and Mark 5B are different. However, the Mark 5B data format has been designed in such a fashion that the Mark 5A can be upgraded to read Mark 5B data and produce VLBA-tape format data. This will allow correlators with only Mark 5A systems to still read and correlate Mark 5B data.

The upgrade of the Mark 5A system to read Mark 5B disks is a significant engineering task and can be avoided if correlators gradually upgrade their playback units to Mark 5B in step with the observing stations. It now appears likely that this may happen and the engineering expenditure to upgrade the Mark 5A system may be avoided.

8. Mark 5B Station Unit Capabilities

As indicated earlier, the Mark 5B playback system will support a mode of operation that emulates the Mark 4 Station Unit and allows the current Mark 4 Station Units on the Mark 4 correlators to be retired. Figure 3 shows a simplified block diagram of the Mark 5B Station Unit capability. A station-delay model is applied to the data during playback to the correlator; the delay model, as well as model phase and delay-rate are also inserted into the data stream and sent to the correlator.

A built-in phase-calibration tone extractor will analyze the amplitude and phase of up to 16 individual tones in each of up to 16 channels of data, and will also measure sample-state statistics to aid in proper correlation-amplitude normalization.

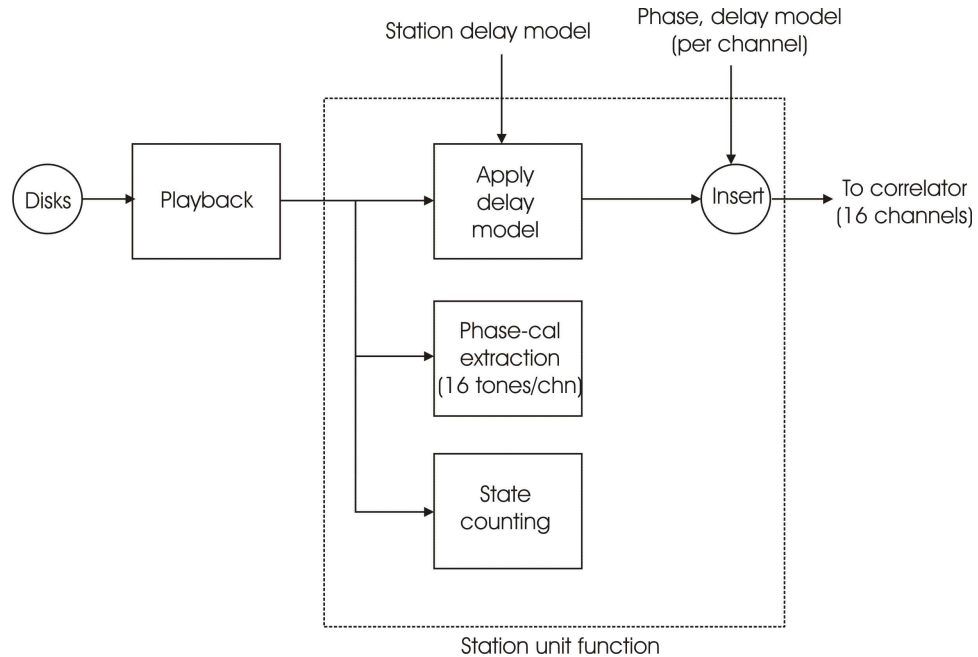


Figure 3. Simplified block diagram of SU function of Mark 5B

9. Mark 5B Status

As of this writing (May 2005), 3 prototype Mark 5B systems are under test. Checkout of the system is a lengthy procedure, particularly for the complicated Station Unit functionality. Though it is difficult to predict, we expect that checkout and interfacing to the Mark 4 correlator will require several months of effort.

Of course, considerable software development is also being undertaken to support Mark 5B, particularly with respect to support of the Mark 5B on the Mark 4 correlator.

Upon completion of the Mark 5B checkout, the design will be transferred to Conduant Corp for replication and sale. We expect the Mark 5B will be somewhat more expensive than the Mark 5A, but not substantially so.

Existing Mark 5A systems will be upgradeable to Mark 5B with the procurement of a Mark 5B I/O interface board to replace the Mark 5A I/O interface board. Of course, new support software will also be required, which will be available from the Haystack web site.

10. Mark 5B Interface Boards

A number of specialized interface boards are required to support the Mark 5B in a world largely populated by the remnants of legacy Mark 4 and VLBA data systems. In particular, four interface boards will be made available to ease the integration of the Mark 5B into the existing VLBI world:

- VSI-4 sampler adapter board
 - Will be mounted inside Mark 4 formatter to provide VSI interface to Mark 5B
 - Uses existing Mark 4 samplers and 1pps generator

- Supports 2 VSI output connectors at 1024Mbps each (though aggregate data rate is restricted to 1792 Mbps by availability of only 14 BBCs)
- Prototype boards ready for checkout
- VSI-C sampler adapter
 - Interfaces VLBA samplers to VSI
 - Designed at Metsahovi [Ref 3]; purchased from Metsahovi
- Correlator Interface Board (CIB)
 - Interface between Mark 5B and Mark 4 correlator
 - Currently in fabrication
- Upgraded Serial Link boards for Mark 4 correlator
 - Designed at MPI
 - Prototypes have been tested; replication underway at MPI

11. Summary

The Mark 5A and Mark 5B disk-based systems represent a new direction in VLBI data technology and have opened new capabilities for higher performance and lower cost than previous tape systems. Because these systems are based on technology that is rapidly developing due to the demands of the global marketplace, we can expect that performance and capabilities for VLBI will dramatically improve in the coming years.

12. References

1. Mark 5 information available at <http://web.haystack.edu/mark5/Mark5.htm>
2. VSI information available at “VLBI Standard Interface Specification - VSI-H,” August 2000, Revision 1.0, available from <http://web.haystack.edu/vsi/index.html>
3. VSI-C information available at <http://kurp.hut.fi/vlbi/instr/>

e-VLBI Development at Haystack Observatory

Alan R. Whitney

MIT Haystack Observatory

e-mail: `awhitney@haystack.mit.edu`

Abstract

Haystack Observatory is engaged in a multi-faceted e-VLBI development program. Real-time experiments using Mark 5A data systems and the Mark 4 correlator have been performed at sustained data rates up to 512 Mbps/station. Specialized algorithms and protocols for e-VLBI are being developed to take advantage of the unique characteristics of e-VLBI. Network performance monitoring tools have been developed. And research is being conducted using dynamically switched optical paths to provide wide dedicated pipes for e-VLBI data transmission. The biggest obstacles to widespread e-VLBI are limited connectivity of telescopes and time-varying end-to-end network performance.

1. Introduction

e-VLBI development has expanded rapidly over the past several years. At Haystack Observatory, a broad program of e-VLBI development is underway, including network strategy and protocol development, optically-switched network development, as well as both experimental and production e-VLBI data transfers. In this paper, we will briefly describe these areas of activity.

2. History of e-VLBI experimental developments

A brief accounting of e-VLBI milestones at Haystack Observatory may be instructive to understand the rate of progress in e-VLBI:

- October 2002:
 - Near real-time VLBI data transferred at ~800 Mbps between Mark 5P (prototype) system at GSFC/GGAO antenna and Mark 5P at Haystack Observatory
 - First intercontinental e-VLBI: Westford-Kashima at ~ 20Mbps
 - Real-time e-VLBI data transfer from GGAO to Mark 5P at Haystack observatory at 288 Mbps
- March 2003:
 - First e-VLBI ‘Intensive’ UT1 result in under 24 hours - Westford-Kashima
- March 2004:
 - First real-time e-VLBI experiment with Mark 5A: Westford-GGAO at 32 Mbps
 - First intercontinental real-time e-VLBI experiment: Westford-Onsala at 32 Mbps
- August 2004:

- Haystack link upgraded to 2.5 Gbps
- Real-time fringes at 128 Mbps, Westford and GGAO antennas, Haystack Correlator
- September 2004:
 - Real-time fringes at 512 Mbps, Westford and GGAO antennas, Haystack Correlator
- October 2004 - present
 - Regular transfers from Kashima ($\sim 300\text{GB}$ per experiment; $\sim 200\text{ Mbps}$)
- November 2004
 - Real-time e-VLBI demonstration at Super Computer 2004 conference (see Figure 1): Westford-GGAO at 512 Mbps; used DRAGON optically-switched light paths on part of network link
- February 2005
 - Real-time fringes Westford-Onsala at 256Mbps
 - Used optically-switched light paths over part of route
- Starting April 2005
 - First transfer from Tsukuba ($\sim 240\text{GB}$; $\sim 240\text{Mbps}$)
 - Preparing for CONT05 experiment in September 2005 (15 days continuously at 256 Mbps)

This succession of events shows the evolution of e-VLBI from short one-time experiments to actual productions transfers over a period of less than 3 years. Though this progress may seem impressive, there are still many problems to overcome before e-VLBI can become routine.

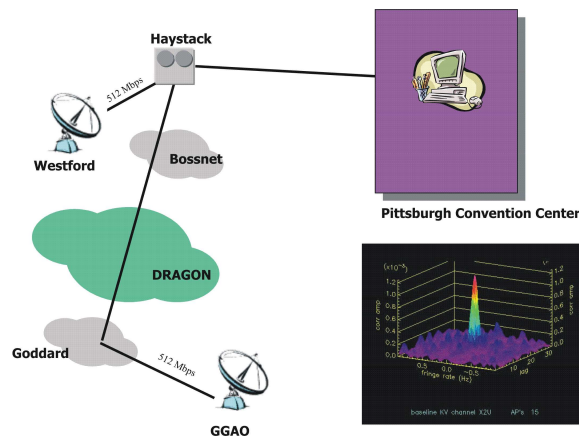


Figure 1. Real-time e-VLBI demo at Super Computer 2004 conference, Nov 2004

3. Challenges of e-VLBI

The list of challenges confronting routine widespread global e-VLBI is significant:

- ‘Last-mile’ connectivity to telescopes
 - Most telescopes are deliberately placed in remote areas
 - Major initiatives are in place in Europe and Japan to connect telescopes; U.S. is lagging
- End-to-end network performance is often well below advertised rates
- Performance of transport protocols
 - untuned TCP stacks, fundamental limits of regular TCP
- Throughput limitations of COTS hardware
 - Disk to/from Network
 - Real-Time data to/from network
- Complexity of e-VLBI experiments
 - e-VLBI experiments currently require significant network expertise to conduct
- Time-varying nature of network
 - R&E networks tend to be unstable, particularly towards end points

In the remainder of this paper, we will discuss these issues and the work at Haystack Observatory related to them.

4. Antenna Connectivity

The following list shows current and prospective high-speed IP network connectivity of the worlds VLBI antennas and correlators (geodetic sites are underlined):

- Current IP connectivity:
 - JIVE Correlator (6 x 1 Gbps)
 - Haystack Correlator (2.5 Gbps)
 - Kashima, Japan (1 Gbps)
 - Tsukuba, Japan (~250 Mbps)
 - GGAO, MD (10 Gbps)
 - Onsala, Sweden (1 Gbps)
 - Torun, Poland (1 Gbps)
 - Westerbork, The Netherlands (1 Gbps)
 - Westford, MA (2 Gbps)
 - Jodrell Bank (1 Gbps?)
 - Medicina (1 Gbps - summer 2005)

- Arecibo, PR (155 Mbps)
- Wettzell, Germany (~30 Mbps)
- Kokee Park, HA (nominally ~30 Mbps, but problems)
- TIGO (~2 Mbps)
- In progress:
 - Hobart - agreement reached to install high-speed fiber
 - NyAlesund - work in progress to provide ~200Mbps link to U.S. as part of NASA/NOAA initiative

Considerable effort is now being expended to connect most of the remaining antennas and correlators, but connections can be quite expensive and are often limited by budgetary resources. One major unconnected resource is the VLBA array of ten 25m antennas.

5. e-VLBI Standardization (VSI-E)

In 1999 a VLBI Technical Working Group was established to develop interface standards for VLBI. The TWG was created as a joint effort under the sponsorship of the Global VLBI Working Group, representing astronomy interests, and IVS, representing geodetic interests. The charge to the TWG was to define a standard interface to and from a VLBI Data Transmission System (DTS) that allows heterogeneous DTSs to be interfaced to both data-acquisition and correlator systems with a minimum of effort. The result of this effort is the VLBI Standard Interface (VSI) specification, which is now being widely adopted [Ref 1].

The VSI specification was originally confined to the local hardware and software interfaces of the DTS, resulting in the VSI-H and VSI-S specifications, respectively. These VSI-H and VSI-S interfaces are shown schematically in Figure 2, showing a Data Input Module (DIM) and Data Output Module (DOM) as connected by an unspecified data-transmission media and data format. VSI-H deals only with the input and output hardware interfaces of the DTS and says nothing about the internal workings of the DTS, including the media or data formats. With the advent of e-VLBI, however, it became clear that a specification for electronic data transmission between the DIM and DOM was necessary to insure efficient electronic transfer of VLBI data between the heterogeneous DTSs; thus was born the VSI-E specification.

Though the VSI-E specification is not yet complete, significant progress has been made. The well known and mature RTP protocol has been chosen as the basis for VSI-E. Among the reasons are:

- RTP allows the reuse of many standard monitoring and analysis tools
- RTP is seen as internet-friendly by the network community:
- Attention to efficiency: protocol designed to have minimum overhead for in-band data
- Attention to resource constraints: won't use up all your bandwidth with control information
- Attention to scaling issues
- Allows choice of underlying transmission protocol (TCP, UDP, UDT, FAST, etc)

In addition, the RTP data transmission is controlled by an independent low-data-rate Real-Time Control Protocol (RTCP) stream that provides many additional features useful to e-VLBI:

- Dissemination of session information
- Monitoring of network and end system performance (by participants and third parties)
- Adaptation to varying network capability and performance
- Appropriate reliability and repair model
- Message Sequencing and reordering
- Multi-cast distribution of statistics, control and data
- RTCP streams occupies $<5\%$ of bandwidth of RTP data stream

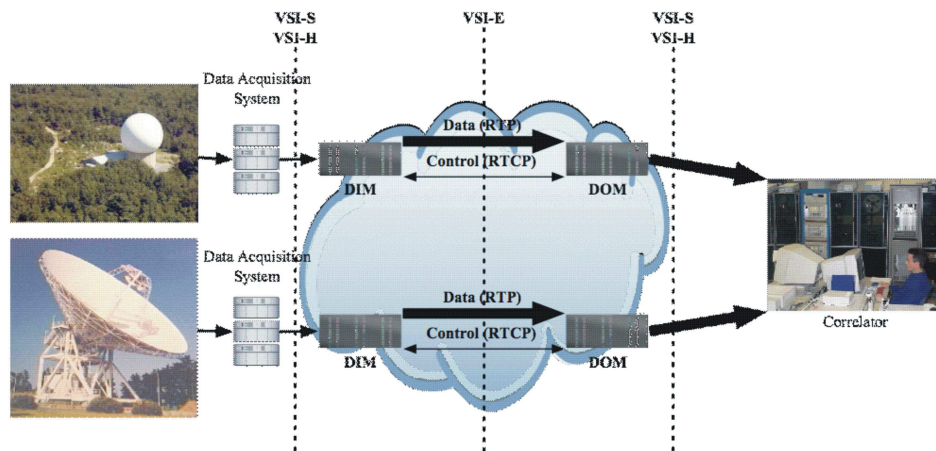


Figure 2. VSI-E architecture

A reference implementation of the draft VSI-E specification has been written by Dr. David Lapsley at Haystack Observatory and is now available for testing; preliminary tests have achieved Haystack-Tokyo data transfer rates in excess of 940 Mbps on a Gigabit Ethernet link. The TWG hopes to finalize and ratify the VSI-E specification before the end of 2005.

6. Throughput Limitation of COTS Hardware

Though the Mark 5 VLBI data system can record and playback at 1 Gbps, it is surprisingly difficult to manage those same data rates to/from network connections. The bottleneck for the Mark 5 and other PC-based systems is usually the PCI bus. Despite the PCI specification that implies data transfer rates of up to $\sim 4\text{Gbps}$ (64bit/66MHz), in practice it is quite difficult to achieve these rates. Additionally, in most systems, including the Mark 5, data must make two passes on the PCI bus, once to/from the network interface and once to/from the data source/sink; this imposes a severe penalty on performance.

Routine operation at 512 Mbps is readily achievable with today's systems, but operation at 1024 Mbps is difficult. In laboratory tests at Haystack Observatory using high-end PC motherboards

with dual bonded Gigabit Ethernet links, data transfer rates of up to ~ 1280 Mbps have been achieved. To date, however, these rates have not yet been achieved in practical e-VLBI experiments.

A new generation of PC motherboards is now appearing which replace the PCI bus with the PCIExpress bus. This high-speed serial bus promises much higher speed operation and should allow routine operation of e-VLBI at rates exceeding 1 Gbps.

7. Intelligent e-VLBI Applications

Based on observed usage statistics of a typical R&E backbone, such as the NSF 10 Gbps Abilene backbone network in the U.S., it is clear that there is much unused capacity. e-VLBI data has some unique qualities that may allow e-VLBI to effectively use some or much of this unused ‘secondary’ network capacity. Special characteristics of e-VLBI that might be taken advantage of include:

- Ability to tolerate some loss of data (up to $\sim 5\%$ or so) in many cases
- Ability to tolerate delay and jitter in data transmission, which can normally be accommodated by large buffers at both transmitting and receiving end

The challenge is to structure e-VLBI network usage so that it can efficiently make use of excess network capacity without interfering with ‘normal’ users. The ‘Experiment Guided Adaptive Endpoint’ (EGAE) is designed to meet this challenge. With funding from the U.S. National Science Foundation, Haystack Observatory is developing the EGAE strategy to make use of “scavenged”, low priority bandwidth to transport e-VLBI data.

Figure 3 shows a simplified block diagram of the EGAE strategy. EGAE performs dynamic adaptation based on a simple high-level description of experiment requirements and the surrounding environment, expressed in language appropriate to the scientific end-user. These requirements are then translated by an application-specific translator into specific network requirements. EGAE controllers at both the network data and control planes gather information and react to network conditions by altering the data flow between the DIM and DOM so as to be a ‘friendly’ user on the network, specifically lowering data rates quickly when higher priority ‘primary’ users demand network bandwidth.

The RTP/RTCP protocol chosen for VSI-E is particularly well-suited to use in the EGAE environment due to the statistical richness of the information it provides to user endpoints.

8. Haystack Production e-VLBI Facility

A simple prototype EGAE implementation is now being used at Haystack Observatory for non-real-time production e-VLBI data transfers (see Figure 4). Typically, about three 24-hr data sets per month from Kashima or Tsukuba are now transferred through this facility, with a typical volume of data around 300 GB/session; we expect usage to ramp up in the near future.

The equipment dedicated to the ‘Production e-VLBI Facility’ includes:

- Two high speed servers for the transfer and conversion of data
 - Turtle (1.266 GHz Intel Pentium III Dell PowerEdge 2500)
 - Enterprise (a dual 2.4 GHz Xeon Dell PowerEdge 2600)

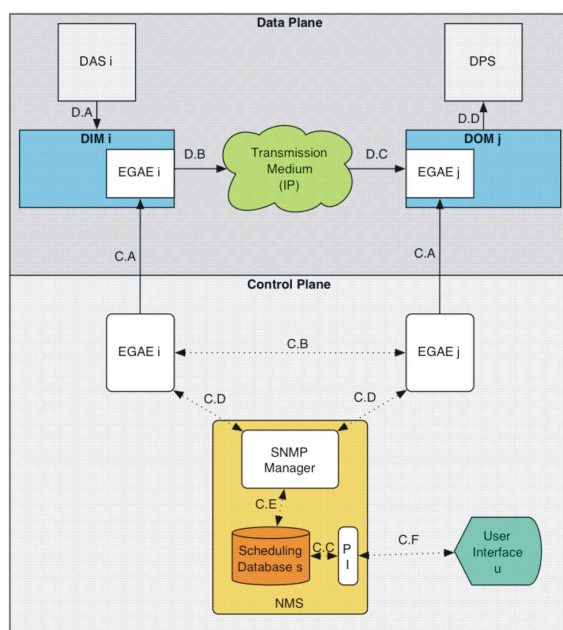


Figure 3. Block diagram of EGAE implementation

- Two 1.0 TB Lacie Bigger Extreme Firewire 800 external hard drives for the temporary storage of data
- A Mark5 for the transfer of data from system disk to Mark5 disk pack
- 3 Dell PowerConnect 5224 Managed Ethernet Switches

After data are collected at Kashima and Tsukuba (both in Japan) on K5 systems, automated procedures are executed to transfer, verify, convert to Mark 5 format, and transfer the data to Mark 5 disk modules [Ref 2]. The process has been structured in a very modular manner to easily accommodate transfers between both heterogeneous and homogeneous data systems. Currently, the system uses ‘bbftp’ for data transfer, but in the near future will be converted to VSI-E. .

9. Automated Network Monitoring

As our work in developing e-VLBI has progressed over the past several years, it has become increasingly evident that it was not possible to trust that a network connection would be there when it is needed. Painful experience taught us that successfully testing a network one week and then trying to use it the next week (with no intervening testing) was, too many times, a recipe for disaster. In the world of shared R&E connections, which e-VLBI largely inhabits, it is not possible to guarantee that network conditions will stay the same from one day to the next or one week to the next.

As a result of this experience, the need for continuous or semi-continuous monitoring became increasingly important. Such automated monitoring both enables the easy identification of bottlenecks (whether a hardware fault or a configuration change), as well as a view of network throughput variations over time. Properly implemented, such a system allows an overview of network behavior



Figure 4. Haystack Observatory ‘production’ e-VLBI facility

at a glance.

A network monitoring system has been developed at Haystack Observatory to meet this need and has the following characteristics:

- Periodic monitoring and logging of:
 - Network performance
 - Configuration of end systems
 - State of end systems
- Built on standard monitoring tools (iperf, nttcp, etc) to provide a single, coherent view of the e-VLBI network state
 - Maintains continuous state monitoring of the entire e-VLBI system
 - Essential for being able to identify issues with network/end system configuration
 - Allows diagnosis at-a-glance

In order for the monitoring data to be of most use, it must be easily accessible to the user. For this purpose, a ‘Network State DataBase’ (NSDB) was constructed that allows instant access and easy interpretation of all the data collected by the monitoring system. A simplified block diagram of the NSDB is shown in Figure 5. Data are collected from the network, performance monitoring, and e-VLBI layers to form a composite picture of network conditions. These data are collected in the NSDB at a central location for easy access.

To make use of the data in the NSDB, a web-based ‘e-VLBI Weather Map’ was constructed, an example of which is shown in Figure 6. By clicking on any gray diamond associated with a

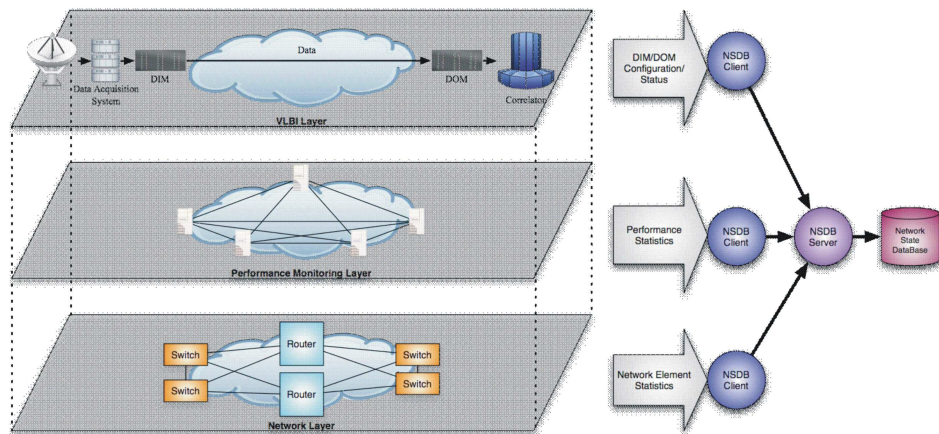


Figure 5. NSDB architecture

particular network link, the history and current performance of that link is displayed. Figure 7 shows the result of clicking on the gray diamond between the ‘ISI-E/Max Network’ and the ‘Juniper WASH’, which show the traffic on the Abilene network at the ISI-E/MAX POP near Washington, D.C.

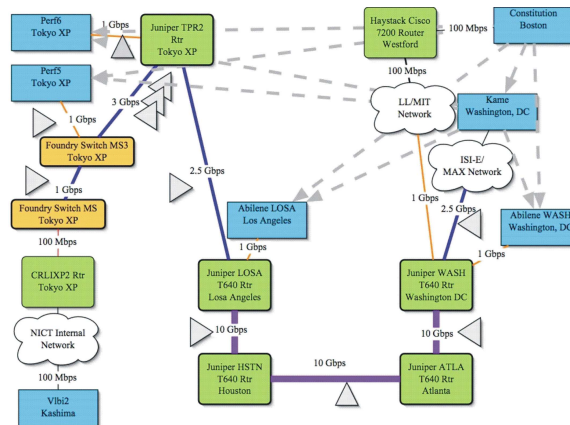


Figure 6. e-VLBI ‘Weather Map’

This type of network monitoring needs to be extended to a global basis before e-VLBI can become truly operational. Other communities, such as the high-energy physics community, are also working on such monitoring systems. In the long term, it seems likely to be of mutual benefit to adopt a single international standard for this type of network monitoring.

10. Dynamically Optically-Switched Light Paths

Haystack Observatory is collaborating with the University of Maryland and others in the DRAGON (Dynamic Resource Allocation via GMPLS Optical Networks) project, under spon-

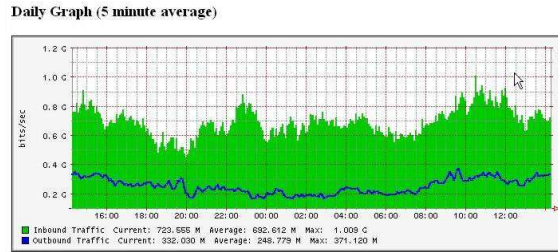


Figure 7. Example network statistics from one network link in the e-VLBI Weather Map

sorship of the National Science Foundation. The objective of the DRAGON Project is to create dynamic and deterministic end-to-end network transport services for high-end e-Science applications, and is concentrating on on-demand creation and teardown of optically-switched light paths. This type of network conditioning is made possible by two fairly recent technological breakthroughs:

1. Dense wave-division multiplex (DWDM) technology, which allows many (more than 100) individual wavelengths to be placed on a single fiber, each capable of carrying at least 10Gbps of data.
2. Optical switches capable of switching individual wavelengths among an array of fibers.

These two capabilities, working together, allow the dynamic creation and teardown of all-optical high-bandwidth paths on user demand. Because the switching is all-optical, expensive routers and switches, which must convert from optical-to-electrical-to-optical, can be eliminated or minimized.

Haystack Observatory is working with the DRAGON project to develop software application interfaces applicable to e-VLBI and other applications that might benefit from this technique. Ultimately, the DRAGON project may allow e-VLBI data to/from Haystack Observatory to be routed entirely (or at least mostly) optically to/from the Abilene backbone network in the U.S. This work will be fully integrated with the EGAE project described above.

11. Summary

Though e-VLBI has been developing rapidly over the past few years, much more work needs to be done before it can become truly operational. This includes not only some of the areas we have described here, but must include others as well. For example, as more high-bandwidth applications compete for limited network bandwidth, bandwidth-reservation systems and direct optically-switched paths become attractive. Many groups in several countries are working on these problems, and e-VLBI will be truly successful only with the close international collaboration of the VLBI and global networking communities.

12. References

1. VSI information available at “VLBI Standard Interface Specification - VSI-H,” August 2000, Revision 1.0, available from <http://web.haystack.edu/vsi/index.html>
2. Mark 5 information available at <http://web.haystack.edu/mark5/Mark5.htm>

The Bonn Astro/Geo MK IV Correlator

Walter Alef¹, Arno Müskens¹

¹) *Max-Planck-Institute for Radioastronomy*

²) *Geodätisches Institut der Universität Bonn*

Contact author: *Walter Alef*, e-mail: `walef@mpifr-bonn.mpg.de`

Abstract

The Bonn MKIV VLBI correlator is operated jointly by the MPIfR and the GIUB in Bonn, and the BKG in Frankfurt. A short overview of the correlator status and recent developments is given. Present and future developments important for the processing of geodetic and astronomical data are discussed. The present efficiency of geodetic correlation and the processor load are shown.

1. Introduction

The Bonn MKIV correlator is hosted at the Max-Planck-Institut für Radioastronomie (MPIfR)¹, Bonn, Germany. It is operated jointly by the MPIfR and by the Bundesamt für Kartographie und Geodäsie (BKG)² in cooperation with the Geodätisches Institut der Universität Bonn (GIUB)³. It is a major correlator for geodetic observations and MPIfR's astronomical projects.

2. Correlator Status and Recent Developments

Nine of the 16 station inputs of the correlator are in use at present. The nine station units, which interface the playback units to the correlator, are connected to eight Mark 5s and nine tape units in parallel. The operator can easily and flexibly configure the correlator for Mark 5 and/or tape playback. Data from 32 tracks can be played back per station in one pass. Mark 5 recordings with 64 tracks can be correlated in one pass, too, by physically changing cables from a tape unit to the corresponding Mark 5 unit.

One of the nine station units is more prone to the typical stability problems which can corrupt correlated data primarily in modes with channel data rates of 32 Msamples/s, limiting the correlator to 8 stations for some observations. The data quality from Mark 5 units is nearly perfect, the tape units deliver good data quality. Occasionally thick tapes from the very few remaining MK III stations has to be correlated. Synchronization of Mark 5 units is nearly instantaneous, tapes need less than 10 seconds.

Observations with bit-rates up to 1 Gbit/s have been correlated successfully with up to 8 stations simultaneously; such observations can only be recorded with Mark 5 systems. 512 Mbit/s observations using tape recordings from VLBA antennas and Mark 5 from European stations are the standard mode of the newly formed global mm-array, whose observations are correlated on the Bonn MKIV correlator. In this mode VLBA antennas record 512 Mbit/s on two tapes simultaneously, and as a consequence the correlation has to be done in two passes. The data can later

¹http://www.mpifr-bonn.mpg.de/div/vlbicor/index_e.html

²http://www.ifag.de/index_english.htm

³<http://www.gib.uni-bonn.de>

be combined in NRAO's AIPS software to form the full cross-spectrum from the two passes. The most recent observations of the global mm-array with 8 antennas of the VLBA and 5 European stations have been recorded solely on disks and are awaiting correlation in Bonn.

The biggest spectral line observation so far was processed recently. One frequency channel with both left and right circular polarization was correlated from 12 stations in 3 passes with 512 lags and 1.2 seconds pre-averaging time. The total volume of correlated data was nearly 50 Gbytes. Fringe-fitting and exporting to AIPS took on the order of two weeks and created an intermediate data set of 200 GB. To efficiently correlate this observation, special correlator and station unit modes had to be designed by K. Dudevoir of Haystack Observatory.

Near real-time fringe tests have been done a few times up to now, mostly to verify the setup of European stations for 3mm-VLBI. Unfortunately the MPIfR is still only connected with 4 Mbit/s to the Internet, so that the data of 30 seconds of observation (= 1.8 GB per station) takes several hours to transfer. It is expected that the institute will be connected to the Internet with 100 Mbit/s in late spring with the option to upgrade to a dedicated fibre for eVLBI.

About 110 8-packs with a total capacity of 175 TB have been assembled at MPIfR up till now, of which 100 packs with 150 TB are the property of MPIfR. Our experience with disk quality and reliability is very mixed. Typically the first batches of disks we bought were of good quality, while when disks became cheaper the quality seemed to drop as well. An exception was a batch of 200 GB Western Digital disks where the first and only batch of 100 disks had a failure rate of nearly 10%. At present we are testing and conditioning 12 8-packs with 400 GB Hitachi disks. So far the results with those disks look promising.

We have successfully played back a few 8-packs with a defective disk. The later versions of the Mark 5A software perform fairly reliably in these cases. Just a few days ago we were able to check a new feature which allows recovery of all the data on a disk-pack which had accidentally been erased with a `reset=erase` command.

3. Geodetic Correlation Status

Our experience from the last 12 months shows that the Mark 5 system has made VLBI data recording and correlation significantly more robust. Both geodetic and astronomical VLBI observing profit from the higher throughput. The correlation process is smoother and faster than with tapes, for which the correlation is often interrupted by time-consuming tape positionings and manual track searches.

To improve the monitoring of the Terrestrial Reference Frame (TRF), the IVS Observing Program Committee (OPC) decided to enlarge the T2 sessions to as many as 16 stations. On the correlator side a 16 stations experiment requires several passes. With a maximum of 8 to 9 stations for every processor run these experiments can be handled in five passes. Baseline repetitions are inevitable, but can be used as a correlation check. (for more details see the IVS-Newsletter, Aug. 2004, p. 6).

For IVS-R1 experiments the processing factor could be improved during the last year. More and more network stations are replacing their old tape recording systems and now operate with Mark 5 recorders. In March 2005 Gilcreek upgraded from tape to disk recording as one of the last network stations in the IVS-R1 series. Now we are able to process an R1 observation in about 24 hours, comparable to the experiment duration. This corresponds to a processing factor of around one — the processing wall-clock time on the correlator over the observe time. Pre- and

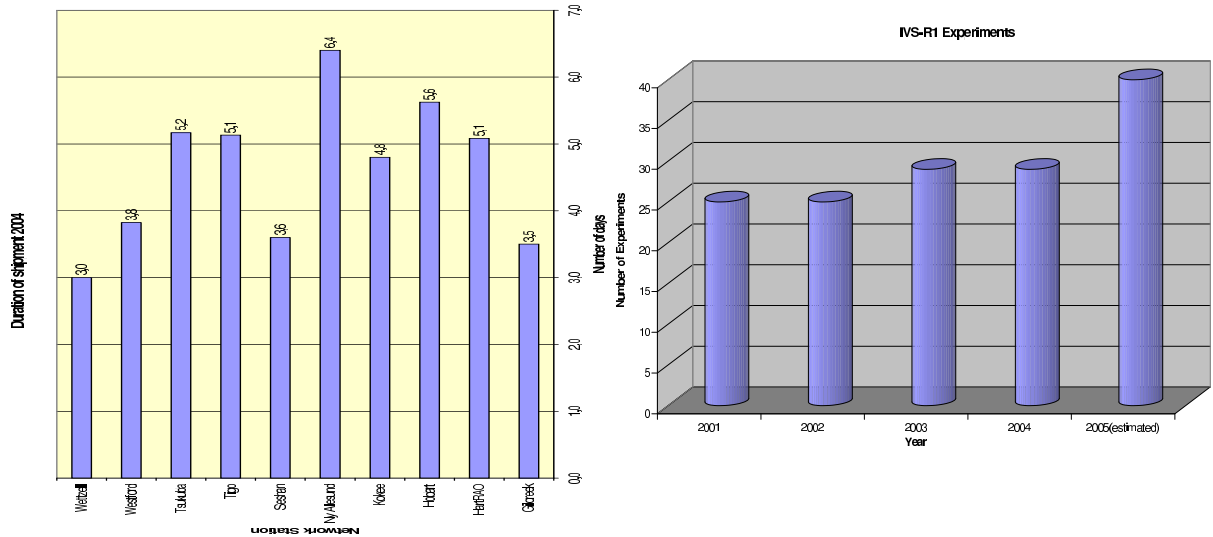


Figure 1. (left) average duration of shipments for R-1 observations in 2004 (right) increase of R-1 experiments over the last years

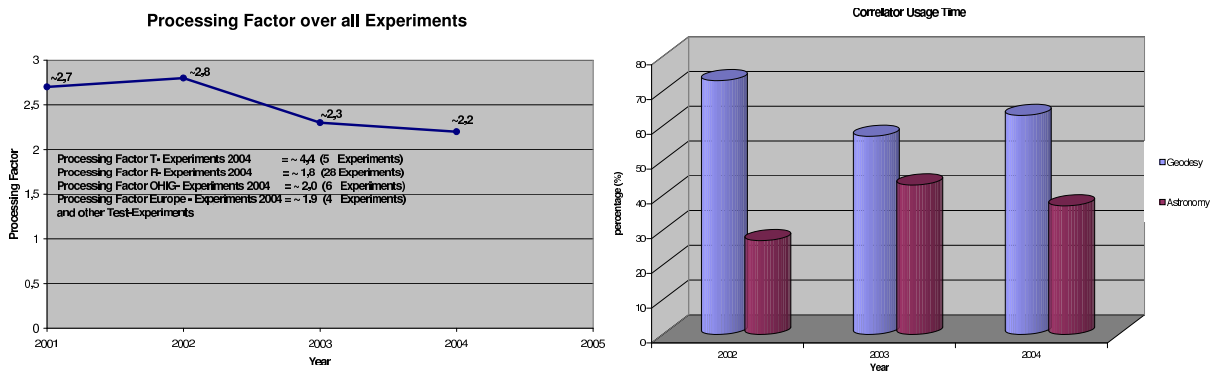


Figure 2. (left) over all experiment processing factor (PF) at Bonn (right) correlator usage time in the last years

post-processing with fringe search, correlator control file setup, fringe-fitting, data analysis and subsequent re-correlation or re-fitting of the correlated data are not included. The improvement of the processing factor allows an increase of the number of IVS-R1 experiments to be correlated at Bonn. In 2005 around 30% more R-1 experiments will be processed at Bonn than in previous years.

The duration of disk/tape shipments from network stations to the correlator center is unchanged compared to previous years. The viewgraph shows the shipping times of some of the stations participating in R1 experiments. Stations which are most distant or are in very extreme locations need the longest time to ship media to the correlator center. Ny Ålesund (Norway/Arctic) is a good example for a European station, where we have sometimes critical weather conditions which can delay shipments. Tigo (Chile) with complicated transport procedures and unreliable infrastructure is another example. All stations are working hard to try to decrease the shipment time, but only eVLBI might eventually solve all the shipment problems so that R1 observations could be correlated within 24 to 48 hours after the observations.

The world-wide supply of Mark 5 modules for geodesy is the main subject of the regular shipment teleconferences of the correlator centers under the auspices of the IVS. The aim is to guarantee a safe supply with Mark 5 modules of the appropriate sizes to all network stations.

The overall load of the Bonn correlator has not changed significantly in the past years. In spite of the official 50 to 50% usage time, the geodetic experiments make use of around 60%. In 2004 around 50 geodetic experiments of type IVS-R1, IVS-T2, Europe and IVS-OHIG were correlated in Bonn. For 2005 we expect the same number, but will have some changes in the different experiments types.

4. Upgrade Plans

BKG and MPIfR have agreed to upgrade the correlator to 12 stations in the course of 2005. This will technically be feasible with Mark 5B units which will have a built-in station unit. The old station units will be decommissioned together with the tape drives probably within the next two years.

The project foresees purchase of four Mark 5Bs and an upgrade of the present eight Mark 5A units. The time-line for the upgrades of the Mark 5As will have to be synchronized with the introduction of Mark 5B systems in the field, as Mark 5B units will not be able to play back Mark 5A recordings.

MPIfR has developed a new version of the serial links which are used to send the data from the station units to the correlator via high-speed data lines. In addition a new correlator control computer and upgrades to the correlator software will be required for which we will have to rely on Haystack Observatory.

An FX software correlator based on Matlab

Thomas Hobiger ¹, Tetsuro Kondo ²

¹⁾ *Institute of Geodesy and Geophysics, University of Technology, Vienna*

²⁾ *Kashima Space Research Center, NICT*

Contact author: Thomas Hobiger, e-mail: `thobiger@mars.hg.tuwien.ac.at`

Abstract

Normally data obtained by very long baseline interferometry (VLBI) are correlated by designated processors containing wired logic components. Additionally, several software correlators, which are able to do the same tasks, were designed in the last years. These software systems are more flexible and can be adopted easier for special tasks than hard-wired correlators. Usually such systems are coded in Assembler, Fortran or C/C++ in order to gain maximum speed. We have chosen MatlabTM6.5, a commercial mathematical software package, to implement an FX correlator including single band delay search. Functionality is similar to IP-VLBI(K5/VSSP) software correlator, developed at Kashima Space Research Center, NICT, and other data formats (Mark5) can be analyzed using conversion tools. The software correlator presented here is not able to provide high data throughput but development and debugging times were much less than with other programming languages.

1. The MatlabTMFX correlator

Starting with the existing K5/VSSP correlation software [1] we have tried to implement the FX correlation engine completely in Matlab. Additional modules were created to perform residual delay and rate search at single band and to provide graphical output for fringe checking and quality control. At the moment apriori files have to be created by program parts from the K5/VSSP software package. According to table 1 several sampling modes as provided by the PCI sampler board (figure 1) are already supported and automatically detected. A graphical user interface (figure 2) can support the user when setting the parameters for correlation runs.

channels	1, 4
quant. levels	1,2,4,8 (bit)
sampl. freq.	40kHz, 100 kHz, 200 kHz, 500 kHz, 1 MHz, 2 MHz 4 MHz, 8 MHz, 16 MHz

Table 1. Capabilities of FX correlator according to K5/VSSP specifications

A graphical user interface (figure 2) can support the user when setting the parameters for correlation runs.

As MatlabTM is optimized to deal with vector data lots of the routines were coded to take advantage of this logic. Loops were avoided whenever possible, but there are still some modules where processing speed can be gained. Table 2 summarizes the supported settings to run FX correlation engine. After correlation is finished a fringe plot for easy fringe checking is created and



Figure 1. PCI sampler board for IP-VLBI system and an auxiliary board for 4 ch inputs

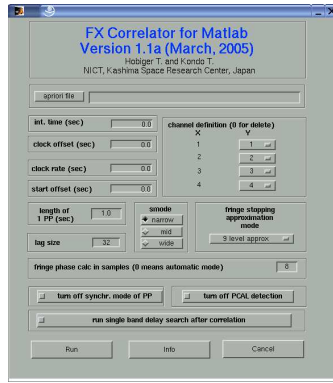


Figure 2. GUI to run FX correlator

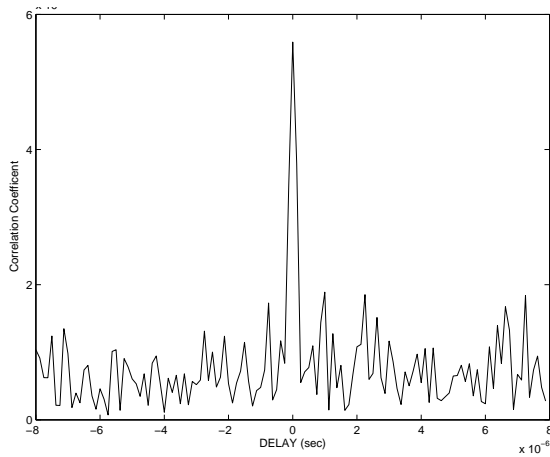
output files containing real and imaginary parts of the correlation function are stored in text files. This output can be used to perform residual delay and rate search at single band and to create the necessary input for band width synthesis, which is not implemented now using MatlabTM.

parameter period length	any
search modes	1000, 2000, 10000, 20000 data points
fringe stopping approx.	exact, 2, 3 ,9 levels
lag size	any
correlation between different BBC	possible
phase cal.	can be turned on/off

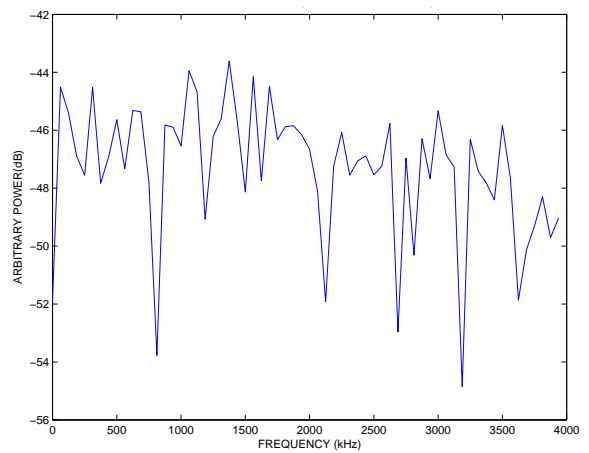
Table 2. Features of the FX correlator

2. Sample outputs

Two different data-sets were analyzed and the obtained plots are presented here. Figures 3 and 4 correspond to a 20 seconds scan of 3C273B at 8209.99 MHz on the baseline Kashima 11m - Tomakomai 11m with 1 bit sampling and a video band width (VBW) of 4 Mhz (sample data 1). Figures 5 and 6 correspond to an observation of Geotail spacecraft made at 8473.6 MHz on the baseline Kashima 34m - Koganei, using 2 bit sampling, a VBW of 2 MHz and a total scan lengths of 109 seconds (sample data 2).

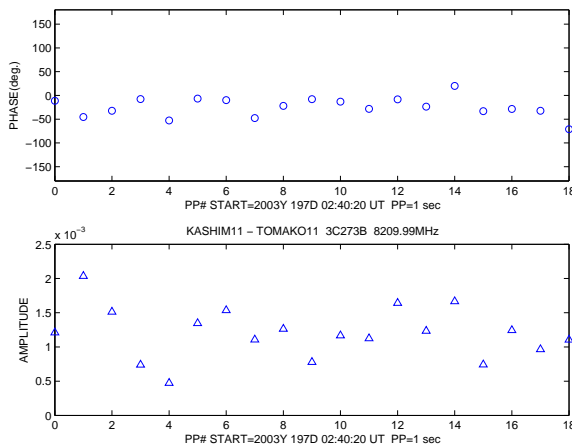


Correlation function from sample data 1

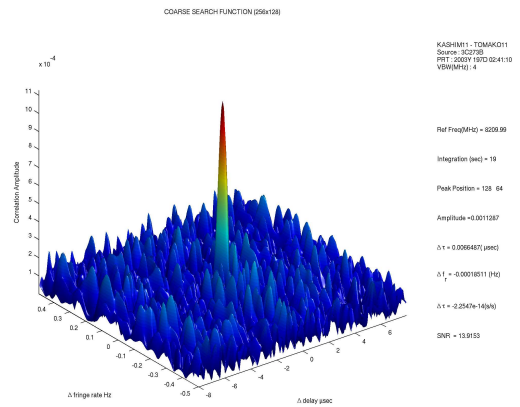


Cross spectrum from sample data 1

Figure 3. Correlation function and cross spectrum from dataset 1

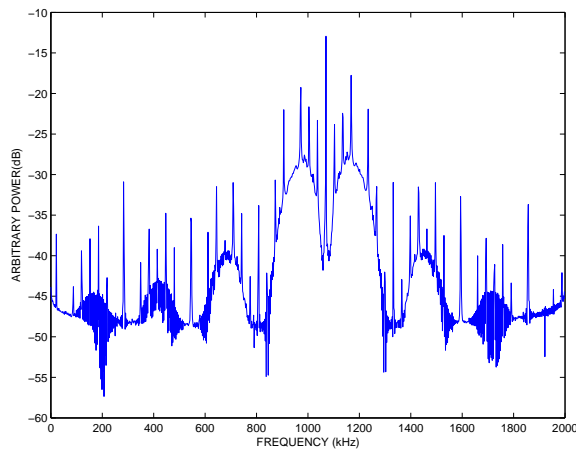


Phases and amplitudes from sample data 1

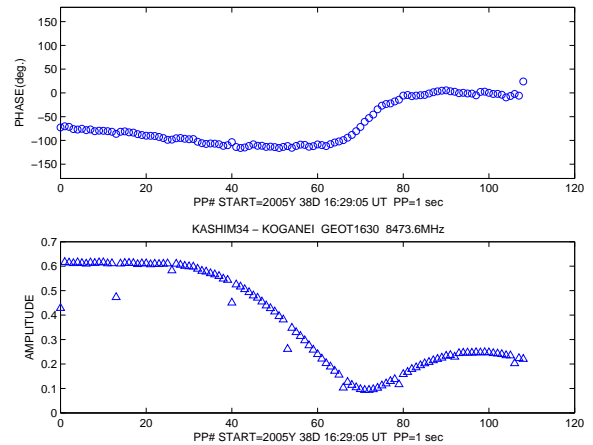


Coarse search function from sample data 1

Figure 4. Phases, amplitudes and coarse search function from dataset 1



Cross spectrum from sample data 2



Phases and amplitudes from sample data 2

Figure 5. Cross spectrum, phases and amplitudes from dataset 2

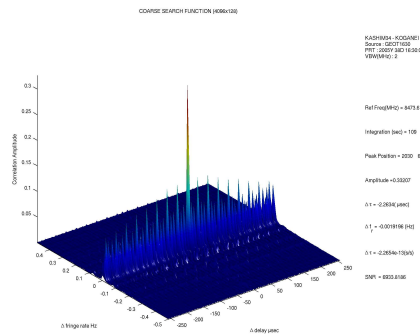


Figure 6. Coarse search function from sample data 2

3. Processing speed

The processing speed of MatlabTMFX correlator is about 10-100 times slower than the corresponding K5/VSSP software correlator. Throughput was measured for different lags and is plotted in figure 7.

4. Conclusions and future plans

We have shown that it is possible to code a software correlator using a high level programming language within very short time. In near future we will run our software under MatlabTM7.0 to take advantage of the FFTW package. Furthermore several parts of the code should be changed to gain more speed from vectorizing. If calculation of apriori delays and band width synthesis are implemented too, our software is able to provide geodetic observables from raw data .

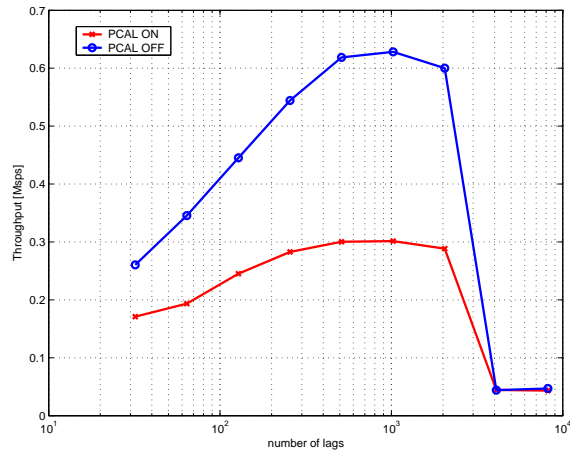


Figure 7. Performance for several lag sizes in Mbps

5. Acknowledgments

The authors want to thank the Japanese Society for the Promotion of Science, JSPS (project PE 04023) and Kashima Space Research Center, NICT for supporting this work.

References

- [1] Kondo T., Y. Koyama, and H. Osaki, “Current Status of the K5 Software Correlator for Geodetic VLBI” IVS CRL-TDC News No. 23, pp.18-20, 2003

Recent Results from the EVN MkIV Data Processor at JIVE

Robert M. Campbell

Joint Institute for VLBI in Europe

e-mail: `campbell@jive.nl`

Abstract

Recent achievements at the EVN MkIV data processor at JIVE include decreasing the read-out time for the whole correlator to 1/4 s (or 1/8 s for half the correlator), developing new astronomical capabilities (*e.g.*, oversampling to $\times 4$, wider-field mapping), and strengthening liaison procedures with PIs (*e.g.*, pipelining, the EVN Archive). Disk-based EVN recording and regular incorporation of FTP fringe-checks are now standard practice, resulting in more reliable data quality. Progress towards real-time *e*-VLBI is underway — so far culminating in 3 real-time science experiments since last autumn.

1. Background

A key item in the MkIV upgrade of the EVN was the construction of the EVN MkIV data processor at the Joint Institute for VLBI in Europe (JIVE). JIVE is hosted by ASTRON in Dwingeloo, the Netherlands, and is funded by science councils of a number of European countries. Special projects have been funded directly by the European Commission. The EVN MkIV data processor [1], [2] was constructed in the context of the International Advanced Correlator Consortium through which the other MkIV correlators were also built, with significant contributions from European partners.

The EVN MkIV data processor had its first fringes on 21 July 1997 and its official inauguration took place on 22 October 1998. We now correlate the vast majority of astronomical EVN experiments, and about half of the global experiments. Altogether, we have processed 210 user and 130 network/test experiments as of 17 May 2005.

This report discusses the capabilities of the correlator system, quickly overviews operations and data flow, and looks towards the future of *e*-VLBI. It concentrates on new features since the Leipzig meeting, illustrated with various milestones achieved along the way. More information about the EVN and JIVE can be found in the websites www.evlbi.org and www.jive.nl.

2. Current Capabilities

The EVN MkIV data processor can correlate simultaneously up to 16 stations with 16 channels per station, each having a maximum sampling rate of 32 Ms/s (thus a total of 1 Gb/s per station for 2-bit recordings). The correlator houses 32 MkIV boards.

2.1. Features Snapshot

The EVN MkIV data processor can currently correlate/provide:

- 1- and 2-bit sampling (all but a handful of experiments use 2-bit sampling).
- MkIII, MkIV, VLBA, and Mk5(A) recordings.

- sustained 1 Gb/s Mk5 recordings, or 512 Mb/s tape recordings, in one pass.
- parallel- and cross-polarization products as desired from dual-polarization observations.
- up to 2048 frequency points per interferometer (see the discussion following equation 1 below).
- full-correlator integration times down to 0.25 s (half-correlator t_{int} down to 0.125 s).
- oversampling at 2 or 4 times the Nyquist frequency in order to provide subband bandwidths down to 500 kHz (the maximum Nyquist-sampled BW_{sb} is 16 MHz).
- multi-pass correlation (*e.g.*, for observations having >16 stations at any given time).
- an improved 2-bit van Vleck correction that accounts for the statistics of high/low bits for each channel’s data stream from each station.

Capabilities whose development is still underway include pulsar gating, speed-up, and phase-cal extraction. Capabilities that are yet to come include sub-netting (although we can manually handle reasonably straightforward instances) and recirculation (achieving greater equivalent correlator capacity, through a time-sharing scheme, for observations that don’t use the maximum BW_{sb}).

2.2. Correlator Capacity

The total correlator capacity can be expressed as:

$$N_{\text{sta}}^2 \cdot N_{\text{sb}} \cdot N_{\text{pol}} \cdot N_{\text{freq}} \leq 131072 \quad (1)$$

Here, N_{freq} is the number of frequency points per interferometer (baseline/subband/polarization). N_{pol} is the number of polarizations in the correlation (1, 2, or 4). N_{sb} represents the number of different subbands, counting lower- and upper-sidebands from the same BBC as distinct subbands. The value to use for N_{sta} is “granular” in multiples of 4: *e.g.*, 5–8 stations is the same as 8 stations. Independent of this equation, the maximum number of channels ($N_{\text{sb}} \cdot N_{\text{pol}}$) is 16 (a station-unit limitation), and the maximum N_{freq} is 2048 (a single interferometer must fit onto a single correlator board). Table 1 shows some examples of correlator configurations for which increasing any parameter would require a compensatory decrease in some other parameter(s). All capabilities discussed in this report assume the use of local validity, which avoids problems ensuing from the MkIV-format data-replacement headers correlating with each other in certain baseline-source geometries — but at the expense of a factor of two in correlator capacity.

2.3. Output Capacity

The minimum t_{int} for a configuration using the whole correlator is now 1/4 s; configurations that use no more than one-half of the correlator can achieve minimum t_{int} of 1/8 s (both correspond to a raw-data output rate of 6 MB/s). In the future, the Post-Correlator Integrator (PCI) aims to provide a minimum t_{int} for the whole correlator of 1/64 s.

These low integration times, together with the spectral resolution afforded by large N_{freq} , provide the possibility to map considerably wider fields of view through reduced bandwidth- and time-smearing effects in the u - v plane [3]. For example, the fields of view having $\leq 10\%$ decrease in the response to a point source arising from each of these two effects are ([4] §21.7.5):

$$FoV_{\text{BW}} \lesssim 49'' \frac{1}{B} \frac{N_{\text{freq}}}{BW_{\text{sb}}}; \quad FoV_{\text{time}} \lesssim 18'' \frac{\lambda}{B} \frac{1}{t_{\text{int}}} \quad (2)$$

Table 1. Example “maximal” correlator configurations (local validity)

N_{sta}	N_{sb}	N_{pol}	N_{frq}	comment
5–8	1	1	2048	EVN spectral-line
9–16	1	1	512	9 th sta: $N_{\text{frq}} \rightarrow N_{\text{frq}}/4$ (N_{frq} must be 2^n)
9–16	8	4	16	global cross-polarization
9–16	2	2	128	re-arranging $\{N_{\text{sb}}, N_{\text{pol}}, N_{\text{frq}}\}$
5–8	16	1	128	How N_{sta} increase can be absorbed by
9–12	14	1	64	N_{sb} (which is not constrained to be 2^n)
9–16	16	1	32	and N_{frq} (which is)

In equation 2, non-SI units apply for B [1000 km], λ [cm], and BW_{sb} [MHz]. A primary goal of such wide-field correlations would be to map the entire primary beam of each antenna composing the array in a single correlation pass. With our existing N_{frq} and t_{int} capabilities, we can approach this for some observing configurations. More details can be found in www.evlbi.org/user_guide/fov. Of course, one drawback to such wide-field correlations is the rapid growth of the size of the FITS file seen by the user — at our current maximum, ~ 7 –12 GB per hour of observation, depending on the “efficiency” of FITS-file storage for the specific configuration correlated.

2.4. Highlights from Recent Sessions

The following “firsts” refer explicitly to the EVN MkIV Data Processor, although some may indeed have global bearing. Our first sub-second integration-time user experiments came in the Feb’04 session. By the Oct’04 session, we had our first experiments producing overwhelmingly large data sets (our current single-experiment record stands at 260 GB of FITS files). In the course of the observations of the descent of the Huygens probe onto the surface of Titan, we had our first fringes from Australian and Japanese stations. The Feb’05 session had our first successfully correlated and distributed 1 Gb/s user experiment. From the very first use of Mk5A recordings in EVN observations (Nov’03), the number of stations regularly recording onto Mk5A has increased from 3–4 (Feb’04), through 8 (May’04), to our first all-disk experiments (Oct’04). The Huygens observations provided our first Mk5A recordings from VLBA stations, and also saw simultaneous correlation of the most Mk5A stations to date (15). The EVN has by now essentially entirely converted to Mk5A recording. In the longer term, with Mk5B recordings, the possibility exists to move away from using local validity, effectively doubling the correlator capacity as described in equation (1) and the maximum N_{frq} (the impact on the minimum t_{int} could be more complicated, depending on the stage of PCI development).

3. Operations & Data Flow

We operate the correlator 80 hours per week, from which time system testing and development must also come; typically 45–60 hours per week are production. We have 16 Mk5A playback units and 13 tape DPUs, enough to handle any currently feasible global observation. For further practical information from an EVN user’s point of view, see [5].

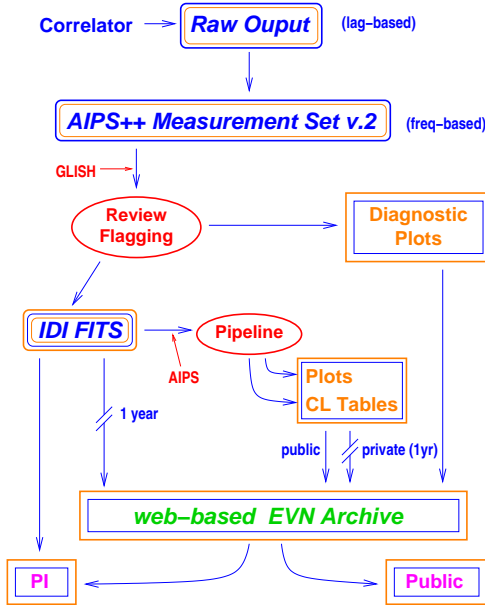


Figure 1. Post-correlation review process for an experiment.

Our internal data review process, as illustrated in Figure 1, begins by transforming the lag-based raw correlator output into an AIPS++ Measurement Set (MS). From the MS, we can investigate slices of the correlation functions in both time and frequency, allowing us to detect and diagnose various problems with the correlation. We can also make various plots to provide feedback to the stations (*e.g.*, parity-error rates, sampler statistics). We apply various corrections to the correlated data at this stage (*e.g.*, the 2-bit van Vleck correction), and flag subsets of the data for low weights and known problems resulting in (uncorrectable) spurious correlation amplitudes and/or phases. Finally, we convert the final MS into FITS format, which can be read into AIPS directly using FITLD. At this stage, we send e-mail to the PI describing the correlation and any points of interest noticed during our data review.

During the course of the post-correlation review, we also begin populating the EVN Archive (www.jive.nl/archive/scripts/listarch.php). This provides web access to the station feedback, standard plots, pipeline results, and FITS files. Feedback from the stations and the diagnostic plots from the MS-based data review go into the Archive and are accessible immediately. The EVN Pipeline is an automated AIPS script that performs the following steps (for more details, see www.evlbi.org/pipeline/user_expts.html): flags data known to be invalid, applies an *a priori* amplitude calibration using the T_{sys} and gain curves from the stations, fringe-fits the data, makes preliminary CLEAN images using a fixed scheme for phase and amplitude self-calibration, and saves a set of AIPS tables and plots from various stages of the calibration/fringe-fitting/imaging process. The AIPS tables produced by the pipeline may help to simplify the initial stages of the analysis. The quality of the preliminary images may be affected by the lack of interactive data editing inherent in the pipeline concept. Prior to correlation, we ask the PI how to treat each of the sources in the experiment in terms of public accessibility via the Archive (see the *EVN Data Access Policy* — linked from the main EVN web page). In short, pipeline results for “public”

sources are immediately accessible on the Archive. The FITS files and results for all pipelined sources are made public after a one-year proprietary period. The PI can arrange for a password to access “private” Archive material. This provides the possibility to download all the FITS data directly — as some PIs have already started to do — eschewing the more traditional DAT-by-mail distribution channel.

There are two independent ways to search the Archive other than by direct entry via a specific experiment. The EVN catalog of observations (kept by Bologna) can be used to search for past observations of particular sources, and provides a link to the relevant experiment(s) correlated at JIVE. In addition, a FITS-finder utility allows searching the archived data by name/coordinates, observing frequency, participating telescopes, and/or various correlation parameters. Both have direct links from the initial EVN Archive page.

Each experiment is assigned a JIVE support scientist. We encourage users to arrange a visit JIVE for help in data reduction if desired. In order to facilitate such visits, financial support through the Trans-National Access activity of the EC’s RadioNet program is available to eligible experiments — see www.evlbi.org/access.

4. *e*-VLBI Overview

The essence of *e*-VLBI lies in the transfer of observed data from the stations to the correlator over a network rather than by shipping recordings made onto physical media. This transfer can occur in various modes: ftp, doubly- or singly-disk buffered, or real-time (ordered in a sense of increasing “*e*-ness”). The advantages of an established real-time *e*-VLBI network range from simplified logistics (no recording media to pre-position at the stations), to increased network reliability (continuous monitoring, real-time feedback to the stations), to new types of science opened up to VLBI (*e.g.*, target-of-opportunity observations of transients), to shortening the ultimate delivery time of the data to the PI.

We have already enjoyed tangible operational benefits from ftp fringe-checks. We have been inserting ftp scans into the standard Network Monitoring Experiments during EVN sessions since May 2003. We process these ftp scans using the NICT Software Correlator (`fx_cor`) [6]. We run the NICT software correlator on an 8-node, dual-processor PC cluster, where independent baselines are assigned to different nodes/processors. Each of the past four sessions has had one or two instances of station problems that, thanks to these ftp fringe-checks, we were able to identify — and more importantly the stations were able to repair — before subsequent user experiments were affected. Without the ftp fringe-checks, we would have discovered the problems far too late to take any meaningful action, and user experiments would have lost the station.

Over the past two years, we have made considerable progress towards real-time *e*-VLBI in the EVN, under the auspices of a proof-of-concept program in collaboration with the national research and education networks in various European countries and DANTE, the operators of the pan-European research network GÉANT. Up through the winter of 2004 we focused on disk-buffered tests, achieving fringes at 256 Mb/s in January 2004. Since the spring of 2004, we have been turned our efforts primarily towards real-time tests and observations. Our first (3-station) real-time image came in April 2004 at 32 Mb/s. The EVN has conducted three peer-reviewed real-time *e*-VLBI user experiments: two spectral-line experiments with 5 stations at 32 Mb/s in September 2004 (see [7]), and a 6-station continuum experiment at 64 Mb/s in March 2005 [8]. To date, our highest-rate sustained real-time fringes are also at 256 Mb/s.

The available connections at the stations obviously play a major role in the establishment of an operational *e*-VLBI array. Currently, JIVE has six 1 Gb/s fibres leading into the data processor. Five EVN stations have connections at 1 Gb/s or better (Jb, Cm, On, Tr, Wb). Arecibo has a 155 Mb/s connection. These six stations and JIVE have formed the nexus driving the EVN's *e*-VLBI observing to date. Some EVN stations expect 1 Gb/s connections within the year (Mc, Mh, Yb). Some stations have more serious issues, in either the local last-mile hook-up (Ef, Nt) or the connectivity between continents (Hh, Sh, Ur, Tigo).

More details about the various *e*-VLBI tests conducted by the EVN can be found in www.evlbi.org/evlbi. A recent summary of technical tests related to protocols, parameter tuning, and the ilk can be found in [9]. JIVE is co-ordinating a proposal, called *EXPR*e*S*, which was recently submitted to the EC in response to a Research Infrastructures call for “*e*Infrastructure: Consolidating Initiatives.” The overall objective of *EXPR*e*S* is to establish a production-level real-time *e*-VLBI service. Among other things, this includes seed money to tackle the last-mile connections at stations and a joint-research activity looking into *e*-VLBI at >1 Gb/s (which would require significant upgrades to our Mk IV Data Processor) and distributed software correlation.

References

- [1] Casse, J.L., “The European VLBI Network MkIV Data Processor,” in *Proceedings of the 4th EVN/JIVE Symposium*, eds. M.A. Garrett, R.M. Campbell, & L.I. Gurvits, *New Astron. Rev.*, **43**, 503–508, 1999.
- [2] Schilizzi, R.T., Aldrich, W., Anderson, B., *et al.* “The EVN-MarkIV VLBI Data Processor,” *Exper. Astron.*, **12**, 49–67, 2001.
- [3] Bridle, A.H. & Schwab, F.R., “Wide Field Imaging I: Bandwidth and Time-Average Smearing,” in *Synthesis Imaging in Radio Astronomy*, eds. R.A. Perley, F.R. Schwab, & A.H. Bridle (ASP: San Francisco), 247–258, 1989.
- [4] Wrobel, J.M., “VLBI Observing Strategies,” in *VLBI and the VLBA*, eds. J.A. Zensus, P.J. Diamond, & P.J. Napier (ASP: San Francisco), 411–427, 1995.
- [5] Campbell, R.M., “Recent Results from the MkIV Data Processor at JIVE,” in *Proceedings of the 7th EVN Symposium*, eds. R. Bachiller, F. Colomer, J.F. Desmurs, & P. de Vincente, (OAN: Alcalá de Henares), 245–248, 2004. (also astro-ph/0412684).
- [6] Kondo, T., Koyama, Y., Takeuchi, H., & Kimura, M., “Current Status of the K5 Software Correlator,” *IVS NICT-TDC News*, **25**, 23–27, 2004. (also www2.nict.go.jp/ka/radioastro/tdc/news25/pdf/tdcnews25.pdf)
- [7] Richards, A., Diamond, P., Bains, I, *et al.*, “The Search for AGB-PNe Transition Sources Using New Technologies (Virtual Observatories and *e*-VLBI,” *Mem. Soc. Astron. Ital.*, in press.
- [8] Paragi, Z., Garrett, M.A., Paczyński, B., *et al.*, “*e*-VLBI Observations of SN2001em — an Off-Axis GRB Candidate,” *Mem. Soc. Astron. Ital.*, in press.
- [9] Szomoru, A., Biggs, A., Garrett, M, *et al.* “From Truck to Optical Fibre: the Coming-of-Age of *e*-VLBI,” in *Proceedings of the 7th EVN Symposium*, eds. R. Bachiller, F. Colomer, J.F. Desmurs, & P. de Vincente, (OAN: Alcalá de Henares), 257–260, 2004. (also astro-ph/0412686).

Thermal deformation of VLBI antennas

Joerg Wresnik¹, Rüdiger Haas², Johannes Boehm¹, Harald Schuh¹

¹) IGG, Vienna University of Technology

²) OSO, Onsala Space Observatory, Chalmers University of Technology

Contact author: Joerg Wresnik, e-mail: wresnik@mars.hg.tuwien.ac.at

Abstract

Geodetic VLBI is one of the major space geodetic techniques that contributes to the International Terrestrial Reference Frame (ITRF). Errors due to atmospheric propagation effects, loading phenomena and technical reasons have been minimized during the last years. Today the results of geodetic VLBI are accurate on the sub-cm level. For further improvements thermal deformations of the radio telescopes have to be taken into account in the analysis of geodetic VLBI data. Thermal deformation effects can reach several millimeters, in particular for the vertical position of the antenna reference point. The magnitude depends on the design of the antenna structure, the material, and environmental influences. The variations typically have seasonal and daily signatures. Two radio telescopes, Onsala (Sweden) and Wettzell (Germany), are equipped with measurement systems that are based on invar rods or invar wires and provide direct observations of the vertical variation of the telescope reference points. Based on these measurements we developed models of thermal deformations as a function of observed environmental temperatures. These thermal deformation models can also be applied to other radio telescopes that are not equipped with invar measurement devices.

1. The existing model

Most VLBI telescopes are of Cassegrain type with alt-azimuth or polar mount and secondary focus. Figure 1, from Haas et al. (1999, [1]), based on Nothnagel et al. (1995, [3]), shows the principles of these antenna mounts. The height of the concrete foundation is denoted by h_f , the height of the antenna pillar by h_p , the height of the vertex by h_v , the height of the subreflector by h_s and the declination shaft by h_d (Haas et al., 1999, [1]). For these antennas the correction $\Delta\tau$ in [sec] on the VLBI delay measurement τ due to thermal deformation can be modeled as follows (Haas et al., 1999, [1]) for alt-azimuth mounts:

$$\Delta\tau = \frac{1}{c} \cdot [\gamma_f \cdot (T(t - \Delta t_f) - T_0) \cdot (h_f \cdot \sin e) + \gamma_a \cdot (T(t - \Delta t_a) - T_0) \cdot (h_p \cdot \sin e + h_v - 1.8 \cdot h_s)] \quad (1)$$

For polar mounts the relations are:

$$\Delta\tau = \frac{1}{c} \cdot [\gamma_f \cdot (T(t - \Delta t_f) - T_0) \cdot (h_f \cdot \sin e) + \gamma_a \cdot (T(t - \Delta t_a) - T_0) \cdot (h_p \cdot \sin e + h_v - 1.8 \cdot h_s) + h_d \cdot \cos \delta] \quad (2)$$

In the above equations c in [m/sec] is the speed of light, γ_f and γ_a in [$1/^\circ C$] are the expansion coefficients for the foundation and for the antenna, respectively, and h_f , h_p , h_v , h_s and h_d are the dimensions of the telescopes in [m]. For prime focus antennas, the factor for h_s is 0.9 instead of 1.8. The temperature of the telescope structure is denoted by T , and T_0 is a reference temperature.

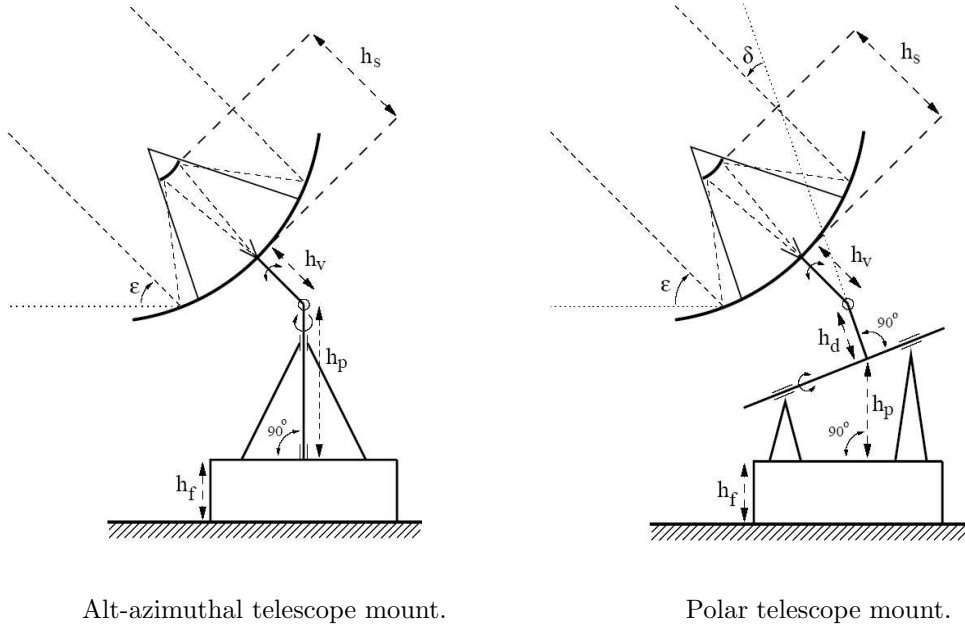


Figure 1. Alt-azimuthal and polar telescope mount (Haas et al., 1999).

The time delay between the change in the surrounding air temperature and the expansion of the telescope structure is denoted by Δt_f for the foundation part and by Δt_a for the antenna part. The elevation and declination of the observed radio source are denoted by e and δ (Haas et al., 1999, [1]). For large VLBI telescopes, variations in the VLBI delay observations of several picoseconds can occur. Regarding a baseline of two telescopes with the signal from the radio source arriving first at site A, the total effect on the measured delay on the baseline is:

$$\Delta\tau_{baseline} = \Delta\tau_A - \Delta\tau_B \quad (3)$$

2. Effect of thermal deformation

As we can see from Equation 1 and Equation 2, the thermal deformation depends on the temperature difference and position of the radio source. Figure 2 shows the effect of the thermal deformation on the baseline between Wettzell (Germany) and Gilcreek (U.S.A.) for the continuous VLBI campaign CONT02 using the above explained model. To point out the influence of the elevation we have calculated the thermal deformation for the antenna at Wettzell for different elevations. The first calculation used an elevation of 90° and the second used 5° . The corresponding results are shown in Figure 3.

We analyzed all IVS-R1 and IVS-R4 VLBI sessions between January 2002 and August 2004 with and without using the model for thermal deformation. Figure 4 shows the repeatabilities of baseline length measurements on the 61 baselines (left) and the difference of the repeatabilities in millimeters (right). For 47 baselines the repeatability improved with an average improvement of 3.5 percent when the thermal deformation model was used in the VLBI analysis. For 14 baselines the application of the thermal deformation model resulted in a degradation of repeatability.

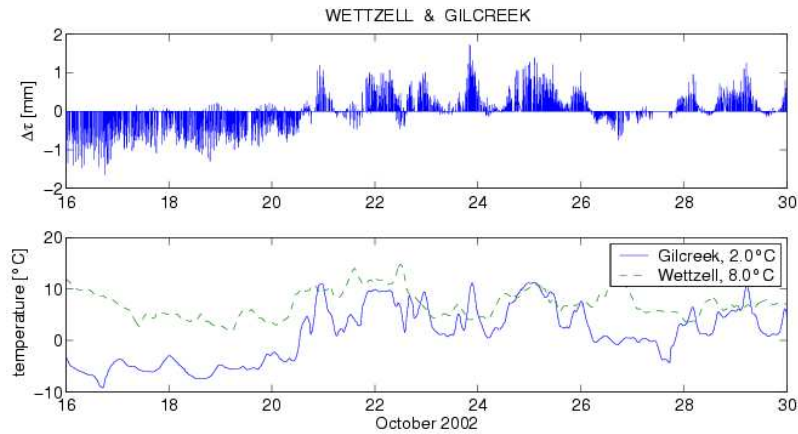


Figure 2. The upper plot shows the modelled effect of thermal deformation on the baseline between Wettzell (Germany) and Gilcreek (U.S.A.) during CONT02, which was a continuous VLBI campaign from October 16, 2002 till October 30, 2002. The correction of $\Delta\tau$ is in a range of ± 3 mm. The lower plot shows the air temperature at both stations. The reference temperatures are mean temperatures at the stations of the last 40 years.

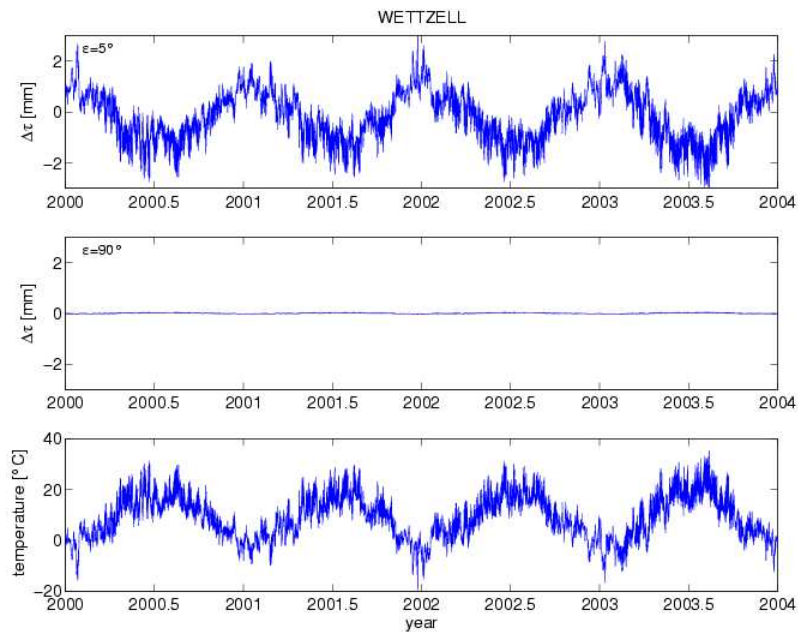
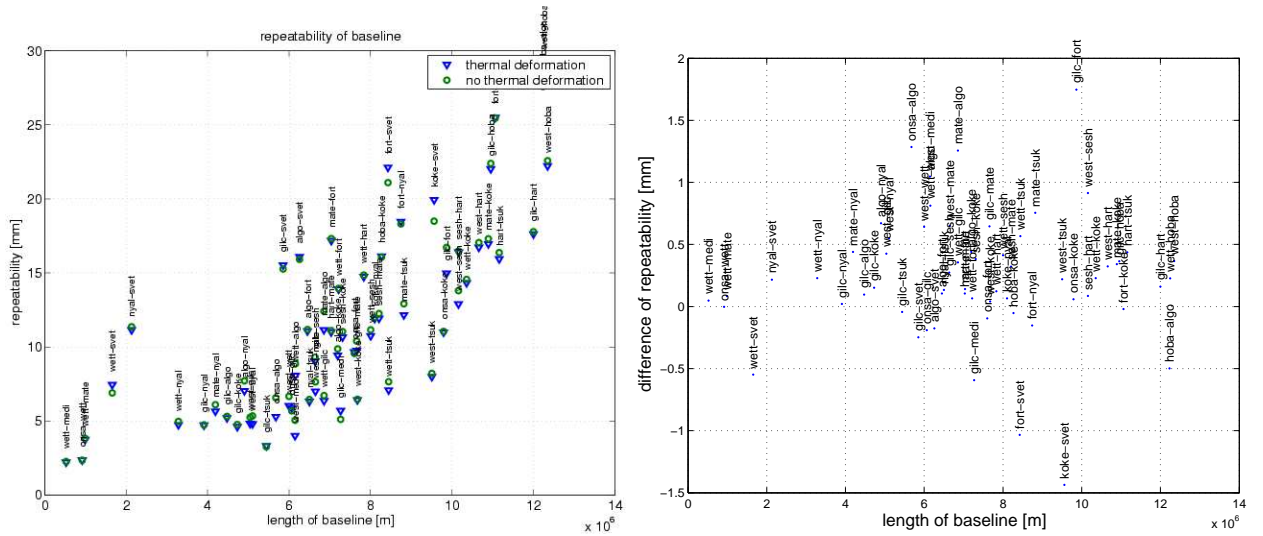


Figure 3. Dependence on elevation angle in the model for thermal deformation. The correction $\Delta\tau$ was calculated for a time period of four years. The elevation e was set to 5° in the upper plot and to 90° in the middle plot. The results for the observation in zenith show a correction nearly zero. For the 5° observation we can see a diurnal and an annual variation in the range of ± 5 mm (upper plot). The lower plot shows the air temperature at station Wettzell.



Repeatability of baselines length measurements with using the correction of thermal deformation (triangle) and without (circle).

Difference of repeatabilities without and with modeling of thermal deformation effects.

Figure 4. Baseline length repeatabilities from the analysis of all IVS-R1 and IVS-R4 VLBI sessions between January 2002 and August 2004.

3. Improved thermal deformation model for the Onsala 20 m telescope

The model for thermal deformation effects described by Haas et al. (1999, [1]) uses the environmental air temperatures that are recorded at the observing VLBI stations and logged in the VLBI log-files. However, these air temperatures are usually measured at some distance to the telescopes and thus are not representative for the temperature of the telescope structures themselves. Some of the IVS radio telescopes are even protected by radome buildings, e.g. Onsala (Sweden) and Westford (U.S.A), so that the outside measured air temperature can deviate quite a lot from the temperature of the telescope structure.

The height and temperature monitoring systems at Onsala (Johansson et al., 1996, [2]) and Wettzell (Zerneck, 1999, [4]) show that the measured vertical height changes are highly correlated to the temperatures of the telescope structure. Figure 5 shows a scatter plot of the vertical height changes and temperature for the Onsala 20 m telescope. Therefore the idea was to model the temperature of the telescope structure based on the outside air temperature and use to this modelled telescope temperature as the input for an improved thermal deformation model.

The approach for the improved thermal deformation model is a mathematical model that is based on digital filter technique. It includes an exponential modeling of environmental heating and cooling of the telescope structure and also memory effects. The modelled temperature of the telescope structure is described as:

$$T_{m,i} = f_{short} \cdot \frac{\sum_{j=i-z_{short}}^i T_{Aj} \cdot q_{short}^{(z_{short}-(i-j) \cdot d)}}{\sum_{j=i-z_{short}}^i q_{short}^{(z_{short}-(i-j) \cdot d)}} + f_{long} \cdot \frac{\sum_{j=i-z_{long}}^i T_{Aj} \cdot q_{long}^{(z_{long}-(i-j) \cdot d)}}{\sum_{j=i-z_{long}}^i q_{long}^{(z_{long}-(i-j) \cdot d)}} + \text{offset} \quad (4)$$

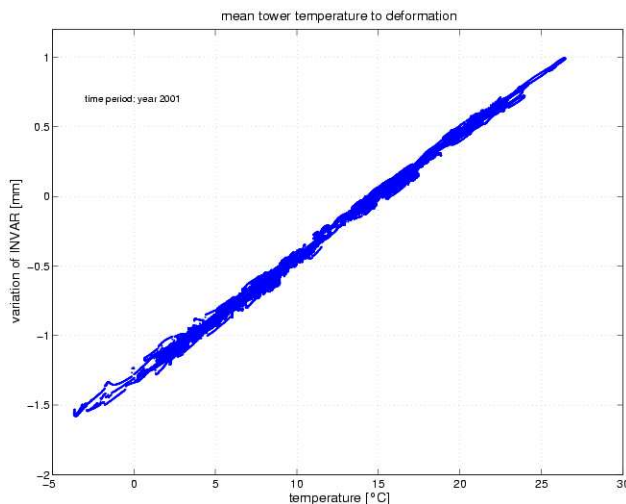


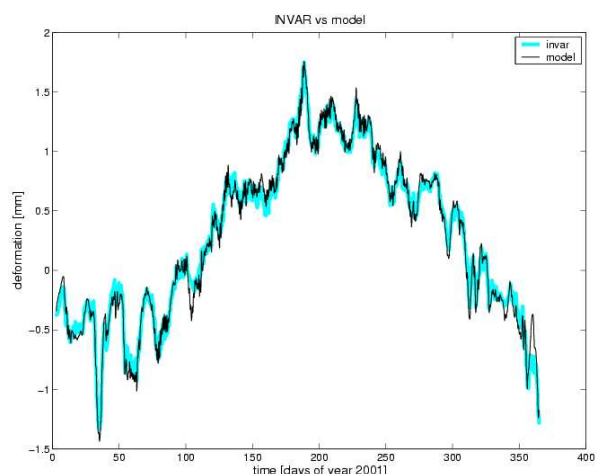
Figure 5. Measured vertical height changes of the telescope tower of the Onsala 20 m telescope versus mean temperature of all 16 temperature sensors in the antenna tower.

The parameters of this model are $T_{m,i}$, and $T_{A,j}$ which represent the modelled telescope temperature at time i and the observed air temperature at time j , the sampling rate d (e.g. 5 min), the coefficients q_{short} and q_{long} for long period and short period variations in outside temperature, the weight factors f_{short} and f_{long} for the short and long periodic terms, and finally z_{long} and z_{short} which express memory effect for 12 hours and 3 days, respectively. The parameters of this model were determined for the Onsala telescope by least-squares estimation based on the time series of outside air temperature and temperature of the telescope structure.

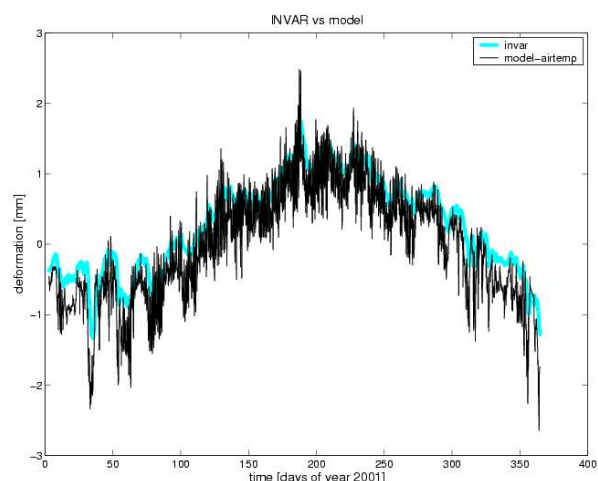
The result of this digital filtering are model parameters that allow to calculate a time series of modelled telescope temperature that fits better the measured antenna temperature much better than the original outside air temperature. The root-mean-square (rms) agreement between modelled and measured temperature of the telescope structure is 0.65°C . Based on this new temperature we are able to calculate the vertical deformation of the antenna with an rms agreement of 0.07 mm with respect to the measured vertical height changes. Figure 6 (left) shows the measured deformation in light grey and the calculated deformation using the modelled temperature in black. Figure 6 (right) shows the measured deformation in light grey and the calculated deformation using the outside air temperature Onsala in black. The improvement of using the modelled temperature of the telescope structure instead of the outside air temperature is clearly visible.

4. Conclusions

The effect of thermal deformation of VLBI antennas can be on the order of several millimeters and can not be neglected if highly accurate geodetic results shall be achieved. In order to calculate the thermal deformation of a VLBI antenna it is important to know the temperature of its telescope structure. However, at most stations only an air temperature sensor is installed in some distance and stored in the VLBI log-files. Thus, we developed a model to determine the temperature of the



Measured vertical deformation (grey) and the calculated antenna deformation using the modelled telescope temperature (black).



Measured vertical deformation (grey) and the calculated antenna deformation using the outside air temperature (black).

Figure 6. Comparison of modelled and measured vertical height changes of the Onsala 20 m telescope.

telescope structure from the recorded air temperature.

The model was calculated for the 20 m telescope at Onsala for the years 2001 to 2004. The rms of the modelled temperature with respect to measured telescope temperature is 0.82°C . The rms agreement of modelled and measured vertical height changes is 0.10 mm. The same strategy was also used to derive a corresponding model for the telescope at Wettzell. For this telescope during the years 2001 to 2003 the rms agreement of modelled and measured telescope temperatures is 1.42°C , and for the modelled and measured vertical deformation the rms agreement is 0.13 mm.

The two telescopes at Onsala and Wettzell might be used as a kind of calibrators for this improved thermal deformation model. The hope is that this improved model for thermal deformation in the future also can be applied to other IVS telescopes.

References

- [1] Haas, R., Nothnagel, A., Schuh, H., and Titov, O.: Explanatory Supplement to the Section "Antenna Deformation" of the IERS Conventions (1996), DGFI Report No.71, Deutsches Geodätisches Forschungsinstitut (DGFI), 26-29, München, 1999.
- [2] Johansson, L.A., Stodne, F., and Wolf, S.: The Pisa Project, Variations in the height of the foundation of the 20 meter radio telescope, Research Report No 178, Chalmers University of Technology, 1996.
- [3] Nothnagel, A., Pilhatsch, M. and Haas, R.: Investigations of Thermal Height Changes of Geodetic VLBI Radio Telescopes, Proceedings of the 10th Working Meeting on European VLBI for Geodesy and Astrometry, 121-133, edited by R. Lanotte and G. Bianco, Matera, 1995.
- [4] Zerneck, R., Seasonal Variations in Height demonstrated at the Radiotelescope Reference Point, 13th Working Meeting on European VLBI for Geodesy and Astronomy, 1999

GPS - VLBI eccentricity at Noto Observatory: June 2003 survey results

Pierguido Sarti¹, Monia Negusini¹, Luca Vittuari², Simonetta Montaguti¹,
Paolo Tomasi¹

¹) *Istituto di Radioastronomia, INAF, Bologna, Italy*

²) *DISTART - Topografia e Geodesia, Universita' di Bologna, Italy*

Contact author: Pierguido Sarti, e-mail: p.sarti@ira.cnr.it

Abstract

The local eccentricity vector between the AZ-EL VLBI antenna Reference Point (12717S001) and the new GPS tracking point (12717M004) has been measured, in June 2003, using terrestrial observations. The adjusted coordinates of the Reference Points (RPs) as well as the coordinates of six pillars that are part of the local network have been extracted and used to generate a SINEX file, performing an alignment of the solution, expressed in the local frame, into ITRF2000. GPS observations have been performed on three pillars of the ground control network (P3: 12717M005; P4: 12717M006 and P10: 12717M012) and on two L-shaped devices mounted on the VLBI antenna. These latter observations correspond to a rapid static survey of different azimuth and elevation positions of the radiotelescope and will be used to recover the VLBI RP by means of GPS technique. A comparison between GPS-derived and terrestrial-derived heights of the local ground pillars has highlighted an interesting systematic bias that is most likely related to the local undulation of the geoid.

1. Upgrade and survey of the local network

The survey approach that was adopted in Noto follows from the positive experience developed during the surveys performed in 2000, 2001 and 2002 at Medicina observatory (e.g.: [1], [2], [3]). 3-D Wild type markers were installed on top of all pillars that establish the local ground control network; these new markers allow a forced centering set-up of devices and instruments and, consequentially, a precise horizontal positioning. Instrumental heights were measured with two different approaches: the height differences between the markers and the tribrachs were determined with levelling and using especially designed devices (see Figure 1). The survey was performed using a couple of high precision total stations (TDA5005 and TC2003): the network and all targets installed on the VLBI antenna were trilaterated and triangulated from the pillars and from daily installed tripods. Tripods were installed with the purpose of improving the geometric distribution of ground observations, especially for surveying the IGS-GPS RP antenna NOT1, and ensuring a reliable connection between the pillars situated at the two sides of the VLBI antenna: P3, P4 and P7 on one side and P9, P10 and P11 on the other side (see Figure 2).

2. Data analysis and results

The eccentricity vector was estimated in the local frame and it was aligned in ITRF following the approach described in [4]. A part of the SINEX file containing the coordinates of six markers of the local ground control network and the RPs of the two co-located space geodetic instruments is shown in Figure 3.

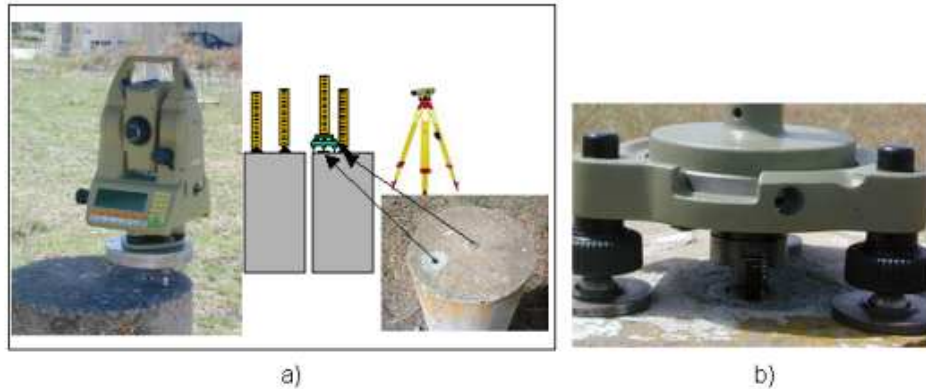


Figure 1. Systems used for total station centering. a) Determination of instrumental height using levelling. b) Direct measurement of instrumental height.

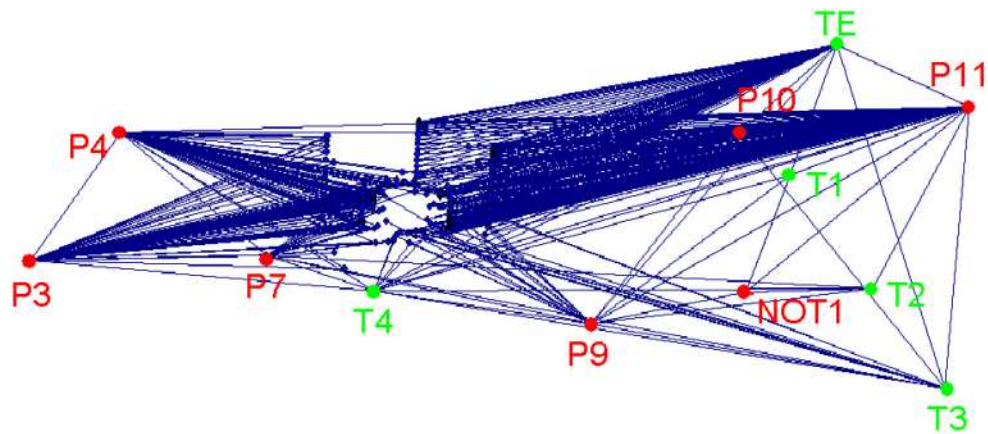


Figure 2. Scheme of the Noto ground control network (P are permanent concrete pillars defined by an ITRF DOMES, T are temporary points materialized by tripods).

A comparison between GPS derived height differences of markers P3, P4, NOT1, P10 and corresponding differences derived by terrestrial observations are reported in Table 1.

P4 has been set as reference for both determinations. Column five shows the differences originated subtracting the relative ellipsoidal height differences obtained with GPS to the corresponding values obtained with terrestrial measurements. Taking into account the distances involved (< 130 m), these latter can be considered as referred to a surface parallel to the local geoid and actually as approximating orthometric height differences (see Figure 4).

A computation of geoid undulations on the four markers was kindly performed by Riccardo Barzaghi, Polytechnic of Milano, using the determination of the Italian geoid ITALGEO1999 ([5]).

```

%-SNX 1.00
*-----
+FILE/COMMENT
* File created by CLEMEnt
* The DOMES are correct
* Variance factor equal to 1.00
-FILE/COMMENT
*-----
+SITE/ID
*CODE PT _DOMES_ T _STATION DESCRIPTION_ APPROX_LON_ APPROX_LAT_ _APP_H_
P10 A -----
P3 A -----
P4 A -----
P11 A -----
P7 A -----
P9 A -----
VLBR A 12717S001
GPSR A 12717M004
-SITE/ID
*-----
+SOLUTION/ESTIMATE
*INDEX TYPE CODE PT SOLN REF_EPOCH UNIT S ESTIMATED VALUE STD_DEV
1 STAX P10 A 1 03:176:00000 m 2 4.934528428365759E+06 1.72272E-004
2 STAY P10 A 1 03:176:00000 m 2 1.321262342867066E+06 1.79313E-004
3 STAZ P10 A 1 03:176:00000 m 2 3.806479664140819E+06 1.48333E-004
4 STAX P3 A 1 03:176:00000 m 2 4.934569832999114E+06 1.71816E-004
5 STAY P3 A 1 03:176:00000 m 2 1.321124416294927E+06 1.34440E-004
6 STAZ P3 A 1 03:176:00000 m 2 3.806472580746669E+06 1.85519E-004
7 STAX P4 A 1 03:176:00000 m 2 4.934552432148709E+06 1.05523E-004
8 STAY P4 A 1 03:176:00000 m 2 1.321141034678117E+06 1.05523E-004
9 STAZ P4 A 1 03:176:00000 m 2 3.806490303368096E+06 1.05523E-004
10 STAX P11 A 1 03:176:00000 m 2 4.934516979307425E+06 2.19757E-004
11 STAY P11 A 1 03:176:00000 m 2 1.321307342902795E+06 1.79279E-004
12 STAZ P11 A 1 03:176:00000 m 2 3.806479875565058E+06 2.36768E-004
13 STAX P7 A 1 03:176:00000 m 2 4.934561768121127E+06 1.65831E-004
14 STAY P7 A 1 03:176:00000 m 2 1.321171140155365E+06 1.71527E-004
15 STAZ P7 A 1 03:176:00000 m 2 3.806470533152924E+06 1.66387E-004
16 STAX P9 A 1 03:176:00000 m 2 4.934554836996763E+06 1.90104E-004
17 STAY P9 A 1 03:176:00000 m 2 1.321234820390432E+06 1.90457E-004
18 STAZ P9 A 1 03:176:00000 m 2 3.806453470841092E+06 1.78465E-004
19 STAX VLBR A 1 03:176:00000 m 2 4.934563006537265E+06 3.89756E-004
20 STAY VLBR A 1 03:176:00000 m 2 1.321201373798122E+06 1.84159E-004
21 STAZ VLBR A 1 03:176:00000 m 2 3.806484578024003E+06 3.23217E-004
22 STAX GPSR A 1 03:176:00000 m 2 4.934546259223840E+06 3.23563E-004
23 STAY GPSR A 1 03:176:00000 m 2 1.321264982513176E+06 6.37154E-004
24 STAZ GPSR A 1 03:176:00000 m 2 3.806456083761341E+06 2.72649E-004
-SOLUTION/ESTIMATE

```

Figure 3. Partial representation of the SINEX file generated for Noto 2003 survey.

Geoid undulation values are reported in Table 2.

The last column of Table 2 confirms the general trend reported in the corresponding column of Table 1. There is a constant bias of approximately 5 mm on all three points. This could be related by a local effect that is smoothed out by the regional geoid model. Further investigations are needed in order to assess the reliability of the discrepancies originated by space and terrestrial techniques. In particular, a new survey is planned for September 2005. Then, an extensive geometric levelling survey as well as a GPS survey are going to be performed on selected markers of the local network and, possibly, on a wider area around the observatory, with the purpose of assess the causes of these discrepancies.

Acknowledgments

Authors would like to thank Prof. Riccardo Barzaghi, Polytechnic of Milano, for computing the geoid undulation on the four markers of the local network. Authors sincerely thank Mr. Carlo Nocita, Mr. Corrado Contavalle and Mr. Mario Paterno', staff members of Istituto di Radioastronomia - Noto Station, for their fundamental support during the survey.

Table 1. Relative height differences determined with GPS and terrestrial measurements

	Local Heights (m)	GPS Heights (m)	GPS diff(m)	Diff Loc-GPS(m)
NOT1	0.3558	126.3399	0.3406	0.0152
P10	0.1771	126.1607	0.1614	0.0157
P3	-0.6253	125.3699	-0.6294	0.0041
P4	0	125.9993	0	0

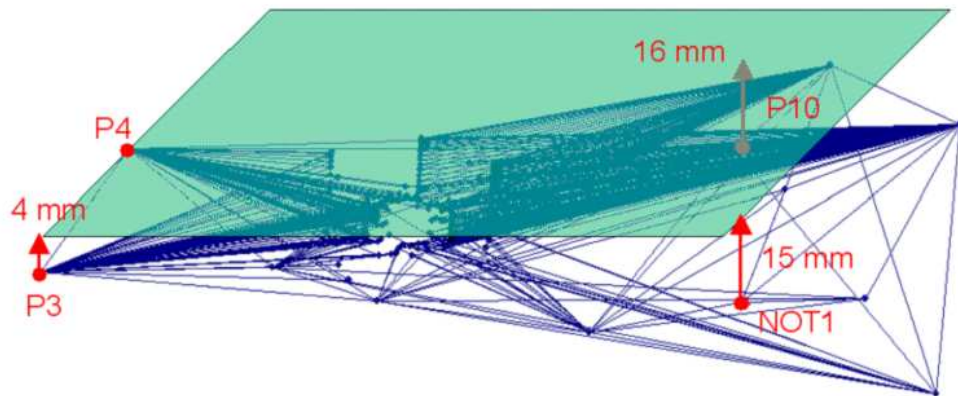


Figure 4. The discrepancies obtained subtracting the GPS derived height differences from the corresponding height differences derived with terrestrial observations (see also Table 1)

Table 2. Latitude, longitude, ellipsoidal height, geoid height and undulation of the four markers of the local network

	Lat (deg)	Lon (deg)	h(m)	N(m)	dN NOT1-others(m)
NOT1	36.875844	14.989787	126.3399	41.374	0.010
P10	36.876111	14.989810	126.1607	41.375	0.009
P3	36.876036	14.988196	125.3699	41.384	0.000
P4	36.876232	14.988426	125.9993	41.384	0.000

References

- [1] Sarti P., Vittuari L., Tomasi P., “GPS and classical survey of the VLBI antenna in Medicina: invariant point determination”, in *Proceedings 14th Working Meeting on European VLBI for Geodesy and Astrometry*, Castel San Pietro Terme (Bologna), Italy, 8-9 Settembre 2000, 67-72, 2000.
- [2] Vittuari L., Sarti P., Tomasi P., “2001 GPS and classical survey at Medicina observatory: local tie and VLBI antenna’s reference point determination”, in *Proceedings 15th Working Meeting on European VLBI for Geodesy and Astrometry*, Institut d’Estudis de Catalunya, Consejo Superior de Investigaciones Científicas, Barcelona, Spain, D. Behrend and A. Rius (Eds.), 161-167, 2001.

- [3] Tomasi P., Sarti P., Vittuari L., Negusini M., “2002 local geodetic survey of VLBI and GPS reference points and ex-centre at Medicina” in *Proceedings 16th Working Meeting on European VLBI for Geodesy and Astrometry*, held at Leipzig, May 09-10, 2003, edited by W. Schwegmann and V. Thorandt, Bundesamt für Kartographie und Geodäsie, Frankfurt/Leipzig, 91-98, 2003.
- [4] Sarti P., Sillard P., Vittuari L., “ Surveying co-located space-geodetic instruments for ITRF computation”, in *J. of Geodesy*. 78:210-222 - DOI 10.1007/s00190-004-0387-0, 2004.
- [5] Barzaghi R., Betti B., Borghi A., Sona G., Tornatore V., ”The Italian quasi-geoid ITALGEO99” , in *Bollettino di Geodesia e Scienze Affini*, n. 1, Istituto Geografico Militare, Firenze, Italy, 33-51, 2002.

Determination of vertical motion from levelling data in the wider area of Medicina and the Apennine foothills

*Bitelli, G.*¹, *Campbell, J.*², *Negusini, M.*³, *Sarti, P.*³, *Vittuari, L.*¹

¹) *DISTART Dept. - University of Bologna*

²) *Geodetic Institute, University Bonn*

³) *IRA - INAF - Bologna*

Contact author: Campbell, J., e-mail: campbell@uni-bonn.de

Abstract

The vertical motion of the Medicina Radio Telescope with respect to the north-central European "stable platform" has been determined from both VLBI and GPS with a clear tendency towards subsidence on the order of 3 to 4 mm/yr. Here, we present investigations of the local motion of the site in the context of groundwater level evolution in the southeastern Po-Plain. From levelling data which are connected to the foothills of the Apennine it appears that the subsidence is indeed closely related to groundwater withdrawal in the region.

1. Introduction

The Medicina Radio Telescope of the IRA has been part of the European Geodetic VLBI Network since the start of its operations in 1984 and has contributed considerably to both astronomical and geodetic observation campaigns (Mantovani 1987, Tomasi and Mantovani 1989). The existing IRA site of the Northern Cross with its technical and logistical infrastructure was a natural selection for the site of the new telescope. However, already in the planning phase of its construction, there was a full awareness of the problems connected with the geological and stratigraphic characteristics of the ground in this area of the south-eastern Po Plain. Accordingly, a deep reaching concrete foundation with pillars reaching down to 20 m was provided to create the best possible stability under the prevailing conditions. Monumentation was established after geotechnical and engineering surveys carried out on site.

During the following years, several local measurement campaigns were carried out to monitor the stability of the VLBI telescope and to determine its geodetic reference point (Tomasi and Mantovani 1989, Del Rosso and Ambrico 1995; Cenci et al. 1998; Nothnagel and Binnenbruck 2000, Vittuari et al. 2001, Sarti et al. 2004).

2. Vertical motion of Medicina from space techniques

Over the past decade, the vertical motion of the Medicina primary observing station has been determined by VLBI and GPS in diverse global as well as regional reference frames. In the context of European geotectonics and intra plate motion, the motion of any station of a given network can best be studied by considering a European based reference system (Campbell and Richter 2001). One rather simple way to realise such a system is by fixing a suitably chosen station and discuss the relative motions of the other stations with respect to this station. This approach has the advantage of a simple and unambiguous definition, but it has to rely on the proper functioning



Figure 1. Typical setting of the Medicina radio telescope in the south-eastern Po-plain

of all observational systems of the chosen reference station at all epochs. In this respect, the Wettzell station in central Europe has an exemplary record of integrity and operational stability. At the same time we have to be sure that the reference site is not subject to local motion of any type, geological or structural. This, in turn, can be verified for example by comparison with data from other stations in the central part of Europe, such as Potsdam, Prague and Brussels in the European Network of Permanent GPS stations.

The behaviour of some of the principal stations in relation to Wettzell fixed can be seen in Fig. 2 where we have listed the vertical motion going from South to North and clearly expose the significant post glacial uplift of the Northern stations (Campbell 2004). This is a firm indication that the rates derived from the GPS time series of different analysis centers are showing real motion at the accuracy level of 1 mm/yr or even better. The comparison of GPS with several VLBI solutions and the ITRF2000 values (Fig. 3) shows a similar picture (here the sites have been arranged from North (left) to South). A more recent VLBI solution of the European VLBI campaigns (using data from Jan. 1990 to July 2004 and again Wettzell as a fixed reference) has yielded a rate of -3.42 ± 0.23 mm/yr for Medicina.

In this scenario of European vertical motions, the large subsidence of the Medicina site is highly significant and has to find a convincing explanation. Vertical tectonic motions are mostly smaller by at least one order of magnitude, so that anthropogenic causes certainly are in the foreground. As already mentioned, the groundwater level and its medium term change have to be considered a major factor in the observed process.

3. Local investigations of the Medicina site

Local and regional investigations on vertical ground movements can best be performed by:

- a.) small scale and regional GPS networks
- b.) levelling networks

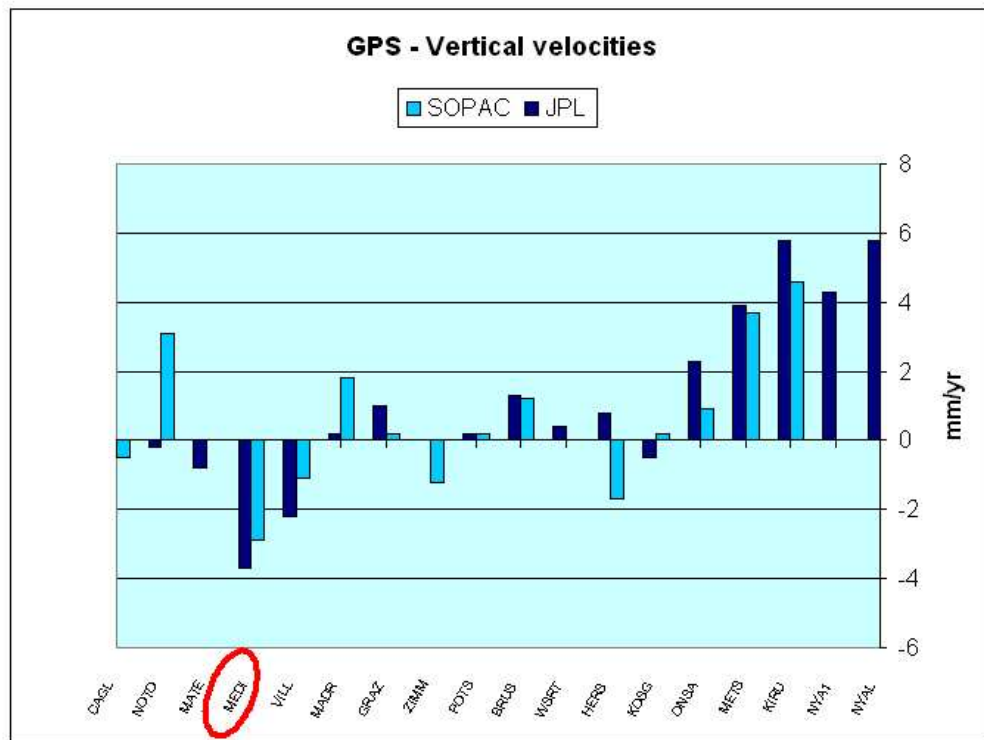


Figure 2. Vertical velocity of Medicina in a Wettzell-fixed European frame. (Medicina GPS data used from 1996.5 to 2002.5)

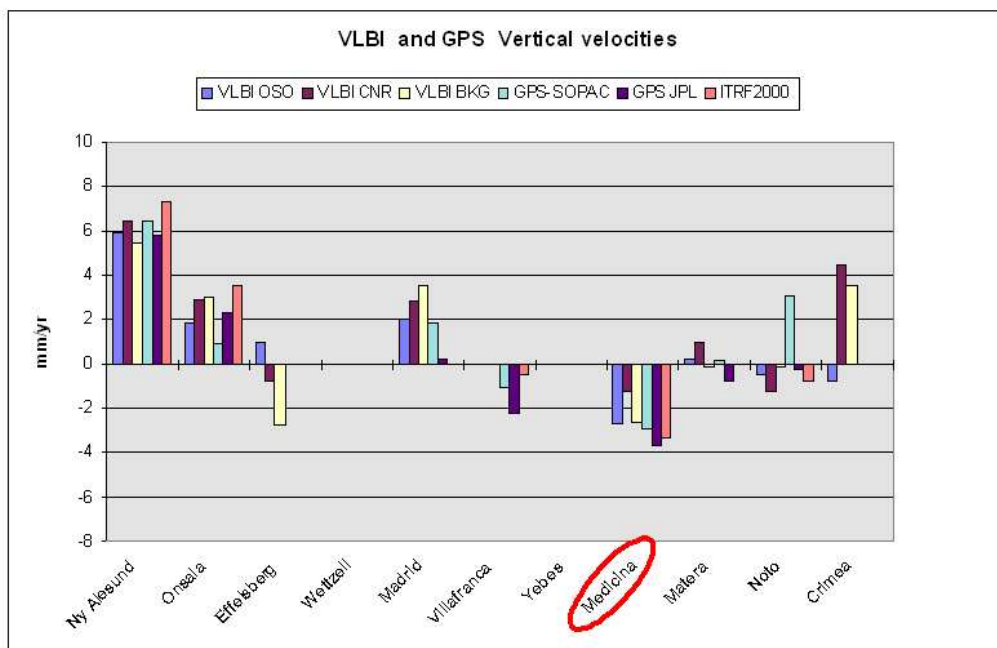


Figure 3. VLBI, GPS and ITRF solutions for geodetic VLBI stations in Europe. (VLBI-Data from 1990-2001, GPS data from 1996.5-2002)

Here, we shall concentrate on precision levelling networks existing in the Bologna-Medicina area, which have been observed at repeated epochs by a number of different public institutes and authorities in the region, such as "Autorità di Bacino del Reno", "Provincia di Bologna", "ARPA", etc. In parallel, the department of civil engineering (DISTART) at the University of Bologna has a long standing project of investigations in geodetic control networks (Baldi and Unguendoli 1987, Bitelli et al, 2000) which includes the combined adjustment of local and regional levelling networks in the Southern Po Plain with the aim to determine the magnitude and distribution of anthropogenic ground motion in this area. As an example, we show the configuration of the lines and markers in the levelling network of Bologna Province (survey 1999) (Fig. 4).

4. First results and discussion

A first preliminary analysis of a combined network of the ARPA Agency Emilia Romagna provides an insight in the pattern of subsidence, indicating the presence of wells for heavy groundwater withdrawal, in particular near the bigger cities and agglomerations (Fig. 5). Fortunately the site of the Medicina observatory does not belong to the worst affected parts, i.e. the subsidence rate in this area appears to be settled at a level of about -1 cm/yr; this value must be regarded with caution due to the long period examined, the effects of interpolation and the different paths of the levelling lines.

The rate for the telescope, more precisely for the markers on its foundation, can be obtained with higher accuracy with respect to a regional interpretation by considering a levelling line connecting the nodal point of Idice with the Medicina observatory, surveyed in 1992 and 1999 (Fig. 6).

The node Idice is connected to the two stable reference points in the foothills of the Apennine, the main reference Sasso Marconi and by a separate line to a secondary reference Castel de' Britti. In Fig. 7 the annual rates for the markers on both levelling lines are shown, as derived from the levelling epochs of 1992 and 1999 (data from Bologna Municipality, Province of Bologna, ARPA). In this period a subsidence of -0.024 m has been obtained for the benchmarks fixed to the VLBI-telescope basement, i.e. an annual vertical motion with respect to the levelling reference point at Sasso Marconi in the foothills of the Apennine of

$$v = -3.4 \text{ mm/yr}$$

The total error is presently estimated to ± 9 mm over the 7 yr time span, i.e. ± 1.2 mm/yr.

This value agrees remarkably well with the vertical rate derived from GPS and VLBI of -3.5 to -4.0 mm/yr. This would mean that the Medicina subsidence is indeed a particular movement pertaining to the effects of water management in the South-Eastern Po-Plain and has to be 'subtracted' when the vertical motion is discussed in a greater geotectonic context. Following this line of thought, the result suggests that the Apennine reference, as used here, is - in the observed period (1992-1999) - in line with the vertical trend of the central European reference (i.e. Wettzell), as well as with Matera and Noto in Southern Italy (see fig. 2 and 3) at the accuracy level of about 1 mm/yr (one sigma).

The results presented here also agree well with the vertical changes determined at Medicina site with the GPS technique (10 yr) in a separate analysis that yields a rate of -3.44 ± 0.03 mm/year (Zerbini et al., 2005).

In the comparison between results from levelling and from space techniques we have tried

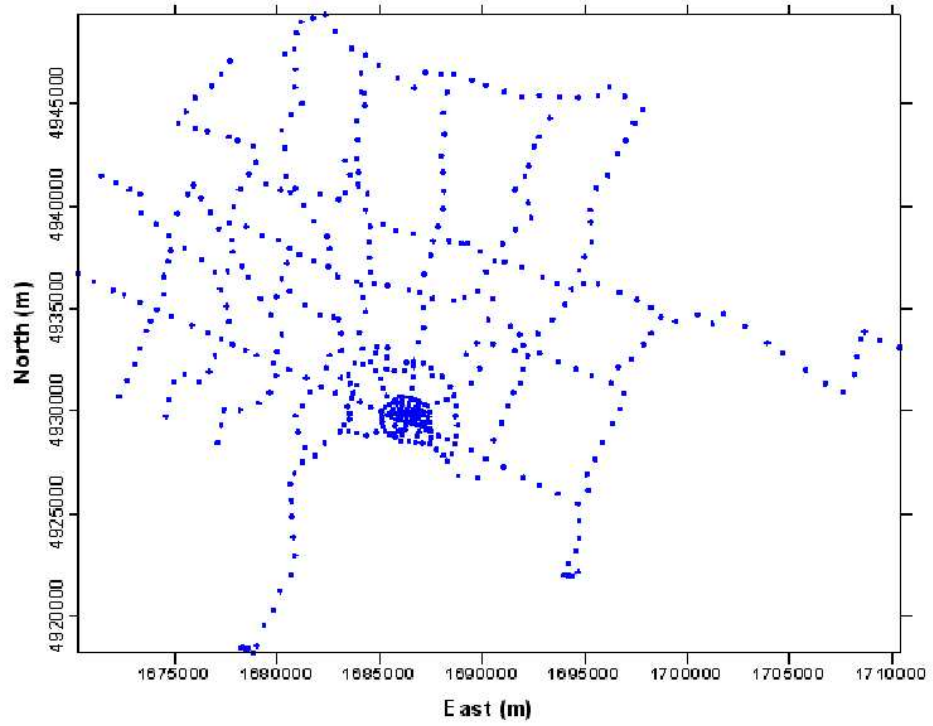


Figure 4. Levelling network of Bologna Province (survey 1999)

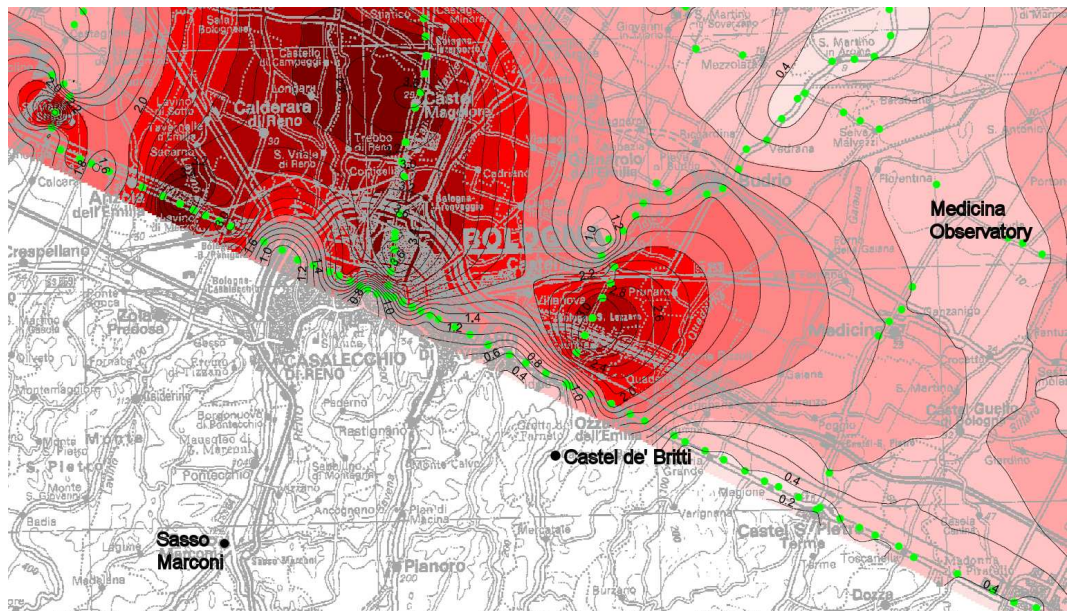


Figure 5. Vertical velocity (cm/year) in the period 1970/93-1999 (adapt. from Bonsignore et al., 2003)

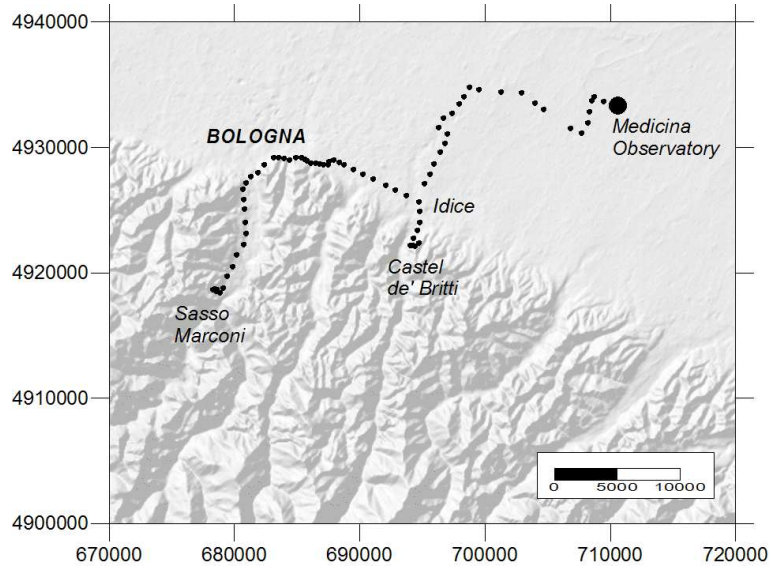


Figure 6. Levelling lines connecting the stable points of Sasso Marconi (reference) and Castel de' Britti with the nodal point of Idice (along Via Emilia) and Medicina Observatory

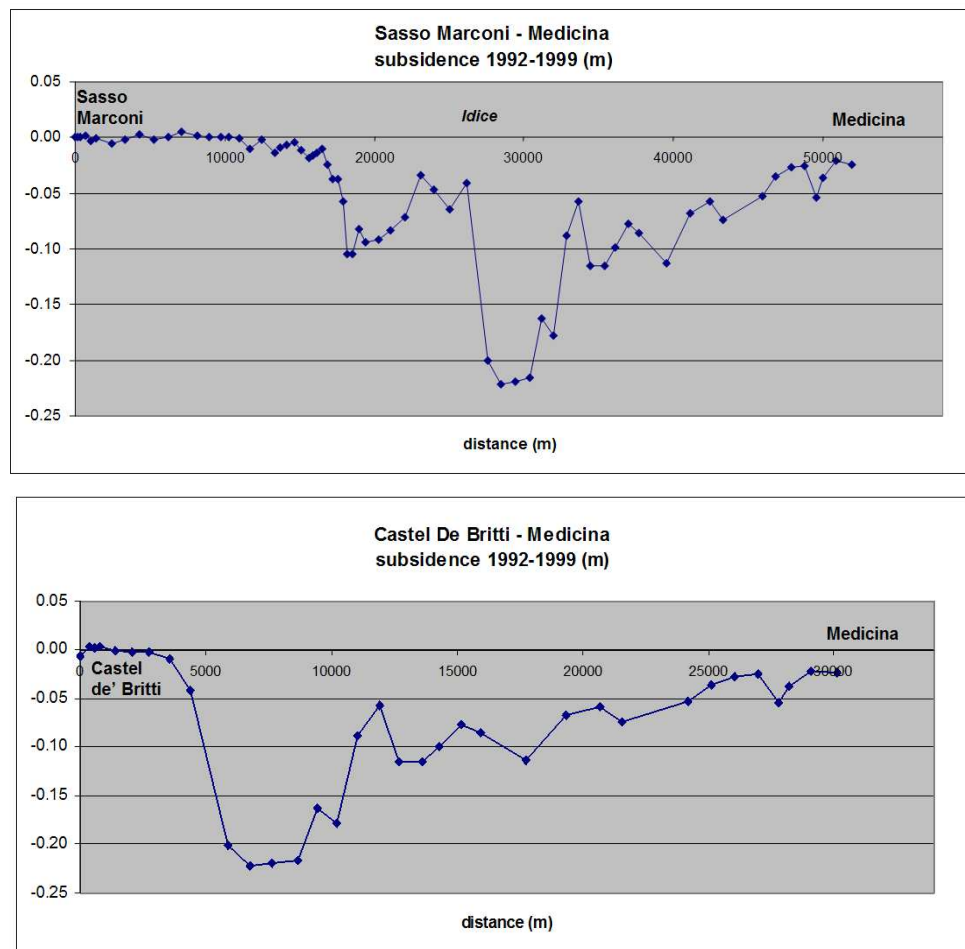


Figure 7. Subsidence rates on two levelling lines connected to the Apennine foothills, (see Fig. 6)

to consider similar time spans where possible, being aware of the fact that the groundwater induced subsidence rates are changing with time. Therefore, in further studies, the recordings of groundwater wells have to be included in the analysis.

References

- [1] Baldi P., Unguendoli M.: Geodetic networks for crustal movement studies. *Lecture Notes in Earth Sciences*, Vol. 12, Applied Geodesy, p. 135-161, 1987
- [2] Benedetti G., Draghetti T., Bitelli G., Unguendoli M., Bonsignore F., Zavatti A.: Land subsidence in the Emilia-Romagna region, Northern Italy. *Proc. Sixth International Symposium on Land Subsidence (SISOL)*, Ravenna, Vol. I, p. 61-76, 2000
- [3] Bitelli G., Bonsignore F., Unguendoli M.: Levelling and GPS networks to monitor ground subsidence in the Southern Po Valley. *Journal of Geodynamics* 30, p. 355-369, 2000
- [4] Bonsignore F., Chahoud A., Cristofori D., Farina M., Martinelli G., Villani B.: Subsidence and groundwater in Emilia-Romagna region: a comparison between subsidence rate and piezometric levels. *Proc. 4th Congress on Regional Geological Cartography and Information Systems*, Bologna, p. 604-605, 2003
- [5] Campbell J.: Accuracy of Vertical Positioning by GPS. *Proc. Workshop on the State of GPS Vertical Positioning Precision*, eds. T. van Dam and O. Francis, *Cahiers du Centre Europeen de Godynamique et de Sismologie*, Vol. 23, p. 17-25, 2004
- [6] Campbell, J. and B. Richter: Towards a stable European vertical velocity reference system using VLBI, GPS and absolute gravity measurements. *Proceedings of the 15th Working Meeting on European VLBI for Geodesy and Astrometry*, held in Barcelona, Spain, Sept. 7-8, 2001, D. Behrend, A. Rius, Eds., IEEC-CSIC Barcelona, p. 65-74, 2001
- [7] Cenci, A., Vicomanni, G., Bianco, G.: Determination of the invariant point and of the axes offset for the VLBI antenna at Medicina, Telespazio, Roma, 1998
- [8] Del Rosso, D., and Ambrico, F. : Survey of the Medicina site - September 1995, Nuova Telespazio, Roma, 1995
- [9] Elmi C., Bergonzoni A., Massa T., Montaletti V.: Il territorio di pianura del Comune di Bologna: aspetti geologici e geotecnici. *Giornale di Geologia*, ser. 3, vol. 46/2, p. 127-152, 1984
- [10] Mantovani F.: The Medicina VLBI Station. *Proc. 5th Working Meeting on European VLBI for Geodesy and Astrometry*, Wettzell, Nov. 1986, *Mitt. Geodt. Inst. der Rhein. Friedr.-Wilh.-Universitt Bonn*, Nr. 71, p. 7-9, 1987
- [11] Nothnagel, A. and Binnenbruck, B.: Determination of the 1996 displacement of the Medicina radio telescope by local surveys", in *Proc. of the XIV Working Meeting on European VLBI for Geodesy and Astrometry*, 61-66, Castel S. Pietro Terme (BO), Italy, 2000
- [12] Sarti P., Sillard P., Vittuari L.: Surveying co-located space-geodetic instruments for ITRF computation, *J. of Geodesy* (2004) 78:210-222 - DOI 10.1007/s00190-004-0387-0, 2004
- [13] Tomasi P., Mantovani F.: The Medicina Station Status Report. *Proc. 7th Working Meeting on European VLBI for Geodesy and Astrometry*, Madrid, Oct. 1989, ed. A. Rius, Instituto de Astronomia y Geodesia Madrid, p. 30-34, 1989
- [14] Vittuari L., Sarti P., Tomasi P.: 2001 GPS and classical Survey at Medicina Observatory: Local Tie and VLBI Antenna's Reference Point Determination *Proc. 15th Working Meeting on European VLBI for Geodesy and Astrometry*, Barcelona, Sept. 2001, ed. D. Behrend and A. Rius, Instituto d'Estudis Espacials de Catalunya, p. 161-167, 2001

- [15] Zerbini S., Cecconi G., Colombo D., Matonti F., Richter B., Rocca F., Van Dam T.: Monitoring natural and anthropogenic subsidence in the northern Adriatic area by space and terrestrial techniques. Poster presented at EGU 2005, Vienna, 2005

Asymmetric Mapping Functions for CONT02 from ECMWF

Johannes Boehm, Marco Ess, Harald Schuh

IGG, Vienna University of Technology

Contact author: Johannes Boehm, e-mail: johannes.boehm@tuwien.ac.at

Abstract

In recent years numerical weather models have been applied to improve mapping functions which are used for tropospheric delay modeling in VLBI and GPS data analyses. The Vienna Mapping Functions (VMF) (Boehm and Schuh, 2004, [1]) assume a symmetric troposphere around the station and are based on raytracing through the numerical weather models at an initial elevation angle of 3.3° . Since the refractivity for the line-of-sight is always taken from the profile above the station, VMF is independent of the azimuth and cannot account for azimuthal asymmetries. With the concept of the Vienna Mapping Function 2 (VMF2), the raytracing is performed every 30° in azimuth with the refractivity determined for the line-of-site by interpolation in a grid of refractivity profiles around the station. Thus, VMF2 depends on the azimuth and abandons the commonly used approach of tropospheric gradients. Baseline length repeatabilities for CONT02 show that VMF2 yields the best results in terms of reduction of variance compared to several other mapping functions presently used in VLBI analyses.

1. Introduction

Troposphere mapping functions like the Niell Mapping Functions (NMF) (Niell, 1996, [7]) or the Vienna Mapping Functions (VMF) (Boehm and Schuh, 2004, [1]) apply the continued fraction form as introduced by Marini (1972, [6]), see equation 1.

$$mf_{h,w}(e) = \frac{1 + \frac{a}{1 + \frac{b}{1+c}}}{\sin(e) + \frac{\frac{b}{\sin(e) + c}}{\sin(e) + c}} \quad (1)$$

In equation 1 the hydrostatic (h) and wet (w) mapping functions depend only on the elevation angle e but not on the azimuth az of the observation. To account for azimuthal asymmetries in the tropospheric path delays at the stations, simple gradient models are applied in VLBI analyses. The most commonly used models are those by Davis et al. (1993, [3]) in the form introduced by MacMillan (1995, [5], see equation 2) or by Chen and Herring (1997, [2], see equation 3). $\Delta L_0(e)$ corresponds to the symmetric path delay at the stations.

$$\Delta L(az, e) = \Delta L_0(e) + mf_h(e) \cdot \cot e \cdot [G_N \cdot \cos az + G_E \cdot \sin az] \quad (2)$$

$$\Delta L(az, e) = \Delta L_0(e) + \frac{1}{\sin e \cdot \tan e + 0.0032} \cdot [G_N \cdot \cos az + G_E \cdot \sin az] \quad (3)$$

The gradient models in equations 2 and 3 correspond to a tilting of the atmosphere, which again is equivalent to tilting the mapping function. Thus, the north and east gradients G_N and G_E can be expressed by the tilting angle β (compare figure 1) and its azimuth.

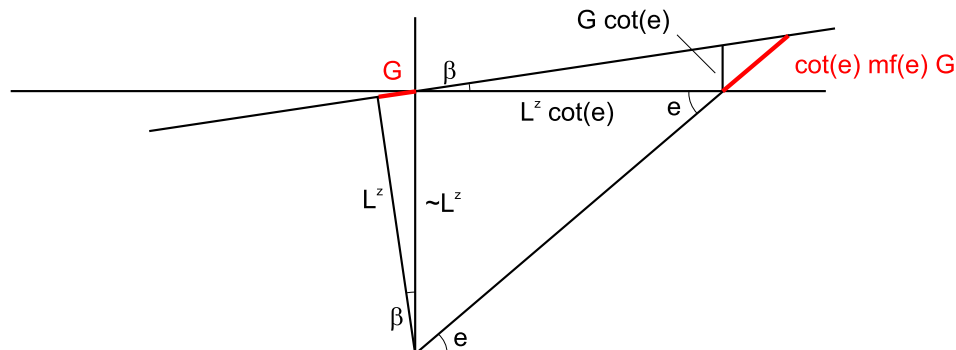


Figure 1. **Tilting of the atmosphere.** Gradient models correspond to a tilting of the atmosphere (or the mapping function), i.e. north gradient and east gradient are equivalent to a tilting angle β and its azimuth.

2. Determination of the Vienna Mapping Function 2 (VMF2)

With the symmetric Vienna Mapping Function VMF (Boehm and Schuh, 2004, [1]) pressure level data from the ECMWF (European Centre for Medium-Range Weather Forecasts) are used for the refractivity profile above the site to determine the hydrostatic and wet mapping functions as well as the outgoing (=vacuum) elevation angle e for an initial elevation angle of $e_0 = 3.3^\circ$. Then - using the best b and c coefficients available - the continued fraction form in equation 1 is inverted and the hydrostatic and wet coefficients a are determined. Thus, VMF is realized as time series of the hydrostatic and wet coefficients a once per station every six hours which is the time resolution of ECMWF operational pressure level data.

With the asymmetric VMF2, the refractivity is not just taken from the profile above the site but it is actually taken along the line-of-site (compare figure 2, bended ray path). This requires an interpolation in a grid of refractivity profiles around the station, which is not explained in detail here. The raytracing is then performed every 30° in azimuth, i.e. VMF2 comprises 11 hydrostatic and wet coefficients a per station and time epoch.

For the VLBI campaign CONT02 in the second half of October 2002, the coefficients for VMF2 have been determined from the operational pressure level data of the ECMWF. Figure 3 shows the hydrostatic and wet asymmetries at 5° elevation with respect to the symmetric VMF for station Wettzell in Germany. The behaviour of the hydrostatic part is rather smooth and the asymmetries at the 6-hour epochs approximately describe circles, which means that the hydrostatic asymmetry more or less corresponds to a tilting of the atmosphere. In other words, the hydrostatic asymmetry can be modeled very well with north and east gradients. On the other hand, the wet asymmetries are rather irregular and vary very rapidly, and they do not correspond to a simple tilting model. Thus, the wet asymmetries can hardly be estimated as north and east gradients.

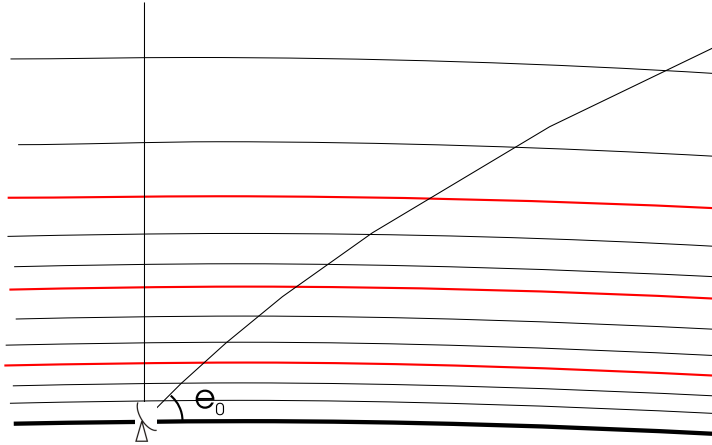
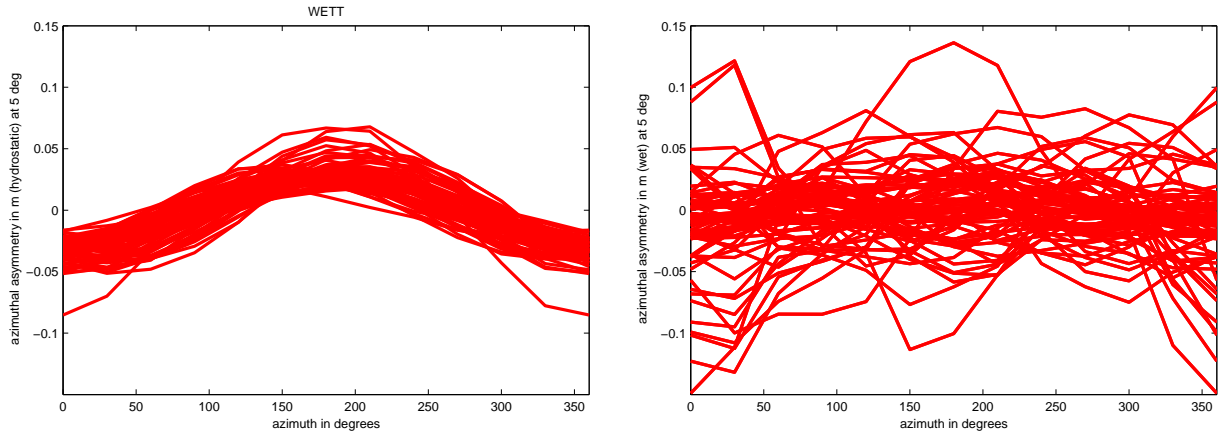


Figure 2. **Pressure levels from the ECMWF.** VMF2 is based on 3D raytracing through the pressure levels, i.e. it is actually taking the refractivity along the line-of-site. Contrarily, the symmetric VMF simply uses the refractivity profile above the site.



Hydrostatic asymmetry at 5° elevation for VMF2 in m.

Wet asymmetry at 5° elevation for VMF2 in m.

Figure 3. **Asymmetries with VMF2 compared to VMF.** Whereas the behaviour of the hydrostatic part is rather smooth and corresponds to the tilting of the atmosphere, the asymmetry of the wet part is more irregular and cannot be easily modeled with a north and east gradient. Each line represents a 6-hour time epoch.

3. Validation of VMF2

For the geodetic VLBI analyses, the classical least-squares method (Gauss-Markov model) of the OCCAM 6.0 VLBI software package (Titov et al., 2001, [11]) is used. Free network solutions with no-net translation and no-net rotation conditions are calculated for the 24-hour sessions with five Earth orientation parameters being estimated (nutations, dUT1, and pole coordinates). Atmospheric loading parameters are obtained from Petrov and Boy (2004, [9]) and ocean loading corrections are calculated from Scherneck and Bos (2002, [10]) using the CSR4.0 model by Eanes

(1994, [4]). The zenith delays are estimated as 1-hour continuous piecewise linear functions, and the cutoff elevation angle is set to 5° for all sessions.

For the analyses here, several different mapping functions have been applied - with and without estimating additional gradients using the model by MacMillan (1995, [5]). The small letter 'o' in the abbreviation indicates that no additional gradients were estimated.

- NMF(o) - the Niell Mapping Functions (Niell, 1996, [7])
- VMF(o) - the Vienna Mapping Functions (Boehm and Schuh, 2004, [1])
- VMF2(o) - the Vienna Mapping Functions 2 (presented here)
- VMF2H(o) - the hydrostatic part from VMF2 and the wet part from VMF
- IMF(o) - the Isobaric Mapping Functions (Niell, 2001, [8]) with a priori hydrostatic gradients from the tilting of the 200hPa pressure level

Figure 4 shows the median reduction of variances (over all 28 baselines) in mm^2 of the baseline length repeatabilities, i.e. the standard deviation with regard to a regression polynomial of first order. Some conclusions can be drawn from figure 4:

- The best improvement is achieved for VMF2 if no additional gradients are estimated.
- If additional gradients are estimated with VMF2, the solution degrades because the gradients are not necessary in this case.
- There is hardly any difference between VMF2H and VMF: This means that it is not important to apply hydrostatic gradients a priori because they can be estimated as north and east gradients very well.
- Repeatabilities are slightly better with VMFo compared to VMF and with VMF2Ho compared to VMF2H: The constraints on the gradients have to be reconsidered in OCCAM because they might be too loose.
- Using a priori gradients from the tilting of the 200 hPa pressure level (IMF) degrades the solution.

4. Conclusions and outlook

For the time period of CONT02, VMF2 has proved to be very successful. However, there is a huge amount of work (downloading, interpolation, raytracing) needed for this approach. Thus, more efficient algorithms and procedures need to be found to provide VMF2 on an operational basis similar to VMF.

5. Acknowledgements

IVS and in particular all network stations that contributed to the CONT02 campaign which provided extremely valuable data are acknowledged. We are very grateful to the Austrian Science Fund (FWF) for supporting our work by research project P16992-N10.

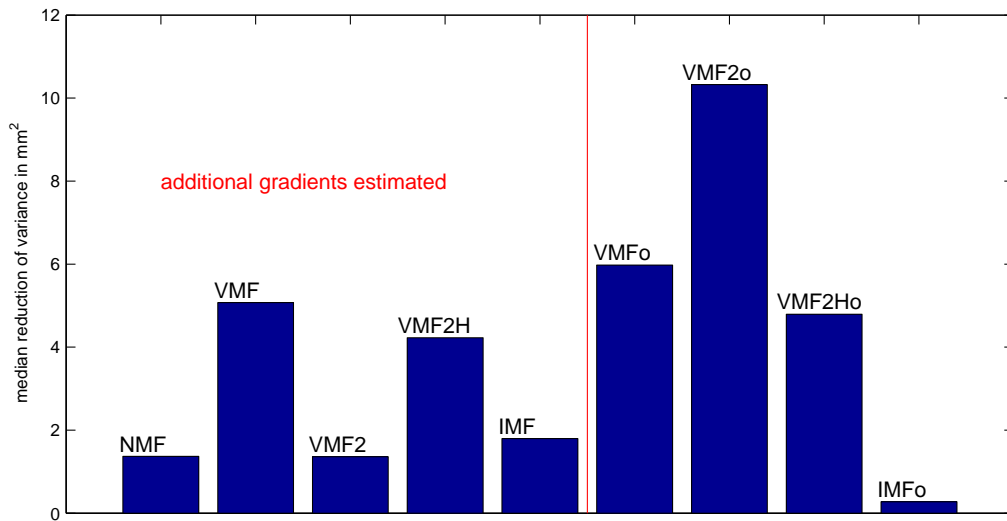


Figure 4. **Reduction of variance in mm^2 of the baseline length repeatabilities with respect to NMFo.** The largest improvement can be seen for VMF2 with no additional gradients being estimated.

References

- [1] Boehm, J. and H. Schuh, Vienna Mapping Functions in VLBI analyses, *Geophys. Res. Lett.*, 31, L01603, doi:10.1029/2003GL018984, 2004.
- [2] Chen, G. and T.A. Herring, Effects of atmospheric azimuthal asymmetry on the analysis of space geodetic data, *Journal of Geophysical Research*, Vol. 102, No. B9, pp. 20489-20502, 1997.
- [3] Davis, J.L., G. Elgered, A.E. Niell, C.E. Kuehn, Ground-based measurement of gradients in the 'wet' radio refractivity of air, *Radio Science*, Vol. 28, No. 6, 1003-1018, 1993.
- [4] Eanes, R.J., Diurnal and Semidiurnal tides from TOPEX/POSEIDON altimetry. *Eos Trans. AGU*, 75(16):108, 1994.
- [5] MacMillan, D.S., Atmospheric gradients from very long baseline interferometry observations, *Geoph. Res. Letters*, Vol. 22, No. 9, pp. 1041-1044, 1995.
- [6] Marini, J.W., Correction of satellite tracking data for an arbitrary tropospheric profile, *Radio Science*, Vol. 7, No. 2, pp. 223-231, 1972.
- [7] Niell, A.E., Global mapping functions for the atmosphere delay at radio wavelengths, *JGR*, Vol. 101, No. B2, 3227-3246, 1996.
- [8] Niell, A.E., Preliminary evaluation of atmospheric mapping functions based on numerical weather models, *Phys. Chem. Earth*, 26, 475-480, 2001.
- [9] Petrov, L. and J.P. Boy, Study of the atmospheric pressure loading signal in VLBI observations, submitted to *JGR*, 2004.
- [10] Scherneck, H.-G. and M.S. Bos, Ocean Tide and Atmospheric Loading, *International VLBI Service for Geodesy and Astrometry 2002 General Meeting Proceedings*, edited by Nancy R. Vandenberg and Karen D. Baver, NASA/CP-2002-210002, 205-214, 2002.
- [11] Titov, O., V. Tesmer, and J. Boehm, Occam Version 5.0 Software User Guide, Auslig Technical Report 7, 2001.

IVS long-term series of Tropospheric Parameters

Robert Heinkelmann, Johannes Boehm, Harald Schuh

Institute of Geodesy and Geophysics/University of Technology, Vienna

Contact author: Robert Heinkelmann, e-mail: rob@mars.hg.tuwien.ac.at

Abstract

VLBI provides a consistent set of group delay and meteorological observations for more than twenty years at some stations. Hence VLBI tropospheric estimates could play an important role for climate studies. To detect changes in the water vapor content of the troposphere the long-term characteristics of wet zenith delays (WZD) are investigated, which depend on various parameters. A re-analysis of all VLBI sessions with systematically varying analysis options was performed at the IGG, to understand the sources of influence on the trends of tropospheric parameters. The choice of the terrestrial reference frame (TRF), its treatment in the estimation process, different mapping functions, and cutoff elevation angles are considered in this study.

1. Introduction

Goal of the project is the reliable determination of long time series of tropospheric parameters from VLBI, which is the prerequisite to climate studies. Therefore a re-analysis on the group delay level using all X/S-band 24h-sessions of the global VLBI data set available from IVS Data Centers was performed. Episodic movements due to earthquakes, other seismic events, antenna rail repair, station relocation and a large number of clock jumps were considered to achieve consistency of the about three million observed group delays from November 1981 till July 2004. From the overall number of 152 stations a subset of 50 non-mobile VLBI stations - including the transportable integrated geodetic observatory (TIGO) at Wettzell (TIGOWTZL) and Concepción (TIGOCONC) - were chosen for the study, revealing spatial and temporal inhomogeneity of the VLBI data set (figures 1 and 2). A full re-processing with a modified version of the VLBI analysis software package OCCAM 6.0 takes about 20 hours on a standard PC-system (CPU 3.0 GHz, RAM 512 MB) on LINUX-platform. Analysis options and models were systematically varied to detect possible influences on the long-term characteristics of tropospheric parameters.

2. Data analysis

Source coordinates were taken from the ICRF-ext.1 catalogue and kept fixed. Earth orientation parameters (EOP) were estimated as 24h-offsets using the IERS C04 as a prioris and the MHB2000 nutation model without the terms for free core nutation. The terrestrial reference frame (TRF) was realized by coordinates and velocities of the 50 stations taken from ITRF2000 or VTRF2003, respectively. During the least-squares fit they were either kept fixed or no-net-rotation (NNR) and no-net-translation (NNT) conditions were applied ('free adjustment') to define the geodetic datum. Corrections of the station coordinates were applied due to solid Earth tides using the solar system ephemerides DE405/LE405 of JPL and due to ocean loading with coefficients from the GOT00p2 model. Site displacements caused by atmospheric loading were considered, too, as well as thermal

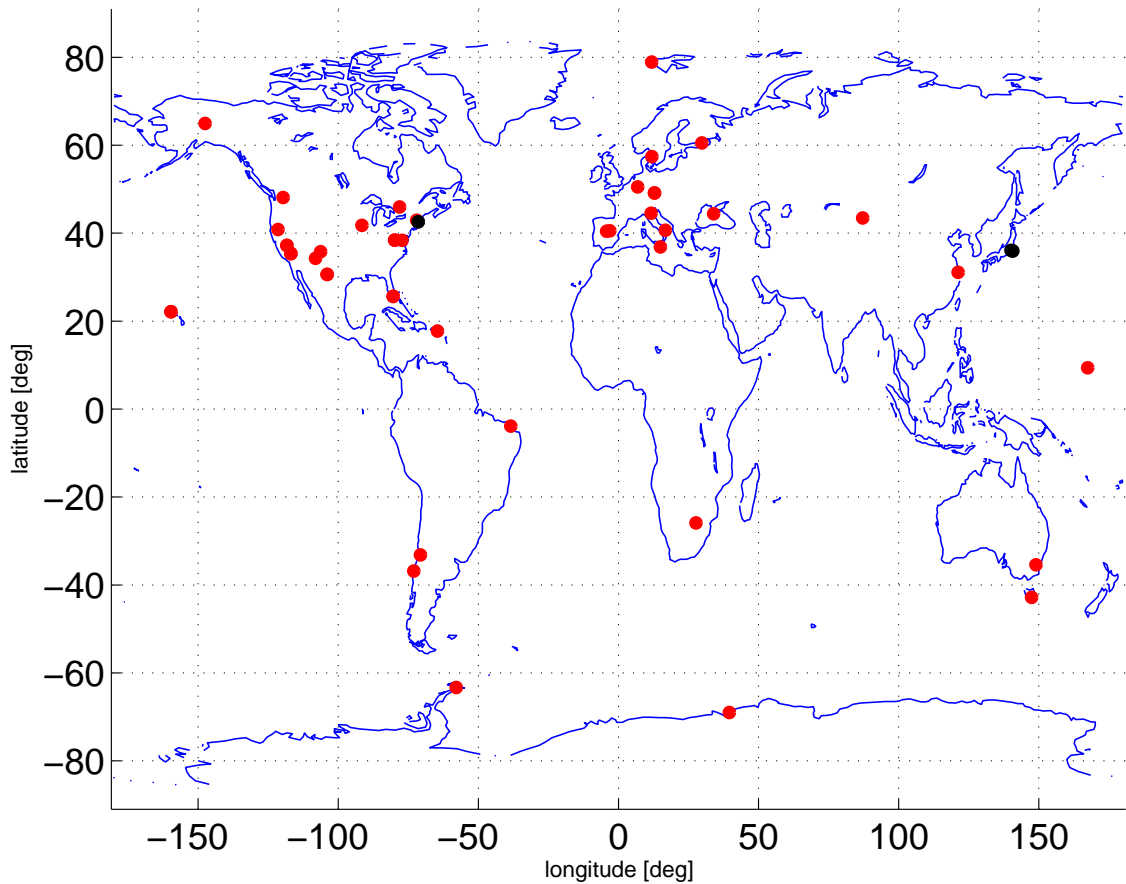


Figure 1. Spatial distribution of VLBI sites of this study shows an accumulation on the northern and a sparse density of observing sites on the southern hemisphere. Each red dot represents one telescope, each black dot more than one telescope.

deformations of the VLBI antennas. The hydrostatic and wet zenith delays were mapped using isobaric (IMF), Niell (NMF), or Vienna (VMF) mapping functions and elevation cutoff angles varying from 15° to 0° . Tropospheric parameters were modelled as piece-wise linear functions (PWLf) with interval lengths of 1 hour. Tropospheric gradients in N-S and E-W directions were estimated as one offset and 6-hourly rates for each session. All rates were constrained to zero by pseudo-observations with empirically determined small weights to prevent the normal equation matrix from singularity.

3. Determination of linear trends

The long time series - some stations have observed for more than twenty years - were analysed solving for offset, linear trend, and annual and semi-annual harmonic functions (equ. 1). Formal errors were considered, too. All estimated parameters are significant; the size of the coefficients extends their standard deviations by far. The results for station Wettzell, Germany are given in tables 1 and 2.

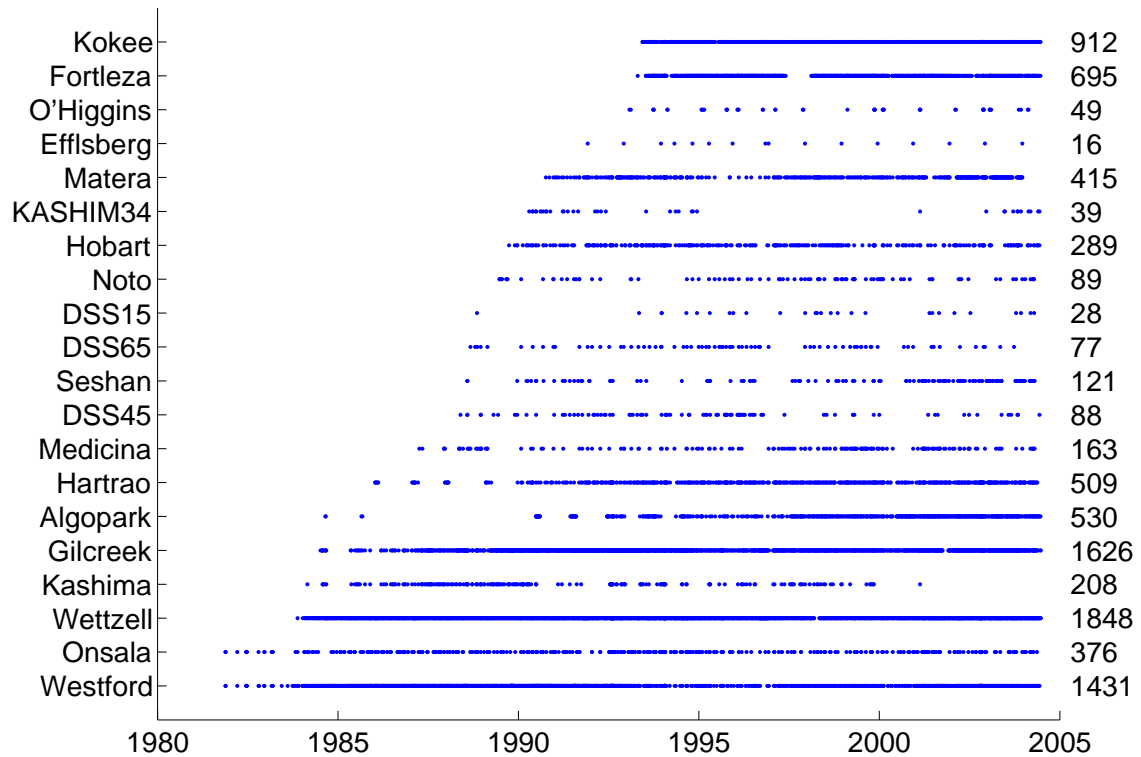


Figure 2. Most prominent VLBI sites and their observational history. The numbers at the right side of the figure denote the total numbers of observed sessions used for this study. Each blue dot represents one 24h-session.

$$F(t) = x_0 + x_1 \cdot t + x_2 \cdot \sin(\omega_1 \cdot t + \varphi_1) + x_3 \cdot \sin(\omega_2 \cdot t + \varphi_2) \quad (1)$$

x_i, φ_i coefficients determined by least-squares fit
 ω_i periods set to $1y, \frac{1}{2}y$, respectively.

Wettzell and some other stations provide long and stable time series. The trends of these stations are rather reliable and the seasonal coefficients disagree only slightly, also when comparing the time series submitted by various IVS Analysis Centers (fig. 3). Stations with longer gaps in their observational history or with a few observations only still show very good agreement of seasonal terms and offset, but their linear trends tend to disagree.

4. Outlook

It has to be investigated which additional effects and errors influence the long-term characteristics of tropospheric parameters from VLBI. From the mathematical point of view the role of outliers, the temporal inhomogeneity of the particular time series and the computational method for the trend have to be studied in more detail to finally set up a combination procedure of long time series of tropospheric parameters. These combined time series will be the basis for climatological interpretation.

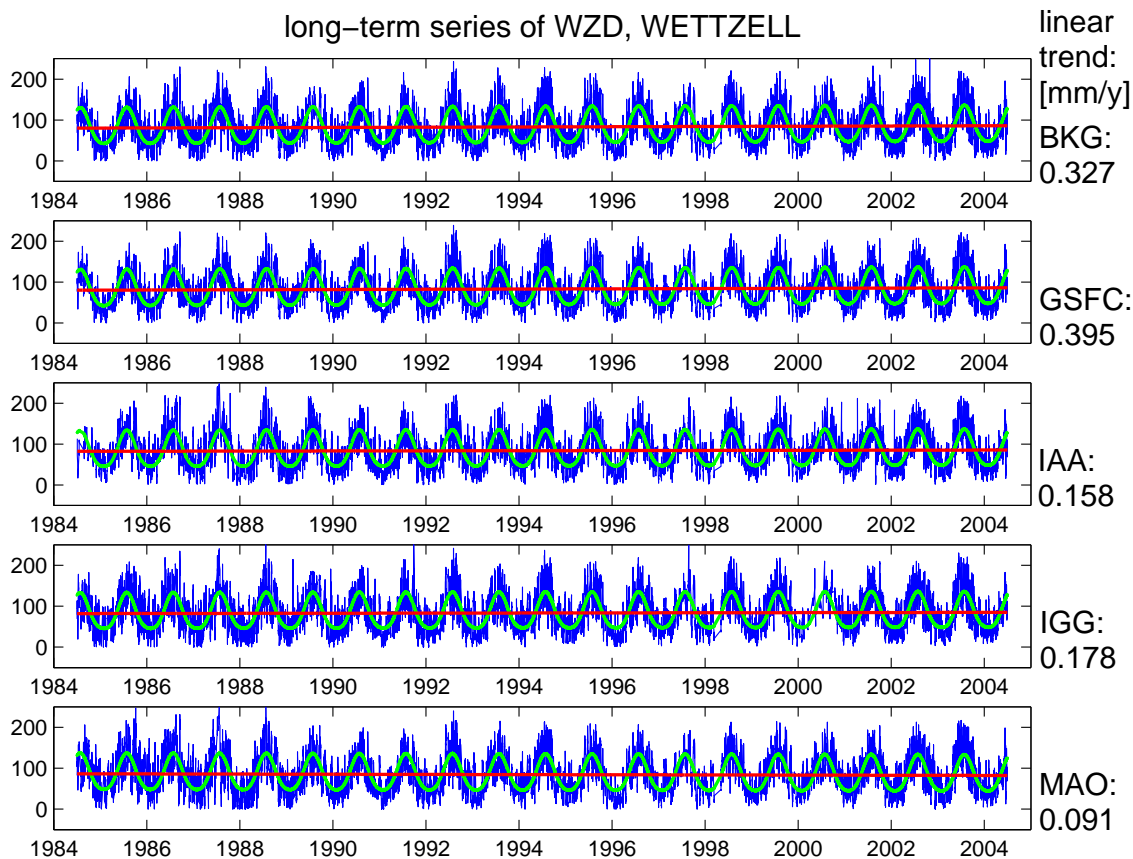


Figure 3. Long time series of WZD from different IVS Analysis Centers at Wettzell, Germany in mm. Time span: 1984.5 - 2004.5. Annual and semi-annual harmonics and offsets agree very well, while the trends slightly disagree. The blue lines signify the WZD estimates, green curves represent an approximation by seasonal terms, and the red line shows the linear trend in mm/y.

5. Acknowledgements

The following agencies are acknowledged for providing their time series of tropospheric parameters: Bundesamt für Kartographie und Geodäsie (BKG), Leipzig, Germany, Goddard Space Flight Center (GSFC), Greenbelt, USA, Institute of Applied Astronomy (IAA), St. Petersburg, Russia, Main Astronomical Observatory (MAO), Kiev, Ukraine, and Deutsches Geodätisches Forschungsinstitut (DGFI), Munich, Germany. Thanks to the IVS and its member institutions. We are very grateful to the Austrian Science Fund (FWF) for supporting our work by research project P16992-N10.

	ITRF2000		VTRF2003		DGFI-TRF	
radial velocity	-0.97 [mm/y]		-1.09 [mm/y]		-1.13 [mm/y]	
	WZD	TZD	WZD	TZD	WZD	TZD
fixed station coordinates	IGG: +0.104	IGG: -0.051	IGG: -0.104 IAA: 0.158	IGG: -0.261 IAA: -0.087		
NNR/NNT conditions ('free adjustment')	IGG: -0.738 GSFC: +0.293 MAO: -0.203	IGG: -0.894 GSFC: +0.040 MAO: -0.436	IGG: -0.923 BKG: +0.292	IGG: -1.079 BKG: +0.016	DGFI: +0.418	DGFI: +0.122

Table 1. Linear trend of wet zenith delays (WZD) and total zenith delays (TZD) using various TRF and applying different analysis strategies at Wettzell, Germany in mm/y. The acronyms of the Analysis Centers can be seen from the acknowledgements.

	VMF		NMF		IMF	
cutoff elevation angle	WZD	TZD	WZD	TZD	WZD	TZD
0°	+0.103	-0.052	+0.084	-0.059	+0.041	-0.103
5°	+0.104	-0.051	+0.084	-0.059	+0.042	-0.102
10°	+0.125	-0.031	+0.089	-0.049	+0.063	-0.077
15°	-0.079	-0.235	-0.192	-0.322	-0.322	-0.327

Table 2. Linear trend of WZD and TZD using elevation cutoff angles between 0° and 15° and three different mapping functions at Wettzell, Germany in mm/y. All results from IGG. Applying the Vienna Mapping Function (VMF), Niell Mapping Function (NMF), or Isobaric Mapping Function (IMF) influences the determination of long-term trends.

References

- [1] Boehm J., H. Schuh, V. Tesmer, and H. Schmitz-Hübsch: Determination of tropospheric parameters by VLBI as a contribution to climatological studies, In: Proceedings of the 16th Working Meeting on European VLBI for Geodesy and Astrometry, edited by W. Schwegmann and V. Thorandt, Leipzig, Germany, 237-245, May 9-10, 2003
- [2] MacMillan D.: Atmospheric Gradients from Very Long Baseline Interferometry Observations, Geophys. Res. Lett., 22, 1041-1044, 1995
- [3] Niell A.E.: A role for VLBI in Climate Studies, IVS Newsletter, issue 5, May, 2003
- [4] Titov O., V. Tesmer, and J. Boehm: OCCAM v.6.0 Software for VLBI Data Analysis, IVS 2004 General Meeting Proceedings, NASA/CP-2004-212255, 267-271, Ottawa, Canada, 9-11 February, 2004

Homogenization of surface pressure recordings and its impact on long-term series of VLBI tropospheric parameters

Robert Heinkelmann, Johannes Boehm, Harald Schuh

Institute of Geodesy and Geophysics/University of Technology, Vienna

Contact author: Robert Heinkelmann, e-mail: rob@mars.hg.tuwien.ac.at

Abstract

The surface meteorological data recorded at the IVS Network Stations allow to separate the wet zenith delays (WZD) from the total zenith delays (TZD). Thus, climate quantities can be determined such as the integrated precipitable water, which corresponds to the amount of water vapor above a station. The original meteorological data recorded at the stations, however, are contaminated by outliers, missing data points, and breaks due to various instrumental and environmental reasons. In this study we show that discontinuities in the pressure time series significantly tamper the determination of the trends of tropospheric parameters and we present an approved test method to detect and eliminate them.

1. Introduction

One can identify large breaks in any given data set empirically by simply looking at an appropriate visualization of the "contaminated" data set. In simple cases the visual inspection will be sufficient. However, if the number of breaks is considerably high, or the significance has to be tested, a quantification instead of the visual appearance is preferred. In particular, in order to obtain a certain degree of automation of the procedure, an objective decision method has to be considered. The homogenization of meteorological data in climatology has a long history [Peterson et al., 1998]. In most cases the standard normal homogeneity test (SNHT) as applied by Alexandersson [1986] is widely used and taken as a reference in the climate sciences. The method is simple, approved, and allows flexible application.

2. Preparation of reference time series from numerical weather model ECMWF

SNHT uses standardized series of the differences between time series of the candidate site and one or more neighbouring reference sites. It is obvious that the reference time series are to be most homogenous in order not to introduce additional inconsistencies. For the globally distributed VLBI sites a large number of local references or one global reference are required. A global and consistent reference is given by numerical weather models (NWM), e.g. provided by the European Centre for Medium-Range Weather Forecasts (ECMWF): <http://www.ecmwf.int/>. A re-assimilation of meteorological data such as the ERA-40 Reanalysis [Uppala et al., 2004; Haimberger, 2005 and priv. comm.] provides a homogenous pressure reference during most of VLBI observational history from 1979 till the end of 2001 for all VLBI sites. Thereafter the operational data set of the ECMWF maintains equivalent information. From the NWM, which is given on a grid the geopotential height of pressure levels at the VLBI sites can be obtained by bi-linear interpolation between four neighbouring grid points. From the geopotential height a geometrical height, e.g. the

ellipsoidal height can be obtained. To determine the surface pressure at the VLBI antenna with the given height of the next pressure level the hypsometric formula (1) can be used. The pressure data from ECMWF are provided at six hour intervals which can be linearly interpolated to derive reference pressure series at the time of each group delay measurement.

$$p_0 = p \cdot \exp\left(\frac{(h-h_0) \cdot g}{R_d \cdot T_v}\right) \quad (1)$$

$$T_v = T \cdot \frac{p}{p - \left(1 - \frac{M_w}{M_d}\right) \cdot e}, \text{ virtual temperature [K] ,}$$

p_0 pressure referring to height h_0 [hPa] ,
 p given pressure referring to height h [hPa] ,
 g gravitational acceleration [m s^{-2}] ,
 R_d specific gas constant [$\text{Pa m}^3\text{K}^{-1}\text{g}^{-1}$] ,
 $M_{d,w}$ molar mass of dry constituents of atmosphere, resp. water [g mol^{-1}] ,
 T absolute temperature at height h [K] ,
 e relative humidity [%] .

3. Height reference of the pressure records

The surface pressure corresponds to the mass of the atmosphere above the sensor, thus every pressure measurement refers to a certain height. The height reference of the raw pressure readings from VLBI stations is usually given for the height of the pressure sensor above the geoid. To obtain the pressure at the VLBI reference point (VRP) the raw pressure records have to be referred to the height of the VRP using equation (1). Considering the spatial and temporal interpolation necessary to obtain the reference pressure series we expect the mean value of the original time series with reference to the VRP to be more reliable. Hence, the reference time series mean level is adjusted to the mean level of the original pressure series referring to the VRP after an outer control.

4. Standard normal homogeneity test (SNHT) method

After the original and reference time series have been prepared, the residual time series is obtained by forming the difference:

$$q_i = (p_0)_i - \hat{p}_i \quad (2)$$

$(p_0)_i$ denotes the original pressure series and
 \hat{p}_i the mean adjusted reference pressure series .

Large outliers should be eliminated e.g. by an $k\sigma$ -criterion outlier elimination (with $k \approx 5$) in a next step to prevent the further calculations from distortions. Standardizing the residual time series

$$z_i = (q_i - \bar{q}) / \sigma_q \quad (3)$$

allows the simple formulation of the two hypotheses characterizing the test of a single shift of the mean:

$$\begin{array}{ll} \text{Null hypothesis} & H_0: z_i \in N(0, 1) \quad i \in \{1, \dots, n\}, \quad n: \text{length of time series}, \\ \text{Alternative hypothesis} & H_1: z_i \in N(\mu_1, 1) \quad i \in \{1, \dots, a\}, \\ & z_i \in N(\mu_2, 1) \quad i \in \{a + 1, \dots, n\}. \end{array}$$

With the test quantity

$$T(a) = a \cdot (\bar{z}_1)^2 + (n - a) \cdot (\bar{z}_2)^2 \quad (4)$$

the decision between the two hypotheses can be taken on an objective basis,

$$\begin{array}{ll} a & a \in \{1, \dots, n\} | T(a) = \max [T(a)], \text{ most probable break}, \\ \bar{z}_{1,2} & \text{mean value before resp. after } a. \end{array}$$

If the maximum of T is significant, a will denote the time of the shift and the break will be corrected with $\bar{z}_{1,2}$. For the significance of the break critical levels are given [Tuomenvirta et Alexandersson 1996] but they have to be adopted to the very much larger number of observations n in our case. The presence of a break should be verified then by using meta data (dates of replacement, relocation, calibration, etc.) of the pressure sensor. If a break has been successfully detected it can be easily removed keeping the overall weighted mean by adjusting the mean values before and after the break, or it can be removed from the part before the break, keeping the mean value of the current readings. The procedure can be repeated by iterative determination of (4) from the adjusted series and further breaks can be removed. The SNHT can also be used for other purposes like testing a shift in the standard deviation, or a trend in the mean level. Alexandersson et Moberg [1996] suggest that short trend intervals should be handled as abrupt breaks. Besides the application for the homogenization of surface pressure the test can be applied to any time series, in particular residual time series, which don't suffer from large systematically changes of the mean level, e.g. clock breaks, shifts due to episodic motions in the time series of station positions, etc.. Figure 1 shows examples of detected breaks of surface pressure recordings from VLBI sites.

5. Impact of breaks on the tropospheric parameters

From the homogenized pressure data the wet zenith delays (WZD) are affected, while the total zenith delays (TZD) remain almost constant. Referring the pressure at the VLBI reference point (VRP) changes the absolute values of the WZD: A height correction of $\Delta h = 1m$ is equivalent to a pressure correction of $\Delta p \approx 0.13hPa$. A pressure correction of $\Delta p = 1hPa$ results in a change of the wet zenith delay of $\Delta WZD \approx 2.7mm$. The correction of breaks of the pressure series leads

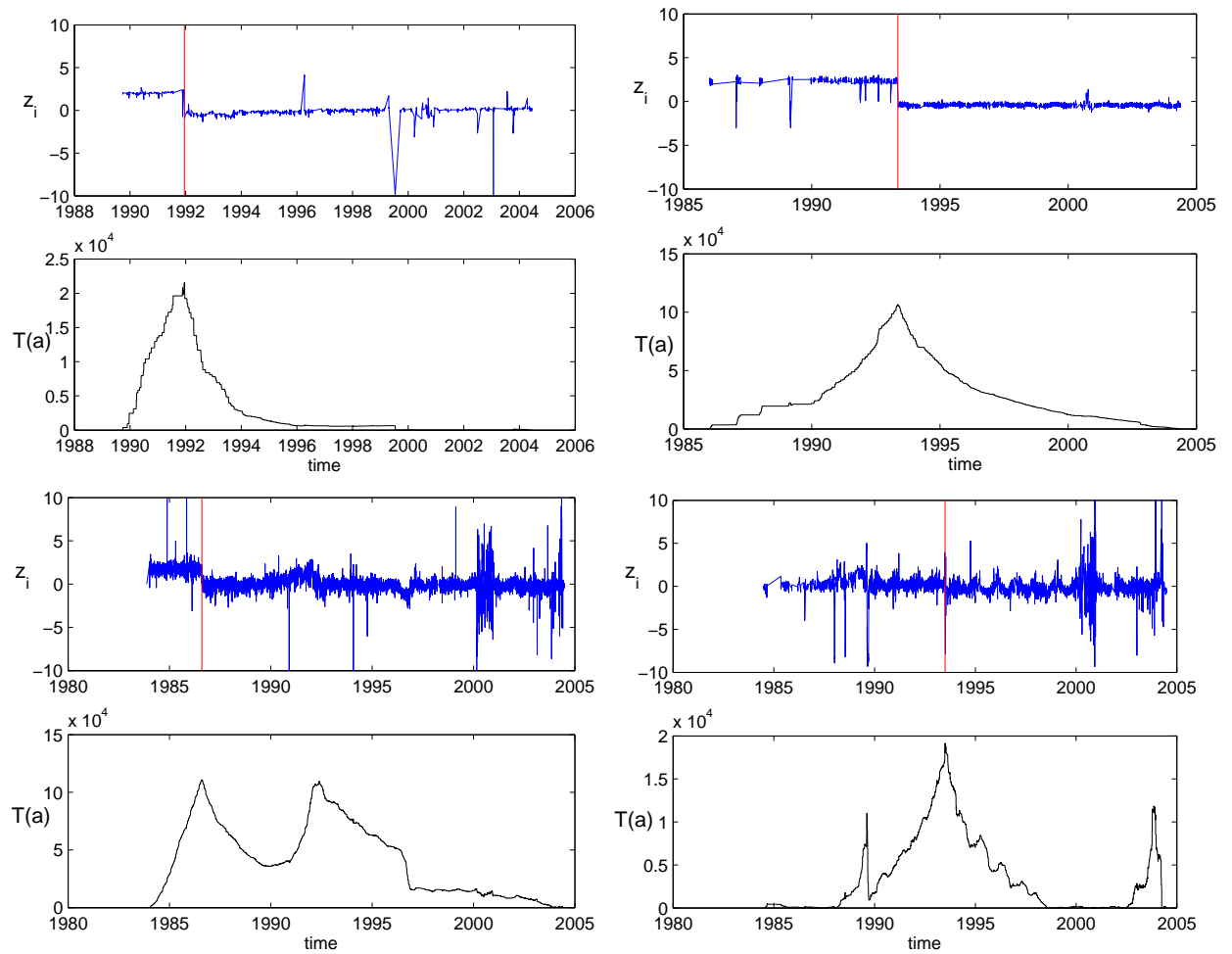


Figure 1. The SNHT applied to pressure series of four stations. In the upper figures blue lines denote the residual time series q_i , the red lines the most probable breaks at time a and the black curves in the plots below display the corresponding test quantity T . Detected breaks: Hobart, Tasmania (top, left), 1991-12-11, $\Delta p = 17.4$ hPa, Hartebeesthoek, South Africa (top, right), 1993-05-04, $\Delta p = 14.0$ hPa, Wetzell, Germany (bottom, left), 1986-08-07, $\Delta p = 1.9$ hPa, and Gilmoore Creek, Alaska (bottom, right), 1993-06-26, $\Delta p = 1.4$ hPa. The two upper breaks are extreme in size, but all are highly significant and have to be corrected. The test function of Wetzell shows two peaks almost similarly large. Obviously the test for a single shift also could be used to detect more than one break at the same time. The second break refers to a short interval trend rather than to a shift. Treating short interval trends in the same way as shifts does not tamper the trend determined from wet zenith delays. The test statistics at Gilmoore Creek shows some small systematic (seasonal) effects, which don't disturb the test, thus proving its robustness. If the systematic effects exceed a certain level relative to the size of the break, they have to be eliminated in order to find shifts of the same size or smaller. The residual time series can be used to identify outliers, too. These outliers and the missing values can be easily replaced by the corresponding values from the adjusted reference series.

to a different trend of the wet zenith delays. How strong the trend varies, depends on the size and position of the break in the time series and cannot be generalized. Figure 2 shows an example.

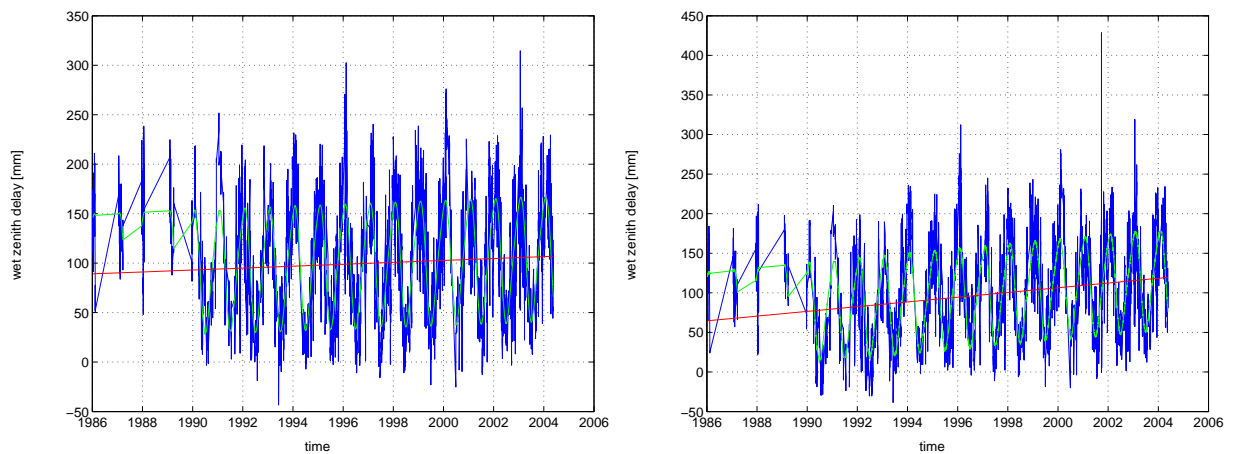


Figure 2. Impact of a break at trends determined from wet zenith delays at Hartebeesthoek, South Africa. The left plot displays the trend using homogenized pressure data, trend = 1.0 mm/y, the right plot using original pressure data, trend = 3.0 mm/y. The trends from total zenith delays (not displayed) were almost stable at 0.9 mm/y.

References

- [1] Alexandersson H.: A Homogeneity test applied to Precipitation Data, *Journ. of Clim.*, Vol. 6, pp. 661-675, 1986
- [2] Alexandersson H. and A. Moberg: Homogenization of Swedish Temperature Data. Part I: Homogeneity Test for Linear Trends. *Int. Journ. of Clim.*, Vol. 17, pp. 25-34, 1997
- [3] Boehm, J., H. Schuh, V. Tesmer, and H. Schmitz-Hübsch: Determination of tropospheric parameters by VLBI as a contribution to climatological studies, In: *Proceedings of the 16th Working Meeting on European VLBI for Geodesy and Astrometry*, edited by W. Schwegmann and V. Thorandt, Leipzig, Germany, pp. 237-245, May 9-10, 2003
- [4] Haimberger L.: Homogenization of Radiosonde Temperature Time Series using ERA-40 Analysis Feedback Information, ERA-40 Project Report Series No. 22, European Centre for Medium Range Weather Forecasts, Reading, England, February, 2005
- [5] Niell A.E.: A role for VLBI in Climate Studies, *IVS Newsletter*, issue 5, p. 5, May, 2003
- [6] Peterson T.C., D.R. Easterling, T.R. Karl, et al: Homogeneity Adjustments of In Situ Atmospheric Climate Data: A Review, *Int. Journ. of Clim.*, Vol. 18, pp. 1493-1517, 1998
- [7] Tuomenvirta H. and H. Alexandersson: Review on the Methodology of the Standard Normal Homogeneity Test (SNHT), In: *Proceedings of the 1st Seminar for Homogenization of Surface Climatological Data*, edited by the Hungarian Meteorological Service, Budapest, Hungary, pp. 35-45, 6-12 October, 1996
- [8] Uppala, S.M., P.W. Kallberg, A.J. Simmons, et al: The ERA-40 Reanalysis, submitted for publication to *Q.J.R. Meteorol. Soc.*, 2004

Combination of tropospheric parameters within IVS project TROPO

Robert Heinkelmann, Johannes Boehm, Harald Schuh

Institute of Geodesy and Geophysics/University of Technology, Vienna

Contact author: Robert Heinkelmann, e-mail: rob@mars.hg.tuwien.ac.at

Abstract

Since January 2002 tropospheric parameters have been combined on a weekly basis at the Institute of Geodesy and Geophysics (IGG), Vienna. The results from individual solutions agree within a few mm, but differ in bias and standard deviation. Recently the IVS tropospheric combination was extended by two more contributions, the new axis offsets were considered in the analysis, and a new tropospheric product webpage was set up at the IGG.

1. Introduction

Goal of IVS project TROPO is to provide tropospheric parameters from VLBI:

- total zenith delays (TZD),
- wet zenith delays (WZD),
- total N-S and E-W tropospheric gradients (GRN, GRE),
- and their standard deviations.

Within four weeks after the correlation process each participating IVS Analysis Center (AC) solves for tropospheric parameters from IVS-R1 and IVS-R4 sessions, which usually take place every Monday and Thursday and submits its estimates to one of the IVS Data Centers. Then the tropospheric parameters are combined on the result level to an IVS weekly solution adding the files from eight ACs together. In a two-step procedure appropriate weights are obtained to determine the combined IVS solution for each station (fig. 1).

2. Intra-comparison of tropospheric parameters

The ACs are not restricted in the choice of analysis options. The only agreement is to deliver total and wet zenith delays with one hour resolution. To obtain the tropospheric parameters at integer hours of each session, piece-wise linear functions (PWLF) estimates are linearly interpolated or stochastic process results are averaged by the ACs, respectively. Despite of the variety of analysis options the tropospheric parameters agree within a few mm in terms of bias and standard deviation (fig. 2). Possible causes for the remaining differences might be:

- different clock models,
- different analysis options,
- different geophysical and astrometric models,

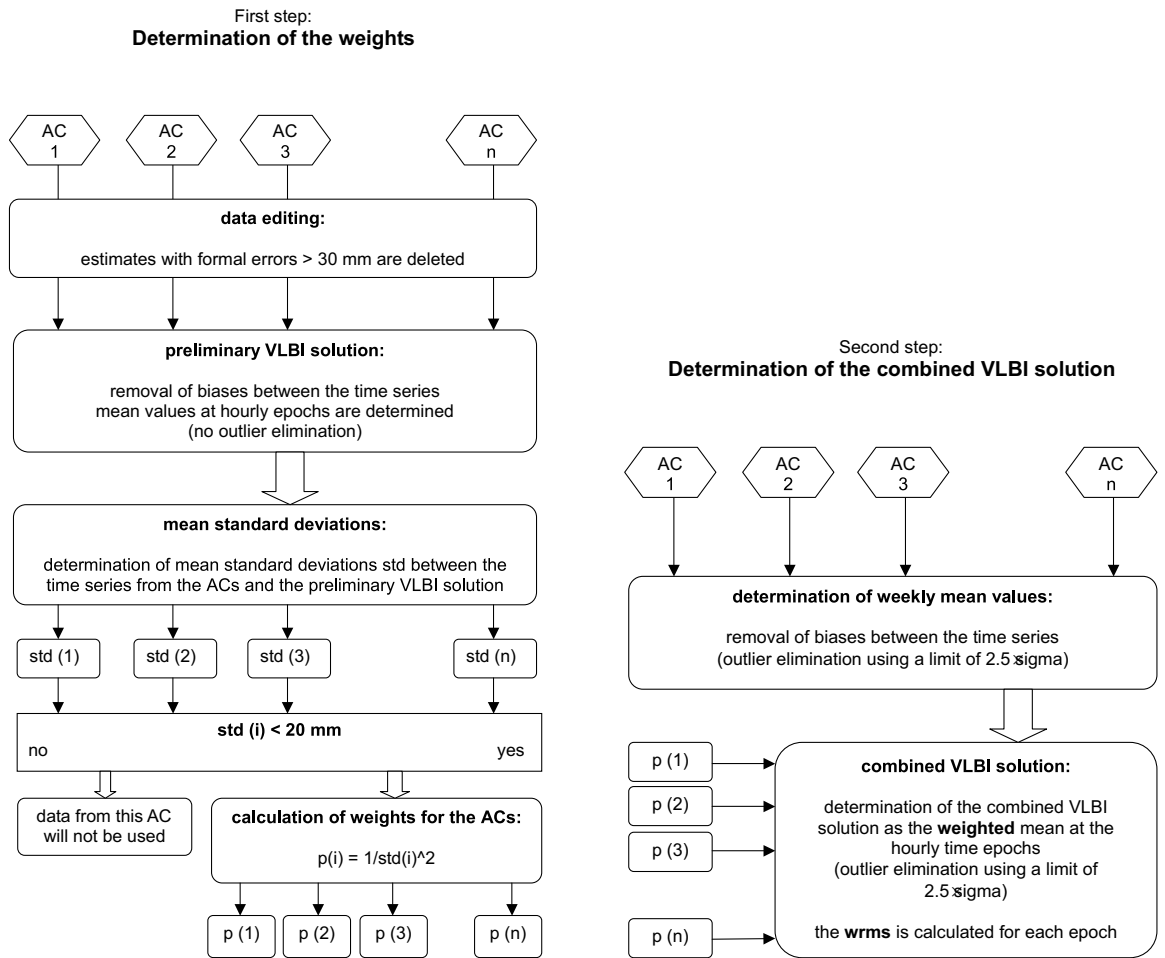


Figure 1. Combination strategy of tropospheric parameters at IGG: In a two-step approach the weights are obtained (left) to determine the final combined IVS solution (right). The flow charts are taken from Schuh and Boehm [2003b].

- erroneous or inhomogenous surface pressure data,
- errors of the terrestrial reference frames (TRF), in particular, if coordinates are fixed,
- different analysis software packages and versions,
- different observations (elevation cutoff angle, outlier elimination) and their treatment (down-weighting of low observations),
- different models of the tropospheric parameters (Gauss-Markov model, Kalman filter, least-squares filter).

	BKG	CGS	CNR	GSFC	IAA	IGG	MAO	OSO
software	Calc/Solve	Calc/Solve	Calc/Solve	Calc/Solve	Occam	Occam	SteelBreeze	Calc/Solve
elevation cut-off angle	5°	3°	5°	3°	0°	5°	0°	5°
downweighting of low obs.	no	no	no	no	yes \leq 10°	no	no	no
TRF	VTRF2003	ITRF2000	ITRF2000	ITRF2000	VTRF2003	ITRF2000	ITRF2000	ITRF2000
treatment of TRF	NNT/NNR	NNT/NNR	NNT/NNR	NNT/NNR	fixed station coordinates	fixed station coordinates	NNT/NNR	fixed station coordinates
mapping function	NMF	NMF	NMF	NMF	VMF	VMF	MTT/NMF	NMF
hydrostatic delay a priori	Saastamoinen	Saastamoinen	Saastamoinen	Saastamoinen	Saastamoinen	Saastamoinen	Saastamoinen	Saastamoinen
delay model	PWLF	PWLF	PWLF	PWLF	Kalman filter	PWLF	least-squares filter	PWLF
constraint rate	50 psec/h	50 psec/h	50 psec/h	50 psec/h	no	20 mm/h ^{1/2}	2.56 cm ² /h	20 mm/h ^{1/2}
gradient resolution	24h	3h	24h	8h	1h	6h	1h	6h
gradient a priori	no	no	no	dry+wet GSFC/DAO	no	no	no	no
gradient model	PWLF	PWLF	PWLF	PWLF	offset	PWLF	least-squares filter	PWLF
constraint rate	0.5 mm/d	2.0 mm/d	2.0 mm/d	2.0 mm/d	no	0.4 mm/d	8.64 mm ² /d	2.0 mm/d
constraint offset	0.5mm	5.0mm	0.5mm	0.5mm	10mm	no	no	2.0mm

Table 1. Analysis options for the determination of tropospheric parameters by the eight ACs mentioned in the acknowledgements. All a priori hydrostatic delays are obtained with the modified formula of Saastamoinen as presented in the IERS Conventions 2003. The dry and wet a priori gradients are obtained using forecast data from the NASA Goddard Space Flight Center Data Assimilation Office (GSFC/DAO).

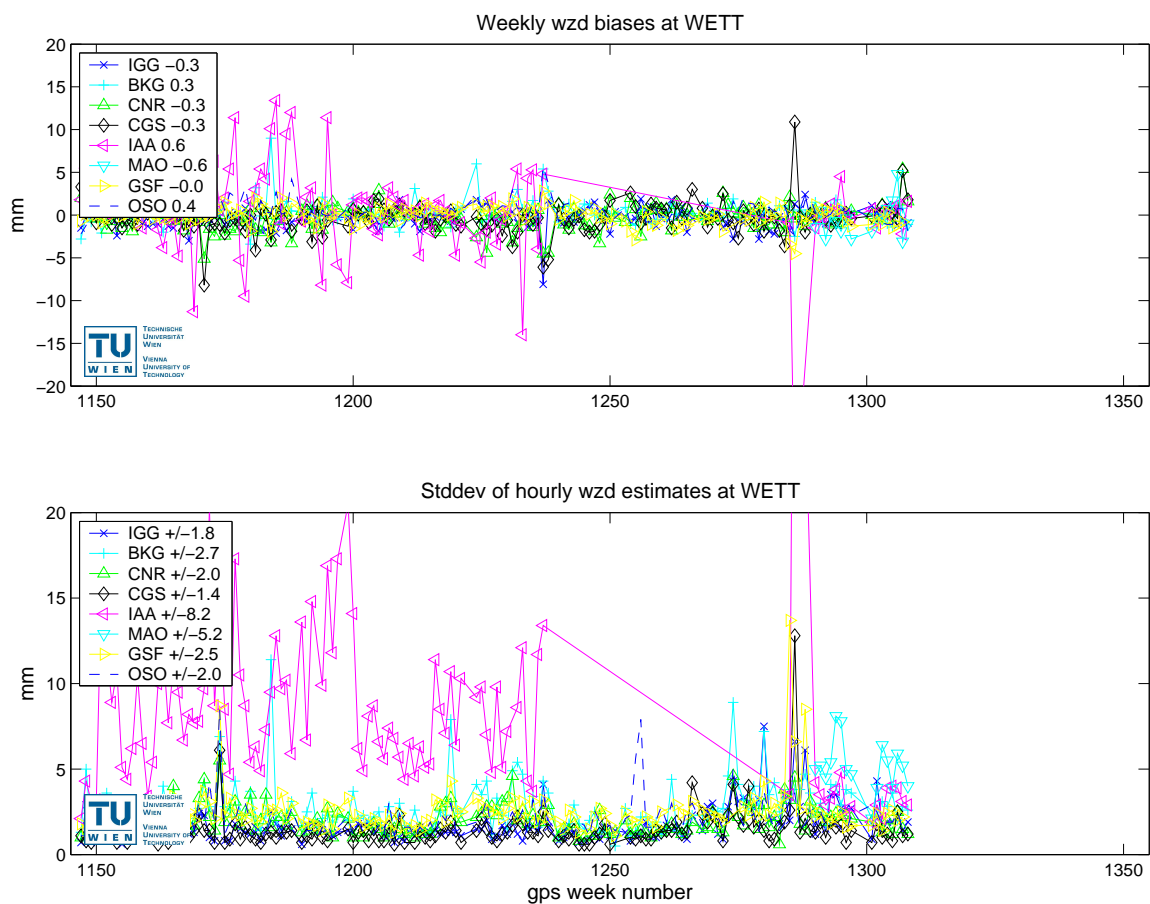


Figure 2. Bias and standard deviations of wet zenith delays (WZD) at Wetzell, Germany since the beginning of 2002. The IAA solution using the QUASAR software (until GPS week 1234) and the IAA solution using the OCCAM software (after GPS week 1286) have to be distinguished.

3. Recent developments and outlook

- 2004-09-01: The Main Astronomical Observatory (MAO), Kiev, Ukraine, joined the project and the Institute of Applied Astronomy (IAA), St. Petersburg, Russia, rejoined after about one year break, now using the OCCAM software instead of the QUASAR VLBI package. The two new contributions are of particular importance for the combination due to the application of an additional software (Steelbreeze), a second solution with the OCCAM package, and additional models of the tropospheric parameters (Kalman filter, least-squares filter).
- 2005-01-21: New axis offsets were published by the IVS Analysis Coordinator, which had to be considered for the determination of tropospheric parameters due to the correlations between the zenith delays and the vertical site positions (mean correlation = -0.4). The ACs were asked to apply the new axis offsets in their analysis.
- At the IGG a combination webpage has been set up <http://www.hg.tuwien.ac.at/~ivstrop> holding plots and reports of the individual and combined IVS tropospheric products.

- It is planned to compare and combine tropospheric gradients, too, and to establish an automated outlier warning system.

4. Acknowledgements

The following agencies are acknowledged for providing their tropospheric parameters: Bundesamt für Kartographie und Geodäsie (BKG), Leipzig, Germany, Istituto di Radioastronomia (CNR), Bologna, Italy, Centro di Geodesia Spaziale (CGS), Matera, Italy, Goddard Space Flight Center (GSFC), Maryland, USA, Institute of Applied Astronomy, St. Petersburg, Russia, Main Astronomical Observatory (MAO), Kiev, Ukraine, and Onsala Space Observatory (OSO), Onsala, Sweden. Thanks to the IVS and its member institutions. We are very grateful to the Austrian Science Fund (FWF) for supporting our work by research project P16992-N10.

References

- [1] Boehm J. and H. Schuh: Vienna Mapping Functions in VLBI analyses, *Geophys. Res. Lett.*, 31, L01603, doi:10.1029/2003GL018984, 2004.
- [2] Gendt G.: Comparison of IGS tropospheric estimates, In: *Proceedings of the IGS Analysis Center Workshop*, edited by R.E. Neilan, P.A. van Scoy, J.F. Zumberge, Silver-Spring, USA, March 19-21, 1996
- [3] Schuh H., J. Boehm, G. Engelhardt, D. MacMillan, R. Lanotte, P. Tomasi, M. Negusini, I. Vereshchagina, V. Gubanov, and R. Haas: Determination of Tropospheric Parameters within the new IVS Pilot Project, In: *International Association of Geodesy Symposia 128*, edited by F. Sanso, pp. 125-130, Sapporo, Japan, June 30 - July 11, 2003
- [4] Schuh H. and J. Boehm: Determination of Tropospheric Parameters Within the new IVS Pilot Project, In: *Proceedings of the 16th Working Meeting on European VLBI for Geodesy and Astrometry*, held at Leipzig, May 9-10, 2003, edited by W. Schwegmann and V. Thorandt, Bundesamt für Kartographie und Geodäsie, Frankfurt/Leipzig, pp. 257 - 264, 2003a.
- [5] Schuh H. and J. Boehm: IVS Pilot Project - Tropospheric Parameters, *sterreichische Zeitschrift für Vermessung & Geoinformation*, Heft 1/2003, pp. 14-20, Wien, sterreich, 2003b.
- [6] Schuh H. and J. Boehm: Status Report of the IVS Pilot Project - Tropospheric Parameters, In: *International VLBI Service for Geodesy and Astrometry 2002 Annual Report*, edited by N.R. Vandenberg, K.D. Baver, NASA/TP-2003-211619, pp. 261-264, 2003c.

Water vapour content and variation estimated at European VLBI sites

Monia Negusini, Paolo Tomasi

Istituto di Radioastronomia, INAF, Bologna, Italy

Contact author: Monia Negusini, e-mail: negusini@ira.cnr.it

Abstract

Space geodetic techniques are proving to be a powerful tool for supplying additional information for climate change and global warming studies. Water vapour is an important greenhouse gas that can be monitored using VLBI observations. VLBI can determine its decennial behaviour through computation of time series of troposphere parameters. The estimates of Zenith Total Delay (ZTD) and Zenith Wet Delay (ZWD) from 2000 till 2004 using all databases available at the IVS Data Centre are presented. On this time span, VLBI-derived ZTDs have been compared with analogous GPS-derived estimates. In order to validate VLBI results, Integrated Precipitable Water Vapour (IPWV) obtained using VLBI observations performed at Medicina station has been compared to IPWV derived by radiosoundings. Furthermore, long time series of VLBI-derived ZWD values have been computed at European sites using the datasets stored at our analysis center since 1987, thus spanning a 17 years period.

1. Introduction

Space geodetic techniques are proving to be a powerful tool for supplying additional information for climate change and global warming studies. One of the most important greenhouse gases is water vapour and it can be monitored using VLBI observations. For the VLBI data analysis a 5 degrees elevation cut-off angle and Niell mapping functions are used. The solution is computed into ITRF2000 without fixing the stations' coordinates, using a no-net-translation constraint. One total and one wet zenith delay parameter per hour for all the stations involved into the experiment and only one value for both east and north gradient per station per session are computed. Our Analysis Center participates to the IVS TROP project on Tropospheric Parameters, submitting the estimates of tropospheric parameters for all IVS-R1 and IVS-R4 experiments. The data submitted by the different ACs are combined at the IVS Tropospheric Combination Center at IGG in Vienna in order to obtain IVS combined products [1] and, as a feedback, a check on the quality of the solutions.

2. Results of VLBI data analysis of 2000-2004 experiments.

In order to monitor the behaviour of water vapour, we analyzed all the 2000-2004 databases available on the IVS Data Centers, using a set up identical to the one described above. As a product of this analysis we obtained tropospheric parameters for each station and for every experiment available in our catalogue and the relevant time series. In Figure 1 the total and wet zenith path delay time series for some selected European VLBI stations are shown. For Wettzell we have quite a continuous time series unlike other stations, such as Medicina or Onsala, where very sparse data are present. A strong annual signal is easily recognized at each station and it

is highly related to the variation of the wet component of the delay. This has been confirmed by spectral analysis performed on each time series.

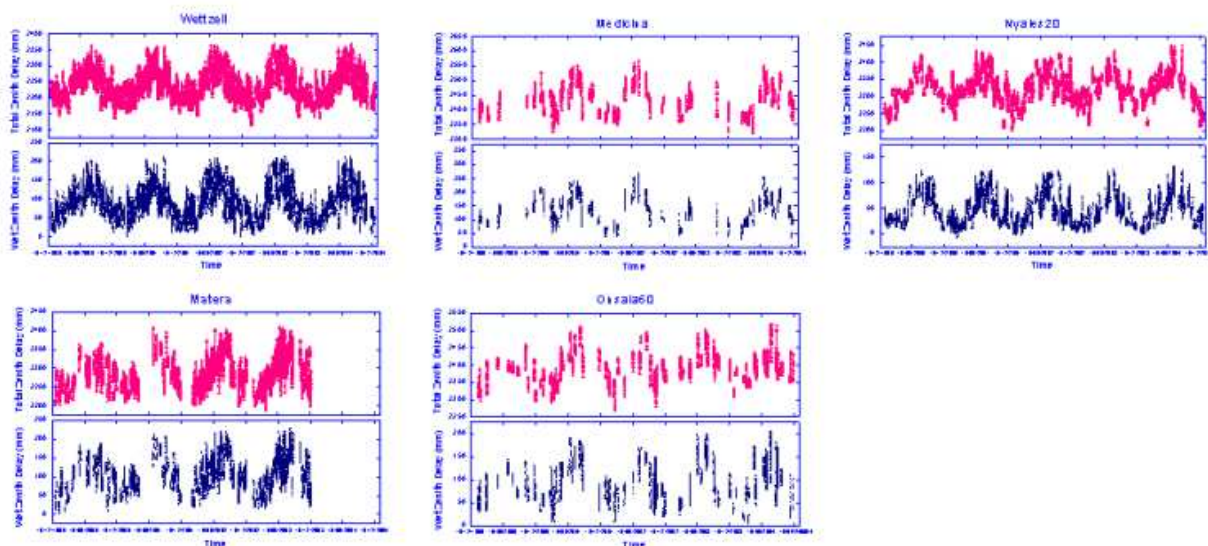


Figure 1. **Total (up) and Wet (down) zenith delay time series for: Wettzell, Medicina, Nyales20, Matera and Onsala60, respectively.**

3. Post-processing of the time series

The time series of zenith path delay for the stations present in this analysis is an interesting set of data that can be compared with the results coming from independent techniques, like GPS. For that we decided to carry out a comparison between the VLBI-derived ZTDs values and the analogous GPS-derived estimates at co-located sites. We used GPS data available on the web site of the CODE Analysis Center and in particular the COE EUREF daily solutions, where the troposphere parameters have 1-hour resolution and, thus, they are directly comparable with the parameters computed by our VLBI data analysis. For stations not included into EUREF analysis we used the COD solutions, where every 2-hour parameters were estimated. As an example we plotted in Figure 2 Wettzell time series, both VLBI and GPS, and the seasonal signals highlighted by spectral analysis, performed in order to derive the properties of the dominant signals. We computed amplitudes and phases by means of a best-fit wave. VLBI and GPS seasonal signals have quite the same amplitudes and phases. For VLBI we found a period of 365 ± 4 days and for GPS 356 ± 2 days. For the amplitude we found 45.4 ± 0.8 mm for VLBI and 45.7 ± 0.4 mm for GPS. Similar behaviour has been found for the other stations.

Since signals present in both VLBI and GPS data were comparable, we computed the differences between the two time series and we obtained the relevant residuals, for all the stations. A bias is present on all series and it is most probably related to GPS data analysis strategy. For this reason, we looked into different GPS solutions' setups in order to explain the meaning of this bias. Figure 3 shows the results for Wettzell. The cut-off angle seems to have a major impact on results.

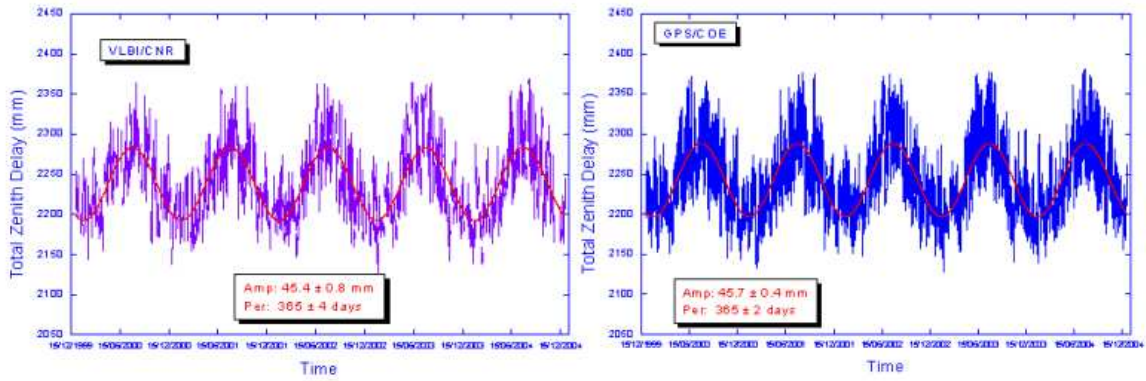


Figure 2. VLBI (left) and GPS (right) time series and best-fit annual waves for Wettzell.

The graph on the left represents differences computed between COE (cut-off angle of 15 deg before 01/09/01 and 10 deg after) and VLBI solutions. The graph on the right shows differences between COD (cut-off 10 deg before 19/08/01 and 3 deg after) and VLBI solutions. The difference becomes smaller when a cut-off of 3 degrees is applied. Furthermore, this latter GPS solution is more similar to VLBI: horizontal gradients are estimated once per day.

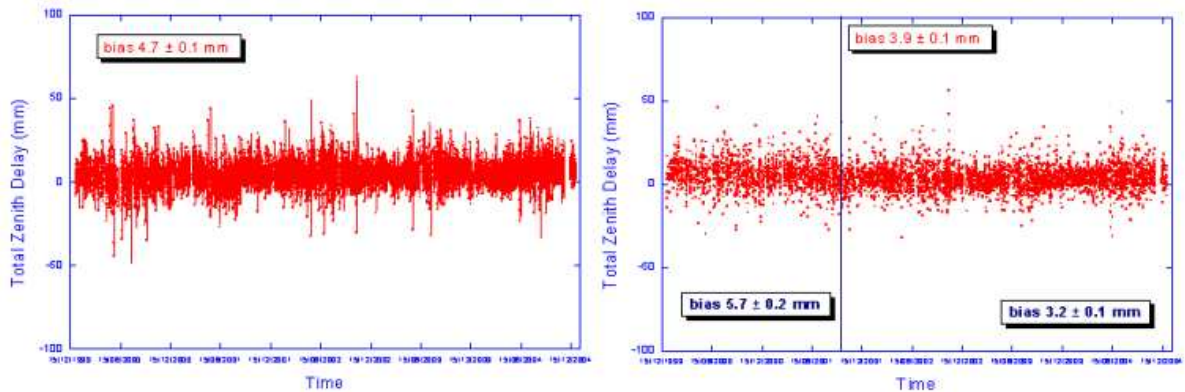


Figure 3. Differences between COE and VLBI solutions (left) and differences between COD (before and after 19/08/01) and VLBI solutions (right) for Wettzell.

One known effect, that has to be taken into account, is the difference in height of the reference points of the different instruments. Thus, for a precise comparison, we have to take into account these differences in height, convert them into differences of tropospheric zenith delay and correct the residuals time series. That is quite easy for the dry component, but not for the wet component. In fact, for the first component we can assume that the delay is a fraction, proportional to the difference in height, of all the dry delay, but that assumption is not true for the wet path delay. Table 1 shows the results for 5 European co-located sites. The first two rows represent the different GPS solutions for Wettzell (COE and COD), respectively. If we take into account only the

COD solution after 19/08/01, a bias of 2.2 ± 0.1 mm can be obtained, after applying the height correction. For Medicina, only COD solution is available and the bias, after 19/08/01 and height correction applied, is again 2.2 ± 0.1 mm. For the other stations, only COE solution is available. Positive biases are still present after height correction for all the stations, indicating that further investigations are needed.

Table 1. Biases between VLBI and GPS tropospheric zenith delay before and after height corrections

VLBI	GPS	Height diff.(m)	Bias(mm)	Bias(mm) b. corr.	Bias(mm) a. corr.
Wettzell	WTZR	3.1	1.0	4.7 ± 0.1	3.7 ± 0.1
Wettzell	WTZR	3.1	1.0	3.9 ± 0.1	2.9 ± 0.1
Medicina	MEDI	17.1	6.3	9.3 ± 0.3	3.0 ± 0.3
Matera	MATE	7.7	2.5	7.3 ± 0.1	4.8 ± 0.1
Nyales20	NYA1	3.1	1.1	5.7 ± 0.1	4.6 ± 0.1
Onsala60	ONSA	13.7	5.1	6.4 ± 0.2	1.3 ± 0.2

4. Comparison with radiosonde data

In order to validate VLBI results, Integrated Precipitable Water Vapour (IPWV) obtained using VLBI observations performed at Medicina has been compared to IPWV derived by radiosoundings, performed in the vicinity of the radiotelescope. To compare the two time series, we transformed the ZWDs into IPWV using a well-known conversion ratio. Figure 4 shows, on the left, the IPWV time series obtained with VLBI and radiosoundings for Medicina station. Radiosoundings are performed every 12 hours at San Pietro Capofiume, approximately 8 km apart from Medicina. The periodic signals are similar in amplitude and phase. There is no bias between the two series that are highly correlated.

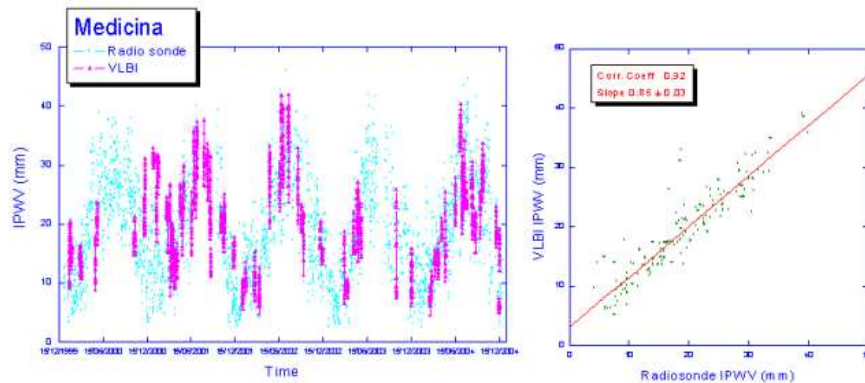


Figure 4. IPWV observed by Radiosonde and VLBI (left) and scatter plot between the two series (right) at Medicina.

5. Long-term time series

Very long-term time series of tropospheric parameters, particularly of wet zenith delay representing the content of water vapor in the atmosphere and one of the greenhouse gases, are useful for meteorological and climatologic studies. Therefore, we decided to analyze all the databases included in our AC catalogue, considering the fact that the time series can go back for about 17 years, including, for the most part, experiments that contain at least three European stations. We re-analyzed all these databases in order to obtain a homogenous set of tropospheric parameters. In Figure 5 there are the results for the wet zenith delay at the station of Wettzell since 1987 till 2004. The series is very uneven and with a strong annual signal. We performed a spectral analysis and fitted the wet delay time series with the annual wave and we subtracted the best-fit wave from the data. On the residual series we computed the linear trend and we obtained any significant variation, -0.08 ± 0.06 mm/yr, not different from our previous results [2]. We performed the same analysis also for the other stations, as shown in Figure 6. The trends are quite different, with both positive and negative values.

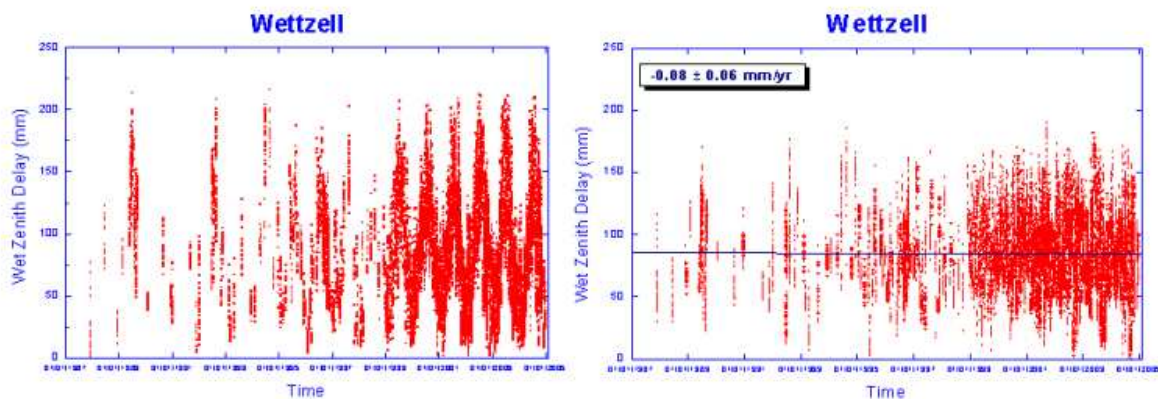


Figure 5. Wet zenith delay time series for Wettzell (left). On the right, residual series after subtracting the estimated annual signal and corresponding trend.

6. Conclusion

VLBI has proved to be an efficient tool for studying contents, trends and variations of atmospheric water vapour. When compared to traditional methods (e.g. radiosoundings) the estimates are very satisfactory, especially when taking into account errors deriving from radiosonde sensors. When compared to other space geodetic techniques (GPS) results appear similar in amplitude and trend. A small bias can be highlighted between GPS and VLBI estimates and its origin can be related, at least, to a couple of causes: the analysis strategy and the height difference between reference points of the two techniques. Long time trends of ZWD computed for European sites show a different behaviour of water vapour content: it is highly dependent on site location. It is not possible to highlight a common behaviour on a European scale.

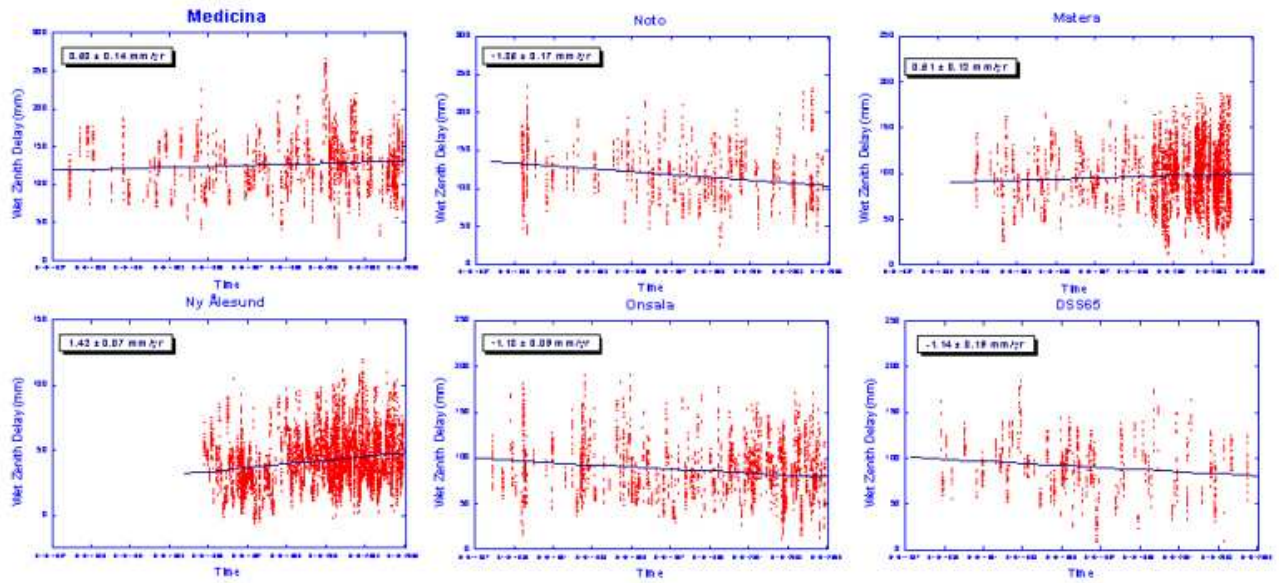


Figure 6. Long time trends obtained subtracting the annual signal from each ZWD time series for some European stations: Medicina, Noto, Matera Nyales20, Onsala60 and DSS65, respectively.

References

- [1] Schuh, H., Boehm J., “Status Report of the IVS Pilot Project - Tropospheric Parameters”, in *International VLBI Service for Geodesy And Astrometry 2002 Annual Report*, edited by N. R. Vandenberg and K. D. Baver, NASA/TP-2003-211619, 13-21, 2002.
- [2] Negusini, M., Tomasi P., “Tropospheric Parameters Estimated by Geodetic VLBI Data”, in: *International VLBI Service for Geodesy and Astrometry 2004 General Meeting Proceedings*, edited by Nancy R. Vandenberg and Karen D. Baver, NASA/CP-2004-212255, 456-460, 2004.

An Investigation of Water Vapor Trends in Europe

Rüdiger Haas, Camilla Granström, Jan Johansson

Onsala Space Observatory, Department of Radio and Space Science, Chalmers University of Technology

Contact author: Rüdiger Haas, e-mail: haas@oso.chalmers.se

Abstract

Long term variations in the amount of tropospheric water vapor are an ongoing and important topic of meteorological research. This is in particular due to the possible drastic consequences for society in connection with global climate change processes. The meteorological community aims at modeling the dynamic processes in the atmosphere. Traditionally, one important input for these models are meteorological observations with radiosonde balloons. Ground based space geodetic techniques like Very Long Baseline Interferometry (VLBI) and the Global Positioning System (GPS) are also sensitive to the amount of tropospheric water vapor. Thus, these techniques promise to be able to add important additional information to the meteorological modeling. To assess this possible contribution of space geodesy to meteorological research, we investigate trends in the amount of water vapor in Europe. For this purpose we use six space geodetic stations in Europe that are collocated with several space geodetic techniques and have relatively close by radiosonde launch sites.

1. Introduction

Possible natural and/or man-made global change effects could have drastic consequences for society (IPPC, 2001,[8]). The European climate could change, e.g. in the future some regions could experience a more wet climate than today, others a more dry climate. Furthermore, the risk for extreme weather events with disastrous consequences might increase. Therefore, it is important to monitor the amount of tropospheric water vapor and to understand the physical processes that determine climate change. This might allow to reduce the possible man-made impact on global change.

Traditionally, the meteorological community uses observations taken by radiosonde (RS) balloons that provide atmospheric profiles of temperature, pressure and humidity as one important data set for the meteorological modeling. One disadvantage of this data set is its relatively sparse distribution in time and space. Figure 1a shows the location of European radiosonde launch sites as black triangles. Usually, RS balloons are launched two to four times per day. Some of the sites that are shown in Fig. 1a are not active anymore, but observational data is available in the archives of the European meteorological agencies.

During the last decades networks of space geodetic techniques have been established in Europe. The black triangles in Figure 1b depict continuously operating ground based GPS sites in Europe. The large black symbols with a white star on black ground show space geodetic sites with collocated GPS and VLBI equipment. Some of these collocation sites are also equipped with ground based microwave radiometers and/or equipment for further space geodetic techniques like for Satellite Laser Ranging (SLR), Lunar Laser ranging (LLR) and Doppler Orbitography by Radiopositioning Integrated on Satellite (DORIS). These space geodetic techniques are sensitive to the amount of atmospheric water vapor. Thus, they might possibly contribute to monitoring the atmospheric water vapor content and possible climate change.

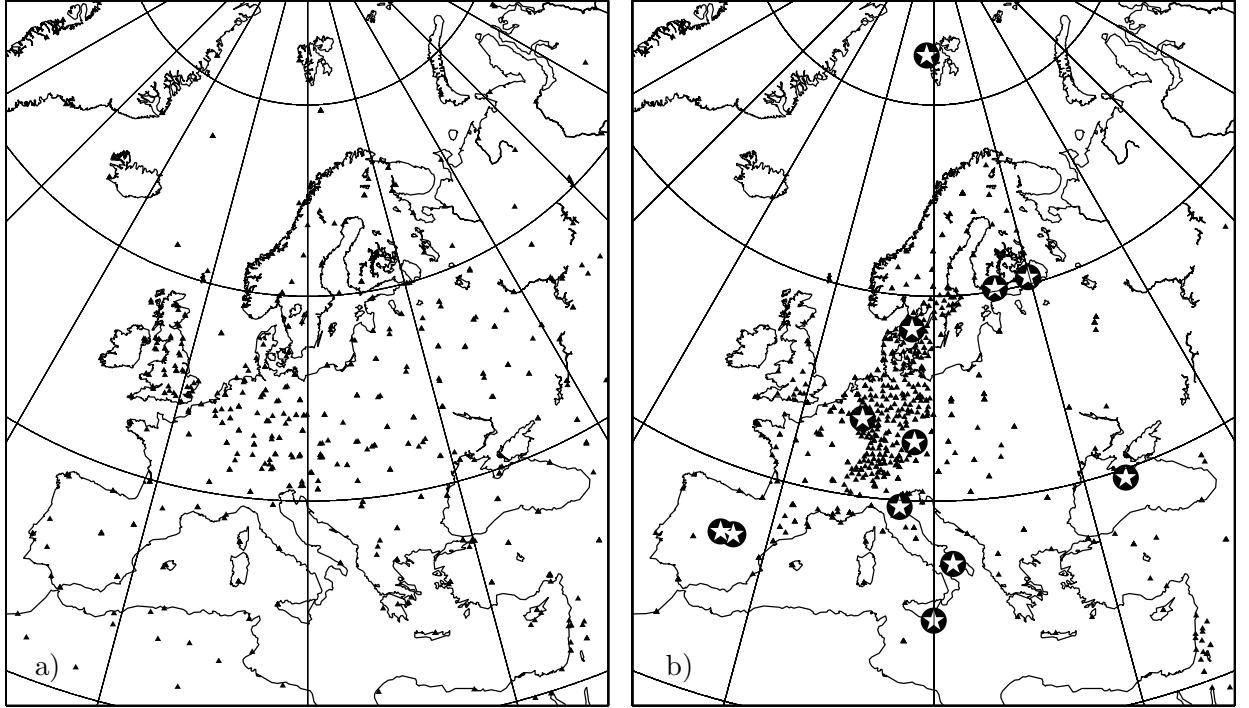


Figure 1. Left: The black triangles represent radiosonde launch sites in Europe. Right: The black triangles represent continuously operating ground based GPS sites in Europe. The large symbols with a white star on black ground show space geodetic sites with collocated equipment. See text for further details.

In the following we concentrate on six European space geodetic stations that are equipped both with VLBI and GPS equipment and also have a radiosonde launch site relatively close by. Table 1 gives an overview about these stations. We combine the atmospheric water vapor results derived with the space geodetic techniques with data obtained by radiosondes. These combined results are compared to the trends in atmospheric water vapor derived from the ERA40 data set [4] of the European Centre for Medium-Range Weather Forecast (ECMWF) [2].

Table 1. The space geodetic stations in Europe with collocated VLBI and GPS equipment and relatively close by RS launch sites that were used for this study.

Station	longitude (°)	latitude (°)	distance to RS
Ny-Ålesund	12.00	78.99	ca. 5 km
Onsala	11.93	57.45	ca. 40 km
Wettzell	12.88	49.15	ca. 170 km
Medicina	11.65	44.52	ca. 10 km
Matera	16.70	40.65	ca. 130 km
Madrid	-4.25	40.43	ca. 70 km

2. Observations of Integrated Precipitable Water Vapor

The microwave based space geodetic techniques VLBI and GPS experience signal propagation delays that are related to the amount of atmospheric water vapor. Using appropriate mapping functions, e.g. the New Mapping Functions (Niell, 1996, [11]), corresponding atmospheric zenith delay parameters can be determined from the data analysis. Usually, for VLBI analysis the locally measured and recorded pressure data is used to model the hydrostatic delays, so that the VLBI analysis directly provides zenith wet delay (ZWD) results.

On the contrary to that, for GPS analysis usually only some average station pressure is applied in the data analysis, so that the primary GPS result are zenith total delay (ZTD) values. Thus, to derive zenith wet delay from GPS the hydrostatic contribution has to be subtracted in a post-processing step. To be able to compare the space geodesy results for atmospheric water vapor to results provided by the meteorological agencies, the ZWD values have to be converted into Integrated Perceptible Water Vapor (IPWV). For Europe the algorithms described by Emaradson and Derks (2000, [3]) can be used.

We analyzed a global VLBI data set with the CALC/SOLVE analysis software (Ma et al., 1990, [10]) and determined ZWD results with an temporal resolution of 1 hour. The NMF mapping functions (Niell, 1996, [11]) were applied in the analysis. The resulting ZWD values were converted into IPWV using the approach described by Emaradson and Derks (2000, [3]). Figure 2 shows the time series of VLBI derived IPWV results.

The Tropospheric Working Group of the International GPS Service (IGS) [7] provides time series of combined total zenith delay values for about 150 IGS GPS stations (Gendt, 2004 [5]). These results have a temporal resolution of 2 hours and are combinations of results derived by different IGS analysis centers that use different analysis strategies and software packages. We downloaded IGS ZTD time series and post-processed the data to derive IPWV time series. For the hydrostatic pressure correction we used local pressure data observed at the sites where these data were available, and interpolated pressure data based ECMWF pressure fields for the other stations. Then the same conversion algorithms to derive IPWV were used as for the VLBI results. The resulting data are shown in Figure 2.

Radiosonde profiles were provided by the British Atmospheric Data Centre (BADC, [1]). We used the in-house RS analysis software to derive IPWV time series from these RS profiles. The resulting data are displayed in Figure 2, too.

Figure 2 shows that all techniques sense IPWV time series that have a predominantly annual variation. Some techniques suffer from data gaps, others from a relatively short observational history. In general, the individual series have very similar shape and signature so that combinations of the individual results appear to be a reasonable approach.

3. Combination of RS, VLBI and GPS results

The different collocated techniques have technique specific advantages and disadvantages. The instrumental stability, temporal resolution, measurement uncertainty and the observation history of the techniques are different. Thus, for the determination of robust estimates of possible long term changes in atmospheric water vapor, a combined analysis appears to be promising. First experience from a combined analysis of IPWV time series for Onsala were reported in Haas et al. (2003, [6]). A simple mathematical model was applied that allowed to estimate individual offsets,

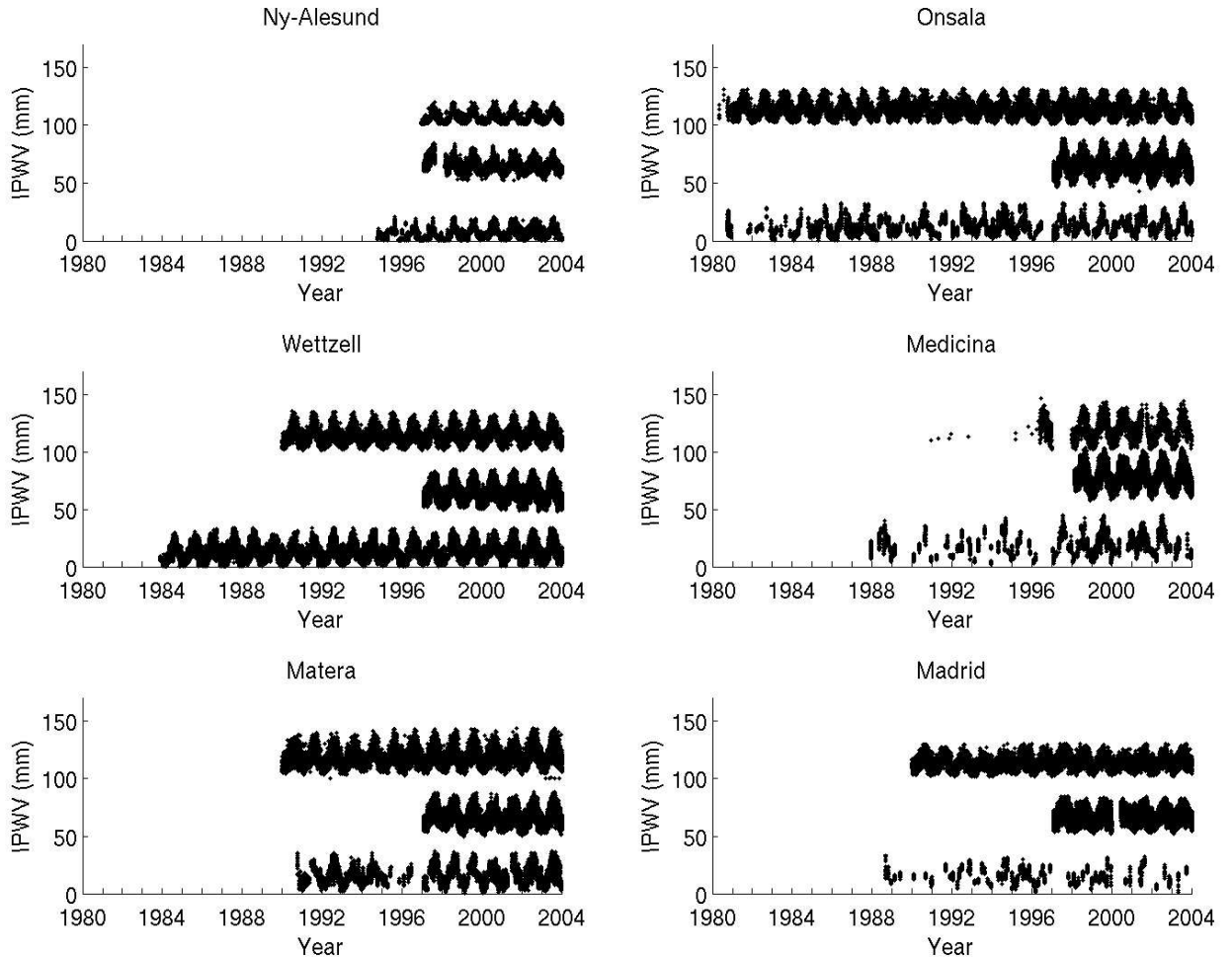


Figure 2. Time series of IPWV for six space geodetic station in Europe. In each picture the displayed data show from the bottom to the top IPWV results for VLBI, GPS, and RS, respectively. Offsets of 50 mm and 100 mm are added for GPS and RS, respectively, in order to improve readability of the graphs.

a common trend parameter and amplitudes of annual variations. The difficulty of this approach lies in particular in the relative weights that have to be attributed to the individual time series.

For the current study we therefore applied a variance-covariance estimation strategy (Koch, 1987, [9]) that allows to iteratively determine weights for the individual input data sets. The results for the IPWV trends that were determined with this approach are given in Table 2 and compared to trends derived from the ERA40 data set. The ERA40 data set is given on a grid of 2.5° times 2.5° resolution, and thus the data had to be interpolated to the positions of the space geodetic stations. We determined ERA40 trends for the interval 1980 to mid 2002. Unfortunately, the ERA40 data set ends in mid 2002 and does not extend until the end of the space geodetic time series.

The results listed in Table 2 show a good agreement between the IPWV trends derived from combination of collocated techniques and the ERA40 IPWV trends only for Onsala and Medicina.

Table 2. Trends in IPWV derived from a combined analysis of VLBI, GPS and RS using a variance-covariance estimation approach, and corresponding IPWV trends derived from the ERA40 data set.

Station	Combined IPWV trend (mm/yr)	ERA40 IPWV trend (mm/yr)
Ny-Ålesund	-0.16 ± 0.01	$+0.01 \pm 0.01$
Onsala	$+0.03 \pm 0.01$	$+0.04 \pm 0.01$
Wettzell	$+0.04 \pm 0.01$	-0.03 ± 0.01
Medicina	$+0.04 \pm 0.01$	$+0.05 \pm 0.01$
Matera	$+0.11 \pm 0.01$	$+0.05 \pm 0.01$
Madrid	$+0.03 \pm 0.01$	-0.02 ± 0.01

For Ny-Ålesund, Wettzell and Madrid, the sign of the trends is opposite and for Matera the ERA40 trend is only about half of the combined trend from VLBI, GPS and RS. The discrepancy at Ny-Ålesund might be due to the relatively short data sets that are available from space geodesy. Among the six studied stations Ny-Ålesund is the one with the shortest observational history which makes the analysis more sensitive to short-time fluctuations and temporary anomalies. The discrepancy at Matera could be due to a dominance of the RS results. Unfortunately the RS launch site is not that close to Matera and thus the combined trend could be influenced. The deviations at Wettzell and Madrid are hard to explain.

4. Study of elevation cutoff effects

The elevation cutoff used in the data processing is one possible reason for discrepancies between the results of the different space geodetic techniques. Therefore we investigated this effect by analyzing GPS data of three of the six space geodetic stations with the Gipsy-Oasis-II software (Webb and Zumberge, 1993, [12]). in precise-point-positioning (PPP) mode. We applied elevation cutoff values between 5 and 20 degrees. The resulting ZTD were converted to ZWD using time series of locally measured pressure data, and then to IPWV using the above mentioned algorithms. The resulting IPWV time series were analyzed to determine offset, trend and amplitudes of annual variations. Table 3 shows the trend results for the three stations and the different elevation cutoff angles. It becomes clear that the choice of elevation cutoff angle can influence the trend results on the order of the discrepancies seen in Table 2.

Table 3. IPWV trends derived from GPS point-positioning using different elevation cutoff angles in the GPS data processing.

Station elevation cutoff	trend (mm/yr) 5°	trend (mm/yr) 10°	trend (mm/yr) 15°	trend (mm/yr) 20°
Onsala	$+0.12 \pm 0.01$	$+0.15 \pm 0.01$	$+0.12 \pm 0.01$	-0.05 ± 0.01
Wettzell	-0.03 ± 0.01	$+0.00 \pm 0.01$	$+0.05 \pm 0.01$	$+0.02 \pm 0.01$
Matera	-0.09 ± 0.01	-0.09 ± 0.01	-0.08 ± 0.01	-0.11 ± 0.01

5. Conclusions and outlook

We analyzed atmospheric water vapor derived for six space geodetic stations in Europe. These stations have collocated equipment and radiosonde launch sites are located relatively close by. The IPWV trend results of the individual techniques agree reasonably well and an analysis approach based on variance-covariance estimation gives useful combination results. However, the combined IPWV trends agree only to some extent with the results based on the ERA40 data set. The effect of the elevation cutoff on the GPS IPWV trends has been studied. Changes in elevation cutoff can cause changes in the IPWV trends that are on the same order of magnitude as the discrepancies between the combined trend results and results from ERA40. In order to better understand the robustness of IPWV trends derived from space geodetic techniques and their value for climate research, this study has to be continued including also ground based radiometry.

Acknowledgement

This study used data of the 40 Years Re-Analysis Project (ERA40) that were supplied by the European Centre for Medium-Range Weather Forecast (ECMWF). Atmospheric pressure files were also provided by the ECMWF.

References

- [1] British Atmospheric Data Centre (BADC): <http://badc.nerc.ac.uk/home/>
- [2] European Centre for Medium-Range Weather Forecast (ECMWF): <http://www.ecmwf.int/>
- [3] Emardson, T.R., Derks, H.J.P.: On the relation between the wet delay and the integrated precipitable water vapour in the European atmosphere. *Meteorological Applications*, **7(1)**, 61–68, 2000.
- [4] ERA40: (<http://data.ecmwf.int/research/era/>)
- [5] Gendt, G.: Report of the Tropospheric Working Group for 2002, 2001-2002 Technical Report IGS Central Bureau, Jet Propulsion Laboratory, Pasadena, 2004.
- [6] Haas, R., Elgered, G., Gradinarsky, L., Johansson, J.: Assessing long term trends in the atmospheric water vapor content by combining data from VLBI, GPS, radiosondes and microwave radiometry. In: V. Thorandt, G. Engelhardt, D. Ullrich and R. Wojdziak (eds.): *Proc. of the 16'th Working Meeting on European VLBI for Geodesy and Astrometry*, Bundesamt für Kartographie und Geodäsie, 279–288, 2003.
- [7] IGS: International GPS Service (IGS) homepage <http://igsceb.jpl.nasa.gov>
- [8] IPCC, Climate Change 2001: The Scientific Basis. Contribution of Working Group 1 to the Third Assessment Report of the Intergovernmental Panel on Climate Change, *Cambridge University Press*, 2001
- [9] Koch, K. R.: Paramaterschätzung und Hypothesentests in linearen Modellen, Dümmlers Verlag, 1987.
- [10] Ma, C., Sauber, J.M., Bell, L.J., Clark, T.A., Gordon, D., Himwich, W.E., and Ryan, J.W.: Measurements of horizontal motions in Alaska using very long baseline interferometry. *J. Geophys. Res.*, **95(2)**, 21991–22011, 1990.
- [11] Niell, A., Global mapping functions for the atmosphere delay at radio wavelength. *Journal of Geophysical Research*, **101(B8)**, 3227–3246, 1996
- [12] Webb, F., H., and Zumbege, J. F.: An introduction to GIPSY/OASIS II. *JPL Publication D-11088*, Jet Propulsion Laboratory, Pasadena, CA, 1993.

Preliminary results of applying WVR calibration to European VLBI data

J. Cho, A. Nothnagel, M. Vennebusch, D. Fischer

Geodätisches Institut der Universität Bonn, Korea Astronomy and Space-science Institute

Contact author: J. Cho, e-mail: jojh@kasi.re.kr

Abstract

Tropospheric delay caused by water vapor is one of the main error sources in space geodetic techniques. To correct the tropospheric delay, several independent instruments have been used. Among them, WVR (Water Vapor Radiometer) are sensitive to the amount of water vapor in the atmosphere. Radiometers measure the brightness temperature (TB) of water vapor, liquid water and oxygen. To get the water vapor induced effects from WVR observations it is necessary to convert the brightness temperature into the atmospheric PD (Path Delay) corrections. We applied calibrated WVR PD to VLBI data for improving the repeatability of site positions. For the first step of this study, we have applied different WVR calibration methods to Madrid (DSS65) data. The level of improvement was analyzed by comparing standard deviations of baselines and vertical components.

1. WVR Data Calibration and PD Calculation

We have calibrated WVR data to extract the PD from the TB of the radiometer. The radiometer measures TB, which correspond to the spectral line intensity of water vapor, liquid water and oxygen in the troposphere. The water vapor part can be extracted from those composition using an optimal choice of frequency pairs [6].

To get proper values of PD, the raw measurements of TB have to be calibrated for instrumental effects. In a first step, a water vapor saturation-correction has to be applied. Here we used a linearization method according to Claffin *et al.* [1]. Then the instrumental gain was calculated. After determination of the gain, one unknown constant is left which is called correction of hot load temperature.

To determine the proper correction of the hot load temperature, the so-called tipping curve method was used. In addition to the tipping curve method, we can also use the information of the cosmic background temperature known to be 2.7K. As a result, we can determine the correction of the brightness temperature using a linear relationship between the brightness temperatures and the air mass values [2].

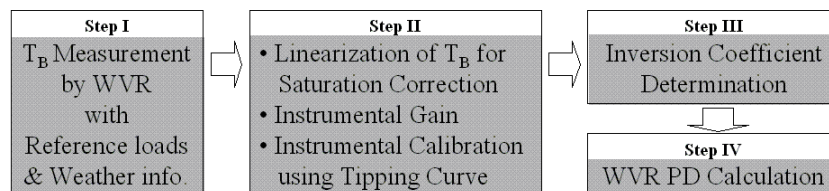


Figure 1. Overview of WVR pre-processing

Now we can determine the inversion coefficient for converting calibrated brightness temperatures to the PD. In general radiosonde observables are used to determine these coefficients. Figure 1 shows an overview of the WVR measurement calibration and PD calculation process, which we call pre-processing.

2. Preparation for Data Processing

Currently, three European VLBI stations are equipped with different types of WVR instruments. WVR data is provided by the Madrid Deep Space Complex and Onsala Space Observatory corresponding to the dates of different European VLBI sessions. Wettzell data will be collected in the near future. Unfortunately there is only a small number of European geodetic VLBI sessions where WVR data is available for Madrid. Some detailed information related to the WVR instruments and their status are listed in table 1.

Table 1. WVR station summary

Station	Number of Sessions	WVR Type	Freq.(GHz)	Status
Madrid	9	JPL D2	21.0/31.4	Step IV
Onsala	37	Astrid	20.7/31.4	Step II
Wettzell	-	ETHZ White	23.8/31.5	Collecting

Onsala WVR data has been provided in pre-processed form. Madrid data has been pre-processed at GIUB following the scheme described in section 1. We have adopted a linearization method and two sets of inversion coefficients. A summary of the different methods, which were adopted for Madrid WVR data calibration, is listed in table 2.

Table 2. Applied model for pre-processing of WVR data

Step	Applied Method
Linearization	Clafin <i>et al.</i> [1]
Inversion Coefficients	Resch[4], Johanssen <i>et al.</i> [3]

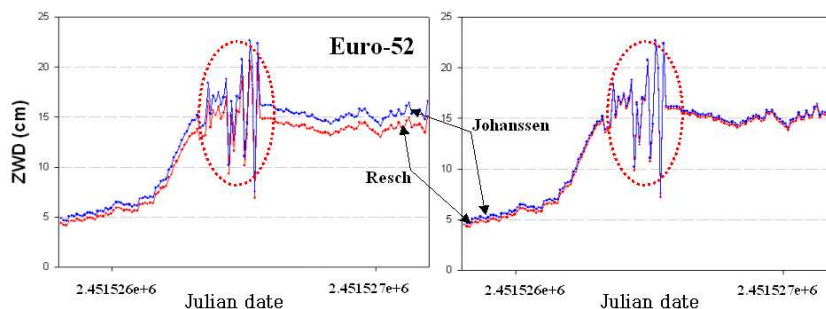


Figure 2. Zenith wet delay (ZWD) at Madrid (DSS65) for EURO-52 session before linearization (left) and after (right) with period of heavily increased noise level probably due to rainy conditions.

Figure 2 shows an example of the ZWD at Madrid (DSS65) for session EURO-52 before and after linearization. A period of heavily increased noise is clearly discernable, probably caused by rainy weather conditions. Periods like this are present also in some of the other sessions.

3. Data Processing and Analysis

The VLBI data has been analysed with the Calc/Solve software and program DBCAL has been used for inserting WVR data into VLBI databases. During pre-processing periods with obvious deficiencies due to increased noise have been replaced with interpolated data. The estimates of atmosphere parameters were improved after the periods of increased noise were removed as shown in figure 3.

The VLBI data of each session was processed in two different ways. We distinguished it by name: 1) Standard solution, 2) WVR solution. The standard solutions were determined by estimating tropospheric parameters in the usual way with rate changes at every hour (see Fig. 3). In one case the hydrostatic part was corrected using the CfA2.2 model, and the wet part was estimated (a). In the second case the hydrostatic and the wet part were calibrated, the latter one with surface meteorologica data, and the wet part was still estimated (b). In the WVR solution we used the WVR data directly to correct the wet delay. In a separate solution of the latter type zenith wet delays were estimated in addition to the calibration of the data with WVR induced zenith wet delays (c). It should be noted here that if in solution type (c) the WVR

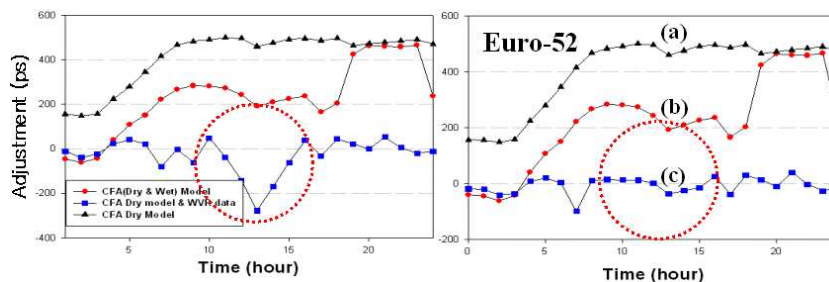


Figure 3. Wet delay estimates. a) only hydrostatic part calibrated using surface met data; b) hydrostatic and wet part calibrated using surface met data; c) hydrostatic part calibrated with surface met data and wet part calibrated with WVR data. Left side includes period with increased noise, right side uses interpolated data for this period.

calibrations comprise the wet refraction effect completely the estimates of the wet delays should be zero throughout. However, the estimates are sometimes negative. Since the refraction effect by water vapor can never have a decreasing effect on the zenith wet delay, we assume that the WVR data in its present state over-calibrates the wet component. This issue is currently being investigated.

The impact of applying WVR data to VLBI data has been checked by looking at the standard deviations of linear fits of several VLBI sessions and the associated repeatabilities of selected baselines. The repeatabilities are represented by the weighted root mean squared errors (WRMS). In addition, the effect of water vapor radiometer corrections can also be found in the variations of the vertical components [5].

4. Results

We have compared the standard and the WVR solutions for each baseline as shown in figures 4 and 5. In table 3, the different types of solutions for each baseline are summarized. While the first three columns of table 3 are results of baseline lengths and UD (Up-Down) components, the last three columns are baseline-rate related values from a linear regression analysis. The results of the Wettzell–Onsala baseline are also shown in figure 4. The WRMS of the baseline-rate from the standard and WVR solutions are similar. The WRMS of WVR solution is slightly bigger than of the standard solution. But there are some improvements on the standard deviations of the baseline lengths and UD components as listed in table 3. Considering the fact that WVR data for Wettzell station was not used, it is expected that the formal errors would be improved if Wettzell WVR data will be introduced.

Figure 5 shows the Wettzell–Madrid and the Onsala–Madrid baseline results. Each baseline has a relatively small number of sessions used to determine the values in table 3. Except for the Onsala–Madrid baseline, there is a similar tendency between standard and WVR solution. Especially for the Onsala–Madrid baseline there is relatively big degradation of the WRMS. But we have to note that there are only four sessions included. This means that the Onsala–Madrid result is easily changed by a single value.

The UD results in table 3 have been computed with respect to the standard solution. Therefore, the reference UD component is set to zero and the other results are reported relative to this. The average vertical components are all smaller when WVR data has been used.

Table 3. Summary of the results

Baseline	Mode	σ of Bl	UD Comp.	σ	B-rate	σ	WRMS
		(mm)	(mm) Average	(mm)	(mm/yr)	(mm) Regression	(mm)
Wettzell- Onsala	Standard	1.89	0.00	6.86	-0.41	0.17	3.51
	WVR	1.79	-6.27	5.38	-0.58	0.18	3.61
Wettzell- Madrid	Standard	2.04	0.00	8.01	0.80	0.51	2.39
	Resch	1.84	-27.80	5.42	0.44	0.56	2.61
	Johanssen	1.84	-22.76	5.42	0.59	0.53	2.49
Onsala- Madrid	Standard	2.15	0.00	6.58	-0.04	0.55	1.60
	Resch	1.78	-32.09	4.68	-0.43	1.28	3.74
	Johanssen	1.78	-32.18	4.68	-0.20	1.50	4.37

5. Conclusion

WVR data gathered at Madrid and Onsala have been used to check the possibility of improving the repeatability of baseline and vertical component result. We found that WVR corrections applied instead of model corrections decrease the station heights. Another preliminary result is that the formal errors of the baseline length results are reduced by 10% and vertical components by 30%. However, these results are very preliminary and further investigations have still to be carried out. The fact that different results are obtained from different WVR calibration and inversion methods means that we have to perform detailed comparisons of the models available today before we can safely apply WVR data to VLBI data processing.

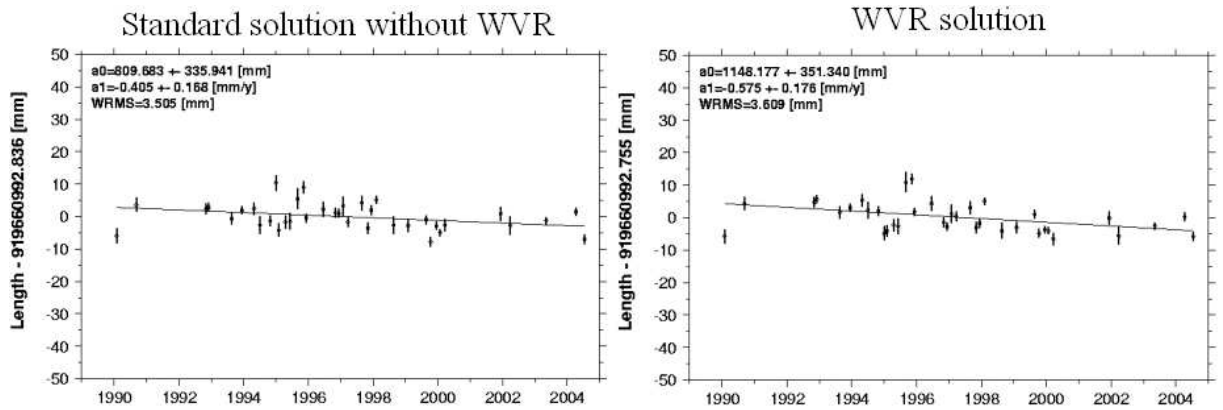


Figure 4. Baseline length results of Wettzell–Onsala with standard solution and using WVR calibrations at Onsala

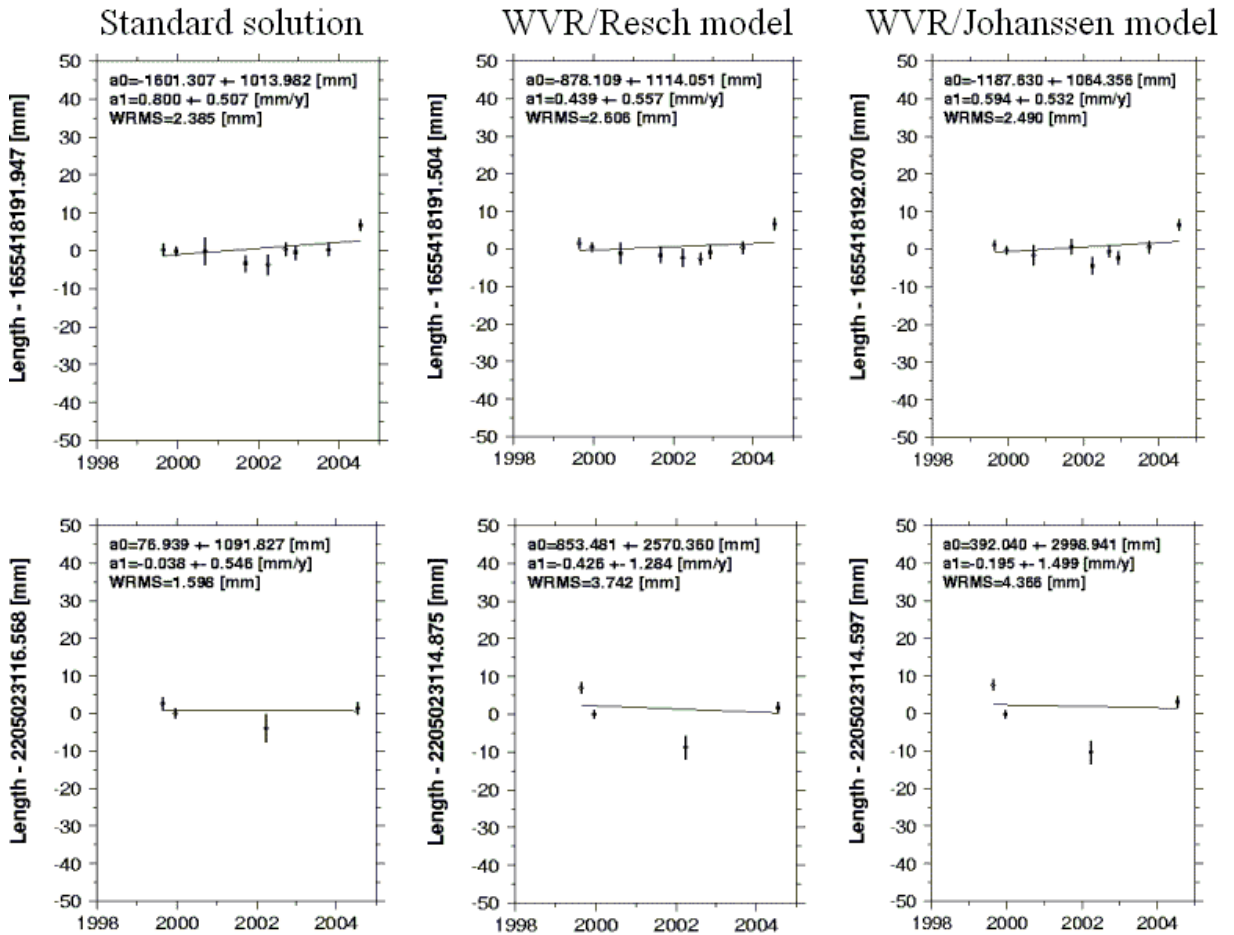


Figure 5. Top: Wettzell–Madrid baseline length results applying three different calibration methods. Bottom: Onsala–Madrid baseline length results.

6. Future Tasks

- Wettzell data calibrating and processing,
- Comparison of various WVR calibration and inversion methods,
- Hybrid tropospheric correction using WVR+GPS for rainy condition,
- Including WVR data from Effelsberg.

Acknowledgements

We would like to thank Rüdiger Haas of Onsala Space Observatory of Chalmers Technical University and Stephen J. Keihm of NASA JPL for providing the WVR data used in this study.

References

- [1] Claffin, E.S., S.C. Wu, G.M. Resch, Microwave Radiometer Measurement of Water Vapor Path Delay: Data Reduction Techniques, DSN Progress Report No. 42-48, September and October 1978, pp.24-27
- [2] Elgered, G., Tropospheric Radio Path Delay from Ground-based Microwave Radiometry, Atmospheric Remote Sensing by Microwave Radiometry, Ed. M.A. Jansen, John Wiley & Sons, New York, 1993
- [3] Johanssen, J.M., G. Elgered, J.L. Davis, Wet Path Delay Algorithm for Use with Microwave Radiometer Data, Contribution of Space Geodesy to Geodynamics: Technology Vol. 25, AGU, Washington, D.C.,1993, pp.81-98
- [4] Resch, G.M., Inversion Algorithms for Water Vapor Radiometers Operating at 20.7 and 31.4 GHz, TDA Progress Report No.42-76, 1983, pp.12-19
- [5] Ware, R., C. Rocken, F. Solheim, T.V. Hove, C. Alber, J. Johnson, Pointed Water Vapor Radiometer Corrections for Accurate Global Positioning System Surveying, Geophysical Research Letters Vol.20, No.23, 1993, pp.2635-2638
- [6] Wu, S.C., Frequency Selection and Calibration of a Water Vapor Radiometer, DSN Progress Report No. 42-43, February 1978, pp.67-81

Estimation of absolute TEC values by VLBI

Thomas Hobiger ¹, Tetsuro Kondo ², Harald Schuh ¹

¹⁾ *Institute of Geodesy and Geophysics, University of Technology, Vienna*

²⁾ *Kashima Space Research Center, NICT*

Contact author: Thomas Hobiger, e-mail: `thobiger@mars.hg.tuwien.ac.at`

Abstract

Geodetic VLBI observations are carried out at two distinct frequencies in order to determine ionospheric delay corrections. Each ionospheric delay corresponds to the total electron content (TEC) along the ray path through the ionosphere. Because VLBI is a differential technique the observed ionospheric delays represent the differences of the behavior of the propagation media above each two stations. Additionally, there is a constant instrumental delay offset per baseline that contributes to the observed ionospheric delay. This instrumental offset is independent of azimuth and elevation in which the antennas point what allows to separate it from the variable ionospheric parameters for each station which can be represented by different functional approaches. Instrumental offsets can be separated from the ionospheric parameters by a least-squares fit. Additional parameters of a model, which relates TEC values measured at the intersection point of the ray path with the infinitely thin ionospheric layer to vertical TEC values above the station, are estimated. The results agree well with other techniques like GPS, what will be shown, too.

1. Estimation of ionospheric parameters

Each dual-frequency VLBI observation provides the baseline dependent ionospheric delay ($\tau_{measured}$) in the form of equation (1).

$$\tau_{measured}(t) = \tau_{ion,1}(t) - \tau_{ion,2}(t) + \tau_{offset,1} - \tau_{offset,2} \quad (1)$$

The ionospheric delay at X-band measured at station i can be described by equation (2) with an appropriate mapping function $M_f(\varepsilon_i)$ depending on the elevation angle ε_i (e.g., Schaer, 1999, [1], Hobiger and Schuh, 2004, [2]).

$$\tau_{ion,i}(t) = \frac{1.34 \cdot 10^{-7}}{f_x^2} \cdot M_f(\varepsilon_i) \cdot VTEC_i(t) \quad (2)$$

If the Vertical Total Electron Content (VTEC) above a single station shall be estimated the problem occurs that each measurement contains four unknowns. Thus, some assumptions and simplifications have to be made and an estimation method has to be used that takes the physical behavior of the ionosphere into account (e.g. TEC values cannot be negative).

1. As indicated in equation (1), instrumental offsets caused by the receiving system (e.g., Ray, 1991, [3]) are supposed to be constant within a 24h VLBI session. In GPS there is a similar problem called differential code biases, DCBs, [1] when solving for absolute ionospheric parameters. In VLBI the same assumption as in GPS is applied by postulating that the sum of all station-dependent offsets equals to zero.

$$\sum_{i=1}^{N_{stat}} \tau_{offset,i} = 0 \quad (3)$$

2. However, measurements are made at different elevation angles and azimuths and the observed VTEC value has to be assigned to the intersection point of the ray path with the ionospheric shell which is not vertically located above the station. Taking into account that the ionosphere is mainly traveling with the sun's position any measurement can be rotated in the meridian of the station by the introduction of an artificial observation time.
3. Setting up a linear north-south gradient for each station allows to deduce VTEC values above the station from the time-transformed measurements.
4. Under the previous assumptions VTEC values for each station can be modeled by means of least-squares. Different elevation angles for each station will enable the separation of the station-dependent parameters.

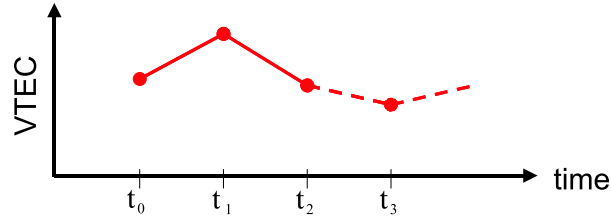


Figure 1. Piece-wise linear function as a representation of vertical total electron content

5. The ionospheric parameters are modeled in the form of piece-wise linear functions (figure 1, equation (4)) with only positive VTEC values allowed (solution within positive half-space).

$$VTEC_{PLF}(t) = offset + rate_1(t_1 - t_0) + rate_2(t_2 - t_1) + \dots + rate_n(t_n - t) \quad (4)$$

$$\begin{aligned}
 (offset_0 + \Delta offset) & \geq 0 \\
 (offset_0 + \Delta offset) + (rate_{1,0} + \Delta rate_1)(t_1 - t_0) & \geq 0 \\
 (offset_0 + \Delta offset) + (rate_{1,0} + \Delta rate_1)(t_1 - t_0) + (rate_{2,0} + \Delta rate_2)(t_2 - t_1) & \geq 0 \\
 & \vdots \\
 & \vdots
 \end{aligned} \quad (5)$$

Applying the non-negative constraint to all points at the interval boundaries yields equation (5). Parameters indicated with \mathbf{x}_0 stand for the initial guess and a $\Delta \mathbf{x}$ symbolizes the improvement from the adjustment process. If all conditions are summed up using matrix notation equation (6) is obtained.

$$\underbrace{\begin{pmatrix} 1 & 0 & 0 & 0 & \dots \\ 1 & t_1 - t_0 & 0 & 0 & \dots \\ 1 & t_1 - t_0 & t_2 - t_1 & 0 & \dots \\ \vdots & \vdots & \vdots & \vdots & \ddots \end{pmatrix}}_{\mathbf{B}} \mathbf{x}_0 + \underbrace{\begin{pmatrix} 1 & 0 & 0 & 0 & \dots \\ 1 & t_1 - t_0 & 0 & 0 & \dots \\ 1 & t_1 - t_0 & t_2 - t_1 & 0 & \dots \\ \vdots & \vdots & \vdots & \vdots & \ddots \end{pmatrix}}_{\mathbf{B}} \Delta \mathbf{x} \geq 0 \quad (6)$$

Re-arranging equation (6) yields

$$\mathbf{B} \cdot \Delta \mathbf{x} \geq -\mathbf{B} \cdot \mathbf{x}_0 \quad \Rightarrow \quad \mathbf{B} \cdot \Delta \mathbf{x} \geq \mathbf{C} \quad (7)$$

Incorporation of equation (7) into the adjustment process leads to

$$\min_{\Delta \mathbf{x}} \left(\Delta \mathbf{x}^T \underbrace{\mathbf{A}^T \mathbf{P} \mathbf{A}}_{\mathbf{H}} \Delta \mathbf{x} - 2 \underbrace{\mathbf{A}^T \mathbf{P} \Delta \mathbf{Y}}_{-\mathbf{f}^T} \Delta \mathbf{x} + \underbrace{\Delta \mathbf{Y}^T \mathbf{P} \Delta \mathbf{Y}}_{const > 0} \right) \left. \vphantom{\min_{\Delta \mathbf{x}}} \right\} \rightarrow \text{reflective Newton method}$$

$$\mathbf{B} \cdot \Delta \mathbf{x} \geq \mathbf{C}$$
(8)

As pointed out by equation (8) the usage of a reflective Newton method allows to obtain the unknown parameters under non-negative conditions.

6. Normally piece-wise linear functions are modeled with constant interval lengths (figure 2). For periods with no data additional constraints are needed to stabilize the solution. To

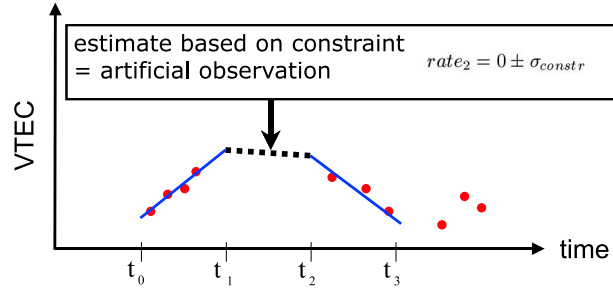


Figure 2. Piece-wise linear function - constant interval lengths

avoid the introduction of constraints an adaptive piece-wise linear function was developed which shifts the interval boundaries that every interval contains the same (given) number of observations (figure 3).

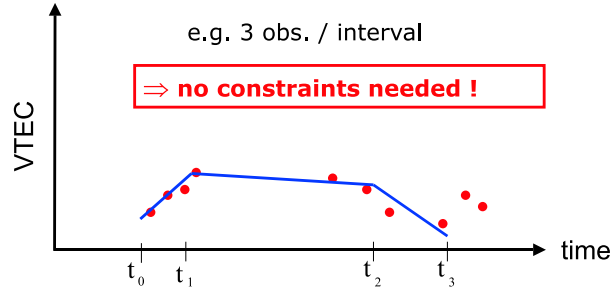


Figure 3. Piece-wise linear function - adaptive interval lengths with 3 observations per interval

2. Results - comparison to GPS

As an example, the results for station Wettzell, Germany, are shown in figure 4 upper part. Values obtained from global VTEC models derived from the Center for Orbit Determination in

Europe (CODE) at the Astronomical Institute of Berne and plotted in the lower part of figure 4. When calculating the difference between both series it seems that GPS provides slightly higher values with a mean bias of 1.95 TECU and a standard deviation of about ± 6 TECU.

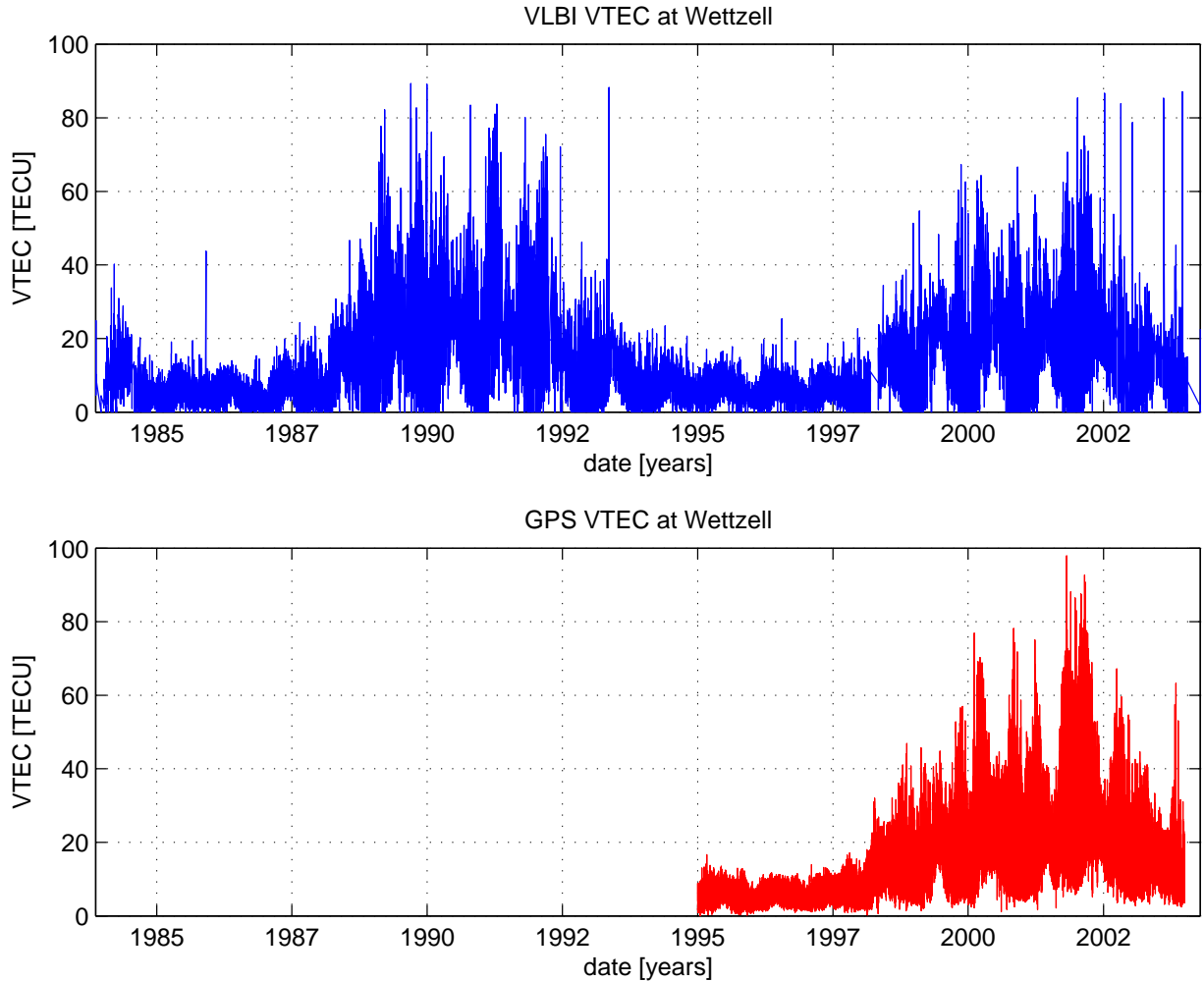


Figure 4. VTEC values for station Wettzell, Germany from VLBI (upper plot) and CODE-GIM (lower plot).

3. Conclusions and Outlook

VLBI is able to provide absolute ionospheric parameters above globally distributed stations. Our first results agree well with values derived by GPS and it is possible to study the behavior of the ionosphere on long- and short-term time scales. Therefore, VLBI can be used as a source for global ionospheric models.

4. Acknowledgments

Research project P16136-N06 "Investigation of the ionosphere by geodetic VLBI" is funded by the Austrian Science Fund (FWF). Furthermore the authors want to thank the Japanese Society for the Promotion of Science, JSPS (project PE 04023) and Kashima Space Research Center, NICT for supporting this work. The International VLBI Service for Geodesy and Astrometry (IVS) and the International GPS Service (IGS) are acknowledged for providing data.

References

- [1] Schaer, S., Mapping and Predicting the Earth's Ionosphere Using the Global Positioning System, Inaugural Dissertation der Philosophisch-naturwissenschaftlichen Fakultät der Universität Bern, Bern, 1999
- [2] Hobiger, T., H. Schuh, Modeling Vertical Total Electron Content from VLBI Observations, in International VLBI Service for Geodesy and Astrometry 2004 General Meeting Proceedings, edited by Nancy R. Vandenberg and Karen D. Baver, NASA/CP-2004-212255, 2004.
- [3] Ray, J.R., B.E. Corey, Current Precision of VLBI Multi-Band Delay Observables, Proceedings AGU Chapman Conference on Geodetic VLBI: Monitoring Global Change, Washington D.C., 22-26 April, 1991
- [4] Hobiger, T., S. Todorova, H. Schuh, Ionospheric Parameters Obtained by Different Space Geodetic Techniques During CONT02, in International VLBI Service for Geodesy and Astrometry 2004 General Meeting Proceedings, edited by Nancy R. Vandenberg and Karen D. Baver, NASA/CP-2004-212255, 2004.
- [5] http://igs.cb.jpl.nasa.gov/components/dcnav/cddis_products_ionex.html

Status of SINEX combination - IVS' Contribution to the IERS Combination Pilot Project

Markus Vennebusch, Andreas Weinberger

Geodätisches Institut der Universität Bonn

Contact author: Markus Vennebusch, e-mail: vennebusch@uni-bonn.de

Abstract

A new approach for the combination of geodetic space techniques has been established by the IERS, called "IERS Combination Pilot Project" (IERS CPP). This approach is based on the accumulation of "weekly" or session-wise normal equation matrices. Therefore, the IVS has to perform a so-called intra-technique combination to provide one official IVS solution per session to the IERS CPP. The intra-technique combination is carried out by the Geodetic Institute of the University of Bonn, Germany. The status of this work is described in this paper.

1. Introduction

1.1. IERS Combination Pilot Project

The IERS Combination Pilot Project (IERS CPP) has been established in 2004 and will be a major step towards more consistent, routinely generated IERS products [2]. Within this project different geodetic space techniques (GPS, VLBI, SLR/LLR, DORIS) are combined applying the entire covariance information of the parameters. This combination approach is based on the usage of either variance/covariance matrices or normal equation matrices (also known as adjustment of groups of observations, [6]).

Usually all techniques provide their solutions as "weekly" SINEX files containing information on site coordinates, EOPs and sometimes also auxiliary parameters, e.g. for atmospheric behaviour. However, in the case of VLBI *session-wise* solutions are provided which also contain information on station positions, EOP and their rates. For this combination approach each technique has to combine the individual solutions of the technique's analysis centers and has to generate one official "weekly" solution (see figure 1). This is done at the different services and is called "intra-technique combination". Since VLBI networks do not observe permanently the International VLBI Service for Geodesy and Astrometry (IVS) provides one official solution per VLBI observing session of about 24 hours of duration to the IERS CPP.

After submitting the official intra-technique solutions to the IERS CPP data center these solutions are combined by various IERS Combination Centers. This process is called "Inter-technique combination".

This new session-wise combination approach will replace the current way of combining VLBI EOP time series on the basis of results soon. The new approach has some important advantages:

- All solutions can be transformed to a common set of apriori values. After such a transformation solutions of different analysis centers of the same session can be compared more easily.

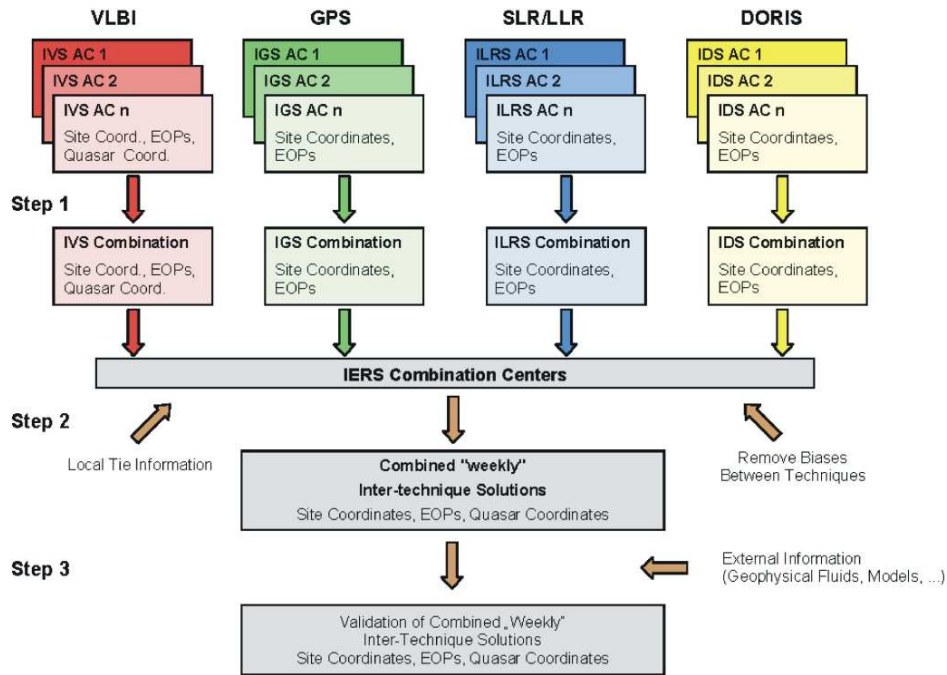


Figure 1. Concept of the IERS Combination Pilot Project (IERS CPP Call for Participation)

- All the relations between parameters (correlations) are carried over through the process and will be considered correctly
- The geodetic datum can be imposed by the combination center providing an identical datum for all input series

2. The IVS Contribution to the IERS CPP

2.1. VLBI data analysis software

In order to contribute VLBI solutions to the IERS CPP some efforts have been made by the VLBI data analysis software developers to generate the solutions in the required SINEX format (Solution INdependent EXchange format) [7]. These files contain both datum-free normal equation matrices as well as their right hand sides and further statistical information needed for a combination on the basis of normal equations [6].

Currently, the following VLBI data analysis software packages are capable to generate SINEX output:

- CALC/SOLVE, classical least-squares approach, developed at GSFC
- OCCAM (LSM), classical least-squares approach, developed at DGFI, TU Vienna
- OCCAM (Kalman), Kalman-filter approach, developed at AUS

- SteelBreeze, square-root information filter (SRIF), developed at MAO

At the moment (May 2005) there are seven analysis centers preparing or already prepared for a regular submission of SINEX files for the intra-technique combination:

- Geoscience Australia (AUS), Australia
- Bundesamt für Kartographie und Geodäsie (BKG), Germany
- Deutsches Geodätisches Forschungsinstitut (DGFI), Germany
- Goddard Space Flight Center (GSFC), USA
- Main Astronomical Observatory (MAO), Ukraine
- United States Naval Observatory (USNO), USA
- Shanghai Observatory (SHA), China

2.2. VLBI-Intra-technique combination

For the VLBI-intra-technique combination at GIUB the combination software DOGS-CS developed at the German Geodetic Research Institute (DGFI), Munich is used. As mentioned above, further software for quality checks and for controlling DOGS-CS has been developed at GIUB. For the VLBI Intra-technique combination different tasks had to be solved:

- Implementation of automated downloading procedures and programs for quality checks of the input files have been developed. These quality checks involve different techniques for rank-determination based on eigenvalue and QR-decompositions [5]. (Since all station positions, EOP and their rates as well as nutation parameters have been introduced as unknowns for the generation of the SINEX files the resulting normal equation matrices are singular or "datum-free". Therefore the rank deficiency of these matrices should be six).
- Creation of a conversion program (also accounting for different versions of the format) of SINEX files (ASCII) into binary DOGS-CS input files.
- Before combining all different solutions of the same session generated by various IVS Analysis Centers the input solutions have been transformed to an equal set of apriori values for TRF and EOP. After this transformation the solutions are checked for outliers. Therefore, after imposing a common datum definition to all the solutions, EOP or site position can be estimated and compared. Solutions not exceeding a certain threshold (e.g. 0.3 mas for polar motion and 0.02 ms for UT1) will be included in the following combination process.
- In order to balance the influence of Analysis Centers scaling of the normal equation matrices and variance component estimation is necessary [8]. Soon there will be a weighting procedure based on variance component estimation in order to account for different accuracy levels of the contributing solutions at this step of Intra-Technique combination [4].
- Before performing the final combination step it is sometimes necessary to reduce auxiliary parameters like clock or atmosphere parameters (see e.g. [1]) if Analysis Centers also provided normal equation elements for these parameters.

Unfortunately, the IVS Analysis Centers do not use identical nutation models. Therefore, nutation parameters need to be reduced and can (not yet) be included in the combination process.

- After accumulating up to seven individual datum-free normal equation matrices a combined solution can be computed by imposing the same datum definition as mentioned above. An example of the EOPs resulting from an "Intra-Technique combination" can be seen in figure 2.

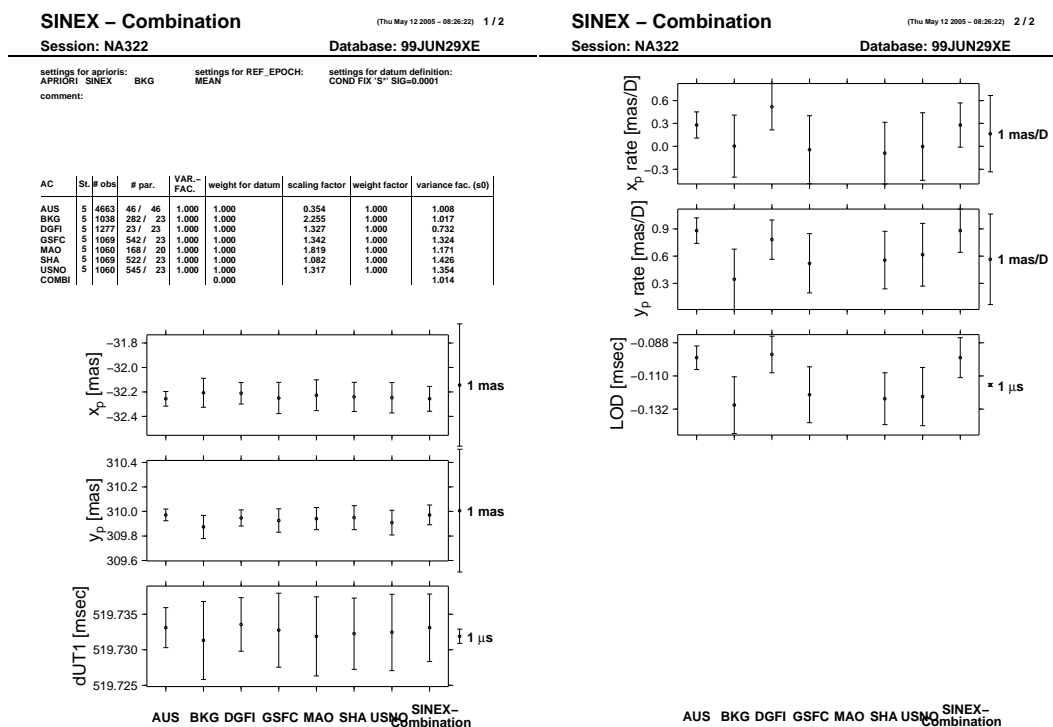


Figure 2. Example for Intra-technique combination results

2.3. Long-term solution of VLBI data from 1980 onwards

For the generation of a so-called long-term solution as a basis for a regular combination the analysis centers mentioned above re-processed almost all available VLBI data from 1980 onwards. Since VLBI is the only technique suitable for a precise UT1 determination this long-term solution is of unique importance for long-term EOP time series generation by the IERS CPP.

At the moment (May 2005) the SINEX statistics is as follows:

IVS Analysis center:	AUS	BKG	DGFI	GSFC	MAO	SHA	USNO	IVS
Sessions processed and submitted:	2481	3107	2642	3940	3441	3508	1220	2038

The current status of submissions of SINEX files is available online at http://miro.geod.uni-bonn.de/vlbi/sinex_combination/SINEX_statistics.html.

For the long-term solution all VLBI sessions with more than three solutions have been combined and submitted to the IERS CPP data center (see item "IVS" in the tabular above). The combined IVS solutions include almost all NEOS-, R1-, R4-, EUROPE-, JADE-, RDV- and other type of sessions. An example for an EOP time series based on SINEX combination is shown in figure 3.

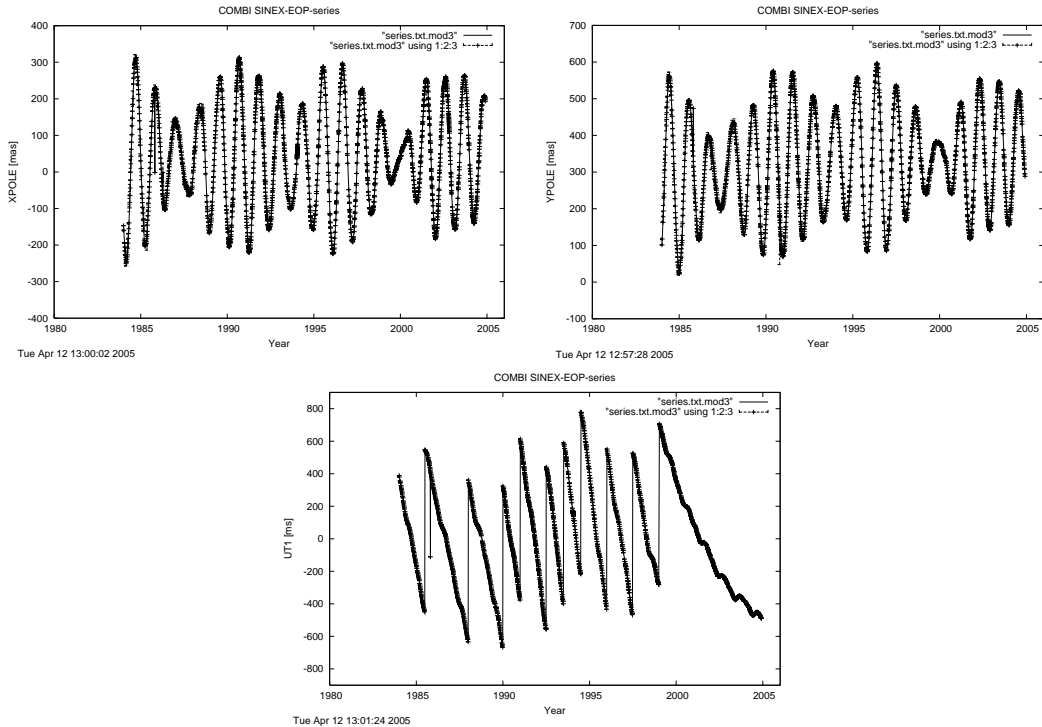


Figure 3. Example for EOP series derived from SINEX combination

3. Future tasks and outlook

VLBI SINEX data can also be used for internal VLBI investigations such as the computation of EOP time series which are based on the same apriori values (e.g. TRF). This kind of investigations can be used to explain the reasons for offsets (more than 100 μs) in EOP time series between different IVS analysis centers revealed in the results of the current combination of VLBI sessions.

Presently, investigations of the input SINEX data from the individual IVS Analysis Centers (and their differences) are in progress. These investigations are necessary for a reasonable combination on a regular basis and for the improvement of the accuracy and reliability of the combined EOP series which are submitted to the IERS CPP. Furthermore, improved strategies for outlier detection, scaling and weighting algorithms for the input matrices and procedures for an automated combination procedure are under development.

Although the IVS is prepared for its contributions to the IERS Combination Pilot Project some improvements of the existing procedures and further investigations on the quality of the input and the combined solutions are still to be done.

Currently GIUB is preparing the IVS contribution to the ITRF2004 which will be completely based on the new combination approach. Data of (about 2000) both global and regional VLBI observing sessions is being re-processed and combined to one official IVS solution per session.

One of the most important requirements for a meaningful contribution of the IVS to the rigorous combination of geodetic space techniques and for internal VLBI investigations is that the IVS Analysis Centers should submit their solutions on a strictly regular basis. We encourage the

analysis centers to concentrate their efforts on submitting their solutions regularly.

Acknowledgements

We would like to thank the software developers and IVS Analysis Centers for their efforts and we appreciate their future contributions to the intra-technique combination and thereby to the IERS CPP.

References

- [1] Brockmann, E.: Combination of Solutions for Geodetic and Geodynamic Applications of the Global Positioning System (GPS), Geodätisch-geophysikalische Arbeiten in der Schweiz, Schweizerische Geodätische Kommission, Band 55, 1997.
- [2] CPP-Call for participation, http://www.iers.org/iers/about/wg/wg3/docs/cfp_cpp.pdf
- [3] GEOTECHNOLOGIEN: Observation of the System Earth from Space, Status Seminar Report, Bavarian State Mapping Agency (BLVA), Munich, Koordinierungsbüro GEOTECHNOLOGIEN, (GEOTECHNOLOGIEN Science Report No. 3), 2003.
- [4] Kelm, R., Rank Defect Analysis and Variance Component Estimation for Inter-Technique Combination, Proceedings of the IERS Workshop on Combination Research and Global Geophysical Fluids. Bavarian Academy of Sciences, Munich, Germany, 18 - 21 November 2002. Edited by Bernd Richter, Wolfgang Schwegmann, and Wolfgang R. Dick. (IERS Technical Note ; 30) Frankfurt am Main: Verlag des Bundesamts für Kartographie und Geodäsie, 2003.
- [5] Lay, D., Linear Algebra and its Applications, Second Edition, Addison-Wesley, 2000.
- [6] Mikhail, Observations and Least Squares, IEP-A Dun-Donnelley Publisher, 1976.
- [7] Ma, C., L. Petrov, SINEX File Implementation in the VLBI Calc/Solve Analysis System, Proceedings of the IERS Workshop on Combination Research and Global Geophysical Fluids. Bavarian Academy of Sciences, Munich, Germany, 18 - 21 November 2002. Edited by Bernd Richter, Wolfgang Schwegmann, and Wolfgang R. Dick. (IERS Technical Note ; 30) Frankfurt am Main: Verlag des Bundesamts für Kartographie und Geodäsie, 2003.
- [8] Nurutdinov, K. et al.: Combination of Terrestrial Reference Frames and ERP at University of Newcastle, Proceedings of the IERS Workshop on Combination Research and Global Geophysical Fluids. Bavarian Academy of Sciences, Munich, Germany, 18 - 21 November 2002. Edited by Bernd Richter, Wolfgang Schwegmann, and Wolfgang R. Dick. (IERS Technical Note ; 30) Frankfurt am Main: Verlag des Bundesamts für Kartographie und Geodäsie, 2003.
- [9] Vennebusch, M.: First results of SINEX combinations, International VLBI Service for Geodesy and Astrometry 2004 General Meeting Proceedings, edited by Nancy R. Vandenberg and Karen D. Baver, NASA/CP-2004-212255, 2004.

Approaches for modeling non-linear site position variations

Leonid Petrov

NVI, Inc./NASA GSFC

e-mail: Leonid.Petrov@lpetrov.net

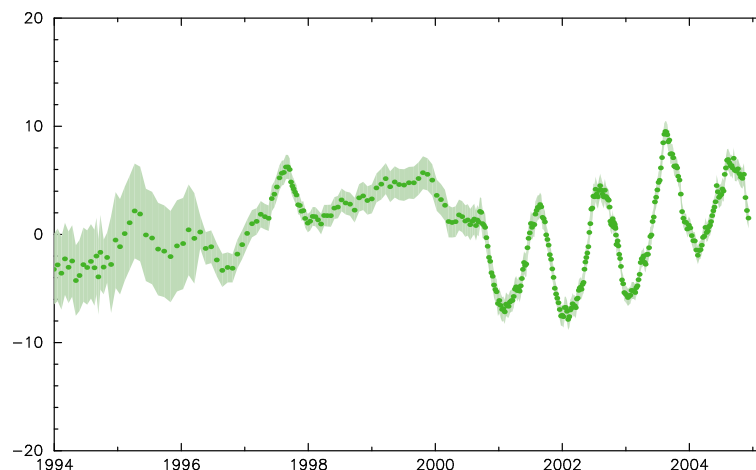
Abstract

Approaches for estimation of site motion beyond linear models are discussed. It is proposed to represent site motion in a sum of three functions: a linear function, an expansion with the B-spline bases, a sum of principal components of the expansion with the Fourier basis. The VLBI dataset from 1979 to 2005 was re-analyzed following this approach. It is concluded that this approach is adequate for describing the non-linear position evolution of VLBI stations.

1. Introduction

Traditionally, the site position evolution is described with a linear model. The technique for this type of motion estimation is well established. However, there is a number of pieces of evidence which show the inadequacy of this model is growing. There are certain phenomena which cause deviation of site motion from a simple linear model: 1) rail repair (for example, DSS65, MEDICINA which results in breaks in a position evolution; 2) seismic slips and transient deformations (TATEYAMA, GILCREEK); 3) seasonal changes in site positions due to mismodeling of mass loading; and 4) poorly understood local phenomena (for example, PIETOWN, HRAS_085). An example of non-linear site motion is shown in figure 1.

Figure 1. Evolution of the length of ALGOPARK/WESTFORD baseline after box-filtering with a width of 60 days. Units: mm.



Due to the presence of systematic errors the accuracy of determination of linear velocity for many stations is approaching the correlation limit. Therefore, no significant accuracy improvement in the framework of the linear model is expected. On the other hand, there is a demand from the

geophysical community to understand better seasonal and inter-annual station position variations. This motivates us to seek an alternative method for site positions estimation.

2. Analysis of the problem

It may seem sufficient to estimate a daily time series of VLBI site positions and then analyze it. However, we should be aware of several complications. The equations of light propagation are differential, they do not determine the solution, but rather a family of solutions. In order to select a member in this family, boundary conditions should be imposed, either explicitly or implicitly in the form of fixing six linear combinations of site coordinates to their a priori values. These boundary conditions make the estimates of site position linearly dependent. This means that variations of position of site A will cause apparent variations in *estimates* of position of site B . These induced variations in estimates of other sites depend on the network configuration and the number of stations. The induced variations in estimates of coordinate of site B due to variations in position of site A will be diluted approximately as $\frac{1}{n}$, where n is the total number of sites in the network. Each network of VLBI sites which participate in an individual experiment is small, typically 5–8 stations, so induced variations are not diluted enough to become negligible. To make things worse, the VLBI network is constantly changing: the set of stations which participate in experiments varies from day to day. These factors make interpretation of changes in *coordinates* as a physical *displacement* very unreliable.

Another complication arises when the Earth orientation parameters are evaluated. The small vector of the Earth rotation determined by the pole coordinates and UT1 is equivalent to the net-rotation of the network of observing stations with respect to some a priori positions. It should be stressed that removal or addition of a station changes the net-rotation of the network which is of the order of magnitude $\frac{\Delta r}{n}$ where Δr is the adjustment to position of an additional site, and n — the total number of stations in the network. Since typically the VLBI network configuration is not held the same in different experiments (during 1979–2005 1240 network configurations were used in 3900 experiments), the Earth orientations parameters evaluated at experiments in different network configurations will have jumps which depend on a priori site coordinates. This will make their interpretation problematic.

Finally, allowing site position to evolve freely on a daily basis reduces the strength of the solution, since its dimension increases. But there is no reason to believe that stations move chaotically at the time scale of 1–30 days. The estimation strategy which evaluates site position independently at adjacent epochs implicitly assumes that stations may have arbitrary large displacements between epochs, and therefore, have arbitrary large accelerations caused by arbitrary large forces. Analysis of the physics of motion can help us to come out with a more realistic model.

2.1. What can cause non-linear site motion?

Understanding causes of non-linear motion helps us to find the optimal parameterization of such a motion. Known causes of the motion can be characterized the following way:

- Antenna displacements due to human activity. Antenna repair can cause an abrupt shift in antenna position at a known epoch.
- Seismic motion. Such a motion is characterized as a sudden jerk in station position at precisely a known epoch which may be followed by an exponential relaxation at time scales

from months to several years.

- Loading mismodeling. Mismodeling an ocean loading results in harmonic site position variations with precisely known frequencies. As was shown in [2], residual errors of ocean loading models are within 1–3 mm. Mismodeling atmospheric pressure loading results mainly in a quasi-random motion with amplitudes with rms less than 1 mm according to [3]. Mismodeling a hydrology loading may result in annual, semi-annual and in some cases ter-annual position variations with an amplitude of 2-8 mm. Currently, it is rather difficult to evaluate the accuracy of hydrological models.
- Unaccounted thermal deformations of the antenna. This signal is mainly diurnal and annual.

3. Mathematical model for non-linear motion

The preferable mathematical model for a non-linear motion should utilize the apriori knowledge about the process under consideration. The solution is sought in the form of an expansion the process with an *appropriate* basis. The coefficients of the expansion are evaluated by using least squares together with linear site velocities, positions at the reference epoch, source coordinates, Earth orientation, and nuisance parameters which characterize clock function and atmospheric path delay. A poorly selected basis requires a dimension of the expansion comparable with the dimension of the initial problem. The process expanded with the appropriate basis will have non-principal components vanishing which allows us to reduce significantly the dimension of the problem.

In this paper I propose to use two bases: the Fourier basis and the B-spline basis.

The components of the Fourier basis which corresponds to the tidal, annual and diurnal frequencies and their multiples are included in the parametric model. These constituents represent the residual tidal, seasonal and diurnal signals. The Fourier basis is the eigenfunction of the linear operator, and it is suitable for describing phenomena which are incessant in the range $[-\infty, +\infty]$.

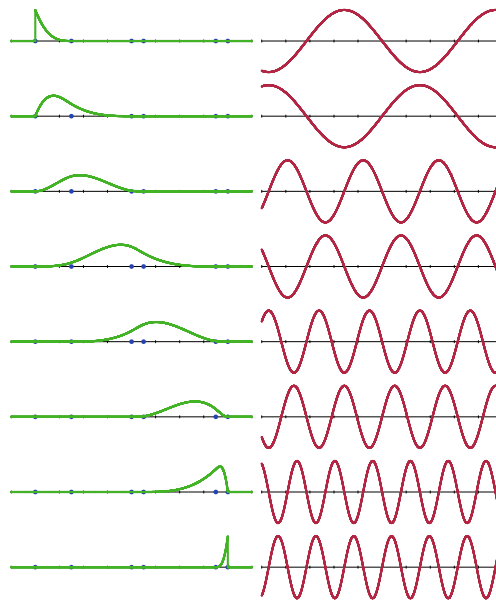
The B-spline basis is suitable for modeling events localized in time. We know [1] that 1) a B-spline of degree k is non-zero at $k + 1$ knots; 2) a B-spline of degree $2k - 1$ provides a minimum to the functional $\int_a^b [f(x)^{(k)}]^2 dx$ which takes specific values at the sequence of knots. In that sense the B-spline is the most smooth function used for approximation.

Since we simultaneously solve for site positions, linear velocities and coefficients of B-spline, we have to impose decorrelation constraints requiring the zeroth and first momentum over the basis functions to be a constant:

$$\int_a^b \sum_i B_i(x) dx = \text{constant} \quad (1)$$

$$\int_a^b \sum_i x B_i(x) dx = \text{constant} \quad (2)$$

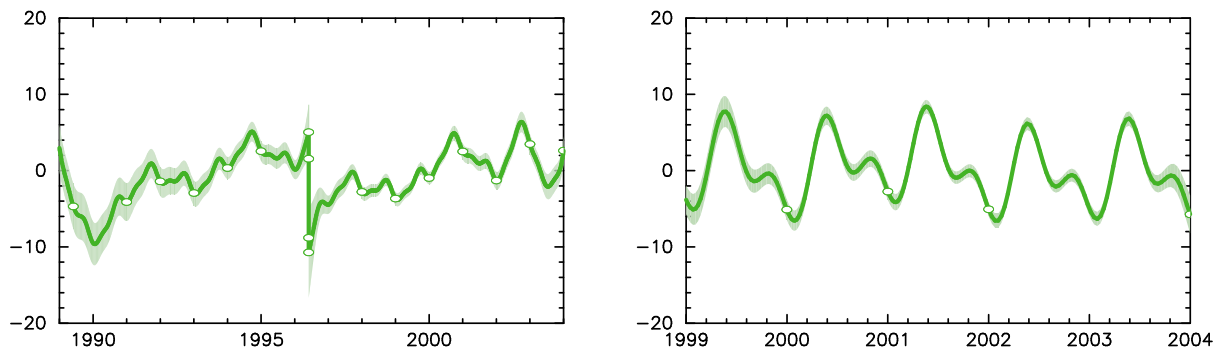
Figure 2. Example of basis functions: the B-spline at six nodes (left) and eight Fourier basis functions



4. Result of analysis

The ability to model non-linear site position variations was added to the VLBI analysis software Calc/Solve¹ in 2005. In trial solutions all VLBI observations from 1979 to 2005 were used. In addition to the traditional set of parameters (site positions at reference epoch, site velocities, the Earth orientation parameters, clock function, atmosphere zenith path delay and the atmosphere tilt), sine and cosine amplitudes at annual, semi-annual, diurnal, semi-diurnal frequencies were evaluated as well as the coefficients of the B-spline expansion of the third degree for 36 sites. The knots of the B-spline were selected equidistantly with the time span of 2 years, except the stations with seismic events, for example, GILCREEK, and stations with rail repairing, DSS65, MEDICINA. For these stations the knots with the multiplicity three were inserted at epochs of events.

Figure 3. The empirical model of non-linear changes in site coordinates. Left: east component of station MEDICINA. Right: up component of the station of TSUKUBA. Units: mm

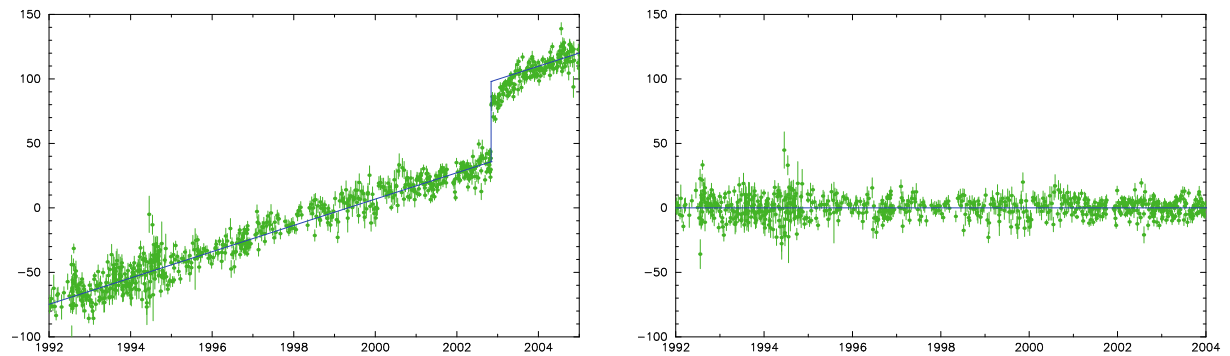


¹<http://gemini.gsfc.nasa.gov/solve>

Examples of the estimates of the empirical model of the non-linear motion are shown in figure 3. Station MEDICINA has a complicated motion: a break caused by rail repairing on 1996.06.01, seasonal variations and inter-annual variations. Non-linear motion of the station of TSUKUBA is mainly seasonal which maybe related to the seasonal changes of the ground water level related to rice fields irrigation.

The empirical model of station motion was substituted in a separate baseline solution. Figure 4 shows results of the substitution for the baseline GILCREEK/WETTZELL affected by Denali earthquake on 2002.11.03.

Figure 4. Evolution of the baseline GILCREEK/WETTZELL. Left: the baseline length time series without modeling non-linear motion. Right: the estimates of baseline lengths after applying the empirical model. Units: mm



5. Conclusions

It was found that the technique of estimation of the coefficients of expansion with the B-spline and Fourier basis is adequate for modeling non-linear site position variations. An addition of new parameters causes a moderate increase of dimension of the problem, but retrieves the signal. When the time span for B-spline is selected to two or even one year, the solution is still stable. 40–50 stations participate in observation during one calendar year. This estimation technique is equivalent to analysis of observations for 1–2 years at a 40–50 station network, in contrast to 4–7 station networks used in each daily individual experiment.

Several problems are still to be solved theoretically: 1) what is the optimal choice of epochs for knots of the B-spline basis?; 2) should constraints on time derivatives of B-spline be applied?; 3) how many harmonics can be included in a solution before it becomes unstable?

References

- [1] G. Nürnberger, Approximation by spline functions, Springer, 1989.
- [2] L. Petrov, C. Ma, Study of harmonic site position variations determined by VLBI, *J. Geophys. Res.*, vol. 108, No. B4, 2190, doi: 10.1029/2002JB001801, 2003. <http://gemini.gsfc.nasa.gov/harpos/>
- [3] L. Petrov, J.-P. Boy, Study of the atmospheric pressure loading signal in VLBI observations, *J. Geophys. Res.*, vol. 109, No. B03405, 10.1029/2003JB002500, 2004. <http://gemini.gsfc.nasa.gov/aplo/>

VTRF2005 - A combined VLBI Terrestrial Reference Frame

Axel Nothnagel

Geodetic Institute, University of Bonn

e-mail: nothnagel@uni-bonn.de

Abstract

Since the ITRF2000 has been based only on observation data until the end of the year 2000 the quality of this TRF deteriorated for the time beyond. In order to provide a terrestrial reference frame (TRF) for operational VLBI determinations of EOP and atmospheric water vapour content, a new conventional TRF of VLBI observatories has been compiled from a combination of five VLBI TRF realisations. At epoch 2000.0 the scale of the new VLBI TRF (VTRF2005) is about 0.5×10^{-9} smaller than ITRF2000 with a scale rate of 0.18×10^{-9} /year.

1. Motivation

The ITRF2000 (Boucher et al. 2004 [1]) has been the terrestrial reference frame (TRF) for operational VLBI earth orientation parameter (EOP) and water vapor content determinations for some time before it was superseded by VTRF2003 (Nothnagel, 2003 [4]). Since then a number of reasons have deemed it necessary to update the VLBI TRF and replace it by a more sophisticated realisation. Within the last year a number of TRF realisations have been computed, this time not only with the Calc/Solve software but also with OCCAM (Tesmer (DGFI), Titov (AUS), pers. communication) and SteelBreeze (Bolotin, pers. communication). For the first time this offers the opportunity to combine and compare TRF realisations of different analysis packages based on Gauß-Markov type least squares adjustments (LSA), square-root information filter (SRIF) and Kalman filtering (KF) as well as on different analysis strategies and data volume (Table 1).

	IVS Analysis Center	Software	Model
AUS	Geoscience Australia, Belconnen, Australia	OCCAM	KF
BKG	Bundesamt für Kartographie und Geodäsie, Leipzig, Germany	Calc/Solve	LSA
DGFI	Deutsches Geodätisches Forschungsinstitut, München, Germany	OCCAM	LSA
GSFC	NASA Goddard Space Flight Center, Greenbelt MD, USA	Calc/Solve	LSA
MAO	Main Astronomical Observatory, Kiev, Ukraine	SteelBreeze	SRIF

Table 1. Contributing analysis centers and software packages used

In addition, the combination process and a detailed analysis of the post-fit residuals provides an ideal opportunity for a quality assessment of the individual solutions. This generates an important feedback to the analysts who may be able to figure out possible areas of improvement in their models and analysis strategies.

2. Combination Process

VTRF2005 is compiled as a combined TRF with the input from the solutions mentioned above. For the combination process the datasets as produced by the analysis centers in the form of coordinates at 1997.0 and velocities were first transformed into coordinate lists at reference epochs 2000.0 and 2010.0. The formal errors of the input series were applied to the error propagation law to end up with the individual formal errors for the respective epochs. The same was done for the ITRF2000 data set of VLBI stations. This preparatory step served the purpose to generate the input data for transforming the VLBI coordinate sets into the ITRF2000 frame using a standard Helmert transformation.

The question which arises at this instant is which stations to use as datum points (identical points). Here, it should be mentioned that currently the twelve radio telescopes employed in the IVS-R1 and IVS-R4 sessions (IVS 2005 [2]) produce about 85% of the observational data in the framework of the IVS (i.e. ALGOPARK, FORTLEZA, GILCREEK, HARTRAO, HOBART26, KOKEE, MATERA, NYALES20, SESHAN25, TSUKUB32, WESTFORD, WETTZELL). For this reason these twelve sites were selected as datum sites for the Helmert transformation. For each individual set of coordinates at epochs 2000.0 and 2010.0 the Helmert parameters for the transformation into the ITRF2000 frame have been estimated yielding the parameters listed in tables 2 and 3.

	AUS	BKG	DGFI	GSFC	MAO	average σ
α [μas]	-29.8	34.6	-96.1	-97.1	63.6	$\pm 50 \mu\text{as}$
β [μas]	47.7	36.5	5.9	-63.4	-39.5	$\pm 46 \mu\text{as}$
γ [μas]	-1.7	25.6	22.8	-49.4	148.1	$\pm 41 \mu\text{as}$
ΔX [mm]	0.5	0.1	-0.8	-2.9	0.4	$\pm 1.3 \text{ mm}$
ΔY [mm]	0.3	0.1	3.0	2.6	-1.5	$\pm 1.2 \text{ mm}$
ΔZ [mm]	0.6	-0.3	1.1	3.7	-1.5	$\pm 1.3 \text{ mm}$
Scale [-]	8.1×10^{-10}	4.6×10^{-10}	8.7×10^{-10}	4.1×10^{-10}	4.4×10^{-10}	$\pm 2.0 \times 10^{-10}$

Table 2. Helmert parameters from analysis center into ITRF2000 for epoch 2000.0

	AUS	BKG	DGFI	GSFC	MAO	average σ
α [μas]	-178.8	38.0	-205.7	-208.9	224.4	$\pm 120 \mu\text{as}$
β [μas]	40.5	2.3	7.6	-138.9	-249.3	$\pm 130 \mu\text{as}$
γ [μas]	-97.1	34.6	44.5	-75.5	572.4	$\pm 80 \mu\text{as}$
ΔX [mm]	-1.7	-1.6	-3.3	-7.2	1.4	$\pm 3.0 \text{ mm}$
ΔY [mm]	2.5	0.5	5.2	4.6	-1.2	$\pm 2.0 \text{ mm}$
ΔZ [mm]	4.6	0.7	6.3	9.2	-6.3	$\pm 3.0 \text{ mm}$
Scale [-]	2.7×10^{-9}	2.3×10^{-9}	2.6×10^{-9}	2.2×10^{-9}	1.2×10^{-9}	$\pm 0.5 \times 10^{-9}$

Table 3. Helmert parameters from analysis center into ITRF2000 for epoch 2010.0

While the rotations and translations are generally only at the few mm level often compensated by the respective rotations, the scale factors deserve a closer look. For the epoch 2000.0 they range from 4.1×10^{-10} to 8.7×10^{-10} with a median of 4.6×10^{-10} resulting in about 2.9 mm at one earth radius with respect to ITRF2000. At epoch 2010.0 the median is 2.3×10^{-9} with an RMS scatter of about 0.6×10^{-9} between the individual solutions (3.8 mm at one earth radius). Considering

the ten year epoch difference, the scale rate between ITRF2000 and the VLBI solutions is about 1.8×10^{-10} per year.

In the actual transformation into the ITRF2000 axis definition, the scale parameters have not been used. The TRF realisations have only been translated and rotated, thus, maintaining the form and size of the polyhedron. In this step not only the datum sites but all other telescopes have been transformed, again propagating also the formal errors.

For the combination process the TRFs of the five analysis centers as transformed into a common frame have been used as input. For both epochs the combination has been carried out on a station by station basis applying input weights of the individual solutions but neglecting the covariances. Considering the fact that other effects still dominate the error budget, the correlations between the coordinate components are deemed to be of a lesser importance at this stage and for this very purpose. A very small number of outliers has been eliminated using a 5-sigma threshold. In the case when only one data set contained a certain station, the coordinates of this realization have been carried over. We may safely apply this procedure since all data sets had been transformed into the common datum beforehand.

In the final step of the process the combined coordinates at epochs 2000.0 and 2010.0 were re-transformed into coordinates at epoch 1997.0 ($X_{1997.0}$) and velocities (v_X) using

$$v_X = \frac{X_{2010.0} - X_{2000.0}}{t_{2010.0} - t_{2000.0}}$$

and

$$X_{1997.0} = X_{2000.0} + v_x \cdot (t_{1997.0} - t_{2000.0})$$

with X_i representing the respective coordinate components and t_i being the respective epochs.

The combined position/velocity model of Gilcreek after the earthquake consists of piece-wise linear "legs". In the coordinate/velocity list the reference coordinates of Gilcreek for each leg could, therefore, not be referred to 1997.0 as is common practice for current terrestrial reference frame realisations. Only for the time prior to the earthquake (between 1979.01.01 and 2002.11.02) the reference epoch of 1997.0 has been chosen. The coordinates of each starting point of a linear leg are referred to the respective epoch. Coordinates of an arbitrary observing epoch can, thus, be computed using the respective period with its coordinates at the reference epoch and the respective velocity.

3. Results

A first interim result giving a direct insight into the level of agreement of the individual TRF realisations is a list of geocentric radii and their differences relative to ITRF2000. The geocentric radii are independent of the rotations of the reference frame and give a clear indication of the scale variations to be expected from the input series. Figures 2 and 3 depict the geocentric radii for the twelve datum sites for the five analysis centers at the two epochs. It can be seen that for the 2000.0 epoch the overall agreement between the individual analysis centers is quite good with only very few exceptions caused by peculiarities in the treatment of individual stations by the analysis centers (e.g. Tsukuba by MAO). On average the scale of the VLBI solutions seems to be slightly smaller than that of ITRF2000. This is supported by the Helmert scale factors in table 2 which is, on average, slightly positive when transforming from the VLBI TRFs to ITRF2000.

Special considerations have to be given in particular to the Gilcreek observatory which has suffered an earthquake induced displacement of several centimeters on November 3, 2002. It is not the fact of the displacement itself but the non-linear behaviour for quite some time after the earthquake. While the AUS, GSFC and DGFI analysis centers developed an exponential decay model (MacMillan 2004 [3]; Titov and Tregoning 2004 [5]) or a piece-wise linear model (Tesmer, pers. comm.), BKG and MAO did not take into account a non-linear station motion. Except of DGFI all analysis centers assumed the same velocity components before and after the earthquake (Fig. 2). In view of the fact that the same velocity components before and after the earthquake seem to be more plausible than a significant change in direction, the DGFI results for Gilcreek were excluded from the combination as were the MAO and BKG results for their lack of a suitable transient model.

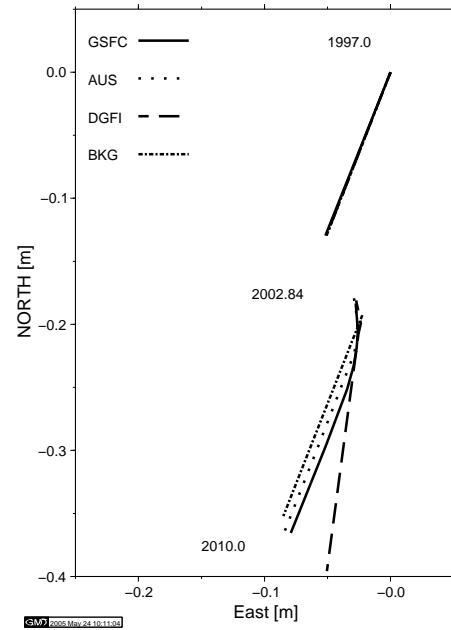


Figure 1. Estimates of Gilcreek observatory for epoch Nov. 3, 2002

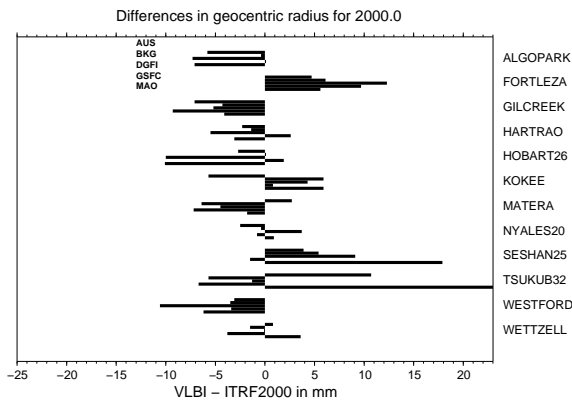


Figure 2. Differences in geocentric radii for epoch 2000.0 (sequence AUS, BKG, DGFI, GSFC, MAO)

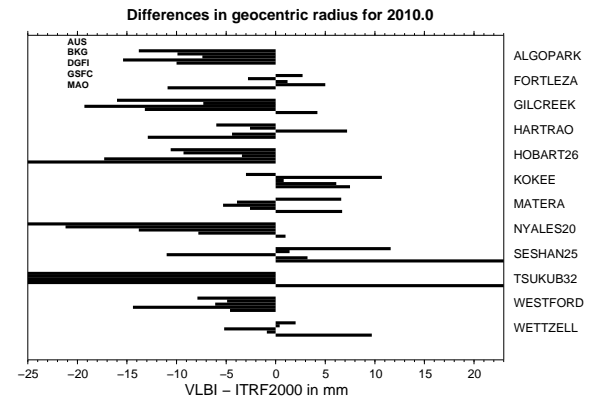


Figure 3. Differences in geocentric radii for epoch 2010.0 (sequence as in figure 2)

For epoch 2010.0 the picture is a bit more scattered predominantly driven by a few sites with larger variations in the geocentric radii. In general, however, the trend of negative differences and,

thus, of a larger scale of the ITRF2000 as compared to the VLBI TRFs remains and even increases towards the future. Again, this is supported by the Helmert scale factors in table 3.

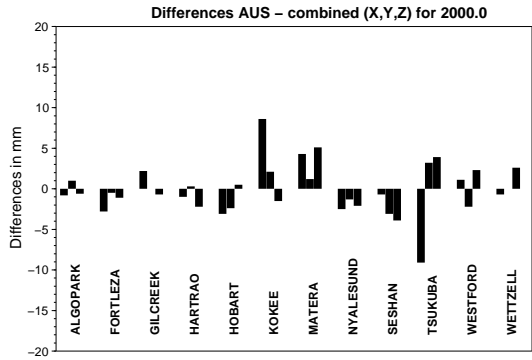


Figure 4. Residuals of AUS results w.r.t. combination for epoch 2000.0 (Sequence X,Y,Z)

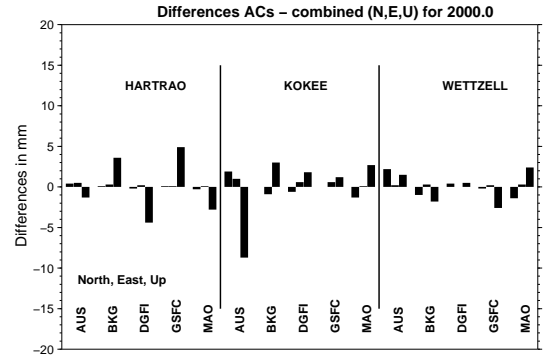


Figure 5. Residuals of selected sites w.r.t. combination for epoch 2000.0 (Sequence N,E,U)

Figures 4 and 5 display a few selected post-fit residuals for epoch 2000.0 and give a good impression of the good agreement of the input series to the combination. The scatter is again slightly larger for the epoch 2010.0 (Figures 6 and 7). As should be expected the vertical components show a larger scatter than the horizontal components.

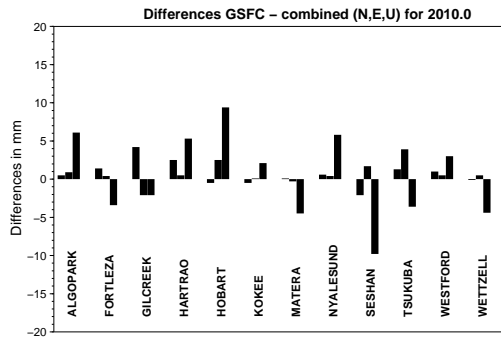


Figure 6. Residuals of GSFC results w.r.t. combination for epoch 2010.0 (Sequence N,E,U)

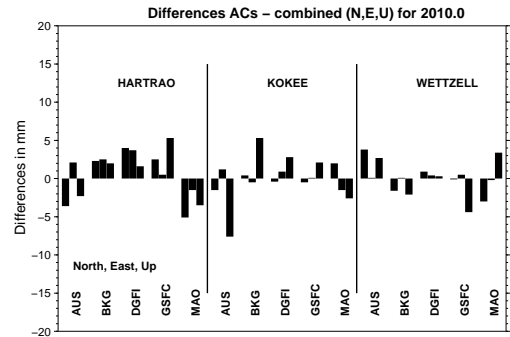


Figure 7. Residuals of selected sites w.r.t. combination for epoch 2010.0

Finally, the residuals of the 35 most important stations are displayed together in figures 8 and 9 to produce a general overview of the quality. The solution of DGFI is chosen here to represent the residuals of an average quality input series. With the exception of only a few components exceeding 5 mm for epoch 2000.0, the agreement of the five input TRFs is very good. For epoch 2010.0 the picture seems to be less favourable. However, the appearance of a few components with slightly larger residuals should not restrict the view of the fact that the WRMS of the residuals are still of the order of below 5 mm.

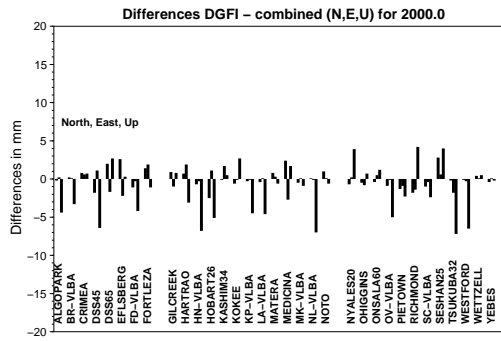


Figure 8. Residuals of 35 major sites in DGFI solution w.r.t. combination for epoch 2000.0

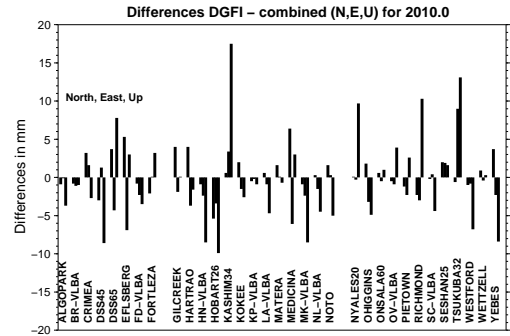


Figure 9. Residuals of 35 major sites in DGFI solution w.r.t. combination for epoch 2010.0

After combination the evolution of the scale can best be depicted again through the differences in geocentric radius of VTRF2005 minus ITRF2000 for both epochs (Figures 10 and 11). It can clearly be seen that in 2010.0 the differences are predominantly negative indicating that the VLBI polyhedron will be significantly smaller than predicted by ITRF2000 (see also table 3).

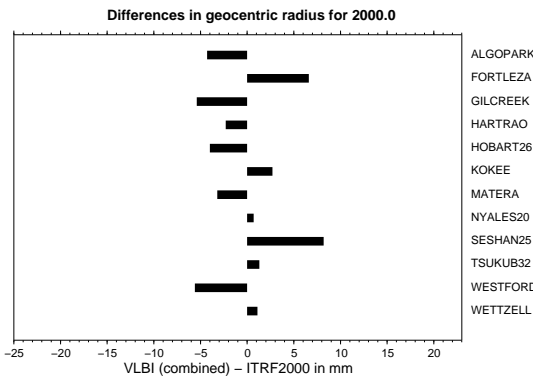


Figure 10. Differences in combined geocentric radii for epoch 2000.0

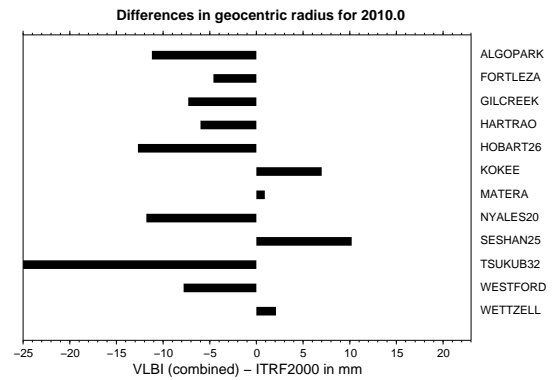


Figure 11. Differences in combined geocentric radii for epoch 2010.0

VTRF2005 is aligned to the axis and origin definition of ITRF2000 but maintains the VLBI scale. This is realised through the translation and rotation of each input TRF into ITRF2000 using the twelve core sites as identical points for the determination of the transformation parameters. The complete list of VTRF2005 coordinates at epoch 1997.0 and their velocities can be found at <http://giub.geod.uni-bonn.de/vlbi/IVS-AC>.

References

- [1] C. Boucher, Z. Altamimi, P. Sillard, M. Feissel-Vernier (2004): The ITRF2000; IERS Technical Note No. 31, Frankfurt a.M.
- [2] IVS (2005): International VLBI Service for Geodesy and Astrometry : Annual Report 2004, edited by D. Behrend and K. Baver, NASA/TP-2005-212772
- [3] D. MacMillan, S. Cohen (2004): Postseismic Transient after the 2002 Denali Fault Earthquake from VLBI Measurements at Fairbanks; Internatioinal VLBI Service for Geodesy and Astrometry 2004 General Meeting Proceedings, NASA/CP-2004-212255, 491-495
- [4] A. Nothnagel (2003): VTRF2003: A Conventional VLBI Terrestrial Reference Frame; Proceedings of the 16th Working Meeting on European VLBI for Geodesy and Astrometry, held at Leipzig, May 09 10, 2003, edited by W. Schwegmann and V. Thorandt, Bundesamt für Kartographie und Geodäsie, Frankfurt/Leipzig, 195 - 205
- [5] O. Titov, P. Tregoning (2004): Post-seismic Motion of Gilcreek Geodetic Sites Following the November 2002 Denali Earthquake; Internatioinal VLBI Service for Geodesy and Astrometry 2004 General Meeting Proceedings, NASA/CP-2004-212255, 496-500

Measurement of core-shifts with astrometric multi-frequency calibration

María Rioja ¹, Richard Dodson ², Richard Porcas ³, Hiroshi Suda ⁴, Francisco Colomer ¹

¹) *Observatorio Astronómico Nacional, Alcalá de Henares, Spain*

²) *Institute of Space and Astronautical Science, JAXA, Sagami-hara, Japan*

³) *Max-Planck-Institut fuer Radioastronomie, Bonn, Germany*

⁴) *VERA Observatory, NAOJ, Mitaka, Tokyo, Japan; Dep. Astronomy, Univ. Tokyo, Japan*

Contact author: María Rioja, e-mail: rioja@oan.es

Abstract

VLBI is unique, among the space geodetic techniques, in its contribution to defining and maintaining the International Celestial Reference Frame, providing precise measurements of coordinates of extragalactic radiosources. The quest for increasing accuracy of VLBI geodetic products has led to a deeper revision of all aspects that might introduce errors in the analysis. The departure of the observed sources from perfect, stable, compact and achromatic celestial targets falls within this category. This paper is concerned with the impact of unaccounted frequency-dependent position shifts of source cores in the analysis of dual-band S/X VLBI geodesy observations, and proposes a new method to measure them. The multi-frequency phase transfer technique developed and demonstrated by Middelberg et al. (2005) increases the high frequency coherence times of VLBI observations, using the observations at a lower frequency. Our proposed SOURCE/FREQUENCY PHASE REFERENCING method endows it with astrometric applications by adding a strategy to estimate the ionospheric contributions. Here we report on the first successful application to measure the core shift of the quasar 1038+528 A at S and X-bands, and validate the results by comparison with those from standard phase referencing techniques. In this particular case, and in general in the cm-wavelength regime, both methods are equivalent. Moreover the proposed method opens a new horizon with targets and fields suitable for high precision astrometric studies with VLBI, especially at high frequencies where severe limitations imposed by the rapid fluctuations in the troposphere prevent the use of standard phase referencing techniques.

1. Introduction

Geodetic VLBI observations with a network of antennas at the Earth are affected by the propagation medium, mainly the ionosphere and the troposphere. It is a basic practice in geodesy to calibrate the ionospheric contribution with simultaneous observations at S/X-bands (2.2GHz/8.4GHz, respectively). The ionospheric-free delay observables at X-band (τ_x^c) are estimated from a combination of observed delays (τ_x, τ_s) at both bands:

$$\tau_x^c = \frac{\nu_x^2}{\nu_x^2 - \nu_s^2} \cdot \tau_x - \frac{\nu_s^2}{\nu_x^2 - \nu_s^2} \cdot \tau_s$$

and used to estimate the geodetic parameters. This approach works under the critical assumption that the brightness distributions for each source are identical and are co-located at both frequencies. In sources for which the VLBI core position is frequency dependent the exact expression must include a 24-hour sinusoidal extra term whose amplitude depends on the magnitude of the shift of the position of the source core (*core shift*):

$$+ \frac{\nu_s^2}{\nu_x^2 - \nu_s^2} * \Delta\tau_{sx}^{geo} \sim 0.08 * \Delta\tau_{sx}^{geo}$$

where $\Delta\tau_{sx}^{geo} = \frac{\vec{D} \cdot \vec{\theta}_{sx}}{c}$, and $\vec{\theta}_{sx}$ corresponds to the *core shift* between S and X-bands.

The non-inclusion of this extra term introduces errors in the estimated ionosphere-free observables, and hence on the astrometric/geodetic products from the analysis. For sources with non-varying (i.e. stable) *core shift* θ_{sx} , the unaccounted extra term will propagate into an offset from the true X-band position, of magnitude ($\theta_{sx} * 0.08$) in the direction away from the S-band position [8]. Instead, unstable *core shifts* can propagate also into uncertainties in the estimated Earth orientation parameters (Engelhardt, these proceedings) in the multi-epoch geodetic analysis. Section 2 is concerned with the origin, magnitude and geodetic impact of core shifts; Section 3 discusses the methods to measure them and Section 4 presents the results of our proposed method.

2. Core shifts do exist

Changes in the observed core positions at different frequencies have been measured in several sources, for example, 1038+528 A [4],[9], 4C39.25 [1], 3C395 [2] and 1823+568 [7]. We propose to classify the core shifts in two groups depending on their origin:

- “Astronomical core shifts” result from opacity effects in the jet. The unresolved “core” of a compact extragalactic radio source is believed to mark the location where the optical depth to synchrotron self absorption ~ 1 . This position changes with observing frequency as $R_{core} \propto \nu^{-1/k_r}$, where k_r depends on physical conditions in the jet. Core position shifts between S and X-bands of up to 1.5 milli-arcsecond (*mas*) are predicted in [3].
- “Instrumental core shifts” result from convolving the source structure with different resolutions at different frequencies, causing core shifts of up to half the beam size at the lower frequency.

While the existence of source “*core shifts*” cannot be predicted, there are some clues which alert one to them. Larger “astronomical core shifts” are expected for flat spectrum sources, where the power index $k_r \sim 1$; “instrumental core shifts” can be expected if the source structure at the higher frequency falls within a small fraction of the beam size at the lower frequency. Regardless of its nature, both core shifts have an identical effect on the analysis of S/X geodesy data. Table 1 lists the propagation of plausible unaccounted stable core shifts into the analysis products.

Observing frequencies	“Astronomical” core shift	“Instrumental” core shift	Source position error
2.2/8.4 GHz	0 – 1 <i>mas</i>	0 – 2 <i>mas</i>	0 – 200 μ <i>as</i>
8.4/30 GHz	0 – 0.25 <i>mas</i>	0 – 0.5 <i>mas</i>	0 – 50 μ <i>as</i>

Table 1: Propagation of unaccounted non-varying core shifts into an offset from the true X and K-band position in the geodetic analysis of 2.2/8.4 GHz (S/X) and 8.4/30 GHz (X/K) observations, respectively.

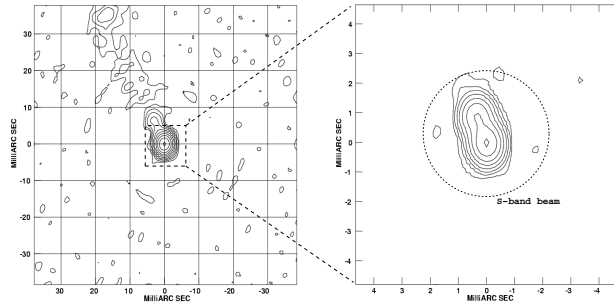


Figure 1. Hybrid map of 1038+528 A at S-band (*left*), and at X-band (*right*). The S-band beam superimposed on the X-band map illustrates the case of structure blending effects from insufficient resolution at lower frequencies, and therefore “instrumental” core shifts.

3. Ways to measure frequency-dependent core shifts

Using closure phase relations in the image processing of VLBI data results in lack of absolute positional information in the hybrid maps. A rigorous alignment of maps at different frequencies, to measure frequency-dependent shifts of the core position, requires absolute astrometry observations, or standard phase-referencing to a nearby (achromatic) radio source. If astrometric observations are not feasible, a simpler but more imprecise procedure for extended sources is to use an optically thin component to align maps at different frequencies, and close epochs, and then estimate the change in the position of the core.

Recently, Middelberg et al. [5, 6] proposed a new astrometric method that uses fast frequency switching observations of the target source and relies on the transfer of calibration from the lower to the higher frequency, after scaling by the frequency ratio. Their implementation proved to be a successful strategy to calibrate the rapid fluctuations of the troposphere, and hence extended the coherence time, in VLBA observations at 86 GHz, using interleaved scans at 15 GHz. This allowed the detection of a very weak, 100 mJy source. It also served to unveil the non-integer frequency ratio problem in the application of this method. On the other hand, the unaccounted dispersive ionospheric contamination, which was non-negligible even at these high frequencies, prevented them from making a proper astrometric measurement of the core shift.

We present an extension of this method, a so-called “SOURCE/FREQUENCY PHASE REFERENCING” which complements the fast frequency switching observing strategy with source switching, in order to calibrate the remaining dispersive contaminating contributions to the observables. Section 4 describes the first successful astrometric measurement of a *core shift* with this method, and Appendix A contains a brief discussion of the basics of the method.

4. Source/frequency phase-referencing

Conventional VLBI at high frequencies is severely constrained by the short coherence times imposed by the rapid fluctuations in the troposphere. The non-dispersive nature of the tropospheric propagation makes it possible to use lower frequency observations to calibrate higher, providing the switching interval between frequencies matches the temporal structure of the tropospheric fluctuations (i.e. coherence time) at the lower frequency. This is the basis of the multi-frequency phase transfer technique developed and demonstrated by Middelberg et al. [5, 6]. Our SOURCE/FREQUENCY PHASE REFERENCING method adds a source switching observing strategy, in addition to the fast frequency switching, to calibrate the dispersive contributions in the phase transfer strategy. The nodding between sources has to match the temporal and spatial structures of ionospheric propagation, and other non-dispersive terms, such as instrumental based contributions. A complete description of the method is given in Appendix A.

We have successfully applied this method to the astrometric analysis of dual-band S/X VLBA observations of the pair of quasars 1038+528 A and B, $33''$ apart, and measured the core shift in the quasar 1038+528 A. The calibration transfer between frequencies involves multiplying the phases by the frequency ratio. The calibration transfer between sources is done as in standard phase referencing. The result is a SOURCE/FREQUENCY PHASE REFERENCED map, shown in figure 2, whose offset from the center is a direct measure of the combined core shifts in the two sources between the two frequencies. The interpretation in terms of individual contributions from each source, assuming that shifts in the core position in each source would occur along the jet axis directions, is simplified by the quasi-orthogonal structures in this pair. The close alignment of the core shift offset with the A quasar source axis suggests a dominant contribution arising from this quasar; moreover, the quantitative agreement between the magnitude of the offset and the separation between the core and second component in the map of quasar A at X-band suggests the “instrumental” dominant nature of the offset. The results from a previous standard phase referencing analysis [9] are in complete agreement with those presented here, validating this new approach.

5. Conclusions

Unaccounted core shifts in the analysis of dual frequency VLBI geodesy observations propagate into offsets from the true X-band positions for the ICRF. We estimate deviations up to $200 \mu as$ and $50 \mu as$, respectively, for S/X and X/K observations, assuming temporally stable core shifts. Moreover, unstable core shifts can also corrupt the estimated Earth orientation parameters.

We have successfully applied the SOURCE/FREQUENCY PHASE REFERENCING method to the analysis of dual band S/X VLBA observations of the pair of quasars 1038+528 A and B, and measured a core shift in quasar 1038+528 A of ca. $800 \mu as$. Our result is equivalent to, within the errors, to those obtained using standard phase referencing techniques [9]. As far as we know this is the first case of successful astrometric application of this multi-frequency phase transfer method. In this case the simultaneous observations of both frequencies and sources allowed solutions despite the non-integer ratio of the observed frequencies. While this new strategy does not present any advantage with respect to traditional techniques in the cm-wavelength regime, it does hold a big potential at high frequencies, which are out of the range of conventional phase-referencing. In particular, we foresee a big impact when applied to observations of molecular line emission, where it

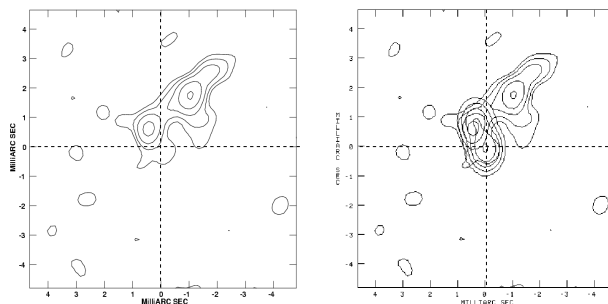


Figure 2. *Left:* SOURCE/FREQUENCY PHASE REFERENCED map of 1038+528 B from S/X VLBA observations; the $\sim 800\mu\text{as}$ offset in NE direction is an estimate of the combined core shift of 1038+528 A and B quasars between S and X bands. *Right:* Same map, with the hybrid map of 1038+528 A quasar superimposed, to show the agreement between the offset and the separation between the 2 components in the hybrid map of A quasar. This is an argument in favor of “instrumental core shift”.

may provide bona fide astrometric alignment of emission arising from different transitions and help to elucidate the controversy between the proposed pumping mechanism for masers in evolved stars.

Appendix A. The basics of the new method

This section outlines the basics of this astrometric method SOURCE/FREQUENCY PHASE REFERENCING aimed to measure core shifts in radio sources. Its application involves observations of the target and a nearby source (in the formulae, A and B) at the two frequencies of interest (here x and s). At the post-processing, the amplitude calibration is done using traditional techniques, for all observations; a pure self-calibration analysis is used to solve for the phase, delay and rate of each low frequency (s) target source (A) observations. Following the standard nomenclature, the phase values ϕ_A^s are shown as a compound of geometric, tropospheric, ionospheric and instrumental terms - assuming that structural contributions $\phi_{A,str}^s$ have been computed using the hybrid maps, and removed:

$$\phi_A^s = \phi_{A,geo}^s + \phi_{A,tro}^s + \phi_{A,ion}^s + \phi_{A,inst}^s + 2\pi n_A^s, \text{ with } n_A^s \text{ integer}$$

These values are scaled by the frequency ratio, R , and used to calibrate the high frequency observations. The resultant high frequency referenced phases to the low frequency are:

$$\begin{aligned} \phi_A^x - R.\phi_A^s &= \phi_{A,str}^x + (\phi_{A,geo}^x - R.\phi_{A,geo}^s) + (\phi_{A,tro}^x - R.\phi_{A,tro}^s) + (\phi_{A,ion}^x - R.\phi_{A,ion}^s) \\ &\quad + (\phi_{A,inst}^x - R.\phi_{A,inst}^s) + 2\pi(n_A^x - R.n_A^s) \end{aligned} \quad (1)$$

This calibration strategy results in perfect cancellation of non-dispersive tropospheric terms: $(\phi_{A,tro}^x - R.\phi_{A,tro}^s) = 0$, but not for the dispersive ionosphere: $(\phi_{A,ion}^x - R.\phi_{A,ion}^s) = (R - \frac{1}{R})\phi_{A,ion}^s$

Taking this into account in Equation (1) above results in:

$$\phi_A^x - R.\phi_A^s = \phi_{A,str}^x + 2\pi\nu \frac{\vec{D} \cdot \vec{\theta}_{A,sx}}{c} + (R - \frac{1}{R})\phi_{A,ion}^s + (\phi_{A,inst}^x - R.\phi_{A,inst}^s) + 2\pi(n_A^x - R.n_A^s) \quad (2)$$

where $2\pi\nu \frac{\vec{D} \cdot \vec{\theta}_{A,sx}}{c} = (\phi_{A,geo}^x - R.\phi_{A,geo}^s)$, and $\vec{\theta}_{A,sx}$ is the core shift in A between s and x .

Similarly, the analysis of the observations of a nearby calibrator, B , after removing structural terms, $\phi_{B,str}^x$ and $\phi_{B,str}^s$ at both frequencies, results in:

$$\phi_B^x - R.\phi_B^s = 2\pi\nu \frac{\vec{D} \cdot \vec{\theta}_{B,sx}}{c} + (R - \frac{1}{R})\phi_{B,ion}^s + (\phi_{B,inst}^x - R.\phi_{B,inst}^s) + 2\pi(n_B^x - R.n_B^s) \quad (3)$$

which are transferred for further calibration of A source observations. The resultant SOURCE/FREQUENCY REFERENCED phases, combining (2) and (3), are:

$$\begin{aligned} (\phi_A^x - R.\phi_A^s) - (\phi_B^x - R.\phi_B^s) &= \phi_{A,str}^x + 2\pi\nu \frac{D \cdot (\vec{\theta}_{A,sx} - \vec{\theta}_{B,sx})}{c} + (R - \frac{1}{R})(\phi_{A,ion}^s - \phi_{B,ion}^s) + (\phi_{A,inst}^x - R.\phi_{A,inst}^s) \\ &\quad - (\phi_{B,inst}^x - R.\phi_{B,inst}^s) + 2\pi[(n_A^x - R.n_A^s) - (n_B^x - R.n_B^s)] \end{aligned}$$

A careful planning of the observations, namely switching between sufficiently nearby sources with a duty cycle which matches the ionospheric/instrumental time-scale variations, would result in negligible differential ionospheric error and instrumental corruption, that is:

$$\begin{aligned} (R - \frac{1}{R})(\phi_{A,ion}^s - \phi_{B,ion}^s) &\sim 0 \\ (\phi_{A,inst}^x - R.\phi_{A,inst}^s) - (\phi_{B,inst}^x - R.\phi_{B,inst}^s) &\sim 0 \end{aligned}$$

which results in an expression for the SOURCE/FREQUENCY REFERENCED phases for the target source free of ionospheric/instrumental corruption:

$$(\phi_A^x - R.\phi_A^s) - (\phi_B^x - R.\phi_B^s) = \phi_{A,str}^x + 2\pi\nu \frac{\vec{D} \cdot (\vec{\theta}_{A,sx} - \vec{\theta}_{B,sx})}{c} + 2\pi n'' , \text{ with } n'' \text{ integer if } R \text{ integer (or } n_A^s = n_B^s)$$

And finally, the calibrated complex visibilities from the target observations are inverted to yield a synthesis image of A at x -band, where the offset from the center is an estimate of the combined core shifts in A and B between s and x -bands.

References

- [1] Guirado, J.C., Marcaide, J.M., Alberdi, A., et al. 1995, AJ, 110, 2586
- [2] Lara, L., Marcaide, J.M., Alberdi, A., Guirado, J.C. 1996, A&A, 314, 672
- [3] Lobanov, A. P. 1998, A&A, **330**, p. 79
- [4] Marcaide, J.M. & Shapiro, I.I. 1984, ApJ, 276, 56
- [5] Middelberg, E., PhD Thesis, 2004
- [6] Middelberg, E., Roy, A. L., Walker, R. C., Falcke, H., 2005, A&A, **433**, p. 897-909
- [7] Paragi, Z., Fejes, I., Frey, S., 2000, Proc. IVS General Meeting, p.342
- [8] Porcas, R., Patnaik, A., 1995, Proc. 10th Working Meeting on European VLBI for Geodesy and Astrometry, p. 188
- [9] Rioja, M.J., Porcas, R.W., 2000, A&A, **355**, p.552-563

Running SKED under Linux

Alexey Melnikov¹, John Gipson²

¹) *Institute of Applied Astronomy RAS*

²) *NVI, Inc/NASA GSFC*

Contact author: Alexey Melnikov, e-mail: melnikov@isida.ipa.rssi.ru

Abstract

Since the early 1980s almost all geodetic VLBI-sessions were scheduled using SKED. A disadvantage of SKED is that it runs only on Hewlett-Packard work stations. There has been interest recently in using personal computers running the Linux operating system. These are much cheaper than the HP work stations, and have the further advantage that the operating system is open-source. This report provides information on the successful porting of Sked to run on PCs with Linux installed.

1. Introduction

SKED is software developed for scheduling VLBI sessions. SKED allows easy creation of geodetic and astrometric schedules. The scheduler can manually choose scans, or have SKED automatically choose scans using a rule-based approach. This allows easy generation of schedules.

SKED has been developed in NASA/GSFC since the late 1970s. Nancy Vandenberg was the initial developer, and continued to maintain and develop it until 2002, when John Gipson took over primary responsibility. The source code is predominately Fortran, together with a few C and Java routines.

Computers have evolved substantially over this time, and along the way SKED has been ported several times to newer, better platforms. There was always a primary platform that was supported, most recently HP-UX.

As the price of personal computers has dropped, and the power increased, there has been much interest in porting applications that once ran only on work stations to run on personal computers, often under the Linux environment.

In 2004 Institute of Applied Astronomy volunteered to help by modifying SKED to run under Linux. The hardware of PCs is different than that of HPs. In addition, the SKED code, which has evolved over time, uses data structures such as Hollerith's which were common at one time, but are no longer so. Because of this conversion of SKED to run under Linux was a non-trivial task.

The SKED port should be considered part of a larger project, which is the port of all VLBI software to run under Linux. The Field System and Drudg already runs under Linux. The Calc/Solve analysis suite is in the final stages of porting.

2. The Port

Alexey Melnikov of the IAA began porting SKED in the summer of 2004.

We initially used the Lahey/Fujitsu Fortran 95 Compiler Linux Edition 6.2. One of us (J. Gipson) had extensive experience using the Windows version of this compiler. In addition the compiler was independently highly rated for catching compile and runtime errors. Because of

subsequent problems in interfacing to the standard C compiler in Mandrake Linux 9.2 we changed to use the Intel Fortran and C compilers. These are available for free download for non-commercial use from Intel's site.

At the second stage the possible problems were analysed. The main problem is that SKED uses Hollerith arrays to represent text information. This caused most of the errors when we tried to run SKED under Linux without any modification. There is a long term project at GSFC to remove all Hollerith strings. However, there are still many places where these strings exist. Most of the problems were related to formatting input/output, and to conversion between ASCII and Hollerith. Fortunately most of these were confined to the library LNFCH. Routines in this library were modified so that they would work correctly under Linux.

Other problems arose because of differences in the default size of integers. SKED was written in standard Fortran 77 where integers were not declared explicitly. So there was the possibility of error, for example, in passing variables to subroutines, the integer size is explicitly declared as integer*2 or integer*4. Also the interaction of the Fortran procedures with C functions were fixed in the terms of variable sizes.

The SKED port was finished in February of 2005. In the meantime, SKED had continued to evolve at NASA GSFC. Because of this, Melnikov ported the SKED source code a second time, starting with the SKED source version of February 2005. Once this port was done, Gipson merged Melnikov's changes back into the standard version. In addition, Gipson did some final debugging, which was only practical because Gipson had access to both HP-UX and Linux machines, and was intimately familiar with the SKED source code.

The main features used for scheduling have been carefully tested. However, in a program of SKED's size it is impossible to test all possible paths. In the testing we have done we have verified that schedules generated under HP-UX and Linux are identical.

The Linux version runs 2-3 times faster than the HP-UX version.

3. Conclusions

We have successfully ported SKED to run under Linux, and the changes made have been merged into the standard source code.

There is now a single version of the source code for both Linux and HP-UX available on NASA's ftp site.

Schedules generated under the two operating system are identical.

SKED runs about 3 times faster under Linux than under HP-UX.

To complete the debugging of SKED, we need schedulers to start using the merged SKED under both HP-UX and Linux. Our commitment is to fix any bugs as quickly as possible, usually within a day or two.

Special thanks to Leonid Petrov for help and to Rüdiger Haas for the access to the HP-UX machine for A. Melnikov.

Densification of the International Celestial Reference Frame: Results of EVN+ Observations

Patrick Charlot¹, Alan Fey², Chris Jacobs³, Chopo Ma⁴, Ojars Sovers⁵, Alain Baudry¹

¹) *Observatoire de Bordeaux (OASU) – CNRS/UMR 5804*

²) *U. S. Naval Observatory*

³) *Jet Propulsion Laboratory, California Institute of Technology*

⁴) *National Aeronautics and Space Administration, Goddard Space Flight Center*

⁵) *Remote Sensing Analysis Systems*

Contact author: Patrick Charlot, e-mail: `charlot@obs.u-bordeaux1.fr`

Abstract

The current realization of the International Celestial Reference Frame (ICRF) comprises a total of 717 extragalactic radio sources distributed over the entire sky. An observing program has been developed to densify the ICRF in the northern sky using the European VLBI network (EVN) and additional geodetic radio telescopes. Altogether, 150 new sources selected from the Jodrell Bank–VLA Astrometric Survey were observed during three such EVN+ experiments conducted in 2000, 2002 and 2003. The sources were selected on the basis of their sky location in order to fill the “empty” regions of the frame. A secondary criterion was based on source compactness to limit structural effects in the astrometric measurements. All 150 new sources have been successfully detected and the precision of the estimated coordinates in right ascension and declination is better than 1 milliarcsecond (mas) for most of them. A comparison with the astrometric positions from the Very Long baseline Array Calibrator Survey for 129 common sources indicates agreement within 2 mas for 80% of the sources.

1. Introduction

The International Celestial Reference Frame (ICRF), the most recent realization of the VLBI celestial frame, is currently defined by the radio positions of 212 extragalactic sources observed by VLBI between August 1979 and July 1995 [1]. These *defining* sources, distributed over the entire sky, set the initial direction of the ICRF axes and were chosen based on their observing histories with the geodetic networks and the accuracy and stability of their position estimates. The accuracy of the individual source positions is as small as 0.25 milliarcsecond (mas) while the orientation of the frame is good to the 0.02 mas level. Positions for 294 less-observed *candidate* sources and 102 *other* sources with less-stable coordinates were also reported, primarily to densify the frame. Continued observations through May 2002 have provided positions for an additional 109 new sources and refined coordinates for candidate and “other” sources [2].

The current ICRF with a total of 717 sources has an average of one source per $8^\circ \times 8^\circ$ on the sky. While this density is sufficient for geodetic applications, it is clearly too sparse for differential-VLBI applications (spacecraft navigation, phase-referencing of weak targets), which require reference calibrators within a-few-degree angular separation, or for linking other reference frames (e.g. at optical wavelengths) to the ICRF. Additionally, the frame suffers from an inhomogeneous distribution of the sources. For example, the angular distance to the nearest ICRF source for any randomly-chosen sky location can be as large as 13° in the northern sky and 15° in the southern sky [3]. This non-uniform source distribution makes it difficult to assess and control any

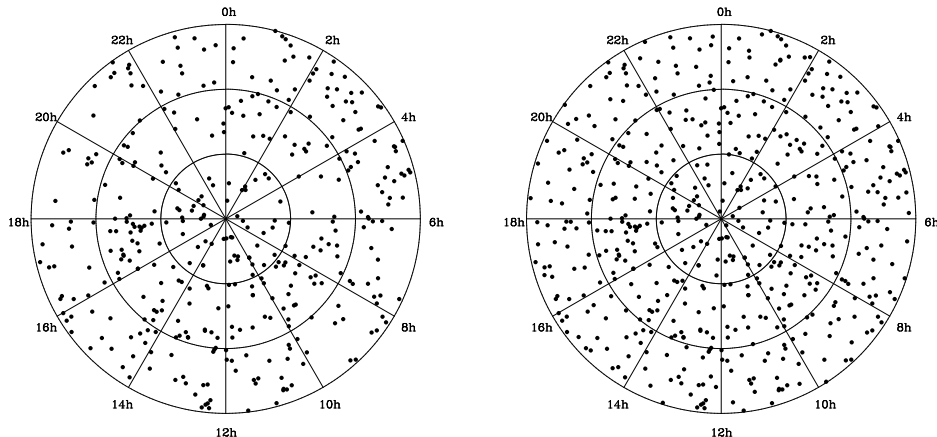


Figure 1. Northern-sky source distribution in polar coordinates. *Left:* for the current ICRF, including defining, candidate, and “other” sources plus the additional sources published in ICRF-Ext.1 [1, 2]. *Right:* same plot after adding the 150 new sources identified to fill the “empty” regions of the frame. The outer circle corresponds to a declination of 0° while the inner central point is for a declination of 90° . The intermediate circles correspond to declinations of 30° and 60° .

local deformations in the frame. Such deformations might be caused by tropospheric propagation effects and apparent source motions due to variable intrinsic structure [1].

This paper reports results of astrometric VLBI observations of 150 new sources to densify the ICRF in the northern sky. These observations were carried out using the European VLBI Network (EVN) and additional geodetic antennas that joined the EVN for this project. The approach used in selecting the new potential ICRF sources was designed to improve the overall source distribution of the ICRF. Sources with no or limited extended emission were preferably selected to guarantee high astrometric suitability. Sections 2 and 3 below describe the source selection strategy in further details, the network and observing scheme used in these EVN+ experiments, and the data analysis. The astrometric results that have been obtained are discussed in Sect. 4, including a comparison with the Very Long Baseline Array (VLBA) Calibrator Survey astrometric positions for 129 common sources.

2. Strategy for Selecting New ICRF Sources

The approach used for selecting new sources to densify the ICRF was to fill first the “empty” regions of the frame. The largest such region for the northern sky is located near $\alpha = 22$ h 05 min, $\delta = 57^\circ$, where no ICRF source is to be found within 13° . A new source should thus be preferably added in that part of the sky. By using this approach again and repeating it many times, it is then possible to progressively fill the “empty” regions of the frame and improve the overall ICRF source distribution. The input catalog for selecting the new sources to observe was the Jodrell Bank–VLA Astrometric Survey (JVAS) which comprises a total 2118 compact radio sources with peak flux density at 8.4 GHz larger than 50 mJy (at a resolution of 200 mas) in the northern sky [4, 5, 6]. For every “empty” ICRF region, all JVAS sources within a radius of 6° (about 10 sources on average) were initially considered. These sources were then filtered out using the VLBA Calibrator Survey,

which includes VLBI images at 8.4 and 2.3 GHz for most JVAS sources [7], to eventually select the source with the most compact structure in each region.

The results of this iterative source selection scheme show that 30 new sources are required to reduce the angular distance to the nearest ICRF source from a maximum of 13° to a maximum of 8° . Another 40 new sources would further reduce this distance to a maximum of 7° while for a maximum distance of 6° , approximately 150 new sources should be added. Carrying this procedure further, it is found that the number of required new sources doubles for any further decrease of this distance of 1° (approximately 300 new sources for a maximum distance of 5° and 600 new sources for a maximum distance of 4°) with the limitation that the JVAS catalog is not uniform enough to fill all the regions below a distance of 6° . Based on this analysis, we have selected the first 150 sources identified through this procedure for observation with the EVN+ network described below. As shown in Fig. 1, the overall source distribution is potentially much improved with these additional 150 sources in the northern sky.

3. Observations and Data Analysis

The observations were carried out in a standard geodetic mode during three 24-hour dual-frequency (2.3 and 8.4 GHz) VLBI experiments conducted on May 31, 2000, June 5, 2002, and October 27, 2003, using the EVN (including the Chinese and South African telescopes) and up to four additional geodetic radio telescopes (Algonquin Park in Canada, Goldstone/DSS 13 and Greenbank/NRAO20 in USA, and Ny-Alesund in Spitsbergen). There were between 10 and 12 telescopes scheduled for each experiment. Such a large network permits a geometrically-strong schedule based on sub-netting which allows tropospheric gradient effects to be estimated from the data. The inclusion of large radio telescopes (Effelsberg, Algonquin Park) in this network was essential because the new sources are much weaker than the ICRF ones (median total flux of 0.26 Jy compared to 0.83 Jy for the ICRF sources, as indicated in [3]). Each experiment observed a total of 50 new sources along with 10 highly-accurate ICRF sources so that the positions of the new sources can be linked directly to the ICRF.

The data were correlated with the Bonn Mark 4 correlator, fringe-fitted using the Haystack software FOURFIT, and exported in the standard way to geodetic data base files. All subsequent analysis employed the models implemented in the VLBI modeling and analysis software MODEST [8]. Standard geodetic VLBI parameters (station clock offsets and rates with breaks when needed, zenith wet tropospheric delays every 3 hours, and Earth orientation) were estimated in each experiment along with the astrometric positions (right ascension and declination) of the new sources. The positions of the 10 ICRF link sources were held fixed as were station coordinates. Observable weighting included added baseline-dependent noise adjusted for each baseline in each experiment in order to make χ^2 per degree of freedom approximately equal to 1.

4. Results

The three EVN+ experiments described above have been very successful in observing the selected targets. All 150 new potential ICRF sources have been detected, hence indicating that the source selection strategy and observing scheme for these experiments were appropriate. In the first two experiments (2000 May 31 and 2002 June 5), there were generally between 20 and 60 pairs of delay and delay rates usable for each source to estimate its astrometric position. Conversely,

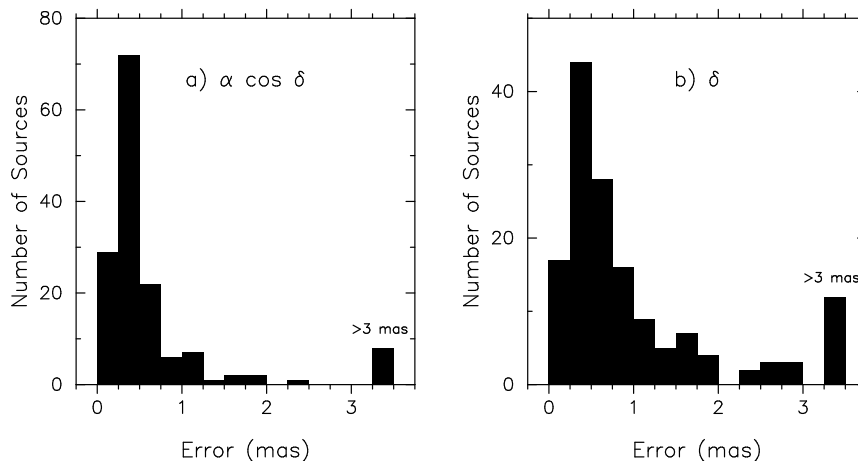


Figure 2. Astrometric precision of the estimated coordinates in *a*) right ascension and *b*) declination for the 150 newly-observed sources. All errors larger than 3 mas are placed in a single bin marked with the label “> 3 mas” on each plot.

more than half of the sources observed in the third experiment (2003 October 27) had less than 20 pairs of usable delay and delay rates because of the failure of three telescopes in that experiment.

Figure 2 shows the error distribution in right ascension and declination for the 150 newly-observed sources. The distribution indicates that about 70% of the sources have position errors smaller than 1 mas, consistent with the high quality level of the ICRF. The median coordinate uncertainty is 0.37 mas in right ascension and 0.63 mas in declination. The larger declination errors are most probably caused by the predominantly East-West network used for these observations. Figure 2 also shows that a dozen sources have very large errors (> 3 mas). Most of these sources were observed during the 2003 October 27 experiment and have only a few available observations or data only on short intra-Europe baselines. Such sources should be re-observed to obtain improved coordinates if these are to be considered for inclusion in the next ICRF realization.

Among our 150 selected targets, 129 sources were found to have astrometric positions available in the VLBA Calibrator Survey [7]. A comparison of these positions with those estimated from our analysis shows agreement within 1 mas for half of the sources and within 2 mas for 80% of the sources. While the magnitude of the differences is consistent with the reported astrometric accuracy of the VLBA Calibrator Survey, further investigation is necessary to determine whether these differences are of random nature or show systematic trends. Such trends might be caused by the limited sky coverage (declination strips) used in observing the VLBA Calibrator Survey [7].

5. Conclusion

A total of 150 new potential ICRF sources have been successfully detected using the EVN and additional geodetic radio telescopes located in USA, Canada and Spitsbergen. About two-third of the sources observed with this EVN+ network have coordinate uncertainties better than 1 mas, and thus constitute valuable candidates for extending the ICRF. The inclusion of these sources would largely improve the ICRF sky distribution by naturally filling the “empty” regions of the current celestial frame. The remaining portion of the sources (those that have coordinate uncertainties

larger than 1 mas) have been re-observed during an additional EVN+ experiment conducted in February 2005 in order to improve their coordinates.

Extending further the ICRF will require observing weaker and weaker sources as the celestial frame fills up and hence will depend closely on how fast the sensitivity of VLBI arrays improves in the future. It is estimated that an extragalactic VLBI celestial frame comprising 10 000 sources may be possible by 2010 considering foreseen improvements in recording data rates (disk-based recording, modern digital videoconverters) and new radio telescopes of the 40–60 meter class that are being built, especially in Spain, Italy and China [9]. In the even longer term, increasing the source density beyond that order of magnitude is likely to require new instruments such as the Square Kilometer Array envisioned by 2015–2020.

6. Acknowledgements

The European VLBI Network (EVN) is a joint facility of European, Chinese, South African and other radio astronomy institutes funded by their national research councils. The geodetic radio telescopes in Algonquin Park (Canada), Ny-Alesund (Spitsbergen), Goldstone (USA), and Greenbank (USA) are sponsored by Natural Resources Canada, the Norwegian Mapping Authority, the National Aeronautics and Space Administration, and the U. S. Naval Observatory, respectively. We thank all participating observatories, with special acknowledgements to the staff of the non-EVN stations for their enthusiasm in participating in this project. We are also grateful to Nancy Vandenberg, Ed Himwich and Dave Graham for help in scheduling, Walter Alef and Arno Mueskens for data correlation and advice in fringe-fitting, and Axel Nothnagel for export of the data to geodetic data base files. This research was supported by the European Commission’s I3 Programme “RADIONET”, under contract No. 505818.

References

- [1] Ma, C., Arias, E. F., Eubanks, T. M., Fey, A. L., Gontier, A.-M., Jacobs, C. S., Sovers, O. J., Archinal, B. A., Charlot, P. 1998, *AJ*, 116, 516
- [2] Fey, A. L., Ma, C., Arias, E. F., Charlot, P., Feissel-Vernier, M., Gontier, A.-M., Jacobs, C. S., Li, J., MacMillan, D. S. 2004, *AJ*, 127, 3587
- [3] Charlot, P., Viateau, B., Baudry, A., Ma, C., Fey, A. L., Eubanks, T. M., Jacobs, C. S., Sovers, O. J. 2000, in *International VLBI Service for Geodesy and Astrometry 2000 General Meeting Proceedings*, eds. N. R. Vandenberg & K. D. Beaver, NASA/CP-2000-209893, 168
- [4] Patnaik, A. R., Browne, I. W. A., Wilkinson, P. N., Wrobel, J. M. 1992, *MNRAS*, 254, 655
- [5] Browne, I. W. A., Patnaik, A. R., Wilkinson, P. N., Wrobel, J. M. 1998, *MNRAS*, 293, 257
- [6] Wilkinson, P. N., Browne, I. W. A., Patnaik, A. R., Wrobel, J. M., Sorathia, B. 1998, *MNRAS*, 300, 790
- [7] Beasley, A. J., Gordon, D., Peck, A. B., Petrov, L., MacMillan, D. S., Fomalont, E. B., Ma, C. 2002, *ApJS*, 141, 13.
- [8] Sovers, O. J., Jacobs, C. S. 1996, *Observation Model and Parameter Partialials for the JPL VLBI Parameter Estimation Software “MODEST”–1996*, JPL Publication 83-89, Rev. 6, August 1996
- [9] Charlot, P. 2004, in *International VLBI Service for Geodesy and Astrometry 2004 General Meeting Proceedings*, eds. N. R. Vandenberg & K. D. Beaver, NASA/CP-2004-212255, 12

Ring Laser "G" and Earth Rotation

Thomas Klügel¹, Wolfgang Schlüter¹, Ulrich Schreiber²

¹) BKG - Wettzell

²) Forschungseinrichtung Satellitengeodäsie, TU München

Contact author: Thomas Klügel, e-mail: thomas.kluegel@bkg.bund.de

1. General Information

Earth rotation plays a fundamental role for maintaining global reference frames. It links the Earth fixed terrestrial reference frame, realized as the International Terrestrial Reference Frame (ITRF) to the space fixed celestial reference frame, realized as International Celestial Reference Frame (ICRF). The techniques used today for monitoring Earth rotation are

Very Long Baseline Interferometry (VLBI), which provides the complete set of Earth rotation parameters, Satellite Laser Ranging (SLR), which contributes to the observation of polar motion, Lunar Laser Ranging which contributes (very little) to the determination of UT1-UTC, the application of the Global Positioning System (GPS), which provides Polar Motion and allows the interpolation of the parameters for the celestial pole and length of day, as well as DORIS (Doppler Orbitography and Radiopositioning Integrated by Satellite) which provides contributions to polar motion.

The so called geodetic space techniques require global infrastructure, as a global observation networks, data transfer and analysis centers.

2. Motivation for ring lasers

Ring lasers by definition operate in an inertial system by themselves (Fermi-System) and are sensitive to rotation. They make use of the relativistic "Sagnac Effect". The measurement of absolute rotation is a fundamental difference to geodetic space techniques, where rotation is measured by observing outside targets. Most applications for ring lasers are found in strap down systems for inertial navigation (INS).

The potential for monitoring Earth rotation has been discussed during the International conference jointly held by the IAG, IAU And IUGG in Columbus Ohio in the Year 1986 by Rotege et. al [1]. The German Research Group for Satellite Geodesy (FGS) included the research and development of such a technique for monitoring Earth rotation in its research program. The motivation in particular was to monitor subdaily variations in the rotation of the Earth. The advantages are

- ring lasers are referenced to an inertial system,
- no need for a global network,

- data access in real time,
- open area for research e. g. Seismology.

The disadvantages are

- the high sensitivity to local influences as tilts,
- numerous environmental observations are required for the correction of local effects,
- absolute orientation is not precisely known,
- some systematic effects are so far still unknown.

3. Principle

Four mirrors with an extreme high reflectivity realize the oscillator for the He-Ne- Laser (Figure 1). Radio frequency excitation starts and maintains the lasing process in both directions, clockwise and counterclockwise. Due to the rotation of the ring laser being attached to the rotating Earth, a difference in the laser frequency occurs, named as Sagnac frequency.

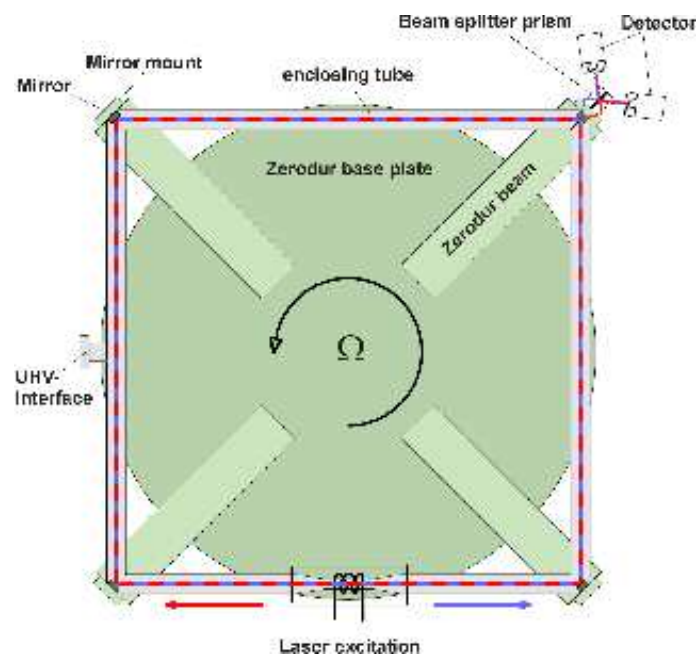


Figure 1. Principle of the Ring laser

The formula describes the relation between the Sagnac frequency and the rotation.

$$\Delta f = \frac{4A}{\lambda L} \vec{n} \vec{\Omega}$$

where

Δf : Sagnac frequency
A: Area enclosed by the laser beam
 λ : wavelength of the laser beam
L: perimeter
 \vec{n} : normal vector of A
 $\vec{\Omega}$: rotation vector.

4. Technical Realization

On behalf of the Research Group Satellite Geodesy (FGS) the Federal Agency of Cartography and Geodesy (BKG) and the Technical University Munich (FESG: Forschungseinrichtung Satellitengeodsie) cooperate with the University of Canterbury, New Zealand on the realization of the ring laser "G". At first prototypes were built in order to derive the technical specifications for the application of monitoring the Earth rotation. In the years before this project the University of Canterbury has built a ring laser, CI, of the size of 1m x 1m and demonstrated the sensitivity for the rotation of the Earth successfully [2]. With respect to the requirements for long and uninterrupted operations, the prototype CII was built based on the CI design and experiences (figure 2), jointly by BKG, FESG and University of Canterbury [3]. The system was set up in a cave in Christchurch which belongs to the University of Canterbury. In addition, an other prototype G0 was built to demonstrate the feasibility of a ring with the size of approximately 4m x 4m.



Figure 2. Ring laser Prototype CII

Based on the experiences gained by CI, CII and G0, the ring laser G, which is used for monitoring the Earth rotation at the Fundamental Station Wettzell was constructed. Figure 3 shows

the construction principles of G. The area enclosed by the laser beam is 4m x 4m, which is required to approach the aimed resolution. The material used as base plate was Zerodur, which has a very low thermal expansion. The reflectivity of the mirrors is better than 5 parts per million. The ultra high vacuum system is constructed for long term operation.

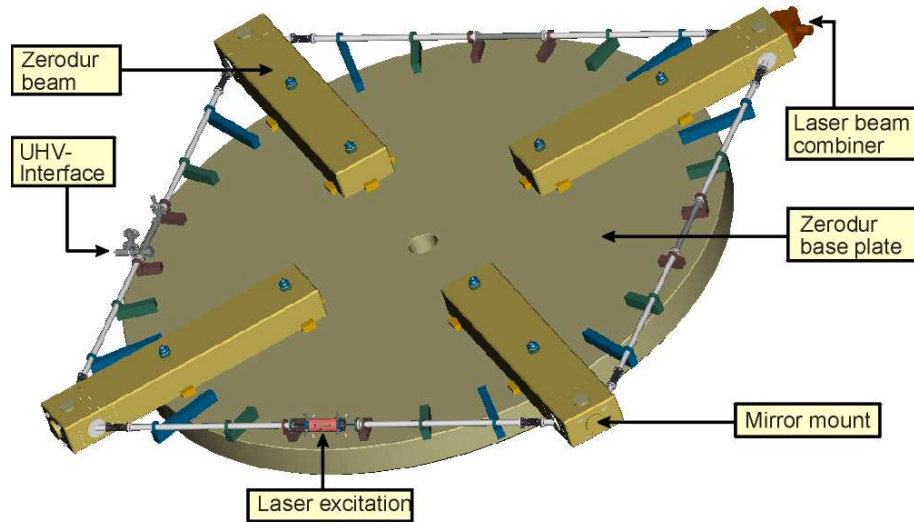


Figure 3. Construction principles of G

In order to minimize local disturbances, an underground laboratory has been built for G. Figure 4 shows the construction of the underground laboratory. Main focus of the building was to guarantee high temperature stability over long periods of time. Local sensors are implemented to monitor tilts and changes of the environment.

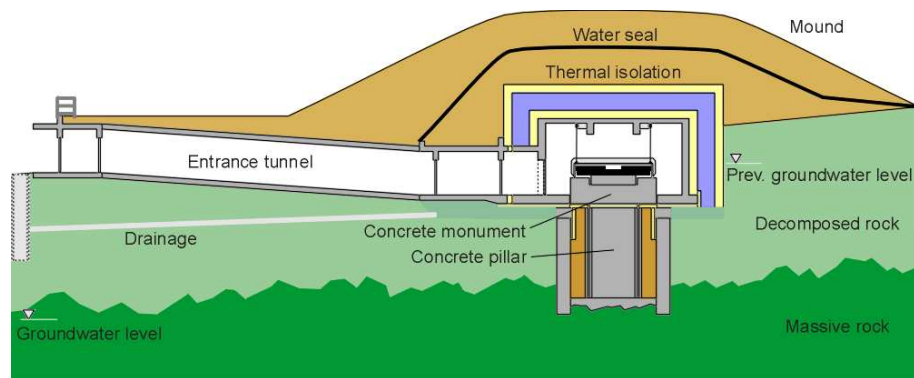


Figure 4. Underground laboratory

G was installed in the underground laboratory in the period from 1998 to 2001. The first Sagnac Signal was detected in June 2001. Figure 5 shows the ring laser G.

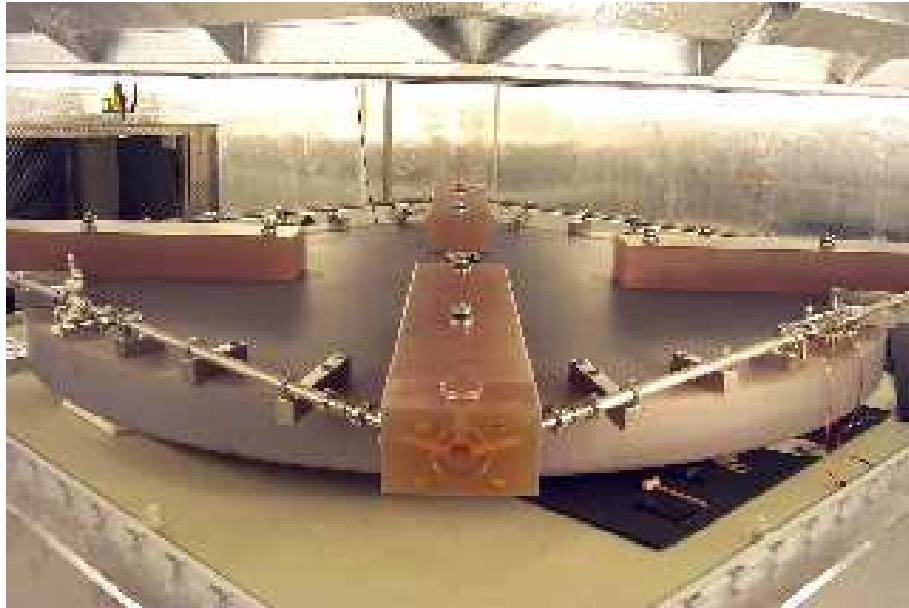


Figure 5. Ring laser G

5. First results

Since October 2001 several time series of the Sagnac frequency, recorded in bins of 30 minutes, could be observed. The resolution and the stability of G is shown in figure 6 with respect to signals which occur from the Earth rotation. The Flicker floor of the Allan variance is reached at the level of 10^{-8} , which clearly shows that the tilt effect of the Earth tides and of the diurnal polar motion is detectable. Tilt and polar motion affect the Sagnac signal, because the projection of the Earth rotation vector on the normal vector of the laser plane changes in both cases. To observe the influence of the Ocean tides and of the Atmospheric momentum, one more order of magnitude in sensitivity is needed.

Resolution and stability of the "G" ring laser with respect to Earth rotation signals

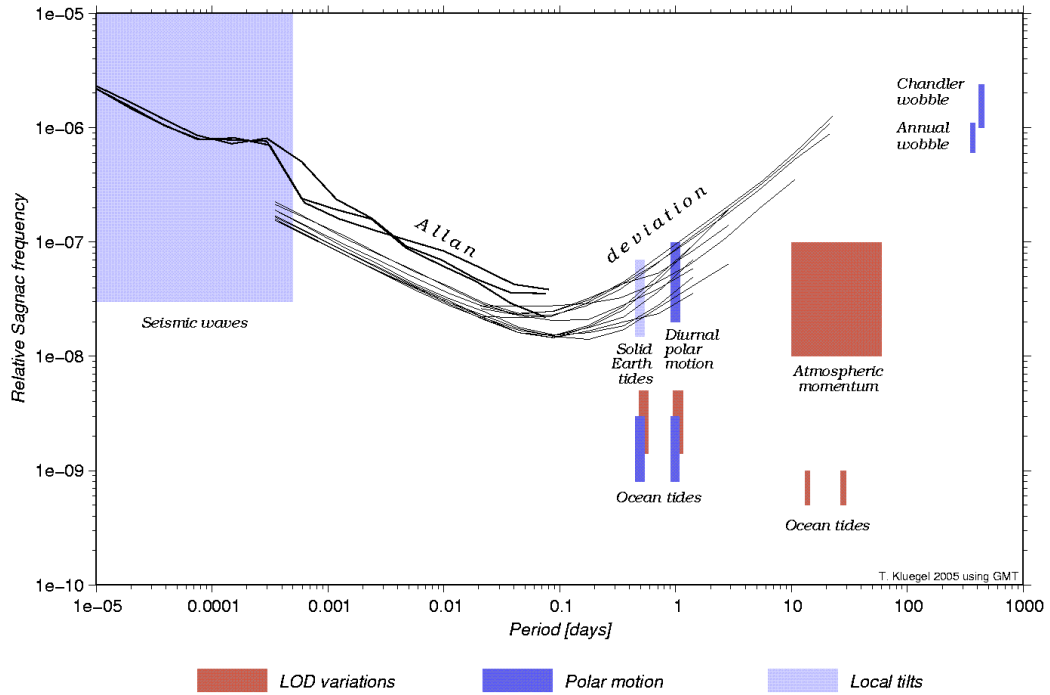


Figure 6. Resolution and stability of the ring laser G, with respect to Earth rotation signals

As example the 35 day time series observed from day 260 to 295 in the year 2005 is shown in figure 7. Results from the spectral analysis are shown in Figure 8. The time series, consists of 30min data. the offset and the drift are reduced and band pass filtered. The two cut off frequencies for the band pass filter was chosen to be 0.02^{-1} to 2^{-1} days $^{-1}$.

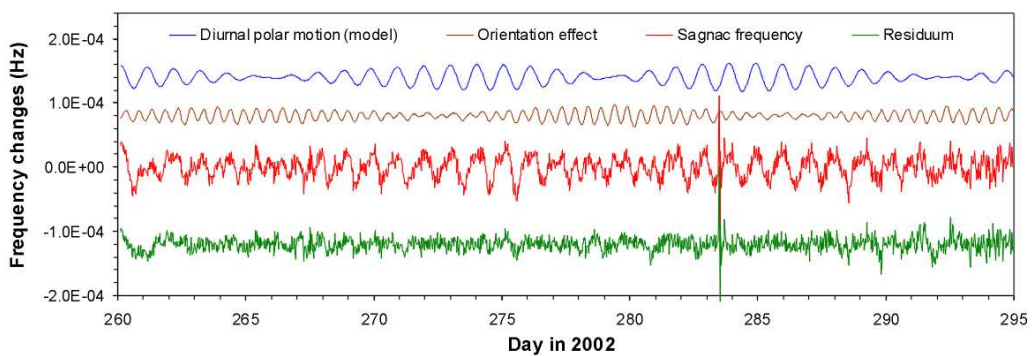


Figure 7. 35 days time series in 2002

The first diagram shows the Spectrum with both signals included, the diurnal polar motion and the tidal tilt effect, the second diagram shows the spectrum with the reduced tidal tilt effect

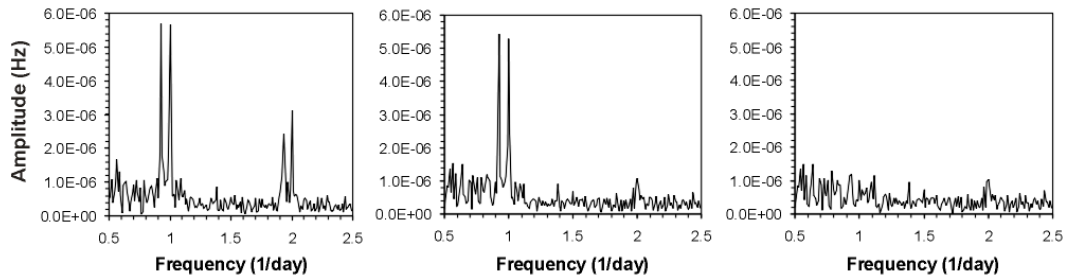


Figure 8. Spectrum of the observed Sagnac frequency

and the third shows the spectrum with diurnal polar motion and tidal tilt effect removed. It could be clearly shown that both effects are seen in the observations [4], [5].

6. Summary and Outlook

The observation of the Earth rotation by employing a ring laser is a complete new technology. The resolution achieved today is in the order of 10^{-8} for a time span of 3h. The signal is sensitive to seismic events, Earth tides and diurnal polar motion. To eliminate drifts and systematic influences after two days of observation external information is required for calibration, e.g. from VLBI. Improvement of 1 order in magnitude is of extreme importance in order to monitor the subdaily Earth rotation variations. It is expected to gain one order of magnitude by employing improved mirrors and improved ultra high vacuum systems. Never the less the models need improvements which require more experiences. It has to be considered that this technology has started right now for this kind of applications and still needs time to mature.

References

- [1] Rotgé, J.R., Shaw, G.L. & Emrick, H.W. (1986): Measuring Earth rate perturbations with a large passive ring laser gyro. - Proc. IAU/IAG/IUGG Int. Conf. On Earth Rotation and Terr. Ref. Frame: 719-729; Columbus/Ohio.
- [2] Stedman, G.E. (1997): Ring laser tests of fundamental physics and geophysics - Reports on progress in physics, vol. 60, no. 6: 615 - 688.
- [3] Schreiber, U. (2000): Ringlasertechnologie für geowissenschaftliche Anwendungen. - Mitt. Bundesamt f. Kartographie u. Geodäsie, Band 8, 97 S., Frankfurt.
- [4] Schreiber, U., Stedman, G.E. and Klügel, T. (2003): Earth tide and tilt detection by a ring laser gyroscope. - J. Geophys. Res. 108 (B) 2, 10.1029/2001JB000569.
- [5] Schreiber, U.; Velikoseltsev, A.; Rothacher, M.; Klügel, T.; Stedman, G.E.; Wiltshire, D.L. (2004): Direct measurement of diurnal polar motion by ring laser gyroscopes, J. Geophys. Res., 109 (B6), 10.1029/2003JB002803, B06405.

Participants of the 17th European VLBI Meeting

Name	Institution	Country	E-mail
Alef, Walter	Max-Planck-Institute for Radioastronomy	Germany	walef@mpifr-bonn.mpg.de
Andersen, Per Helge	FFI	Norway	per-helge.andersen@ffi.no
Barache, Christophe	Syrte / Observatoire de Paris	France	christophe.barache@obspm.fr
Behrend, Dirk	NVI, Inc./GSFC	USA	dbb@ivsc.gsfc.nasa.gov
Boboltz, David	U. S. Naval Observatory	USA	dboboltz@usno.navy.mil
Boehm, Johannes	TU Vienna	Austria	johannes.boehm@tuwien.ac.at
Camargo, Julio	Observatoire de Bordeaux	France	camargo@obs.u-bordeaux1.fr
Campbell, Bob	JIVE	The Netherlands	campbell@jive.nl
Campbell, James	GIUB	Germany	campbell@uni-bonn.de
Charlot, Patrick	Observatoire de Bordeaux	France	charlot@obs.u-bordeaux1.fr
Cho, Jung-ho	Korea Astronomy and Space Science Institute	South Korea	jojh@kasi.re.kr
Engelhardt, Gerald	BKG	Germany	gerald.engelhardt@bkg.bund.de
Fey, Alan	U.S. Naval Observatory	USA	afey@usno.navy.mil
Garramone, Luciano	ASI	Italy	luciano.garramone@asi.it
Gontier, Anne-Marie	Syrte / Observatoire de Paris	France	anne-marie.gontier@obspm.fr
Gordon, David	Raytheon/GSFC	USA	dgg@leo.gsfc.nasa.gov
Haas, Rüdiger	Onsala Space Observatory, Chalmers University of Technology	Sweden	haas@oso.chalmers.se
Heinkelmann, Robert	TU Vienna	Austria	rob@mars.hg.tuwien.ac.at
Himwich, Ed	NASA/GSFC/NVI	USA	weh@ivsc.gsfc.nasa.gov
Hobiger, Thomas	IGG - TU Vienna	Austria	thobiger@mars.hg.tuwien.ac.at
Jike, Takaaki	National Astronomical Observatory of Japan	Japan	jike@miz.nao.ac.jp

Name	Institution	Country	E-mail
Kingham, Kerry	U.S. Naval Observatory	USA	kingham.kerry@usno.navy.mil
Koyama, Yasuhiro	Kashima Space Research Center, NICT	Japan	koyama@nict.go.jp
Lanotte, Roberto	Centro di Geodesia Spaziale - Telespazio - Matera	Italy	roberto.lanotte@asi.it
Leonid, Petrov	NVI, Inc./ NASA GSFC	USA	Leonid.Petrov@lpetrov.net
Ma, Chopo	Goddard Space Flight Center	USA	cma@gemini.gsfc.nasa.gov
MacMillan, Dan	NVI, Inc./NASA GSFC	USA	dsm@leo.gsfc.nasa.gov
Manabe, Seiji	National Astronomical Observatory of Japan	Japan	manabe@miz.nao.ac.jp
Mantovani, Franco	INAF-Istituto di Radioastronomia, Bologna	Italy	fmantovani@ira.cnr.it
Montaguti, Simonetta	IRA - INAF	Italy	montaguti@ira.cnr.it
Mueskens, Arno	GIUB	Germany	mueskens@mpifr-bonn.mpg.de
Negusini, Monia	IRA - INAF	Italy	negusini@ira.cnr.it
Niell, Arthur	MIT Haystack Observatory	USA	aniell@haystack.mit.edu
Nothnagel, Axel	GIUB	Germany	nothnagel@uni-bonn.de
Petrachenko, Bill	Natural Resources Canada (NRCan)	Canada	Bill.Petrachenko@nrc-cnrc.gc.ca
Rioja, Maria	OAN	Spain	rioja@oan.es
Sarti, Pierguido	IRA - INAF	Italy	p.sarti@ira.cnr.it
Schlueter, Wolfgang	BKG, FS Wettzell	Germany	schlueter@wettzell.ifag.de
Schuh, Harald	TU Vienna	Austria	harald.schuh@tuwien.ac.at
Tamura, Yoshiaki	National Astronomical Observatory of Japan	Japan	tamura@miz.nao.ac.jp
Tesmer, Volker	DGFI	Germany	tesmer@dgfi.badw.de
Thorandt, Volkmar	BKG	Germany	volkmar.thorandt@bkg.bund.de
Tornatore, Vincenza	Politecnico di Milano	Italia	vincenza.tornatore@polimi.it
Tuccari, Gino	IRA - INAF	Italy	g.tuccari@ira.cnr.it
Vennebusch, Markus	GIUB	Germany	Vennebusch@uni-bonn.de
Vittuari, Luca	DISTART - Universit di Bologna	Italy	luca.vittuari@mail.ing.unibo.it

Name	Institution	Country	E-mail
Wallace, Patrick	CLRC/RAL	United Kingdom	ptw@star.rl.ac.uk
Whitney, Alan	MIT Haystack Observatory	USA	awhitney@haystack.mit.edu
Wresnik, Jörg	TU Vienna	Austria	joerg@oso.chalmers.se

Programme of the 17th European VLBI Meeting

Friday, 22nd April 2005

Session 1:

Chair: Walter Alef

- 14.00–14.15 Opening of the 17th Working Meeting
14.15–14.30 MANTOVANI, FRANCE
Geodetic VLBI activities in Italy
14.30–14.45 TUCCARI, GINO:
DBBC Development: Status and First Results
14.45–15.00 KOYAMA, YASUHIRO:
Developments of the K5 VLBI System
15.00–15.15 WHITNEY, ALAN:
Mark 5AB Status Update
15.15–15.30 WHITNEY, ALAN:
e-VLBI status update

15.30–16.00 **COFFEE BREAK**

Session 2:

Chair: Gino Tuccari

- 16.00–16.15 ALEF, WALTER ET AL.:
Bonn Correlator Report
16.15–16.30 CAMPBELL, BOB:
Recent Developments at the EVN MkIV Data Processor at JIVE
16.30–16.45 SKURIKHINA, ELENA (cancelled):
VLBI antenna thermal deformation - some results of correct application
16.45–17.00 WRESNIK, JÖRG ET AL.:
Thermal deformation of VLBI antennas
17.00–17.15 SARTI, PIERGUIDO ET AL.:
Terrestrial and GPS survey of co-located geodetic instruments at Noto
Observatory

- 17.15–17.30 BITELLI, G. ET AL.:
Determination of vertical motion from levelling data in the wider area
of Medicina and the Appenine foothills
- 17.30–17.45 Discussion of Sessions 1 and 2

Saturday, 23rd April 2005

Session 3:

Chair: Pierguido Sarti

- 09:00–09:15 BOEHM, J., H. SCHUH:
Troposphere mapping functions from ECMWF operational analysis data
- 09.15–09.30 SKURIKHINA, ELENA (cancelled):
Application of apriori WZD parameters to VLBI data processing
- 09.30–09.45 HEINKELMANN, R., H. SCHUH:
Homogenization of surface pressure and its impact on long-term series
of tropospheric parameters
- 09.45–10.00 HAAS, R. ET AL. (cancelled):
An investigation of water vapor trends in Europe
- 10.00–10.15 HOBIGER T. ET AL.:
Estimation of absolute TEC values by VLBI
- 10.15–10.30 VENNEBUSCH, MARKUS:
Status of SINEX combination - IVS' contribution to the IERS Combi-
nation Pilot Project
- 10.30–10.45 PETROV, LEONID:
Approaches for estimation of non-linear site position variations
- 15.30–16.00 **COFFEE BREAK**

Session 4:

Chair: Franco Mantovani

- 11.15–11.30 NOTHNAGEL, AXEL:
VTRF2005 - A combined VLBI Terrestrial Reference Frame
- 11.30–11.45 TESMER, V. ET AL.:
CONT02: studying rigorously combined GPS and VLBI data

- 11.45–12.00 CHARLOT, P. ET AL.:
Densification of the ICRF: Results of EVN+ Observations
- 12.00–12.15 SOKOLOVA, J. (cancelled):
Study of some methods of radio source catalogues comparison
- 12.15–12.30 RIOJA, M. ET AL.:
Measurement of core-shifts with astrometric multi-frequency calibration
- 12.30–12.45 SCHLUETER, W.:
The Wettzell ring laser and earth rotation
- 12.45–13.00 Discussion of Sessions 3 and 4
- 13.00–14.00 **LUNCH**

Session 5:

Chair: Axel Nothnagel

- 14.00–15.00 EVG - European VLBI Group for Geodesy
- 15.00–16.00 GeoNet - European Network of Terrestrial Reference Points for Geodesy
and Radio Astronomy
- 13:00 **OFFICIAL END OF MEETING**

